Novel Insight into uPAR Function in the Bronchial Epithelium in Asthma Using Functional Genomics

By

Sangita Kumari Bhaker BSc.

Thesis submitted to the University of Nottingham for the degree of Doctor of Philosophy

March 2017



This thesis is dedicated to my Parents, Prempal Singh Bhatti and Krishna Kumari Bhatti and my Grandparents, Ajit Singh Bawa, Koshaliya Kaur Bhatti, Rajinder Singh Digva and Ajit Kaur Digva.

Abstract

The urokinase plasminogen activator receptor (uPAR, *PLAUR*) is a cell surface receptor actively involved in the regulation of cell homeostasis. Expression is elevated in the bronchial epithelium *in vivo* and also in serum and sputum in asthma and elevated expression often indicates poor prognosis in a number of human diseases. The relative contribution of uPAR to asthma disease mechanisms is not fully understood and the functional roles of uPAR isoforms remains to be resolved. The key aims of this thesis were to i) investigate how the uPAR pathway may influence bronchial epithelial barrier properties; ii) investigate the gene expression patterns in the bronchial epithelium in asthma; iii) identify functions of different forms of uPAR in human bronchial epithelial cells (HBEC) and to iv) investigate the association between genetic polymorphisms spanning the *PLAUR* gene with clinical features and the presentation of asthma in moderate to severe asthma.

Using two cell based approaches we identified an inverse relationship between soluble-cleaved uPAR expression and epithelial barrier properties. Importantly, we demonstrated that blocking uPAR-integrin interactions provides a potential therapeutic opportunity to improve epithelial barrier function. Using whole transcriptome analysis genes differentially expressed between cultured asthma and control subjects were identified which were related to cell growth, repair and immune regulation. Furthermore, uPAR expression was elevated in epithelial cells in asthma subjects compared to healthy controls, suggesting expression is inherently altered in the bronchial epithelium in asthma. Transcriptomics was used to provide novel insight into the specific and overlapping functions of uPAR isoforms and to determine the effects of elevated uPAR expression on HBEC function. Finally, the contribution of *PLAUR* genetic variants to clinical and immunological traits within asthma were investigated and found that *PLAUR* single nucleotide polymorphisms (SNPs) did not

show an association with the traits measured in a severe asthma population. Overall this work has provided new insight into the function of uPAR as a regulator of the bronchial epithelium in asthma.

Publications

Miller, S; Henry, AP; Hodge, E; Kheirallah, AK; Charlotte K Billington; Rimington T; **Bhaker, S**; Obeidat, M; Melén, E; Merid, SK; Swan, C; Gowland, C; Nelson, CP; Stewart, CE; Bolton, CE; Kilty, I; Malarstig, A; Parker, SG; Moffatt, MF; Andrew J Wardlaw; Ian P Hall; Ian Sayers; The Ser82 RAGE variant affects lung function and serum RAGE in smokers and sRAGE production in vitro. PLoS ONE 11(10). DOI: 10.1371/journal.pone.0164041

Rimington, T; Hodge, E; Billington, C; **Bhaker, S**; Kilty, 1; Jelinsky, S; Hall, IP; Sayers, I; Defining the Inflammatory Signature of Human Lung Explant Tissue in the Presence and Absence of Glucocorticoid. F1000Research 2017, 6:460. DOI: 10.12688/f1000research.10961.1

Abstracts

Bhaker S, Shaw D, Sayers I. Small airway epithelial cells show distinct growth requirements compared to large airway epithelial cells. [Poster presentation, Respiratory Research Day, Leicester UK 2016]

Bhaker S, Portelli MA, Sayers I. Identification of novel urokinase plasminogen activator receptor function using gene set enrichment analysis. [Poster presentation, The European Respiratory Society Research Seminar, Berlin 2016]

Bhaker S, Portelli MA, Sayers I. Identification of novel urokinase plasminogen activator receptor function using gene set enrichment analysis [Oral presentation, Respiratory Research Day, University of Leicester 2016]

Bhaker S, Shaw D, Sayers I. Investigating the role of the urokinase plasminogen activator receptor (uPAR) in airway epithelial barrier formation using air-liquid interface [Oral presentation, Respiratory Research Day, University of Nottingham 2015]

Bhaker S, Portelli MA, Sayers I. Urokinase plasminogen activator receptor variants drive distinct phenotypes in the bronchial epithelium. [Poster presentation, The European Respiratory Society Annual Meeting, Amsterdam September 2015]

Bhaker S, Portelli MA, Slater M, Shaw D, Sayers I. Differential expression of uPAR in cultured bronchial epithelial cells from asthma patients. [Poster presentation, The European Respiratory Society Annual Meeting, Amsterdam September 2015]

Bhatti S, Slater M, Shaw D, Sayers I. Translating genetic associations to molecular mechanisms in asthma pathogenesis: urokinase plasminogen activator receptor. [Poster presentation, Respiratory Genetics Conference, University of Nottingham UK 2014]

Bhatti S, Portelli MA, Sayers I. Evaluation of bronchial air liquid interface as a model for respiratory research. [Poster presentation, The EMBO/EMBL Epithelia Symposium, Heidelburg 2014]

Acknowledgements

Firstly, I would like to thank Professor Ian Sayers and Dr Dominick Shaw for the opportunity to embark on this PhD and for their support and advice over the last four years. I would especially like to thank them both for pushing me to challenge myself. I would also like to thank Professor Peter Shaw, Dr Thomas Strahl, Janice Saxton and Dr Andrew Knight for the opportunities to work in their labs, and thank you to Professors Ian Hall and Simon Johnson for taking the time to give me very useful pockets of advice.

I owe a great deal to Mike Portelli, Mariel Slater and Emily Hodge for their time and patience when training me. Especially, Mike, who always takes the time out to help regardless of where he is in the world. Thank you to Charlotte Billington, Suzanne Miller, Chris Philp and Aru Dongre-Patel for being great friends and to Alex Kheirellah for the hours of RNA-Seq training. I would like to thank Helen Bailey, Garry Meakin and Carly Clayton for all their help over at City Hospital. Thank you to Vincent Pang, Victoria Wright and Fei Sang for your help with ECIS and RNA-Seq. I am very appreciative of the fact that this project has allowed me to work with so many scientists from whom I have learnt a great deal!

I would also like to thank my parents, especially my mum for demonstrating how to complete a PhD when the odds are stacked against you, and my brothers and sisters for their encouragement and support over the last 4 years. Thank you Harvy and Jave, Kavita, Neesha, Jag and Jamie and most of all Avani and Naya. I would also like to thank my very good friends Ishita and Rozie for being there throughout the journey. Last but definitely not least, I would like to thank my husband and best friend Harry for the late nights, the food drop-offs, fpr putting up with me and for making our wedding possible despite it happening in the middle of this PhD.

Contents

1 General Introduction 19

1.1 Asthma 19

1.1.1 Background 19

1.1.2 Airway Inflammation in Asthma 20

1.1.3 Structural Changes in the Airways in Asthma 22

1.1.4 Asthma Phenotypes 24

1.1.5 Disease Management 29

1.2 Genetics of Asthma 32

1.2.1 Gene-environment Interactions 32

1.2.2 Linkage Analysis and Genome-Wide Association Studies 33

1.2.3 Epigenetics 35

1.3 The Airway Epithelium 37

1.3.1 The Airways 37

1.3.2 Airway Epithelial Cell Types 38

1.3.3 Airway Epithelial Tight Junctions 39

1.3.4 Functions of the Epithelium in Health 40

1.3.5 The Airway Epithelium in Asthma 42

1.3.6 Models of the Airway Epithelium 46

1.4 The Urokinase Plasminogen Activator Receptor 48

1.4.1 Urokinase Plasminogen Activator Receptor Structure 48

1.4.2 uPAR in Health and Disease 50

1.4.3 uPAR in Airway Disease 53

1.5 Summary 56

1.6 Aims 58

2 General Materials and Methods 60

2.1 Mammalian Cell Culture Methods 60

2.1.1 Normal Human Bronchial Epithelial Cells (Commercial) 60

2.1.2 Cell Culture of Mammalian Primary Cells 61

2.1.3 Cryopreservation of Primary HBEC 62

2.1.4 Cell Counting 62

2.2 Molecular biology methods 62

2.2.1 Total RNA Isolation 62

2.2.2 Polymerase Chain Reaction 63

2.2.3 Agarose Gel Electrophoresis 64

2.2.4 Complementary DNA Synthesis 65

2.2.5 Quantitative PCR 67

2.2.6 Transformation of Bacterial Cells 70

2.2.7 Purification of Plasmid DNA 70

2.3 Protein Methods 71

2.3.1 Enzyme-linked immunosorbent assay (ELISA) 71

2.3.2 Luminex Bead-based Multiplex Assay 73

2.3.3 Immunofluorescence 74

2.3.4 Immunofluorescence of Paraffin-Embedded Sections 75

2.3.5 Haemotoxylin and Eosin Staining 76

2.3.6 Alcian Blue Staining 76

2.3.7 Microscopy 77

2.4 Bioinformatics 77

2.4.1 RNA Integrity Analysis 77

2.4.2 RNA Sequencing 79

2.4.3 Processing Sequencing Data 81

2.4.4 Alignment of Reads Using TopHat2 87

2.4.5 Differential Gene Expression Analysis 88

2.4.6 Gene Set Enrichment Analysis 90

2.5 Statistical Analyses 93

2.5.1 Analyses of Variance 93

2.5.2 Linear regression 94

2.5.3 Correlation Analysis 94

3 The Urokinase Pathway as a Regulator of Airway Epithelial Barrier Properties 96

3.1 Introduction 96

3.2 Aims 101

3.2.1 Specific Aims 101

3.3 Methods 102

3.3.1 Air Liquid Interface Culture of Human Bronchial Epithelial Cells 102

3.3.2 Measuring Transepithelial Electrical Resistance 103

3.3.3 Stimulation of ALI Cultures 104

3.3.4 Preparation of Transwell Inserts for Histology of Transwells 106

3.3.5 Antibody Blocking of uPAR Epitopes 106

3.3.6 Electric Cell-substrate Impedance Sensing 106

3.4 Results 109

3.4.1 Bronchial Epithelial Cells Express Epithelial Lineage Markers CK14 and E-Cadherin 109

3.4.2 Bronchial Epithelial Cells Cultured at ALI Develop a Characteristic TEER Profile Indicative of Barrier Formation. 110

3.4.3 uPAR Localizes at the Apical and Basal Membrane of Differentiated Bronchial Epithelial Cells 111

3.4.4 Expression of the uPAR-uPA Pathway during Bronchial Epithelial Cell Differentiation 113

3.4.5 scuPAR, uPA and MMP-9 Expression are Negatively Correlated with Epithelial Barrier Function 114

3.4.6 Treatment with Recombinant uPA and uPAR does not alter TEER of Differentiated Bronchial Epithelial Cells 118

3.4.7 Effects of Elevated uPAR on Cytokine Expression in Differentiated HBEC .. 119

3.4.8 Investigating the Effects of Blocking uPAR on Barrier Formation in HBEC Using Electric Cell Substrate Impedance Sensing 121

3.4.9 scuPAR Expression Correlates with Barrier Properties of Undifferentiated Epithelial Cells 125

3.5 Discussion 128

4 uPAR Expression in Bronchial Epithelial Cells Cultured from Asthma Patients and Healthy Controls 134

4.1 Introduction 134

4.2 Aims 137

4.2.1 Specific aims 137

4.3 Methods 138

4.3.1 Patient Recruitment 138

4.3.2 Isolation of Bronchial Epithelial Cells from Bronchoscopy 139

4.3.3 Cell Culture and RNA Isolation 141

4.3.4 RNA Sequencing 141

4.3.5 Measuring Plasmin Activity in HBEC Supernatants 141

4.4 Results 142

4.4.1 Subject Demographics 142

4.4.2 Morphology and Characterisation of Primary Brush HBEC 143

4.5 Whole Transcriptome Analysis of Primary Cultured HBEC from Asthma and Control Subjects 145

4.5.1 RNA Quality Control Analysis 145

4.5.2 Trimming, Quality Control and Alignment of Sequencing Data 147

4.5.3 Differential Gene Expression Analysis 151

4.5.4 Pathway Analysis Using Gene Set Enrichment Analysis 153

4.5.5 Expression of the uPAR Pathway Genes in Asthma Subjects compared to Healthy Control Subjects 156

4.5.6 Analysis of PLAUR Expression in the Epithelium in Asthma using Gene Expression Omnibus 158

4.6 Expression and Activity of the uPA-uPAR Pathway in the Bronchial Epithelium in Asthma 160

4.6.1 qPCR Analysis of PLAUR Expression in Primary Cultured HBEC from Asthma and Control Subjects 160

4.6.2 Protein Expression of uPAR Pathway Components in the Bronchial Epithelium in Asthma 164

4.7 Discussion 168

5 Whole Transcriptome Analysis of Human Bronchial Epithelial Cells Engineered to Overexpress uPAR Variants 176

5.1 Introduction 176

5.2 Aims 178

5.2.1 Specific aims 178

5.3 Methods 179

5.3.1 Transfecting Human Bronchial Epithelial Cells 179

5.3.2 RNA Sequencing 180

5.3.3 Principle Component Analysis 180

5.3.4 Rank Product Analysis 181

5.3.5 Splice Variant Analysis 183

5.4 Results 185
5.4.1 RNA Integrity Number Analysis 185
5.4.2 Sequencing Data Quality Control Analysis 186
5.4.3 Principle Component Analysis 189
5.4.4 Multiple PLAUR Splice Variants are Expressed in the Bronchial Epithelium 193
5.4.5 Differential Gene Expression Analysis Using the Cuffdiff Tool 194
5.4.6 Differential Gene Expression Analysis using Rank Product Analysis 200
5.4.7 Identification of Cellular Pathways Regulated by uPAR using Gene Set Enrichment Analysis 202
5.4.8 Validation of RNA-Sequencing Using Real-Time PCR 205
5.5 Discussion 210
6 Genetic association study of asthma related phenotypes at chromosome 19q13 (PLAUR) 216
6.1 Introduction 216
6.2 Aims 220
6.2.1 Specific Aims 220
6.3 Methods 221
6.3.1 Study Population and Patient Recruitment 221
6.3.2 Isolation of DNA, Genotyping and Quality Control of Sample Data 222
6.3.3 Clinical Measures for Asthma Traits 223
6.3.4 Association Testing 224
6.3.5 Power Calculations 225

6.4 Results 226

6.4.1 Subject Demographics 226

6.4.2 Quality Control of Sample Data 226

6.4.3 Association of PLAUR Polymorphisms with FEV_1, FEV_1/FVC, Blood Eosinophils, Serum IgE and Atopy 232

6.4.4 Association with Previously Reported Loci 239

6.5 Discussion 243

7 General Discussion 249

7.1 Hypothesis and Aims 249

7.2 Main Findings 251

7.3 Limitations of the Study 256

7.4 Future Directions 259

7.5 Final Conclusion 260

8 Appendices 262

8.1 Appendix 1: Materials and Reagents 262

8.2 Appendix 2: Individual TEER profiles for HBEC donors 265

8.3 Appendix 3: Assay detection ranges of analytes measured using Luminex 266

8.3.1 Chemokine and Cytokine Assay Ranges 266

8.3.2 scuPAR, PAI-1 and uPA Luminex Assay Ranges 266

9 References 267

Abbreviations

ADAM33	Disintegrin and metalloproteinase domain-containing protein 33
AHR	Airway hyperresponsiveness
AJ	Adherens Junctions
ALI	Air liquid interface
AMPA	Aminophenylmercuric acetate
APC	Antigen presenting cell
ASM	Airway smooth muscle
ATS	American Thoracic Society
AUC	Area under the curve
BEBM	Bronchial epithelial basal medium
BEDM	Bronchial epithelial differentiation medium
BEGM	Bronchial epithelial growth medium
BHR	Bronchial hyperresponsiveness
BTS	British Thoracic Society
CF	Cystic fibrosis
CK-14	Anti cytokeratin-14 antibody
CLCAI	Chloride Channel Accessory 1
COPD	Chronic obstructive pulmonary disease
CS	Corticosteroids
DAPI	4',6-diamidino-2-phenylindole
DC	Dendritic cell
DE	Differentially expressed
DMC	Differentially methylated CpG site
DMEM	Dulbecco's Modified Eagle's Medium
DMSO	Dimethyl sulphoxide
ECIS	Electric Cell-substrate Impedance Sensing
ECM	Extracellular matrix
EDTA	Ethylenediaminetetraacetic acid
EGFR	Epidermal growth factor receptor
ELISA	Enzyme-linked immunosorbent assay
EMT	Epithelial-mesenchymal transition
EMTU	Epithelial-mesenchymal trophic unit
eQTLs	Expression quantitative trait loci
ES	Enrichment score
FDR	False discovery rate
FeNO	Fractional exhaled nitric oxide
FEV_1	Forced expiratory volume in 1 second
FITC	Fluorescein isothiocyanate
FPKM	Fragments Per Kilobase of transcript per Million mapped reads
FVC	Forced vital capacity
GASP	Genetics of Asthma Severity and Phenotypes

GINA	Global Initiative for Asthma
GM-CSF	Granulocyte macrophage colony stimulating factor
GPI	Glycosylphosphatidylinositol
GSEA	Gene set enrichment analysis
GWAS	Genome-wide association studies
H&E	Hematoxylin and eosin
HBEC	Human bronchial epithelial cell
HDM	House dust mite
ICS	Inhaled corticosteroids
IL	Interleukin
ILC2	Type 2 innate lymphoid cells
JAM	Junction adhesion molecule
kDa	KiloDalton
LPS	Lipopolysaccharide
MAF	Minor allele freuency
MMP	Matrix metalloproteinase
MUC5AC	Mucin 5AC glycoprotein
NES	Normalised enrichment score
NO	Nitric oxide
OD	Optical density
PAI-1	Serpin family Emember 1
PAI-2	Serpin family B member 2
PAS	Plasminogen activator system
PBS	Phosphate buffered saline
PCR	Polymerase chain reaction
PE	Paired end
PEF	Peak expiratory flow
PLAUR	Urokinase plasminogen activator receptor
POSTN	Periostin
RBI	Right bronchus intermedius
RFU	Relative fluorescent units
RIN	RNA integrity analysis
RUL	Right upper lobe
SERPINB2	Serpin family B member 2
SNP	Single nucleotide polymorphism
TEER	Transepithelial electrical resistance
TGF	Transforming growth factor
Th2	T helper 2
TIMP	Tissue inhibitor of metalloproteinase
TJP	Tight junction protein
TLR	Toll-like receptor
TNF	Tumour necrosis factor
TRITC	Tetramethylrhodamine
TROL	Troleandomycin
TSLP	Thymic stromal lymphopoietin

uPA	Urokinase
uPAR	Urokinase plasminogen activator receptor
VEGF	Vascular endothelial growth factor
WHO	World Health Organisation
ZO-1	Zonula occludens -1 (tight junction protein-1)

Chapter 1: General Introduction

1 General Introduction

The airway epithelium is structurally and functionally altered in asthma and damage to the epithelium is recognised as a contributing factor to airway remodelling. Improved understanding of the mechanisms underlying epithelial dysfunction may lead to the identification of therapeutic targets. The urokinase plasminogen activator receptor (uPAR) is a regulator of bronchial epithelial cell function and expression is elevated in asthma at the gene and protein level. uPAR is expressed in multiple forms which have been shown to have distinct roles in airway epithelial cells. This thesis further investigates the role of uPAR isoforms in regulating the bronchial epithelium in the airways in asthma.

1.1 Asthma

1.1.1 Background

Asthma is heterogeneous disease characterised by chronic airway inflammation (Marcello and Carlo, 2016) affecting an estimated 300 million people worldwide, symptoms include intermittent attacks of breathlessness, wheezing and cough (World Health Organisation, 2016 figures). Disease onset is more common during childhood, which is often associated with allergic disorders, disease may also persist or present in adulthood. The underlying causes of asthma are not fully understood, risk factors include both genetic predisposition and environmental exposure to allergens, pollutants and chemical irritants (Locksley, 2010).

Asthma is an inflammatory disorder of the conducting airways involving distinct inflammatory processes driven by CD4 T helper 2 (Th2) cells and Th2-associated cytokines,

eosinophils and neutrophils (Robinson *et al*., 1992, Wang and Wills-Karp, 2011). The immune response to environmental allergens is thought to drive persistent inflammation in the airways resulting in compensatory structural changes (Al-Muhsen *et al*., 2011). Structural changes in the epithelium include goblet cell metaplasia, smooth muscle hypertrophy and enhanced extracellular matrix (ECM) deposition, collectively referred to as 'airway remodelling' (Locksley, 2010). The reversible airway obstruction and airway hyper-responsiveness (AHR) observed in asthma may in part be a result of airway remodelling processes. Despite advances in our understanding of the pathogenesis of asthma, the underlying cell biology and the contribution of environmental and genetic factors requires further study. Improved characterisation of patients and a stratified, individualised approach to asthma care, as is being seen with severe asthma, is needed to improve disease management in wider asthma populations (Thomas, 2015).

1.1.2 Airway Inflammation in Asthma

Acute inflammation is a rapidly initiated host response to tissue injury, such as damage to the airway epithelium, and is resolved within hours or days of the insult (Dinarello, 2010). Inflammation involves rapid recruitment of granulocytes and is coordinated by pro-inflammatory signalling specific to the nature and location of the site of injury (Lawrence *et al*., 2002). The failure to adequately resolve inflammation in asthma may contribute to structural changes in the airways (Barnig and Levy, 2015). Chronic inflammation is presented in most forms of asthma throughout the respiratory tract (Nakawah *et al*., 2013).

Allergic asthma usually begins with childhood sensitization to allergens, namely house dust mites (HDMs), pollen and moulds and the expansion of T lymphocytes. Th2 type cytokines

(Interleukin (IL)-IL-4, IL-5 and IL-13) drive allergic inflammation via promotion of Th2 cell survival, B cell IgE selection and subsequent mast cell activation and degranulation as shown in Figure 1.1.1. The inflammatory cascade promotes eosinophil maturation and survival and recruitment of inflammatory cells including basophils, mast cells, macrophages and B and T lymphocytes and results in release of pro-inflammatory mediators by airway structural cells (Spahn *et al*., 2002). Dendritic cells (DC) are professional antigen presenting cells (APC) thought to be located close to the basolateral surface of the airway epithelium. On uptake of foreign antigens DC migrate towards draining lymph nodes of the lung where they interact with naive T cells, bridging innate and adaptive immunity (Grayson, 2006).

Other type 2 cytokine producing cells include CD34+ haematopoietic stem cells, eosinophils, basophils, mast cells and type 2 innate lymphoid cells (ILC2). ILC2s are distinct in their role in allergic inflammation in that they do not express T cell antigen receptors (response is not antigen-dependent/ adaptive) and respond to inflammatory signals (Kabata *et al*., 2016). Like eosinophils and mast cells (innate immune response) ILC2s rapidly release type 2 cytokines. Epithelial derived IL-33, IL-25 and thymic stromal lymphopoietin (TSLP) contribute to type 2 inflammation involving Th2 cells, DCs, ILC2s, mast cells and eosinophils (Borish, 2016). Whether the type of inflammation represents a distinct subtype of asthma or differences in response to current medications is not clear (Locksley, 2010).

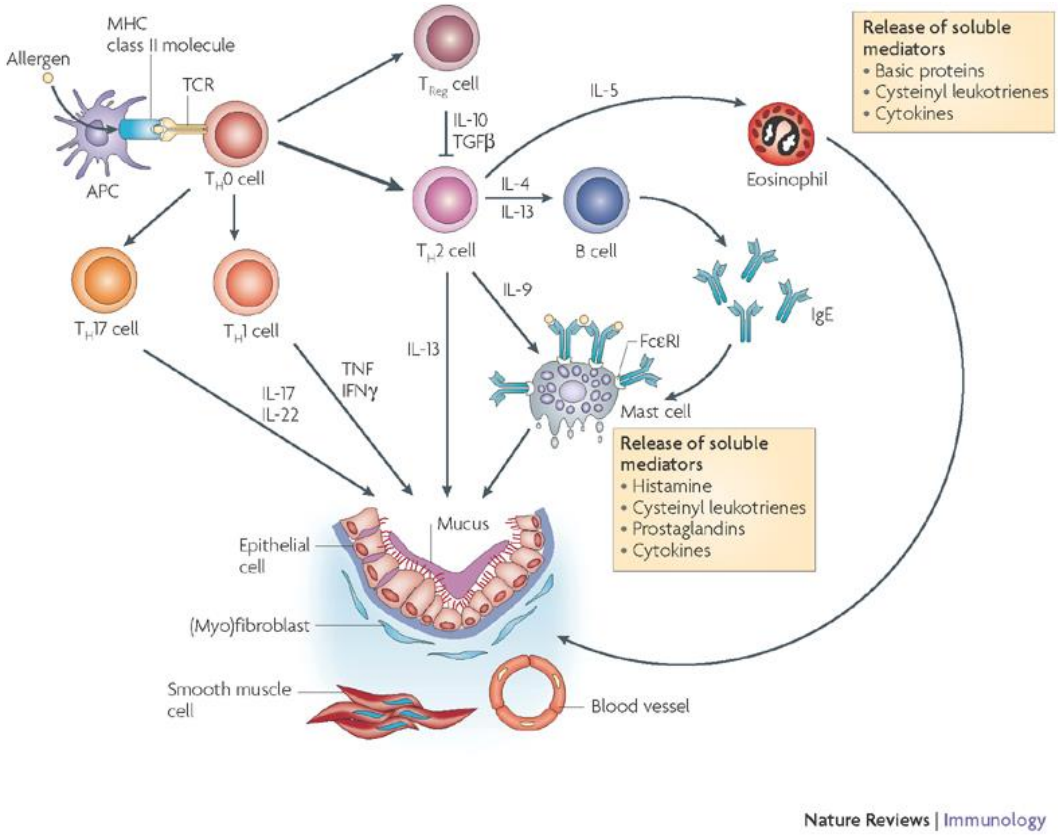


Figure 1.1.1: The Allergic Inflammatory Response. Uptake of allergens by antigen presenting cells and subsequent presentation to naïve T cells drives T cell differentiation. Th2 signalling promotes eosinophil activation, B cell IgE selection and mast cell degranulation. Soluble mediators promote airway remodelling via signalling to airway epithelial cells, airway smooth cells, fibroblasts and endothelial cells (Holgate and Polosa, 2008).

1.1.3 Structural Changes in the Airways in Asthma

The structural changes that occur throughout the airways in asthma and other obstructive lung diseases are termed airway remodelling (Bergeron *et al*., 2010). Remodelling processes refer to the modification of tissue structure and composition caused by mechanical or physiological forms of stress (Al-Muhsen *et al*., 2011). Structural changes characteristic of asthma include goblet cell hyperplasia, thickening of the basement membrane, increased airway smooth muscle (ASM) mass, subepithelial fibrosis and angiogenesis (Durrani *et al*., 2011, Bergeron *et al*., 2010). These changes result in narrowing of the airways, bronchial

hyper-responsiveness (BHR), mucus hyper-secretion and increased blood flow and are associated with poor clinical outcome (Hirota and Martin, 2013).

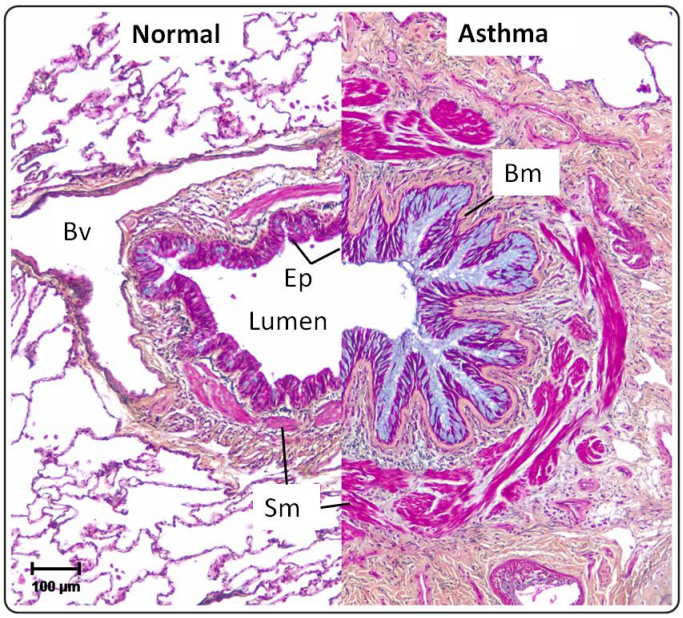


Figure 1.1.2: Structural Remodelling of the Airways in Asthma. Histology of airways from a normal and severe asthmatic shows mucous hyperplasia and hypersecretion (blue) in the epithelium (Ep). The airways in asthma also undergo thickening of the basement membrane (Bm) and smooth muscle (Sm) hyperplasia (Wadsworth *et al*., 2012).

Remodelling processes are complex and involve multiple cell types and complex cell signalling processes. The primary cause of airway obstruction is thought to be due to ASM hyperplasia and hypertrophy. Both HBEC (human bronchial epithelial cells) and ASMs communicate with inflammatory cells via a range of mediators and receptors. The complex interplay between these structural and immune cells may be pivotal in driving remodelling processes in the airways in respiratory diseases (Al-Muhsen *et al*., 2011). Airway inflammation may be required for the initiation of remodelling processes, however the relationship between structural changes in asthma and inflammation is a matter of debate. Airway remodelling has been reported in children in the absence of inflammation therefore raises questions around the classical paradigm that chronic type 2 driven inflammation

underlies defective repair and remodelling (Grainge *et al*., 2011, Berair *et al*., 2013). Treatments targeting the underlying etiology of airway remodelling may improve patient symptoms (Bergeron *et al*., 2010). Proteins associated with airway remodelling include the protease uPAR which is expressed by airway structural cells and immune cells (Ierodiakonou *et al*., 2016b). Transforming growth factor beta (TGF-β), matrix metalloproteinas-9 (MMP-9) and epidermal growth factor receptor (EGFR) have also been shown to induce structural changes in the airways including subepithelial fibrosis and goblet cell hyperplasia, these molecules are potential therapeutic targets for the treatment of asthma (Shifren *et al*., 2012).

1.1.4 Asthma Phenotypes

The advent of corticosteroids (CS), identification of Th2 mediated inflammation and the development of anti-IgE therapies for allergic asthma have highlighted that asthma is not a singular disease and instead encompasses multiple subtypes (Gauthier *et al*., 2015, Wenzel, 2012). Considerable efforts have been made to define these phenotypes in order to manage and treat the disease. Asthma is described phenotypically as an *obstructive lung disease with complete reversibility after the addition of bronchodilators or corticosteroids* (Bostantzoglou *et al*., 2015). The pathologic definition is that *asthma is a disease of eosinophilic bronchitis comprised by robust type 2 cytokine response (IL-4, IL-5 and IL-13) that develops in an allergic setting* (Borish, 2016). However, the presentation of asthma may not fit into the above definitions. For example, airway obstruction may be irreversible and progressive, inflammation may be noneosinophillic and type 2 cytokines and allergies may not be present (Gauthier *et al*., 2015). Several approaches have been used to define and group asthma.

Clinical and Inflammatory phenotypes of asthma

The concept of asthma was historically defined as 'Extrinsic' *vs* 'Intrinsic' disease. Extrinsic asthma was thought to involve allergens and environmental stimuli affecting atopy and was associated with childhood onset. Intrinsic asthma was defined by the individual's biology, was not affected by season or atopy and was associated with adult disease onset (Rackemann, 1947). An adult-onset eosinophilic phenotype was later described (Rackemann, 1950), and by the 2000s with the advancements in the endobronchial biopsy technique a study looking at severe asthma found that atopy and allergic symptoms were associated with early-onset (<12 years) and that individuals with late-onset disease had increased tissue eosinophils and reduced lung function over the duration of disease (Miranda *et al*., 2004). The study also identified a small group of asthma patients with characteristics suggestive of an alternative disease pathway, patients had late-onset disease, lacked increased eosinophils and showed evidence of subepithelial basement membrane thickening. Phenotyping approaches included investigating responses to CS therapy, studies identified that sputum eosinophil counts predicted response to therapy in milder disease (Green *et al*., 2002). However, a separate study of 34 severe asthma patients found that half of the patients who were CS refractory had elevated tissue eosinophils and that half had no or low eosinophil counts. This and similar studies highlighted that some asthma patients show poor response to CS and consequently had severe and poorly controlled disease and emphasised the need to link molecular processes to clinical phenotype (Wenzel *et al*., 1999).

Recent clustering analyses set out to identify clinical phenotypes from well characterised asthma cohorts, the SARP (Severe Asthma Research Program) study identified 5 clinical phenotypes using 34 compressed variables of which age of onset and lung function were the main contributors. This study identified 3 early onset, atopic phenotypes that differed in

baseline lung function and response to medication, and 2 late onset severe phenotypes that were predominantly female (Moore *et al*., 2010).

Eosinophillic vs Noneosinophillic asthma

Distinct asthma phenotypes are described based on their eosinophilic and noneosinophillic presentations. Noneosinophillic asthma can be divided into neutrophilic and paucigranulocytic (normal levels of eosinophils and neutrophils) and is characterised by increased prevalence of airway neutrophils, asthma presentation is often severe and disease is managed using high dose inhaled corticosteroids (ICS) (Douwes *et al*., 2002). ICS inhibit neutrophil apoptosis and may increase numbers in the airway therefore defining this phenotype pathologically is challenging (Borish, 2016). Th17 may play a role in noneosinophillic asthma, a strong association has been found between polymononuclear (PMN) cells (eosinophils, neutrophils and basophils) and IL-17 and also between IL-17 and disease severity (steroid resistant) (Nanzer *et al*., 2013) however the mechanism underlying IL-17 release in asthma is unknown. Eosinophilic asthma phenotypes include childhood-onset allergic asthma and late-onset nonallergic asthma (Pelaia *et al*., 2015). A related phenotype is idiopathic eosinophilic asthma which is characterised by increased eosinophils without specific allergen IgE sensitization. Idiopathic eosinophilic asthma is often a more severe phenotype that presents in adulthood and is associated with aspirin sensitivity (Lötvall *et al*., 2011).

Type 2 high *vs* type 2 low asthma

Molecular phenotypes have been identified by grouping asthma patients based on their response to certain medications (Gauthier *et al*., 2015). Type 2 high asthma is characterised by an inflammatory state driven by Th2 pathway cytokines IL-4, IL-5 and IL-13. These

cytokines are also produced by basophils, mast cells and eosinophils (Tindemans *et al*., 2014) in addition to Th2 CD4 T cells therefore are termed 'type 2' cytokines. The type 2 'signature' was identified by Woodruff *et al*, gene expression profiling of epithelial brush samples (42 asthma *vs* 28 healthy controls) identified 3 differentially expressed genes; *CLCA1* (chloride channel accessory 1), *SERPINB2* (serpin family B member 2), and *POSTN* (periostin). Clustering analysis based on this signature identified 50% of asthma patients as 'type 2 high' which was associated with eosinophilia, AHR, elevated IgE, IL-5 and IL-13, basement membrane thickening and improved FEV_1 in response to ICS. 'Type 2 low' individuals were clustered with healthy, non-atopic controls and did not show improved FEV_1 with ICS (Woodruff *et al*., 2007). The type 2 phenotype however is not yet fully understood, additional sub-phenotypes have been identified within type 2 high asthma e.g. early onset allergic and exercise-induced asthma. Further investigation of these subgroups is needed to identify the complex pathways underlying disease pathobiology (Gauthier *et al*., 2015).

Non-type 2 driven or type 2 low asthma represents almost 50% of the asthma patients studied, who have no evidence for elevated type 2 cytokines and pathways underlying inflammation are less clear (Woodruff *et al*., 2009). Neutrophillic asthma may play a role in non-type 2 asthma however this may differ with the presence or absence of eosinophils (Gauthier *et al*., 2015). Mouse models have suggested IL-17 may play a role in neutrophilic inflammation (McKinley *et al*., 2008) however studies in moderate-severe human studies show poor efficacy (Busse *et al*., 2013). It also remains unclear whether elevated neutrophils underlie disease pathology or are a secondary effect of CS treatment (Gauthier *et al*., 2015). Obesity related asthma shares features with type 2 low asthma however this phenotype is a difficult area of study as obesity is suggested to play a causal role in later onset disease and may be a comorbidity with earlier age onset (Holguin *et al*., 2011). A study comparing

outcome of bariatric surgery in Th1 and Th2 asthma patients found Th1 patients had a reduction in BHR after surgery, whereas Th2 patients did not improve and were less responsive to CS (Wenzel, 2012). Smoking related asthma is also associated with type 1 inflammation, neutrophilia and often shows poor response to therapy (Polosa and Thomson, 2013).

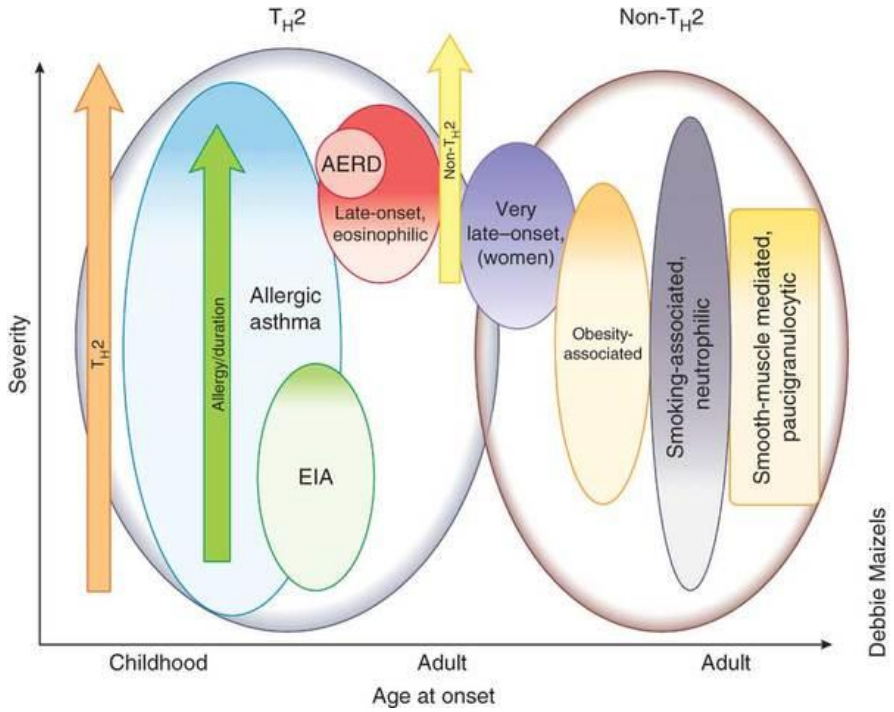


Figure 1.1.3: Emerging Asthma Phenotypes Based on Th2 and non-Th2 Asthma. Th2 asthma varies in disease severity and onset and presents in childhood and adulthood. Early onset allergic asthma and exercise induced asthma (EIA) as generally mild, early onset disease can develop into severe asthma depending on underlying immune responses. Individuals with non-Th2 asthma show less inflammation and phenotypes include very late-onset asthma, obesity-associated asthma, smoking-related and neutrophilic asthma (Wenzel, 2012).

Asthma can be defined as different endotypes, *categorical diagnostic entity based on a distinct pathogenic pathway* (Borish, 2016). A number of studies have proposed asthma endotypes using clustering analyses and argue that clustering allows predictions to be made from the data and that patterns in the data may reflect disease aetiology, including the

genetic basis of the disease and underlying pathways (Lötvall *et al*., 2011). However, there is no universal agreement on pathophysiological mechanisms and biomarkers. Further refinement of the Th2/ type 2 phenotype could improve treatment outcome in subsets of corticosteroid-refractory patients and also in patients who lack underlying type 2 processes (Ray *et al*., 2015).

1.1.5 Disease Management

1.1.5.1 Stepwise Management of Asthma

The aim of asthma management is to control disease (BTS/SIGN, 2016). Asthma control refers to *the extent to which the manifestations of asthma have been reduced or removed by treatment* (Taylor *et al*., 2008). Asthma treatment is based on a step-wise approach where treatment is started at the step most appropriate to the degree of asthma severity and increased or decreased as necessary to achieve and maintain adequate control (BTS/SIGN, 2016), this is summarised in Figure 1.1.4. Most asthma is adequately managed using inhaled and/or oral corticosteroids (CS/ ICS), short and long acting β2-adrenoreceptor agonists (SABA/ LABA) and leukotriene receptor antagonists, however in 5-10% of asthma patients, symptoms persist (Chung, 2015). Effectiveness in part is due to induction of eosinophil apoptosis, it also known that ICS inhibit neutrophil apoptosis (Borish, 2016). This highlights the issue of administering ICS to asthma patients, subsets of the asthma population do not benefit from ICS and treatment may be detrimental to patients with neutrophilic asthma (Green *et al*., 2007).

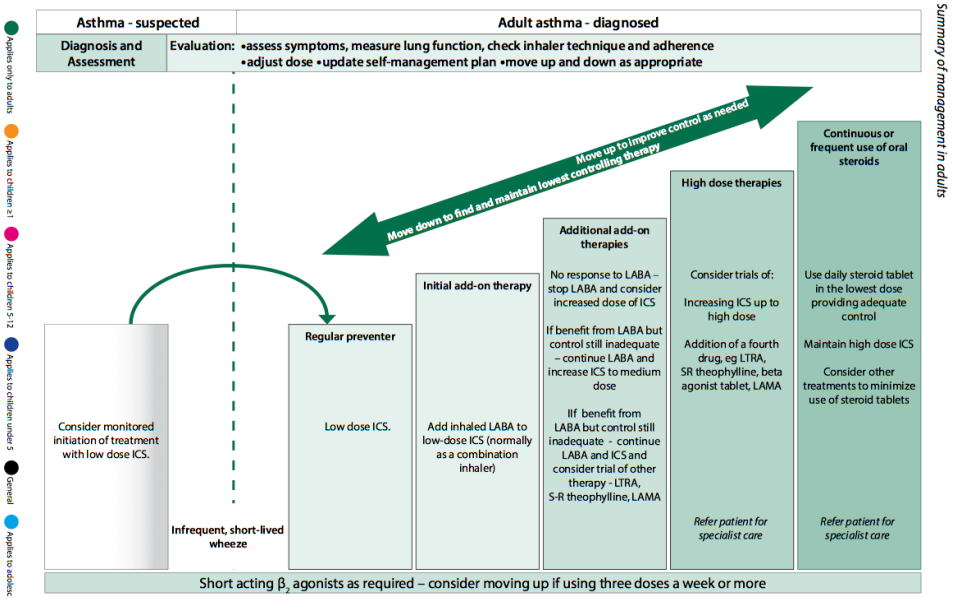


Figure 1.1.4: Stepwise Management of Asthma in Adults. British Thoracic Society (BTS)/ Scottish Intercollegiate Guidelines Network (SIGN) treatment steps described in asthma where BTS steps 1-5 describe severity and treatment options at each step. As asthma severity increases the amount and type of medication changes. Similarly, as symptom severity decreases treatment step-down takes place in order to manage asthma using the least amount of therapy possible. Image taken from (BTS/SIGN, 2016).

1.1.5.2 The Development of Biologics in Asthma

The remaining 5-10% of asthma patients suffer a more severe phenotype and are often refractory to current treatment options (Wenzel, 2012). Long term ICS treatment can have severe side effects, the development of monoclonal antibodies targeting specific inflammatory responses, termed biologic treatments, offer an alternative to conventional asthma therapy (Mitchell *et al*., 2016). Omalizumab is an anti-IgE monoclonal antibody used for the treatment of severe allergic asthma (Lin and Cheng, 2016, Trivedi *et al*., 2016). IL-4 and IL-13 promote IgE switching, antagonists have been developed for glucocorticoid refractory asthma and allergen exacerbated asthma, anti-IL-4 and IL-13 antibodies have shown prevention of asthma exacerbations however airway inflammation and AHR persist (similar to anti IgE therapies) (Borish, 2016, Walsh, 2017). Anti-IL-5 has been studied for the treatment of severe asthma eosinophilic asthma, asthma patients with elevated eosinophil

counts have demonstrated improvement of lung function when treated with anti-IL-5 (Maselli *et al*., 2016). Antibodies blocking IL-17 and IL-25 receptor binding have been used in the context of noneosinophillic asthma however have not been shown to improve asthma control or lung function (Busse *et al*., 2013).

Presentation	Phenotype	Therapeutic intervention
Noneosinophilic	Paucigranulocytic/ Neutrophilic	IL-17 antagonists Macrolide antibiotics methotrexate, phosphodiesterase IV inhibitors
Eosinophilic	Allergen exacerbated	Allergen avoidance immunotherapy, anti-IgE, IL-4 antagonists, IL-13 antagonists, IL-4/IL-13 dual antagonists
	Idiopathic eosinophilic	Corticosteroids IL-5/IL-5 receptor antagonists
	Aspirin-exacerbated respiratory disease	Leukotriene modifiers Aspirin desensitization

Figure 1.1.5: Summary of Therapeutic Intervention of Asthma Based on Phenotype (adapted from Borish 2016).

1.1.5.3 Alternative Treatments

Other less common treatments or procedures for uncontrolled and severe asthma include bronchial thermoplasty, which aims to reduce ASM mass and treat smooth muscle hypertrophy (Trivedi *et al*., 2016). Strategies for allergen avoidance in allergic asthma have been shown to improve symptoms and highlight sensitization to certain allergens that are a risk factor for asthma (Baxi and Phipatanakul, 2010). Macrolides, methotrexate and phosphodiesterase IV inhibitors have also been administered to patients with glucocorticoid refractory asthma (Corrigan, 2002).

1.2 Genetics of Asthma

Asthma is a complex genetic disease involving both gene-gene and gene-environment interactions, environmental triggers include virus, lung microbiota, allergens and pollutants (Ober and Vercelli, 2011). Genetic studies, mainly genome-wide association studies, have made considerable progress in identifying asthma susceptibility loci and improving our understanding of asthma pharmacogenetics.

1.2.1 Gene-environment Interactions

Both genetics and environment play a role in asthma aetiology (Bønnelykke and Ober, 2016) and the complex interaction of genetic and environmental factors differs according to phenotype (Kauffmann and Demenais, 2012). Identifying the genes and genetic variation underlying asthma is challenging as multiple genes are associated with asthma, each contributing a small amount to the overall risk (Halapi and Bjornsdottir, 2009). Epidemiological studies have highlighted environmental exposures associated with asthma risk, children who live on farms in Europe are at a significantly lower risk of developing asthma and allergic disease (von Mutius and Vercelli, 2010). Maternal asthma increases the risk of childhood-onset asthma to a greater extent than paternal asthma (Lim *et al*., 2010) suggesting maternal effect may not be solely due to inheritance. Maternal diet, smoking and viral respiratory tract infections are associated with increased asthma risk (Ober and Vercelli, 2011). Twin and family studies provide evidence that genetic variation is an important factor in asthma risk (Ober and Vercelli, 2011). Twin studies suggest that 50-60% of asthma is heritable (Skadhauge *et al*., 1999; Polderman *et al*., 2015), estimates are higher in early-onset

compared with later-onset asthma (Thomsen *et al*., 2010) and also in boys compared to girls (Polderman *et al*., 2015).

1.2.2 Linkage Analysis and Genome-Wide Association Studies

Advances made in the genetics of airway disease through genome-wide association studies (GWAS) and genome-wide linkage approaches have led to the identification of asthma risk loci (Thomsen, 2015). Linkage analysis commonly uses short tandem repeat markers to follow the transmission of genetic information spanning the entire genome across generations (Bush, 2012). GWAS examine SNPs (single nucleotide polymorphisms) spanning the genome in thousands of individuals to identify disease associated alleles. GWAS are a hypothesis-free approach that rely on information regarding linkage disequilibrium from the HapMap project, variants at a given locus can be used to predict the genetic variance at adjoining loci (Bush, 2012).

ADAM33 is expressed in the airway epithelium and was the first gene identified through linkage analysis, with SNPs affecting baseline lung function (Ober and Vercelli, 2011). Other asthma susceptibility genes expressed in the epithelium include *PCDH1*, *DPP10*, *GPRA*, *SPINK5* and *IRAKM* are associated with airway remodelling, BHR, cell homeostasis and inflammation (Moheimani *et al*., 2016).

GWAS have identified 15-20 asthma loci including genes which regulate immune and allergic responses (*HLA*, *IL13*, *TSLP*, *IL33* and *ST2*) and highlight the role of innate immune responses in activating the Th2 pathway. Novel loci have also been identified (*CDHR3*, *ORMDL3*,

GSDMB), variation at the 17q21 asthma locus, encoding the *ORMDL3* and *GSDML* genes, may be associated with risk for childhood onset asthma (Moffatt *et al*., 2010).

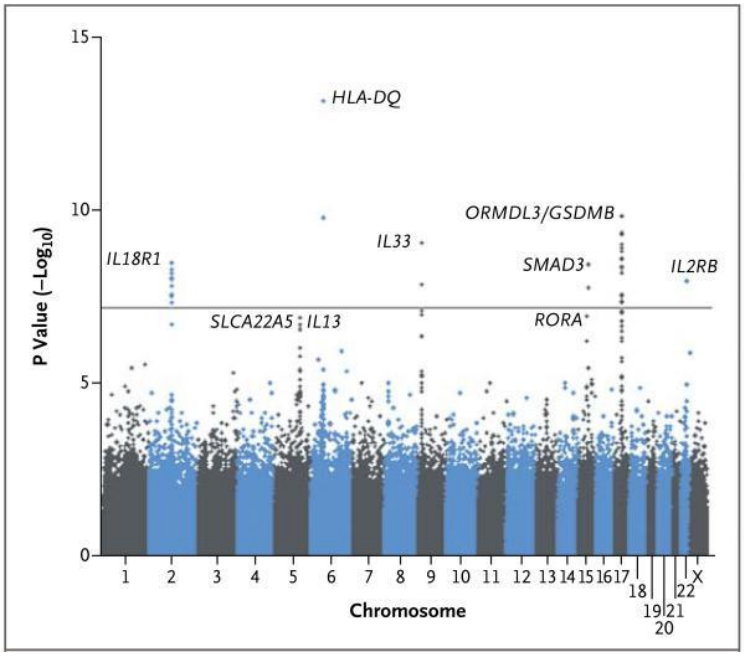


Figure 1.2.1: Manhattan Plot Showing Results of Genome Wide Association Testing of Asthma. Association with the *ORMDL3/GSDMB* locus on chromosome 17q21 was specific to childhood-onset disease. Single nucleotide polymorphisms in *IL1RL1/IL18R1, HLA-DQ, SMAD3, IL33,* IL2RB met genome wide significance (Moffatt *et al*., 2010)

The translation of these findings to disease have had limited success as the contributions of variants to asthma risk is small, this may be due to the heterogeneity in large populations which are required for GWAS (Bønnelykke and Ober, 2016). An integrated approach combining GWAS in asthma subtypes, cell models and gene-environment interaction studies may provide biological insight into the role of genetic variation asthma.

1.2.3 Epigenetics

Epigenetic changes are *heritable changes in gene activity that are independent of alterations in the underlying DNA sequence* and can explain alterations in gene expression due to the environment that might drive a disease phenotype (Jirtle and Skinner, 2007). DNA methylation is the most extensively studied epigenetic mechanism. CpG sites are DNA regions where a cytosine nucleotide (C) is located next to a guanine nucleotide (G), these CG dinucleotides may be clustered in 'CpG islands'. DNA methyl transferases add a methyl group to the cytosine residues, methylation patterns are conserved during cell division and are associated with gene silencing and regulating genes that determine cell type and function (Liang *et al*., 2015). Histone modification by histone acetyl transferase (HAT), histone deactetylase (HDAC) and histone methylation have also been shown to alter gene expression (Bégin and Nadeau, 2014). Epigenetic regulation studies have provided novel insights into disease mechanism and how environmental exposures e.g. air pollution and/or allergen (Clifford *et al*., 2017) may effect gene expression in the lungs and also how DNA methylation can be used to identify molecular pathways important in asthma pathobiology (Nicodemus-Johnson *et al*., 2016a, Kuo *et al*., 2016).

A study investigating methylation levels with IgE levels in asthma families identified correlations between 36 hypomethylated sites (in 34 genes) and IgE levels. Subsequent elevated expression of these genes, some of which are known to encode eosinophil related genes (*GATA1, PRG2*), may contribute to IgE associated inflammation in asthma. The 34 genes were also identified as over active in eosinophils isolated from 24 asthma subjects with high IgE levels (Liang *et al*., 2015).

A recent study using freshly isolated HBEC from asthma and control subjects identified epigenetic signatures of distinct asthma endotypes using genome-wide, epigenetic and whole transcriptome data (Nicodemus-Johnson *et al*., 2016a). The study found that methylation quantitative loci (meQTLs) were enriched for asthma-associated SNPs and the differentially methylated CpG sites (DMCs), but not differentially expressed genes, clustered into co-expression modules (groups of genes with highly correlated expression patterns). These findings strengthen the idea that epigenetic changes in asthma may serve as a more stable marker of disease as opposed to changes in gene expression (Nicodemus-Johnson *et al*., 2016a). Well characterised asthma loci including 17q12-21 have shown alterations in methylation in asthma compared to controls (Acevedo *et al*., 2015). A novel SNP associated with *ORMDL3* methylation and expression detected in HBEC which was not identified in a similar study using blood cells, highlighting the importance of disease relevant and cell specific *omic* studies (Nicodemus-Johnson *et al*., 2016a).

A limitation of case-control studies is that one cannot propose causality as observed profiles may be a result of disease rather than a response to the environment that has predisposed to disease (Moheimani *et al*., 2016). Furthermore, changes in cells may result from prescribed medication such as ICS, investigating findings in cell models must be done to address this issue and draw better conclusions. Ultimately, an integrated approach will help our understanding of how genetic and epigenetic changes contribute to disease onset and progression (Nicodemus-Johnson *et al*., 2016a). Epigenetic studies may be able to identify robust drug targets for allergic disease as well biomarkers that can be used to predict patient response.

1.3 The Airway Epithelium

As discussed, the development and progression of asthma involves a complex interplay between gene and environment interactions. The airway epithelium serves as the initial barrier to environmental insults and GWAS and cell based studies have identified a number of epithelial genes to be associated with disease pathobiology (Moheimani *et al*., 2016). The airway epithelium is therefore an important therapeutic target for the treatment of asthma.

1.3.1 The Airways

The airways of the bronchial tree divide by dichotomous branching (Mauroy *et al*., 2004), the mammalian lung has 23 generations on average (Weibel, 1984). The conducting airways consist of generations 1- 16 and generations 17 to 19 constitute the respiratory bronchioles (Weibel, 1963). The small airways account for 98.8% of the total lung volume, small airways generally have a generation number 8> and an internal diameter <2mm (Virchow, 2009). Small airway function is difficult to assess however studies have shown that the peripheral airways play a role in more severe obstructive disease (Contoli *et al*., 2015). The large airways are defined by an internal diameter of >2mm (Bohadana *et al*., 2004). The airways are lined with a continuous epithelial layer, in the large airways the structure of epithelium is pseudostratified and changes to columnar in the small airways (Crystal *et al*., 2008). We focused to the bronchial epithelium in this thesis due its central role in regulating inflammation, barrier function and airway remodelling.

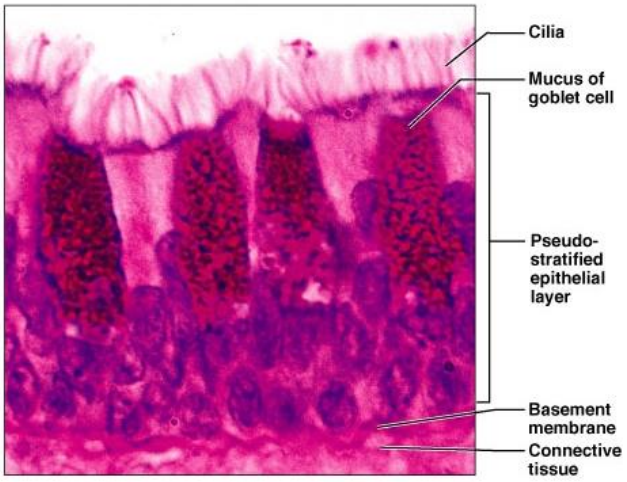


Figure 1.3.1: Pseudostratified Columnar Epithelium Lining the Human Airways. Airway epithelial cells are attached to the basement membrane and cell layer appears stratified. The airway epithelium is composed of ciliated, secretory (goblet and serous cells), basal cells and in the peripheral airways, club cells (not shown) (www.apsubiology.org).

1.3.2 Airway Epithelial Cell Types

The human airway epithelium comprises of specialised cell types that are critical in regulating airway homeostasis (Knight and Holgate, 2003). Basal cells are attached to the basement membrane and mainly serve as progenitor cells, differentiating to mucous and ciliated epithelial cells (Boers *et al*., 1998). Columnar ciliated epithelial cells account for over half of all epithelial cells and their primary role is to carry out mucociliary clearance (Spina, 1998). Mucus is secreted and produced by mucous or goblet cells, these cells are also capable of self-renewal (Evans and Plopper, 1988). Serous cells resemble mucus cells however they produce granules distinct to mucins (Rogers *et al*., 1993). Club cells are also a type of secretory cell that produce bronchiolar surfactant and anti-proteases and are mostly found in the small airways (De Water *et al*., 1986). Amines and peptides that regulate airway development and function are secreted by pulmonary neuroendocrine cells which are found in clusters throughout the bronchial tree (Reynolds *et al*., 2000).

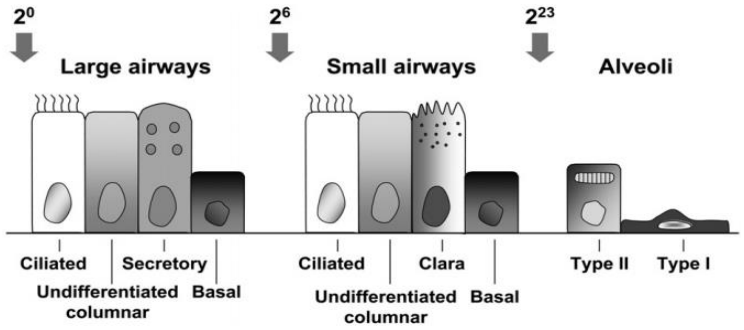
Cell type	Structural features	Primary Function
Columnar ciliated epithelial cells	Predominant cell type. Arise from basal or secretory cells and possess cilia.	Directional movement of mucus from lung to throat
Goblet cells	Characterized by membrane bound mucin granules. May differentiate to ciliated ECs	Secrete mucus to trap foreign particles
Serous cells	Resemble mucous cells. Have been observed in the small airways	Cells may contain neutral mucin.
Basal cells	Only cell firmly attached to basement membrane, numbers correlate to thickness of epithelium. Cytoplasm contains cytokeratin bundles	Provide stem cell/ progenitor cell function, giving rise to goblet and ciliated epithelial cell.
Club cells	Characterised by large granules located basally and a granular endoplasmic reticulum. Cells are non-ciliated and enriched in the small airways	Produce bronchiolar surfactant. May produce anti-proteases and serve as progenitor cell for mucous and ciliated epithelial cells
		

Table 1.3.1: Main Cell Types Present in the Airway Epithelium (Crystal *et al*., 2008).

1.3.3 Airway Epithelial Tight Junctions

Epithelial cells form a barrier comprised of apical tight junctions (TJ) and basolateral adherens junctions (AJ), junctional complexes regulate paracellular transport of ions and molecules via multiple signalling cascades (Georas and Rezaee, 2014). Claudins are the largest family of TJ proteins, 27 proteins have been identified that either promote or disrupt barrier integrity (Mineta *et al*., 2011). Junctional adhesion molecule (JAM) proteins regulate barrier properties after injury and tight junction-associated marvel protein (TAMP) family (occludin, tricellulin and MarvelD3) serve as receptors for viruses (Huber *et al*., 2000,

Excoffon *et al*., 2008). Tight junctions also include the scaffold proteins zona occludens (ZO) 1, 2 and 3, catenins (α-, β- and p120 catenin) and cingulin which bind to cytosolic proteins and the actin cytoskeleton forming the cytosolic plaque which stabilizes junctional complexes (Schneeberger and Lynch, 2004; Kojima *et al*., 2013).

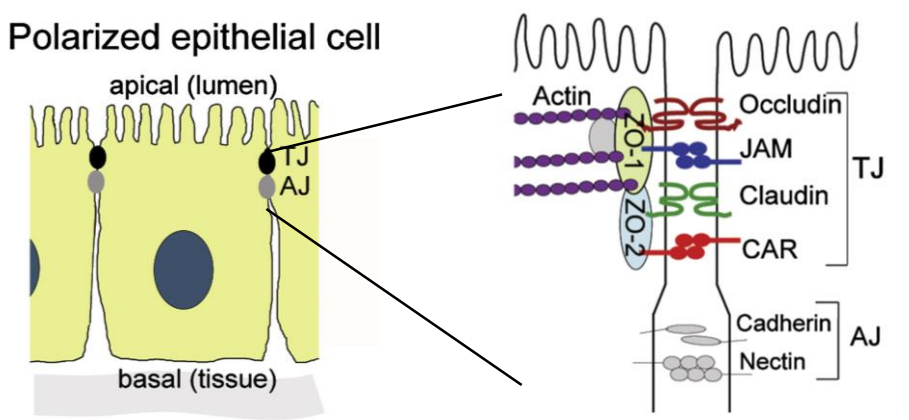


Figure 1.3.2: Structure of Airway Epithelial Tight Junctions. Airway epithelial cells are polarised, apical tight junctions (TJ) and adherens junctions (AJ) form a barrier between adjoining cells and regulate paracellular transport across the epithelium. The transmembrane proteins claudin, occludin, junction adhesion molecules (JAMs) and the coxsackievirus and adenovirus receptor (CAR) extend and form bridges in the intercellular space. Zona-occluden 1 (ZO-1) and 2 (ZO-2) serve as scaffolding proteins between transmembrane proteins and the actin cytoskeleton and intracellular signalling pathways. Adherens junctions are located below the TJ and comprise of nectin and cadherin transmembrane proteins (Bergelson, 2009).

1.3.4 Functions of the Epithelium in Health

The airway epithelium is a barrier between host and environment and regulates secretory processes and immune responses to allergens and damage (Hackett *et al*., 2011). TJs and AJs make up the epithelial barrier and together regulate paracellular solute and water flux (Knight and Holgate, 2003). The production of mucus contributes to barrier function and more crucially acts as an innate defence mechanism against microbes, which are cleared by

beating cilia in a process termed 'mucociliary clearance' (Whitsett and Alenghat, 2015). Epithelial cells also modulate airway mucosal defence and structure via the release of cytokines, chemokines, growth factors and lipid and peptide mediators (Knight and Holgate, 2003, Raeburn and Webber, 1994). A summary of the key molecules is described in Table 1.3.2.

Molecule	Function
Lipid mediators (PGE2, eicosanoids)	Associated with airway smooth muscle tone regulation, mucus secretion and inflammation (Knight and Holgate, 2003)
Nitric oxide	Cell signalling in the epithelium (Gaston *et al*., 1994)
Growth factors (EGF family, TGF-β, PDGF, GM-CSF, IGF)	Regulate epithelial migration, proliferation and repair (Takeyama *et al*., 1999) EGFR complexes with integrins e.g. αvβ5, interaction may enhance signalling (Knight and Holgate, 2003). TGF-β may be involved in epithelial wound repair (Wang *et al*., 1996)
Peptide mediators (e.g. endothelin**)**	Endothelin promotes bronchoconstriction and recruitment of inflammatory cells (Hay, 1999)
Cytokines (IL-1, IL-6, IL-10, IL-11, IL-33, TSLP TNF-α) **and Chemokines** (IL-8, Eotaxin-1-2, RANTES, MIP-1α	Recruitment, activation and regulation of inflammation in response to damage, allergens and viruses (Chung and Barnes, 1999)

Table 1.3.2: Molecules Secreted by Bronchial Epithelial Cells. In health, the airway epithelium regulates airway homeostasis by secreting a range of signalling molecules. PGE2 = Prostaglandin E2, EGF = Epidermal growth factor, TGF-β = Transforming growth factor β, PDGF = Platelet derived growth factor, GM-CSF = Granulocyte-macrophage colony-stimulating factor, IGF = Insulin-like growth factor, IL = Interleukin, TNF-α = Tumour necrosis factor, TSLP = Thymic stromal lymphopoietin, RANTES = Regulated on Activation, Normal T Cell Expressed and Secreted, MIP-1α = Macrophage Inflammatory Proteins.

The epithelium responds to pathogen-associated molecular patterns (PAMPs) and danger-associated molecular patterns (DAMPs) by signalling to the immune system to recruit and coordinate immune cells (Whitsett and Alenghat, 2015). Epithelial cells express pattern

recognition receptors (PRRs) including NOD-like receptors (NLRs) and toll-like receptors (TLRs) which respond to DAMPs and PAMPs and drive mucosal immunity as well as the clearance of pathogens and apoptotic cells (Lambrecht and Hammad, 2012). In addition to regulating host defence mechanisms, epithelial signalling is of importance for epithelial repair processes and epithelial-mesenchymal transition (EMT) during early lung development (Holgate *et al*., 2000).

1.3.5 The Airway Epithelium in Asthma

The epithelium is altered structurally and functionally in asthma (Ierodiakonou *et al*., 2011). Alterations of the epithelium include epithelial shedding, goblet cell hyperplasia, loss of ciliated cells and reduced formation of epithelial tight junctions (Al-Muhsen *et al*., 2011, Knight and Holgate, 2003). How altered signalling and repair processes contribute to airway remodelling and asthma progression is not fully understood (Roth *et al*., 2012). Airway structural changes are also a hallmark feature of chronic obstructive pulmonary disease (COPD), changes result in obstructed airflow which is mostly reversible in asthma and not fully reversible in COPD and there are differences in inflammatory and remodelling processes (Aoshiba and Nagai, 2004).

There is increasing evidence that the integrity of the airway epithelium is impaired in asthma (Maquerlot *et al*., 2006). Defects in TJ proteins such as E-Cadherin and ZO-1 in asthma may result in impaired barrier function and altered TJ signalling (Tsukita *et al*., 2008, Davies, 2014). A defective barrier enables the passage of allergens and tissue damaging agents across the epithelium (Golebski *et al*., 2013) facilitating the inflammatory response which may contribute to BHR in asthma (Holgate and Polosa, 2008). Respiratory tract infections

may trigger exacerbations in chronic airway diseases, and viruses such as rhinovirus (RV) have been shown to disrupt epithelial barrier function via interference with TJPs (Sajjan *et al*., 2008). Restoring normal TJ structure and function in diseased airways may improve barrier integrity, reducing airway susceptibility to environmental insults (Knight and Holgate, 2003). The epithelium produces cytokines including TSLP, IL-25 and IL-33 that promote Th2 responses in asthma (Hammad *et al*., 2009, Erle and Sheppard, 2014). IL-13 is secreted by innate lymphoid cells and Th2 cells and induces changes in epithelial gene expression (Woodruff *et al*., 2007). IL-25 and IL-33 act on dendritic cells, mast cells, and ILC2 cells to recruit both innate and adaptive immune cells naïve CD4 Th cells, promoting the release of type 2 cytokines (Erle and Sheppard, 2014).

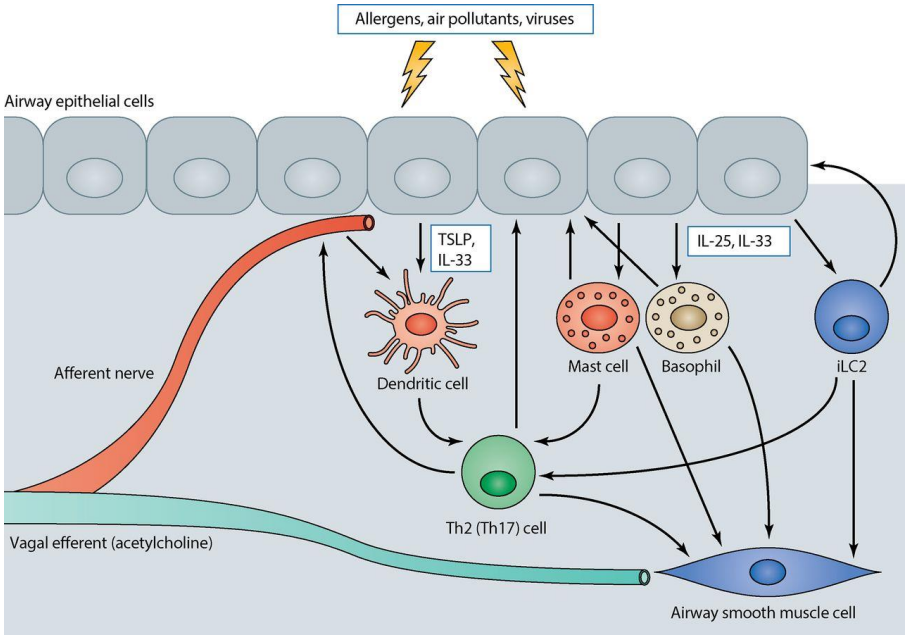


Figure 1.3.3: Airway epithelial signalling in asthma. Airway epithelial cells respond to environmental triggers to initiate responses that contribute to the mucous metaplasia and airway smooth muscle contraction. TSLP and IL-33 act on airway dendritic cells and stimulate dendritic cell maturation and the generation of effector T cells. IL-25 together with IL-33 act on mast cells, basophils, and innate type 2 lymphocytes (ILC2) triggering the release of bronchoconstrictors and type 2 cytokines from innate immune cells, which feedback on both the epithelium and airway smooth muscle and facilitate amplification of airway inflammation (Erle and Sheppard, 2014).

Epigenetic modification of genes may account for changes in the epithelium including cytokine expression, genes associated with goblet cell metaplasia and bronchial hyperactivity (Borish, 2016). Viral infections may also play a role in causing epigenetic changes in epithelial cells. Novel therapeutics target cytokines thought to play a role during exacerbations, these therapies have yielded improvements in airway inflammation and airway hyperactivity. Therefore we must look at the role of epithelial signalling and epigenetic regulations in inflammation and AHR in asthma that may not necessarily be triggered by allergens and other known external triggers (Borish, 2016).

Epithelial hypertrophy, goblet cell metaplasia, subepithelial fibrosis and smooth muscle hypertrophy are airway remodelling processes that occur in the airways in asthma (Elias *et al*., 1999). HBEC derived from bronchial brushings from asthma patients identified more goblet cells and fewer ciliated cells compared to control cells (Parker *et al*., 2010) and remodelling processes have been observed in endobronchial biopsies (Bergeron *et al*., 2010). In normal airways mucus is an important host defence mechanism however in chronic airway diseases mucus hypersecretion contributes to cough and wheezing and impairs mucociliary clearance (Fahy and Dickey, 2010). Obstructing mucus plugs have been found in the small airways in fatal cases of asthma. Targeting the overproduction of mucus in the airways may improve symptoms in asthma patients (Curran and Cohn, 2010). These changes are thought to result from tissue injury caused by inflammatory responses to allergens and pathogens (Holgate *et al*., 2000). These changes however can occur in the absence of infection and injury suggesting other processes may contribute (Ordoñez *et al*., 2000).

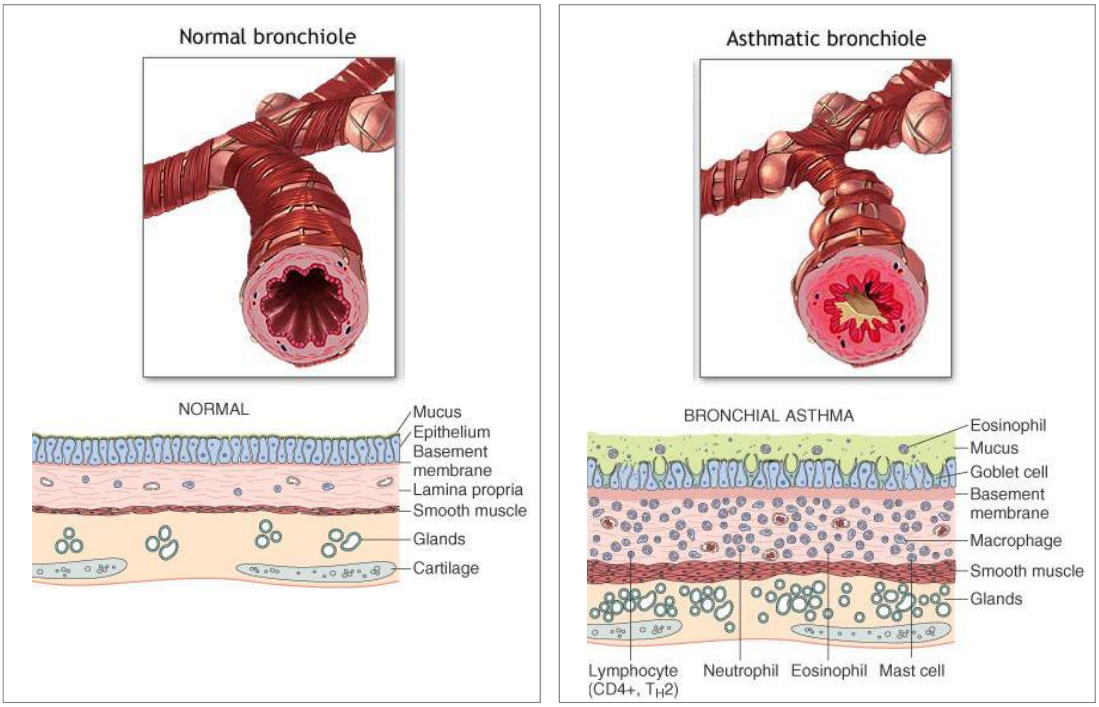


Figure 1.3.4: Airway Remodelling Features Observed in Asthma. The airways in asthma undergo goblet cell hyperplasia resulting in excessive mucus secretion and in some cases the development of mucus plugs. Basement membrane thickening and increased smooth muscle mass result in narrowing of the airways. Altered epithelial signalling promotes infiltration of immune cells and inflammatory responses (Knight and Holgate, 2003) https://marjorieshayene.files.wordpress.com/2011/01/4.jpg).

The airways are subject to environmental, chemical and physical insults, following injury the epithelium acts to restore lung homeostasis (Crosby and Waters, 2010) by inducing regenerative and repair processes to maintain epithelial structure and function via inflammatory and cell signalling events (Roth *et al*., 2012). However, excessive wound healing in the airways is associated with airway remodelling processes (Roth *et al*., 2012, Durrani *et al*., 2011) (Durrani *et al*., 2011). Epithelial repair mechanisms may involve activation of the Epithelial Mesenchymal Tropic Unit (EMTU) (Knight and Holgate, 2003). The EMTU controls the local tissue microenvironement, in asthma an activated EMTU may lead to impaired repair processes and signalling that drive structural changes linked to airway remodelling (Holgate, 2008). Airway epithelial basal cells may undergo EMT in response to

injury and serve as a source of fibroblasts and myofibroblasts contributing to subepithelial fibrosis (Hackett *et al*., 2009). Growth factors, inflammatory cytokines and matrix components released in response to injury inhibit epithelial cell-to-cell adhesion and upregulate mesenchyme gene expression pathways. A better understanding of epithelial remodelling in chronic airway disease could enable identification of epithelial-targeted therapies (Gras *et al*., 2013; Pezzulo *et al*., 2011) which may prevent airway remodelling and inflammation (Holgate and Polosa 2008).

1.3.6 Models of the Airway Epithelium

Primary airway epithelial cells can be cultured and studied using submerged basal cell culture and under air liquid interface (ALI) conditions that drive them to differentiate and form a more physiologically representative model. Cells are cultured on porous membranes in transwell insert, when they have reached confluency media is removed from the apical compartment (Yamaya *et al*., 1992; Gruenert *et a*l.; 1995, Stewart et *al*., 2012c). Primary cells offer a more physiological cell model than immortalized cell lines such as Calu-3 (lung adenocarcinoma derived), BEAS2B (adenovirus-12 SV40 hybrid virus transformed) and 16HBE14o- cells (immortalized by SV40 Large T antigen) (Stewart *et al*., 2012c; Forbes *et al*., 2003). Primary HBEC are obtained from brushing the airways or from collagenase digestion from lung tissue (Aitken *et al*., 1991).

ALI conditions mimic those found in the human airways driving cells towards a mucociliary phenotype, forming tight junctions and differentiating to ciliated, basal and secretory cells producing a robust and reproducible *in vitro* model of the airway epithelium (Stewart *et al*.,

2012c). Importantly, the transcriptional profile of primary airway epithelial cells cultured at ALI shows a high degree of similarity with *in vivo* primary epithelia (Pezzulo *et al*., 2011). ALI co-culture systems can be used to study epithelial-mesenchymal interactions, such systems could help understand how crosstalk between epithelial and mesenchymal cells contribute to mucus overproduction, inflammation and repair processes in the airways (Le Visage *et al*., 2004). This model has been used extensively to study epithelial barrier properties and defective epithelial TJ function in the asthmatic epithelium (Xiao *et al*., 2011, Bai *et al*., 2015).

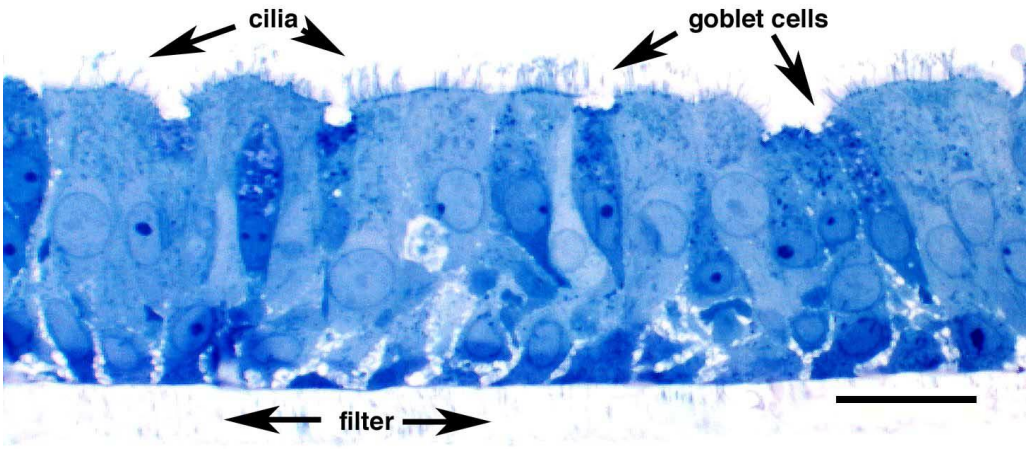


Figure 1.3.5: Air-liquid Interface Cultures of normal HBEC. Airway epithelial cells cultured at air liquid interface are driven to differentiate and cultures exhibit ciliated cells, goblet cells and develop tight junction complexes between neighbouring. Image available http://conner.med.miami.edu/web/conner.html

Electric cell-substrate impedance sensing (ECIS) is an alternative method to ALI and can be used to study multiple characteristics of a cell monolayer (Giaever and Keese, 1991). Cells are cultured under basal conditions on gold electrodes and a small current is applied (~1uA). As the cell monolayer changes impedance is affected and these changes are recorded, from this resistance and capacitance are calculated. At higher frequencies, more current travels through cells indicating monolayer formation. At low frequencies, more current travels through the gaps between cells giving information regarding barrier formation and

permeability (Heijink *et al*., 2010a). Both ALI and ECIS methods allow measurements to be taken in real time and factors can be added directly to media to investigate HBEC response to various stimuli.

1.4 The Urokinase Plasminogen Activator Receptor

The urokinase plasminogen activator receptor (uPAR/ CD87) is a cell surface receptor and serves as a key component of the plasminogen activator system (PAS) (Montuori *et al*., 2005). uPAR belongs to the lymphocyte antigen 6 (Ly6) superfamily of proteins which are characterised by their Ly-6 and uPAR (LU) domain (Mondino *et al*., 1999). uPAR activates the plasminogen pathway which is required for extracellular proteolysis and also initiates non-proteolytic functions in the cell (Smith and Marshall, 2010). uPAR is aberrantly expressed in a number of diseases including asthma and COPD (Almasi *et al*., 2009).

1.4.1 Urokinase Plasminogen Activator Receptor Structure

The uPAR gene is located on chromosome 19q13 and consists of 7 exons. The mature protein is highly glycosylated and is made up of 283 residues, uPAR comprises of 3 domains (D1, D2, and D3) which are similarly sized (~90 amino acids) and is anchored to the plasma membrane by its glycosylphosphatidylinositol (GPI) anchor (Ploug *et al*., 1991).

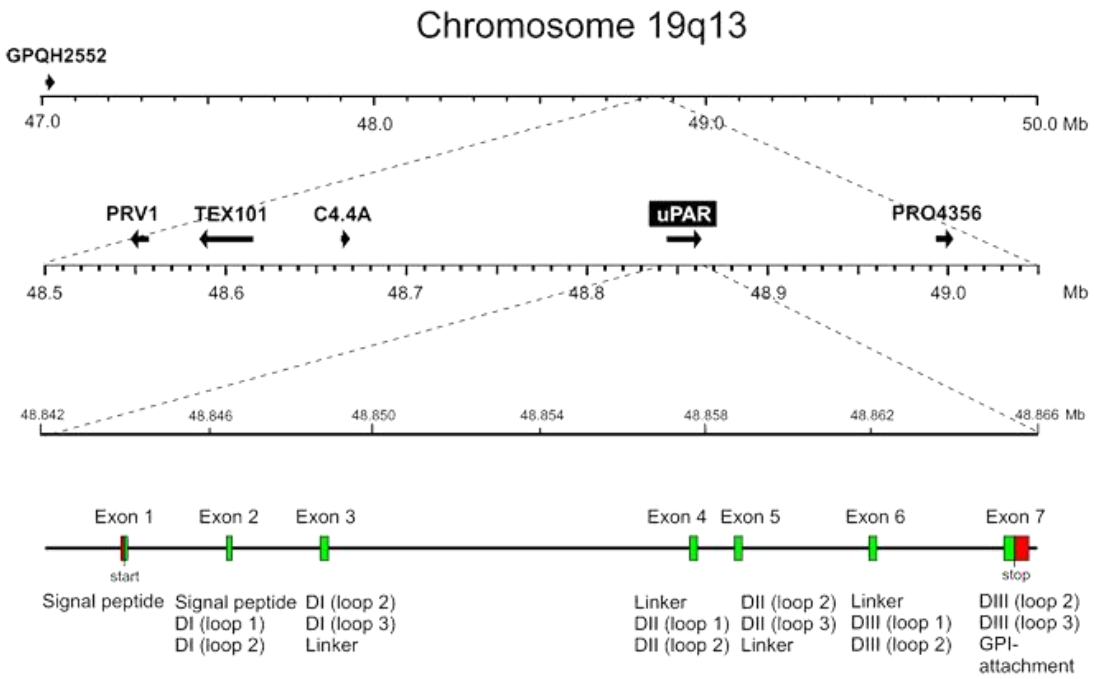


Figure 1.4.1: The *PLAUR* (uPAR) gene locus on chromosome 19q13. The gene for the urokinase-type plasminogen activator receptor (uPAR) is located on chromosome 19q13. Exons 2 and 3, 4 and 5 and 6 and 7 code domains 1, 2 and 3, respectively. Exons 3, 6 and 7 also code linker regions connecting domains 1-3. Exon 7 codes the glycophosphatidylinositol (GPI) anchor (Ploug, 2003).

Multiple uPAR isoforms are generated by alternative splicing which occurs during mRNA processing, the resulting proteins often have different functional properties (Pyke *et al*., 1993). Seven uPAR isoforms have been identified in lung and immune cells at the mRNA level including variants with deletion of exons 3, 5+6, 6 only and a variant with an alternative exon 7b which is predicted to lack the GPI anchor and function as a soluble variant (Stewart and Sayers, 2009). Cleavage of uPAR at the protein level and alternative mRNA splicing generates a number of uPAR variants, some of which have been shown to bind multiple ligands and interact with integrins which may have implications for the role of this receptor in regulating cell functions. Numerous soluble forms have been identified including a D1 and D2-D3 fragment that exhibit chemotactic properties (Blasi and Sidenius, 2010).

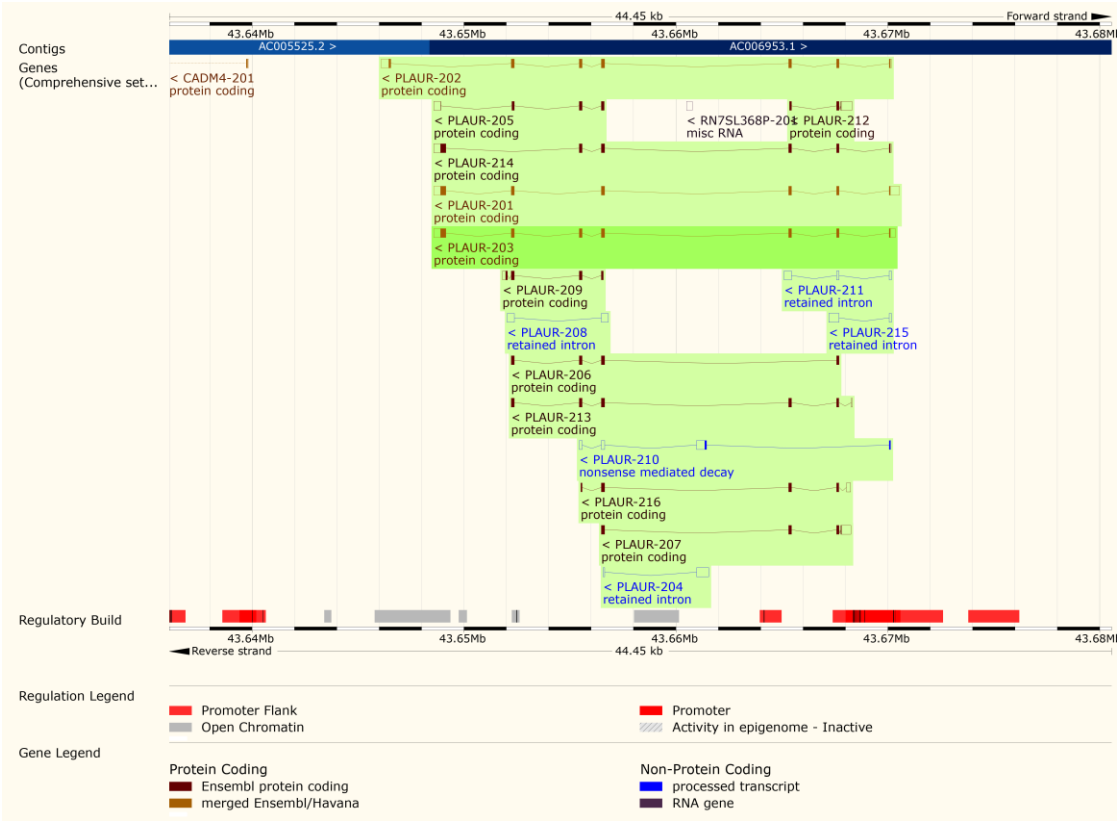


Figure 1.4.2: Annotation of Chromosome 19q13 Mapping Transcripts for the *PLAUR* (uPAR) gene. *PLAUR* maps to 44,150,247-44,174,699 in Human Genome Build GRCh37. There are 16 known transcripts for *PLAUR* 11 of which have been identified as protein coding (Ensembl and Havana databases). PLAUR-203 = full length isoform and PLAUR-202 =soluble isoform. Ensembl transcripts displayed are generated using the Ensembl automatic gene annotation system. Transcripts are based on experimental evidence of mRNAs and protein sequences deposited into public databases from the scientific community. Manually-curated transcripts produced by the HAVANA group at the Welcome Trust Sanger Institute are also displayed. Figure generated using Ensembl.org transcript annotation tool.

1.4.2 uPAR in Health and Disease

uPAR was first identified in monocytes as a cell surface molecule that interacts with urokinase (uPA) (Vassalli *et al*., 1985). In health uPAR is moderately expressed in the lungs, kidneys, spleen, vessels, uterus, bladder, thymus, heart, liver, and cell types include macrophages, neutrophils, endothelial cells (Blasi and Carmeliet, 2002) and bronchial epithelial cells (Stewart *et al*., 2012a).

Cell surface activation of urokinase (uPA) leads to plasmin generation and extracellular proteolysis (Ellis *et al*., 1992). Plasmin activation is required for ECM degradation, fibrinolysis and coagulation, activation is tightly regulated by plasminogen activator inhibitors-1 and -2 (PAI-1 and PAI-2) (Cesarman-Maus and Hajjar, 2005, Deryugina and Quigley, 2012, Myöhänen and Vaheri, 2004). The coagulation cascade results in the generation of fibrin, and is initiated by the classic 'intrinsic pathway' by contact activation of factor XII or the 'extrinsic pathway' in response to tissue injury. Fibrin is degraded by plasmin allowing resolution of fibrin clots (fibrinolysis) to maintain normal blood flow. Protease activated receptors (PAR-1 and PAR-2) may mediate crosstalk between these two pathways (Shetty *et al*., 2010). uPAR interacts with alpha 2-macroglobulin receptor to promote lysosomal degradation of the uPA-PAI-1 complex which leads to the recycling of uPAR to the cell surface and further signalling (Nykjaer *et al*., 1992).

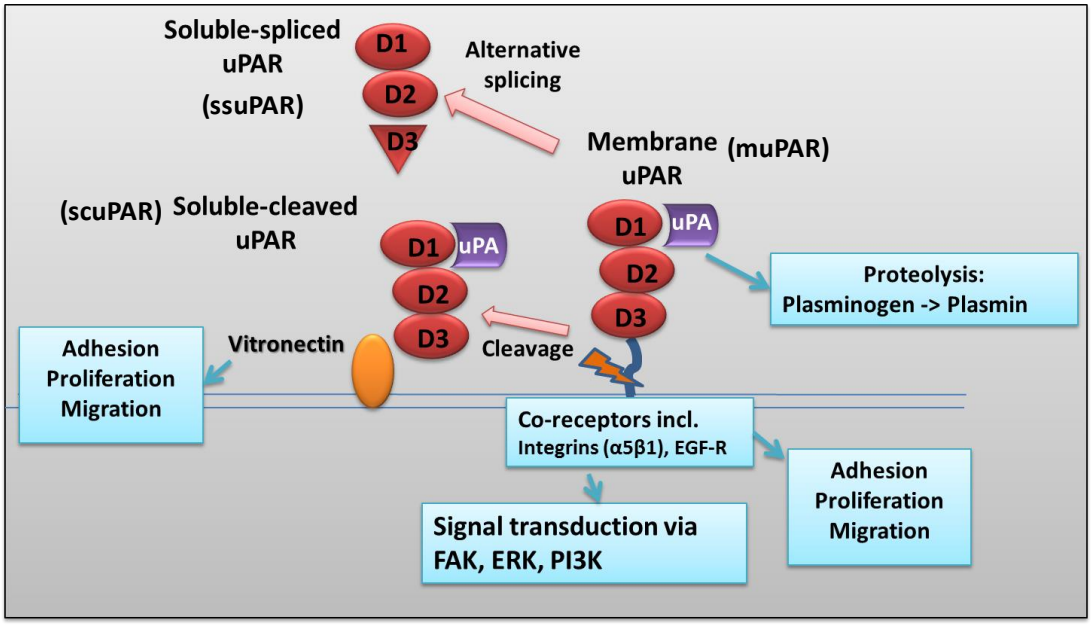


Figure 1.4.3: The Role of the uPA-uPAR Pathway in Cell Homeostasis. Multiple uPAR isoforms exist in the airways, activation of plasmin and interaction a number of membrane receptors together initiate proteolytic and non-proteolytic processes in the cell (Barton *et al*., 2009)

Non-proteolytic uPAR processes such as cell migration, proliferation, invasion and adhesion are mediated by interaction with a range of extracellular ligands such as vitronectin, adhesion receptors, G protein-coupled receptors (GPCRs) and integrins (Ragno, 2006, Degryse *et al*., 2005, Gårdsvoll *et al*., 2006, Madsen *et al*., 2007). uPAR binds vitronectin and uPA at distinct sites therefore regulation of proteolytic and non-proteolytic mechanisms can be coordinated simultaneously (Smith and Marshall, 2010). uPA binds a central cleft in the uPAR protein which consists of residues from all three domains whereas vitronectin interacts with residues in D1 and the D1-D2 linker (Smith and Marshall, 2010). Upregulation of the uPA-uPAR system has been observed in a number of carcinomas, therapies inhibiting uPA activity have had limited success indicating uPAR interaction with other ligands such as membrane proteins are important in modulating cellular processes (Tang and Wei, 2008). uPAR directly binds integrins (β1, β2, and αV) to regulate cellular changes such as adhesion, migration and proliferation in lung, prostate, breast and ovarian cancer (Tang and Wei, 2008). FVII binds domain 2 of uPAR, initiating signalling via uPAR, EGFR and β1 integrin to induce cell proliferation and growth which may play a role in angiogenesis (LaRusch *et al*., 2010).

Soluble full length uPAR (suPAR) lacks the GPI anchor and is detected in serum, uPAR shedding may inactivate or modify uPAR signalling and interfere with the uPAR degradation pathway (Montuori *et al*., 2005, Allgayer, 2010). Membrane bound and soluble cleaved forms of uPAR (muPAR and scuPAR) arise from proteolytic cleavage of the D1-D2 and D2-D3 linker regions by MMPs, uPA, plasmin, chymotrypsin and cathepsin G which generally negatively regulate uPAR (Beaufort *et al*., 2004). Soluble variants, for example the alternate 7b variant (soluble-spliced uPAR/ ssuPAR), can arise from alternative splicing (Stewart and Sayers, 2009).

Both the muPAR and scuPAR have been implicated in cancer biology and more recently asthma and COPD pathogenesis (Blasi and Carmeliet, 2002, Ierodiakonou *et al*., 2016b). The contribution of the plasminogen pathway, specifically uPAR, to the pathobiology of obstructive lung disease is not completely understood. scuPAR has been identified as a marker of various diseases including prostate (Skovgaard *et al*., 2016) and lung cancers (Almasi *et al*., 2009) as well as systemic lupus erythematosus (Enocsson, Sjöwall *et al*. 2015). scuPAR has been proposed as modulator as well as a marker of disease because of its ability to compete with muPAR for the binding of uPA, vitronectin and integrins and thus carry out its own functions (Montuori *et al*., 2005).

1.4.3 uPAR in Airway Disease

Induction of the uPA-uPAR pathway may contribute to airway remodelling in chronic respiratory diseases via the fibrinolysis and coagulation pathways, which are thought to be dysregulated in the airways in asthma, COPD and Idiopathic pulmonary fibrosis (IPF) (Bégin and Nadeau, 2014). The genes encoding uPA, uPAR and PAI-1 are potential asthma susceptibility genes and are upregulated in asthma (Barton *et al*., 2009; Kovacic *et al*., 2011). Genes encoding PAS components are associated with tissue remodelling, BHR and inflammation (Ossovskaya and Bunnett, 2004). uPAR and uPA expression is elevated in airway macrophages and epithelial cells from COPD patients (Wang *et al*., 2008) and in sputum from asthma, COPD and cystic fibrosis patients (Xiao *et al*., 2005a). Studies in COPD patients have also found the uPAR levels correlate with collagen and fibrosis (Zhang *et al*., 2012), airway remodelling and markers of EMT (Wang *et al*., 2013).

Fibrin generation is required for normal epithelial repair, however excessive fibrin deposition in the lungs can enhance inflammatory and fibroproliferative responses which in turn may contribute to tissue remodelling (Chambers and Scotton, 2012). Fibrin deposition is increased in response to lung injury in the asthmatic airway, deposition in the distal airways is associated with BHR and severe asthma (Brims *et al*., 2009). uPAR gene knock-out mice develop tissue fibrosis, and lungs from these mice displayed increased inflammation and collagen deposition (Manetti *et al*., 2014). In a mouse ovalbumin asthma model administration of uPA resulted in reduced subepithelial fibrosis and AHR in groups with upregulated plasmin activity (Kuramoto *et al*., 2009). These data demonstrate that altered expression of uPAR in the lung dysregulate fibrinolytic pathways. In addition to fibrinolysis, uPAR regulates migratory properties of immune cells. As discussed, eosinophils play a key role in inflammation in multiple asthma phenotypes, MMP-9 and uPAR have been shown to mediate eosinophil transmigration in response to the chemotactic factor, eotaxin (Ferland *et al*., 2001). The cysteinyl leukotriene inhibitor Montelukast inhibits protease activity by modifying uPAR expression and MMP-9 activity in eosinophils, and prevent eosinophil migration, which may in part explain the anti-inflammatory properties of this compound in asthma (Langlois *et al*., 2006).

EMT is thought to be an important process in driving invasion and metastasis in cancer, interestingly uPAR expression and signalling is essential for hypoxia induced EMT in breast cancer cells (Jo *et al*., 2009). Importantly, the uPA-uPAR pathway has been implicated in EMT in the airway epithelium of COPD patients (Wang et al., 2013). EMT plays a role in cellular differentiation in tumours and may to contribute to subepithelial fibrosis in the lung, whether EMT is dysregulated in asthma remains unknown (Hackett *et al*., 2009).

In a model of bronchoconstriction, mechanical stimulation of differentiated HBECs leads to upregulation uPA, uPAR, PAI-1 gene expression (Chu *et al*., 2006). Chu *et al* also identified increased immunostaining of uPA and uPAR in the lungs of patients who died from status asthmaticus, these data demonstrate a relationship between mechanical stress (mimicking bronchoconstriction) of the airways and these proteins *in vitro* and *in vivo*. Furthermore, uPAR and PAI-1 are elevated in airway smooth muscle cells stimulated with the pro-remodelling lipid molecule, sphingosine-1-phosphate (Fuerst *et al*., 2014).

uPAR expression is elevated in the bronchial epithelium in asthma patients compared to healthy controls (see Figure 1.4.4), elevated levels correlate with attenuated would healing in HBEC suggesting the uPA-uPAR axis is disturbed in asthma and may be important in repair (Stewart *et al*., 2012a). Multiple uPAR isoforms are expressed in the lung and in the periphery including the exon 7b spliced variant, and may have consequences for downstream signalling (Stewart and Sayers, 2009, Portelli *et al*., 2015). uPAR expression inversely correlates with basal cell epithelial proliferation suggesting the receptor interferes with epithelial regeneration and repair (Ierodiakonou *et al*., 2016b) and elevated expression of scuPAR in serum is related to severe, non-atopic asthma (Portelli *et al*., 2016). The implications of dysregulated uPAR expression in the bronchial epithelium is not known, however evidence suggests the receptor may contribute to of airway remodelling in asthma.

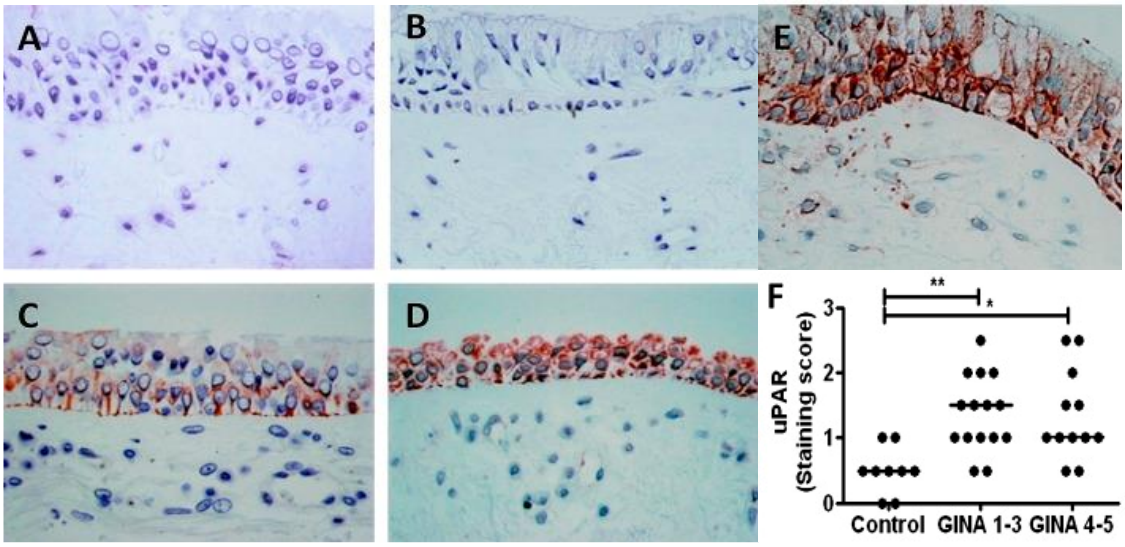


Figure 1.4.4: Urokinase plasminogen activator receptor (uPAR) is increased in asthmatic bronchial epithelium. Bronchial biopsy sections from controls and subjects with asthma were stained with (A) isotype control or (B–E) anti-uPAR antibody. A semiquantitative staining score of 0=none (B), 1=low (C), 2=moderate (D) or 3=high (E) was applied to each section and two sections were scored per subject. (F) uPAR protein levels were higher in the bronchial epithelium of patients with asthma than in normal controls, irrespective of severity (p=0.002). *p<0.05, **p<0.01. GINA, Global Initiative for Asthma. (Stewart *et al*., 2012a).

1.5 Summary

Asthma is a complex genetic disorder involving multiple pathways that drive inflammatory processes and structural changes in the airways (Ober and Vercelli, 2011). There is a need to understand the molecular pathways underlying asthma (endotypes) as current medication does not adequately control all asthma or target specific disease pathways (Lötvall *et al*., 2011). Our understanding of inflammatory processes, particularly Th2 driven asthma, has led to the development of biologics targeting the interleukin pathway (Chung, 2015). These treatments have shown clinical benefit in certain asthma subsets (e.g. severe, eosinophilic) however some patients lack treatment options and their asthma is poorly understood (e.g. noneosinophillic) (Borish, 2016).

There is growing evidence that the airway epithelium plays a central role in the development and progression of asthma and it is therefore an attractive target for therapeutic intervention (Holgate, 2011). Epithelial barrier function, signalling and repair processes are defective in asthma and may promote gross structural changes in the airways. Identifying mechanisms underlying epithelial-driven remodelling may lead to the development of therapies that demonstrate clinical benefit by restoring epithelial function (Knight and Holgate, 2003).

uPAR is elevated in the bronchial epithelium in asthma and is associated with remodelling processes, specifically ECM degradation and wound repair (Stewart *et al*., 2012a). Different forms of the receptor have been shown to differentially regulate airway epithelial homeostasis and elevated levels are associated with basal cell proliferation (Portelli *et al*., 2015, Ierodiakonou *et al*., 2016b). Furthermore, SNPs spanning the gene for uPAR (*PLAUR*) are associated with asthma risk, BHR and baseline lung function (Barton *et al*., 2009). A better understanding of the effects of elevated uPAR in airway epithelial function in asthma is needed to determine whether this receptor can be targeted for therapeutic benefit.

1.6 Aims

A number of studies have shown that uPAR expression is elevated in asthma and that the receptor is associated with bronchial epithelial function and airway remodelling. Whether elevated uPAR expression is cause or consequence of asthma pathobiology remains unclear. Therefore, the aims of this thesis were:

1. To characterise the expression profile of the uPAR and key interacting proteins during differentiation of the airway epithelium and to investigate the role of the uPAR-uPA pathway in regulating bronchial epithelial barrier properties.
2. To investigate gene expression patterns in cultured bronchial epithelial cells isolated from the airways of moderate to severe asthma patients and healthy control subjects and assess the relative expression and activity of uPAR pathway components in the bronchial epithelium in asthma.
3. To determine the effect of elevated membrane uPAR (muPAR), soluble-spliced variant (ssuPAR) and soluble cleaved variant (scuPAR) on bronchial epithelial cell function using whole transcriptome analysis.
4. To define the relative contribution of genetic polymorphisms spanning the *PLAUR* gene to FEV_1, FEV_1/FVC, Atopy, Total serum IgE levels and Blood Eosinophils in moderate to severe asthma patients.

Chapter 2: General Materials and Methods

2 General Materials and Methods

This chapter describes the general methods and techniques used throughout this thesis, methods focused to specific parts of this study are described in their respective chapters. HBEC *in vitro* models are described in Chapter 3 and genetic association analysis methods are detailed in Chapter 6. For specific materials and reagents see Appendix 1.

2.1 Mammalian Cell Culture Methods

2.1.1 Normal Human Bronchial Epithelial Cells (Commercial)

Human bronchial epithelial cells (HBEC) were obtained from the post-mortem lungs of normal, caucasian male subjects sourced from Lonza® (Castleford, UK). Information for the donors used in this thesis are summarised in the Table 2.1.1.

Donor	Donor Number	Age	Gender	Viability	Doubling Time	Seeding Efficiency	Alcohol	Smoker
7F3158	1	56	Male	70%	24.5hrs	31%	Yes	Yes
7F3206	2	50	Male	75%	21hrs	45%	Yes	Yes
124040	3	43	Male	71%	20hrs	60%	No	No
195307	4	19	Male	91%	16hrs	66%	Yes	No
355687	5	38	Male	75%	23hrs	68%	No	No
369144	6	43	Male	87%	18hrs	41%	No	No

Table 2.1.1: Details of Commercially Sourced HBEC. Summary of characteristics of HBEC obtained from Lonza, UK. Data obtained from Lonza® (Castleford, UK).

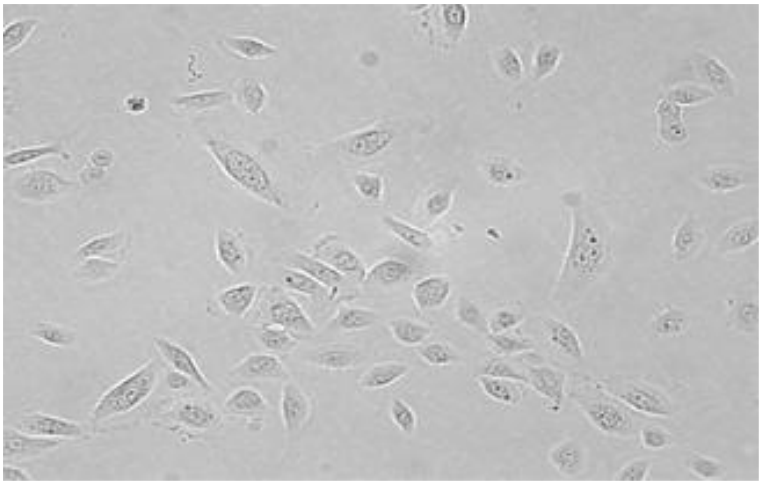


Figure 2.1.1: Morphology of human bronchial epithelial cells (HBEC) in submerged in culture. Commercial normal HBEC (Lonza® Clonetics™) donor 2 (x20 objective).

2.1.2 Cell Culture of Mammalian Primary Cells

Human bronchial epithelial cells (HBEC) were cultured in bronchial epithelial basal medium (BEBM™ Lonza) supplemented with 52 µg/ml bovine pituitary extract, 0.5 µg/ml hydrocortisone, 0.5 ng/ml human epidermal growth factor, 0.5 µg/ml epinephrine, 6.5 ng/ml triiodo-L-thyronine, 5 µg/ml insulin, 0.1 ng/ml retinoic acid, 10 µg/ml transferrin and 0.001% gentamycin (v/v). Cells were initially expanded in a T75 cell culture flask (Corning®), media was replaced every 2-3 days until cells reach ~80% confluency. Cells were detached from culture by the addition of trypsin which is deactivated after 5 minutes by adding trypsin soybean inhibitor. Cells were pelleted by centrifugation at 200 x g for 5 minutes and counted prior to re-plating or cryopreservation. HBEC were seeded at the recommended density of 3,500 cells/cm^2 (Clonetics; Manual - Airway Epithelial Systems - Instructions for use).

2.1.3 Cryopreservation of Primary HBEC

Cryopreservation enables stocks of low passage cells to be stored preventing the need to have all cell lines in culture at all times, which is essential when using cells of limited life span. Cells were detached as described (see Section 2.1.2) and frozen in freezing medium of BEGM + 10% DMSO at a concentration of 2.5 x 10^5 cells/ml per vial. Cells were frozen in a Mr. Frosty™ at rate of approximately -1°C/minute to a maximum of -80°C for 24 hours and were then placed in cryogenic tank filled with liquid nitrogen for long term storage (-180°C).

2.1.4 Cell Counting

Cell were counted using a haemocytometer. Cells were detached and pelleted as described in Section 2.1.2 and re-suspended in 2ml BEGM. 10 µl of the cell suspension was added to the haemocytometer and the cells were examined under the microscope using x 20 magnification. Cells were counted in the four corner squares; the average was taken and multiplied by 10^4 in order to calculate the total number of cells per ml.

2.2 Molecular biology methods

2.2.1 Total RNA Isolation

Total RNA extraction was carried out using the Qiagen RNeasy® Mini Kit in conjunction with the Qiagen QIAShredder Kit as per manufacturer's instructions. This system allows up to 100 µg of RNA longer than 200 bases to bind to the RNeasy silica membrane. Cells are lysed in

the presence of a highly denaturing guanidine-thiocyanate–containing buffer, which inactivates RNases to ensure RNA is intact. Ethanol is added to enhance binding conditions and contaminants are washed resulting in purified RNA. Cells in a T75 cell culture flask were lysed by directly adding 350 µl Buffer RLT and were detached by scraping. The resulting cell lysate was added directly into a QIAshredder spin column placed in a 2 ml collection tube and spun for 2 minutes at 13000 rpm. 1 volume of 70% ethanol was then added to the homogenized lysate and mixed before being added to an RNeasy spin column in a 2 ml collection tube. The lysate was centrifuged for 15 seconds at ≥8000 x g and the flow through discarded. 350 µl Buffer RW1 was then added to the RNeasy spin column and centrifuged as described. DNase I (10 µl DNase I enzyme + 70 µl Buffer (RDD Qiagen RNaseFree DNase Set)) was then incubated on the membrane at room temperature for 15 minutes in order to degrade any genomic DNA. The membrane was then washed with 350 µl of Buffer RW1 followed by 500 µl Buffer RPE+80% v/v ethanol. RNA was eluted by adding 50 µl RNase-free water directly to the column. RNA was visualized using gel electrophoresis and concentration was determined using a Nanodrop 2000c UV/IV Spectrophotometer. RNA is detected at 260 nm and sample purity is assessed using the ratio of absorbance at 260 nm and 280 nm.

2.2.2 Polymerase Chain Reaction

Polymerase Chain Reaction (PCR) is a technique that enables the amplification of a specific sequence of DNA. PCR is highly sensitive and achieves high levels of amplification. A reaction includes target DNA, DNA polymerase, two oligonucleotide primers which are specific to the target sequence, deoxynucleotide triphosphates (dNTPs), reaction buffer and magnesium. The initial step denatures double stranded DNA, followed by 40 cycles of denaturation,

primer annealing and primer extension and a final extension step (Saiki *et al*., 1988). All reactions were carried out on the Techne® PrimeG thermal cycler using Platinum Taq DNA Polymerase and the reaction components listed in Table 2.2.1.

Reagent	Stock Concentration	Final Concentration	Volume (µl)
PCR buffer	10x	1x	2.5
Mg2+	50mM stock	1.5mM	0.75
DNTPs	5mM stock	0.2mM each	1
Forward primer	10µM	0.5µM	1.25
Reverse primer	10µM	0.5µM	1.25
Taq DNA polymerase	1 unit/µl	0.5 units	0.5
Water	-	-	16.65
Total volume			25

Table 2.2.1: Polymerase Chain Reaction Mix. Required volumes and concentrations of reagents required for PCR.

2.2.3 Agarose Gel Electrophoresis

Gel electrophoresis is a technique used to separate DNA fragments by size. An electrical field is applied and causes negatively charged DNA to move towards a positive electrode through agarose gel. Shorter DNA fragments travel faster than longer fragments allowing separation (John F. Robyt, 1987). DNA is loaded using Orange G loading dye (6x) and is run alongside the 1kb Plus DNA ladder. Ethidium bromide is added to the agarose and binds to the DNA allowing visualization of the separated fragments. Gels were 1% w/v and were prepared by dissolving agarose powder in 1 x TAE buffer. Samples and ladder were loaded and gels were run at 75 volts for 35 minutes. DNA fragments were visualized under UV light using the Syngene GeneGenius Gel Doc system and GeneSnap v6.08 software (Syngene).

2.2.4 Complementary DNA Synthesis

The SuperScript® First-Strand Synthesis System for RT-PCR (Thermo Fisher) was used to synthesise complementary DNA (cDNA) from purified RNA. 2 µg RNA was made up to 10 µl with water, DNaseI and DNaseI buffer and incubated at room temperature for 15 minutes.

component	Volume (µl)
RNA (2µg)	*N*
DnaseI	1
DnaseI buffer	1
Water	Make up to 10 µl

Table 2.2.2: DNaseI Pre-treatment of RNA. Required volumes and concentrations of reagents required. Volume of RNA (*N*) was dependant on stock concentration of RNA sample.

1 µl of 25mM EDTA was then then added to each sample and incubated for 15 minutes at 65°C to heat inactivate the DNase I, and then placed on ice for 1 minute. The reaction was collected by brief centrifugation and 5.5 µl was split across 2 Eppendorf tubes to generate a reverse transcriptase positive (RT+ve) and negative control (RT-ve). The following mastermix was made and 4.5 µl was added to each tube.

component	1 rxn
DEPC-treated water	2.5
10 mM dNTP mix	1
random hexamers (50ng/µl)	1

Table 2.2.3: cDNA Synthesis Hexamer-dNTP Mastermix 1

Samples were incubated for 5 minutes at 65°C and then placed on ice for 1 minute. The following mastermix was prepared.

Component	1rxn
10X RT buffer	2
25 mM MgCl2	4
0.1 M DTT	2
RNaseOUT. Recombinant RNase Inhibitor	1
	9

Table 2.2.4: cDNA Synthesis Hexamer-dNTP Mastermix 2

9 µl of reaction mixture added to each RNA/primer mixture, mixed gently, and collected by brief centrifugation and incubated at 25°C for 2 minutes. 1 µl (50 units) of SuperScriptII RT was added to each tube except the RT-ve control and incubated at 25°C for 10 minutes. Samples were then incubated at 42°C for 50 minutes and the reaction was terminated by incubating at 70°C for 15 minutes. Reactions were chilled on ice for 1 min, collected by reactions by brief centrifugation and then 1 µl of RNase H was added to each RT+ve and incubated for 20 minutes at 37°C.

PCR was used to quality control the synthesis of cDNA. PCR was carried out as described in Section 2.2.2 using primers for Glyceraldehyde 3-phosphate dehydrogenase (GAPDH) in RT+ve samples and RT–ve controls. Agarose Gel Electrophoresis was performed as described in Section 2.2.3 to visualize bands with detection of a band at the 306bp position (Forward GAPDH primer 5’-3’ AGGTCATCCATGACAACTTTGG, Reverse GAPDH primer 5’-3’ GCTTCACCACCTTCTTGATGTC).

2.2.5 Quantitative PCR

Quantitative PCR (qPCR) enables quantitative analyses of gene expression in a sample. The presence of a fluorescent reporter in the reaction allows DNA generation to be measured. The qPCR method used was Taqman®, this method utilizes a fluorescent reporter dye and quencher which are attached to the 5' and 3' ends of a gene specific oligonucleotide probe which hybridizes with the PCR product. Gene specific primers bind to the target sequence allowing the probe to be cleaved by the 5' nuclease activity of Taq DNA polymerase during each extension cycle. The reporter dye is cleaved separating it from the quencher and emits its fluorescence (Heid *et al*., 1996). With each cycle additional reporter molecules are cleaved resulting in an increase in fluorescence that is proportional to the amount of amplicon produced in the reaction. The point at which fluorescence becomes measurable is called the Threshold cycle (CT), this is when DNA is in the log linear phase and fluorescence increases above the background. Ct levels are inversely proportional to the amount of target nucleic acid in the sample. All Ct values were calculated using MxPro TM QPCR Software v4.01 and Microsoft Excel. Hypoxanthine phosphoribosyltransferase 1 (HPRT1) was used as the reference gene, variation in cDNA levels across samples was corrected to HPRT1 expression. Plasmid DNA was used a positive control for PLAUR assays and total lung RNA was used as a positive control for RNA seq validation genes. RT-ves and no template controls were run for all assays to test for contamination.

Assay	Target	Forward Primer	Reverse Primer
1	Total PLAUR	PLAUR E1 L258 CTGCTGCTGCTCCACACCT	PLAUR E2 R345 ACTCTTCCACACGGCAATCCC
2	Membrane PLAUR	PLAUR E1 L258 CTGCTGCTGCTCCACACCT	E7V1 R1118 TGGGTGGTTACAGCCACTTT
3	Soluble PLAUR	PLAUR E1 L258 CTGCTGCTGCTCCACACCT	suPAR R1013 TGGCAACCAGCTTCCCCAGAGT
All	Probe	uPAR all CCAGCCTCTTGGGGCCTGCGGT	

Table 2.2.5: Primers and Probes used in the TaqMan™ qPCR. The probe and the forward primer are common to all 3 assays, the reverse primer for each assay specifically targets either total PLAUR, membrane PLAUR or soluble spliced PLAUR. Due to interference between the reference gene (HPRT1) and the assays for membrane and soluble spliced PLAUR, the reference gene was only multiplexed with the total PLAUR assay and so the remaining assays had to be carried out at the same time using the HPRT values from the first assay. The alphanumeric code present in primer names is an experimental cross-reference.

Primer	Sequence	Exon	Location
PLAUR E1 L258	CTGCTGCTGCTCCACACCT	1	44174226 - 44174245
PLAUR E2 R345	ACTCTTCCACACGGCAATCCC	2	44171775 - 44171796
E7V1 R1118	TGGGTGGTTACAGCCACTTT	7a	44153162 - 44153181
sPLAUR R1013	TGGCAACCAGCTTCCCCAGAGT	7b	44150672 - 44150694
Probe	CCAGCCTCTTGGGGCCTGCGGT	2	44171861 - 44171839

Table 2.2.6: Locations of qPCR primers and probe outlined in Table 1.3.5. Locations refer to chromosome 19 build GRCh37.

Assay Target	Assay ID	Exon Boundary	Amplicon Length
CXCL10	Hs04421396_g1	1-2	98
CXCL11	Hs04187682_g1	1-2	96
CXCL8	Hs00174103_m1	1-2	101
IFIT1	Hs03027069_s1	3-3	134
CEACAM5	Hs00944023_m1	4-5	59
COMT	Hs02511558_s1	6-6	135
S100A6	Hs00170953_m1	1-2	94
RPS28	Hs02597258_g1	1-1	74
HPRT1	Hs99999909_m1	6-7	100

Table 2.2.7: Details of Pre-Designed Assay Reagents: Pre-Designed Assay Reagents (PDARs) were used to measure expression of the genes listed using Taqman qPCR. HPRT1 was used as a reference gene for all gene expression assays carried out in this thesis, assays were not multiplexed and HPRT1 controls were included on the same plate for all gene targets.

Each qPCR reaction was carried out in triplicate in a 96 well plate per sample, the reaction volumes are summarised in the Table 2.2.8.

A. Pre-designed assay

Component	Volume
TaqMan Universal PCR Master Mix	10
cDNA (1:5)	5
Pre designed assay	1
water	4
Total	20

B. Custom assay

Component	Volume
TaqMan Universal PCR	10
cDNA (1:5)	5
Forward primer	0.4
Reverse primer	0.4
Probe	1
Water	3.6
Total	20

Table 2.2.8: qPCR Reaction Mix for Pre-designed Assays (A) and Custom Assays (B)

Each assay was run on the Stratagene qPCR machine, data for the ROX™, HEX™ and FAM™ dyes were collected using the cycling parameters listed Table 2.2.9 and 2.2.10.

Temperature	Time	No cycles
50 °C	2 min	1
95 °C	10 min	1
95 °C	15 sec	40
60 °C	1 min	

Table 2.2.9: Cycling Parameters. Pre-designed Assays and Total PLAUR

Temperature	Time	No cycles
50 °C	2 min	1
95 °C	10 min	1
95 °C	20 sec	40
55 °C	20 sec	
65 °C	1 min	

Table 2.2.10: Cycling Parameters. Custom assays: Membrane and Soluble-spliced PLAUR

Data analysis was carried out using the MxPro Mx3005P v4.01 software. The reference dye was set to ROX and data was treated individually and the fluorescence was set to dRN

(baseline corrected normalised fluorescence). Ct (threshold cycle) was determined manually by examining the data as log10 values. Data was exported to Microsoft Excel where fold change was calculated using either the ΔCT or 2-ΔΔCT method.

2.2.6 Transformation of Bacterial Cells

Transformation enables foreign DNA, including plasmid DNA, to be introduced into a cell allowing replication or storage of that DNA (Anthony JF Griffiths, 2000). MAX Efficiency® DH5α™ Competent E.coli Cells were thawed on ice, gently mixed and 50 µl cells were transferred to polypropylene tubes. 1 to 10 ng DNA was added directly to the cells, gently mixed and incubated on ice for 30 minutes. Cells were heat shocked for 45 seconds at 42°C and placed on ice for 2 minutes. 125 µl S.O.C medium was added to the reaction. The polypropylene tubes were then placed on ice and then transferred to a shaking incubator for 30 minutes at 220rpm 37°C. The transformed bacteria were then spread on LB Ampicillin plates and incubated overnight at 37°C. Positive colonies were selected for sub-culturing in 5 ml LB Ampicillin broths.

2.2.7 Purification of Plasmid DNA

The QIAprep Miniprep kit was used for plasmid purification for stocks of pcDNA3™ plasmids containing open reading frames for scuPAR, muPAR and ssuPAR which were used as positive controls for RT-PCR experiments measuring uPAR gene expression. 1500 µl of LB broth was centrifuged at 8,000 rpm for 3 minutes forming a bacterial cell pellet. The pellet was then resuspended in 250 µl of Buffer P1 with RNase A, followed by 250 µl of Buffer P2 to lyse the cells. This lysis reaction is neutralised after 5 minutes by the addition of 350 µl of Buffer N3. The solution was then centrifuged for 10 minutes at 13,000 rpm in a table top centrifuge. A

maximum of 800 µl of the supernatant was added to a QIAprep spin column, centrifuged for 30 seconds and the flow-through discarded. The spin column was then washed with 500 µl of Buffer PE and centrifuged for 30 seconds. This step was repeated with 750 µl of Buffer PE. An additional centrifugation step for 1 minute was carried out to remove residual wash buffer. The column was then placed in a clean 1.5 ml centrifuge tube, 50 µl of Buffer EB was added to the centre of the spin column and after 1 minute was centrifuged at 13,000rpm for 1 minute to elute the DNA. The elution step was repeated to increase the yield.

2.3 Protein Methods

2.3.1 Enzyme-linked immunosorbent assay (ELISA)

An Enzyme-linked immunosorbent assay is a plate based assay used to detect and quantify analytes (e.g. peptides, proteins, antibodies) (Lequin, 2005). DuoSet™ ELISA was used to measure soluble uPAR (assay range 31.20 - 2,000 pg/mL), uPA (assay range 62.5 - 4,000 pg/mL) and MMP-9 (assay range 31.20 - 2,000 pg/mL) (R&D Systems). An analyte specific antibody is bound to a 96 well polystyrene plate, 100 µl of capture antibody was added to each well and incubated overnight on a rocker at room temperature. The following day unbound capture was washed off by washing plates 3 times with Phosphate Buffered Saline with 0.05% Tween (PBST). Plates were then blocked with 300 µl reagent diluent (Phosphate Buffered Saline 1% Bovine Serum Albumin) for 1 hour and washed as described previously. 100 µl of sample or standard was then added to the relevant wells and incubated for 2 hours at room temperature. Analytes present are bound by the immobilized antibody. Plates were washed so that unbound materials are washed away and 100 µl of detection antibody was added to each well and incubated for 2 hours at room temperature. Plates were then washed

and 100 µl of Streptavidin-Horseradish Peroxidase (HRP) was added to each well to bind the detection antibody, plates were covered and incubated for 20 minutes at room temperature. Plates were washed to remove any unbound streptavidin-HRP and 100 µl of substrate solution was added to each well, plates were kept covered at room temperature for 20 minutes. The reaction results in a change in colour which is proportional to the amount of analyte present. The reaction was stopped by adding 50 µl of stop solution (2N H_2SO_4). Absorbance was determined using a microplate reader at 450 nm with a background of 570 nm. This subtraction corrects for optical imperfections in the plate. Readings made directly at 450 nm without correction may be higher and less accurate.

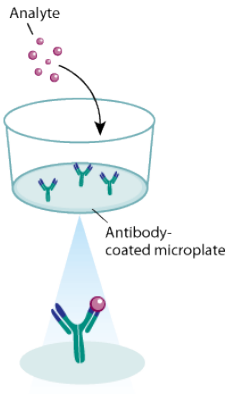
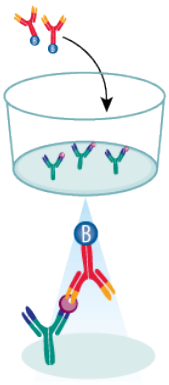
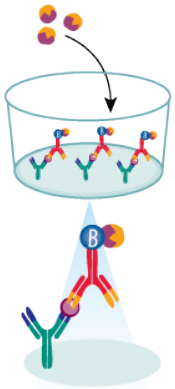
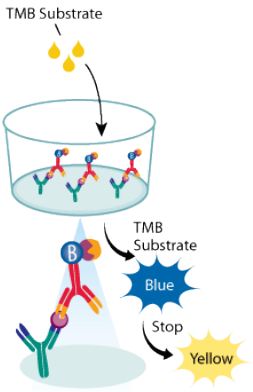
Step 1	Step 2	Step 3	Step 4
			
Analyte-specific capture antibody is bound to a polystyrene microplate. Unbound capture antibody is washed away before plates are blocked and washed.	Samples and standards are added and, the analyte of interest is bound by the immobilized antibody. Unbound materials are washed away.	Streptavidin-Horseradish Peroxidase (HRP) is used to bind to the detection antibody. Unbound streptavidin-HRP is washed away.	Tetramethylbenzidine (TMB) substrate solution is added to the wells and a blue colour develops in proportion to the amount of analyte present in the sample. Colour development is stopped turning the colour in the wells to yellow. The absorbance of the colour at 450 nm is measured.

Figure 2.3.1: ELISA Principle. Adapted from R&D Systems Duoset® ELISA Systems Assay Principle

2.3.2 Luminex Bead-based Multiplex Assay

The Luminex assay is a high-throughput multiplex bead array assay that is capable of quantifying large numbers of analytes (Elshal and McCoy, 2006). Luminex assays were performed using a custom Magnetic Luminex Screening Assay, Human Premixed Multi-Analyte Kit (R&D systems). For the list of analytes measured and assay ranges see Appendix 3. Samples are added to colour coded magnetic beads which are pre-coated with analyte specific antibodies enabling them to bind to the analytes of interest. Biotinylated detection antibodies are then added and form an antibody-antigen sandwich with the analyte they are specific to. Phycoerythrin (PE)-conjugated streptavidin is then added and binds to the biotinylated detection antibodies. The level of each analyte is quantified by illuminating the beads with distinct light-emitting diodes (LEDs). The first LED identifies the analyte that is being detected, the second LED measures the magnitude of the PE-derived signal.

In brief, 50 µl of sample or standard was added to 50 µl of diluted microparticle cocktail in the 96-well microplates provided. Plates were sealed and incubated on a shaker at 200 rpm for 2 hours at room temperature. Using a microplate magnet (Bio-Plex Handheld Magnetic Washer, Bio-Rad) plates were washed three times with wash buffer. 50 µL of diluted Biotin Antibody Cocktail was added to each well. Plates were sealed and incubated on a shaker at 200 rpm for 2 hours at room temperature. Following a further three washes, 50 µL of diluted Streptavidin-PE was added to each well. Plates were sealed and incubated on a shaker at 200 rpm for 2 hours at room temperature. Following a final three washes, microparticles were resuspended by adding 100 µL of wash buffer to each well. Plates were sealed and incubated on a shaker at 200 rpm for 2 hours at room temperature. Plates were read on a

Bio-Rad Bio-Plex analyser using 50 events/bead with sample size set to 50 µL and doublet discriminator gates set to 8000 and 16500.

2.3.3 Immunofluorescence

Immunofluorescence is a powerful technique that utilizes fluorescent-labelled antibodies to detect specific target antigens (Robinson *et al*., 2009). Commercial HBEC and bronchial brush HBEC were immunostained for Cytokeratin 14 (CK-14) and E-cadherin.

Antibody	Clone	Isotype	Stock Concentration	Working Concentration
Anti CK14 fluorescein isothiocyanate (FITC) (Merck Millipore®)	RCK107	Monoclonal mouse IgG3	1mg/ml	5µg/ml
Anti E-Cadherin FITC monoclonal (Merck Millipore®)	67A4	IgG1	1mg/ml	2µg/ml
Anti uPAR monoclonal FITC (Sigma-Aldrich®)	PL231	IgG1	1.5mg/ml	5µg/ml
Mouse IgG3 Isotype Control (Thermofisher®)	-	-	1mg/ml	Dependant on primary
Mouse IgG1 Isotype Control (Sigma-Aldrich®)	-	-	1mg/ml	Dependant on primary
FITC Secondary	-	Goat IgG	1mg/ml	100µg/ml

Table 2.3.1: Details of Primary and Secondary Antibodies and Isotype Controls used for Characterisation of HBEC. Isotype controls were used at the same concentration as the corresponding primary antibody.

Differentiated HBEC were stained for uPAR using a modified method described in section 2.3.4. Cells were washed three times in phosphate buffered saline (PBS, Sigma) and then fixed in 4% formaldehyde for 15mins followed by three PBS washes. Cells were then blocked overnight at 4°C in 1%BSA in PBS +10%goat serum+0.15% triton X. Cells were then washed as described and primary antibody was added and cells were incubated overnight at 4°C.

Primary antibody was then aspirated and cells were washed and incubated with secondary conjugated antibody at 37°C for 45mins. Cells were then washed and mounted using Vectashield hard set media containing DAPI (4',6-diamidino-2-phenylindole) (Vectorlabs). Cells were imaged using a confocal microscope.

2.3.4 Immunofluorescence of Paraffin-Embedded Sections

Immunofluorescence detection of specific target antigens can be performed suing paraffin-embedded sections. Paraffin wax was removed by placing slides in a Coplin jar containing clean Histoclear II for 5 minutes, subsequent washes were carried out for 5 minutes. This was repeated using dirty Histoclear II. Slides were drained and dehydrated in clean absolute ethanol, followed by dirty absolute ethanol and were then re-hydrated in clean 95%v/v ethanol followed by dirty 95%v/v ethanol. Slides were then rinsed in distilled water 1 minute. For the antigen retrieval stage, slides were immersed in warmed Sodium Citrate Buffer (pH 6) for 40 minutes. Slides were washed sterile water. Cells were permeabilised, washed and were blocked by adding blocking solution (10%v/v Goat Serum in PBS) and incubating at room temperature in humidified chamber for 20 minutes. Slides were then washed and incubated with primary antibody overnight at 4^{o}C. Slides were then washed and incubated with the secondary antibody in the sealed chamber for 1 hour at room temperature. Slides were washed and dried before adding mounting media+DAPI onto each slide and a coverslip. Slides were allowed to set overnight at room temperature and cells were imaged using a confocal microscope.

2.3.5 Haemotoxylin and Eosin Staining

Haemotoxylin and Eosin staining is carried out to make cells fixed on histological sections visible. Eosin is an acidic dye which stains basic structures, such as the cytoplasm and some extracellular structures, pink. Haemotoxylin is a basic dye, it binds to tissue bound aluminium salts and stains the nuclei purple (Fischer *et al*., 2008). Firstly, the wax is dissolved and sections are rehydrated by washing for 5 minutes in Histoclear, followed by 100% ethanol and finally 95% ethanol. Sections are then washed in running tap water followed by 5 minutes in Mayers Haematoxylin. Sections are washed again in water and then stained for 5 minutes with Eosin. After a final wash in water, sections are blotted and dehydrated by 10 a second wash in 95% ethanol, followed by 10 a second wash in 100% ethanol and finally 10 seconds in Histoclear. Sections are then mounted using Vectamount and a glass coverslip.

2.3.6 Alcian Blue Staining

Alcian blue stains acidic mucin, the remaining mucins which are Periodic acid–Schiff positive and polysaccharide rich will not react (Bancroft and Gamble, 2008). Sections are deparrafinized and rehydrated as described in Section 2.3.5 and rinsed in 3% Acetic Acid. They are then stained with Alcian blue for 15 minutes. Sections are then washed in running tap water for 2 minutes the distilled water. Sections are rinsed again in 3% acetic acid to remove excess stain and reduce non-specific staining and washed in tap water followed by distilled water. Sections are counterstained in nuclear fast red solution for 5 minutes and washed in running tap water for 1 minute. Sections are then dehydrate as described in 2.3.5 for 3 minutes and mounted.

2.3.7 Microscopy

Fluorescence microscopy of submerged HBEC and ALI HBEC sections were carried out using the Improvision Spinning Disk Confocal Microscope (PerkinElmer UK) and Volocity imaging software with the Hamamatsu camera (C9100-13) (PerkinElmer). Green (fluorescein isothiocyanate, FITC) and blue (4,6-Diamidino-2-phenylindole, dihydrochloride, DAPI) filters were used. Individual images were taken per filter and were merged using Image J.

2.4 Bioinformatics

All RNA samples underwent RNA integrity analysis prior to sequencing. Sequencing was performed using Illumina sequencing machines however two different library preparation protocols are described in this thesis. RNA from HBEC isolated from cultured asthma patient and healthy control brushes was sequenced by the Genome Analysis Facility (GAF), Genomics Coordination Centre (GCC) University Medical Centre Groningen. RNA from engineered HBEC was sequenced by Deep Seq, University of Nottingham. All bioinformatics analyses were carried out using the Ubuntu Linux operating system version 12.04 LTS.

2.4.1 RNA Integrity Analysis

RNA was extracted using the RNeasy extraction kit (see Section 2.2.1), RNA integrity (RIN) analysis was carried out to assess the integrity of total RNA and the suitability for RNA sequencing and samples with RIN scores >8 are suitable for sequencing (Schroeder *et al*., 2006). RIN analysis was performed using the Agilent 2100 bioanalyser (Post Genomics Facility, University of Nottingham) and the Agilent RNA 6000 Nano kit (Agilent) which

included Agilent RNA 6000 Nano gel matrix and loading dye. In brief, RNA matrix gel was centrifuged at 1500 rpm for 10 minutes at room temperature. RNA dye was spun down and 1 µl was added per 65 µl of RNA matrix gel. The solution was then vortexed and spun at 13000 rpm for 10 minutes at room temperature. A RNA chip was placed in a chip priming station, 9 µl of the RNA matrix gel was loaded into the specified well and the chip priming station was closed for 30 seconds. The chip priming station was opened and 9 µl of the RNA matrix gel was pipetted into the same well. 5 µl of RNA marker was loaded into the sample and ladder wells. 1 µl of ladder and RNA sample was loaded into the specified wells, the chip was then vortexed at 2400 rpm for 5 minutes and immediately run on the Agilent 2100 Bioanalyser. The assay output includes an electropherogram of the ladder and sample well results (Figure 2.4.1) and RNA concentration, ribosomal ratio and the RNA Integrity Number (RIN).

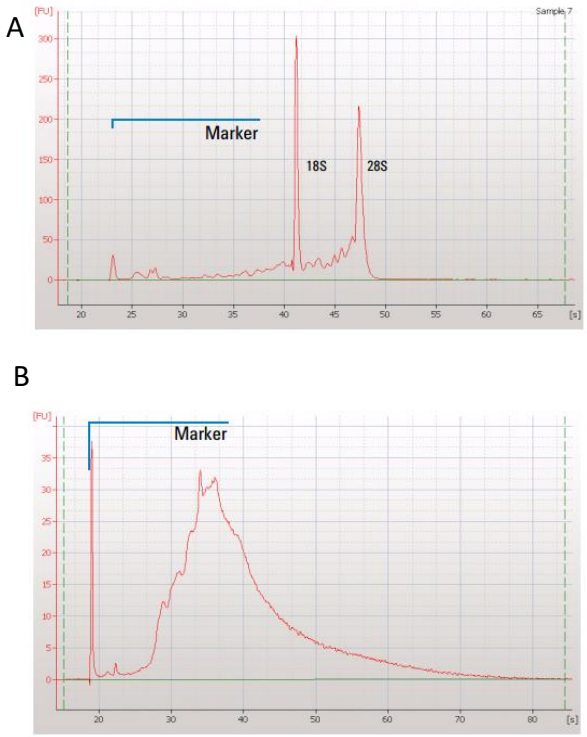


Figure 2.4.1: RNA Analysis Outputs from Agilent Bioanalyzer. (A) RNA peaks of a successful sample run for 18S and 28S rRNA and (B) mRNA peaks of a successful sample run. Key features of a successful sample run is the presence of 1 marker peak and a broad second hump indicating successful sample preparation.

2.4.2 RNA Sequencing

RNA sequencing (RNA-seq) uses next generation sequencing (NGS) to analyse RNA in biological samples, NGS is the collective term for high-throughput DNA and RNA sequencing methods (Finotello and Di Camillo, 2015). The 'flow cell' is a glass slide where the sequencing reaction occurs. Strands of cDNA are clonally amplified on the surface of the flow cell in a process termed bridge amplification, each strand is amplified many times forming clonal clusters. Flow cell bound cDNA templates are read by incorporating labelled nucleotides that compete for addition to the template. After each cycle a light source excites the bound nucleotide which then emits a characteristic fluorescent signal (base-calling), the number of cycles determines the length of the read.

2.4.2.1 Library Preparation and Sequencing of Patient RNA

Library preparation and sequencing was performed by Genome Analysis Facility (GAF), Genomics Coordination Centre (GCC) University Medical Centre Groningen. Initial quality check of and RNA quantification of the samples was performed by capillary electrophoresis using the LabChip GX (Perkin Elmer). Non-degraded RNA-samples were selected for subsequent sequencing analysis. Sequence libraries were generated using the TruSeq RNA sample preparation kits (Illumina) using the Sciclone NGS Liquid Handler (Perkin Elmer). In case of contamination of adapter duplexes an extra purification of the libraries was performed with the automated agarose gel separation system Labchip XT (PerkinElmer). The obtained cDNA fragment libraries were sequenced on an Illumina HiSeq2500 using default parameters (Paired End 2 x 100 bp) in pools of multiple samples. 51 RNA samples were

sequenced (asthma *n* = 33, healthy control *n* = 18) (for patient details and isolation of HBEC brush samples see section 4.3.2).

2.4.2.2 Library Preparation and Sequencing genetically engineered HBEC RNA

Two HBEC donors were genetically engineered to overexpress variants of uPAR, for sample details see section 5.4.1. Library preparation and sequencing was performed by Deep Seq, University of Nottingham. Paired end sequencing was performed using the Illumina NextSeq500 and generated 60 million paired end reads (75bp) for each sample. RNA concentrations were measured using Qubit RNA BR assay and RNA Integrity was assessed using the Agilent Bioanalyser. For mRNA enrichment and quality control 10 µg of total RNA was taken forward for polyA enrichment using Dynabeads Oligo (dT)25 (Life technologies, 610.02), two rounds of polyA enrichment were performed and mRNA was eluted in 7 µl. Following purification 1 µl of the polyA enriched mRNA was run on the Agilent Bioanalyser RNA pico 6000 chip. 50 ng of mRNA was used for library construction was used to construct sequencing libraries according to NEB Next Ultra Directional RNA Library Prep kit for Illumina (New England Biolabs, E7420S). 12 rounds of PCR cycles were used for library amplification, NEB next indexing kits (NEB, E7335S and E7500) were used for the amplification. Library quality control and quantification was carried out by diluting libraries 5-fold, libraries were run on the Agilent Bioanalyser high sensitivity chip to check the library fragment size and presence of adapter sequences. Libraries were quantified using qPCR (Kapa biosystems). Libraries were diluted to 4nM and pooled equally for sequencing runs, the library pool was denatured and diluted to 1.3pM and loaded onto the sequencer. Three runs were carried out for each sample, the libraries were re-pooled for second and third runs to account for

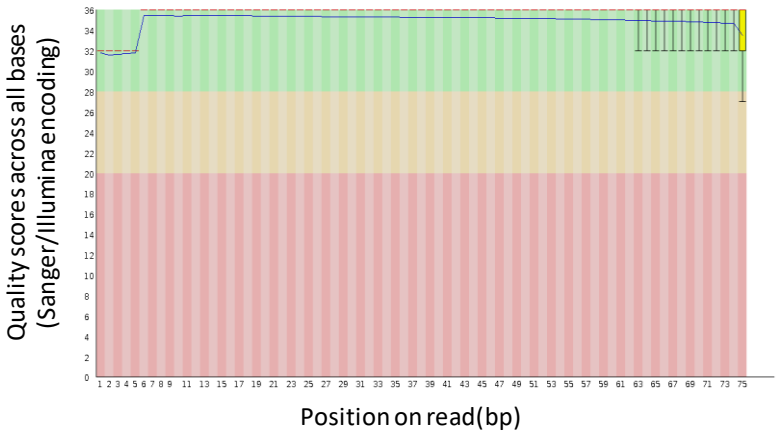
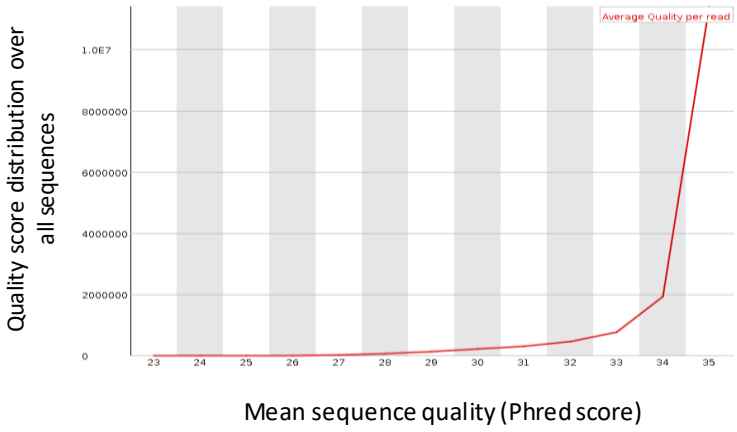
the difference in clustering, in order to balance the reads evenly across all samples. 12 FASTQ files were outputted for the forward and reverse reads for each sample.

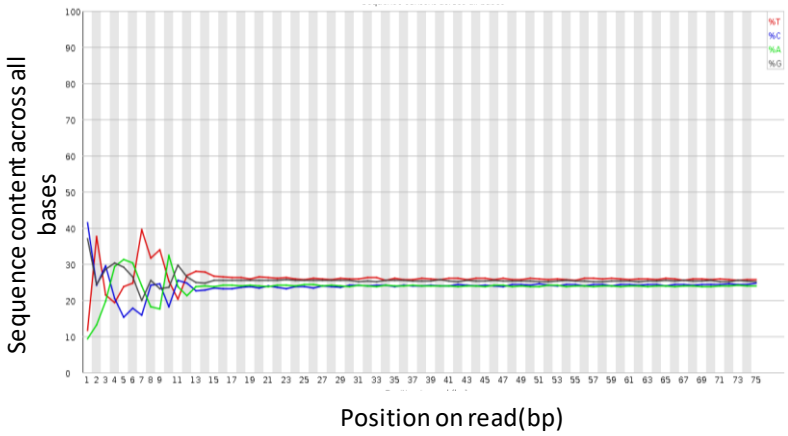
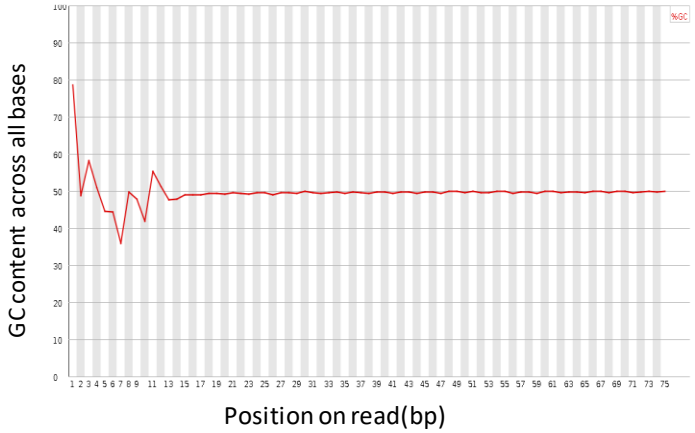
2.4.3 Processing Sequencing Data

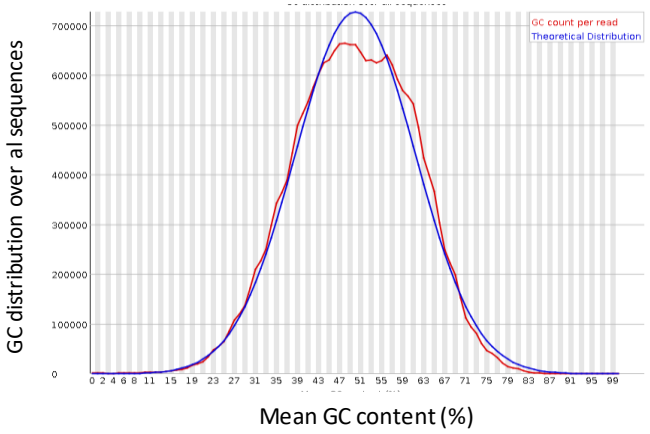
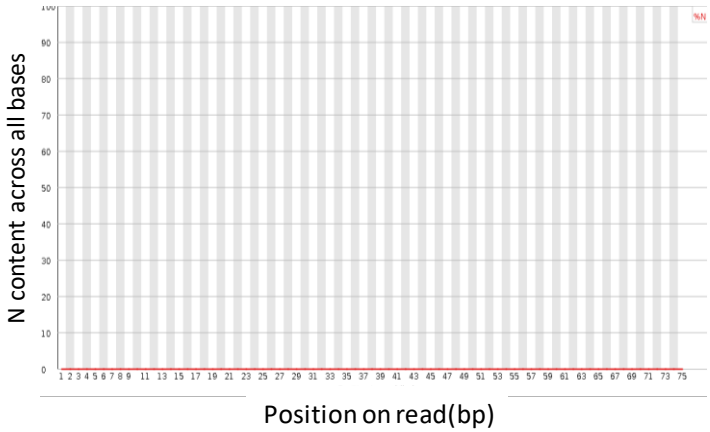
Raw RNA-seq data is outputted in FASTQ format, in the FASTQ format each nucleotide is associated to an encoded quality number corresponding to a Phred score (Q), which is a measure of the accuracy of base calling (and hence a measure of the quality of the sequencing). The presence of low quality nucleotides can have implications for downstream analysis. Regions of low quality can be identified and removed by read "quality trimming" (Del Fabbro *et al*., 2013).

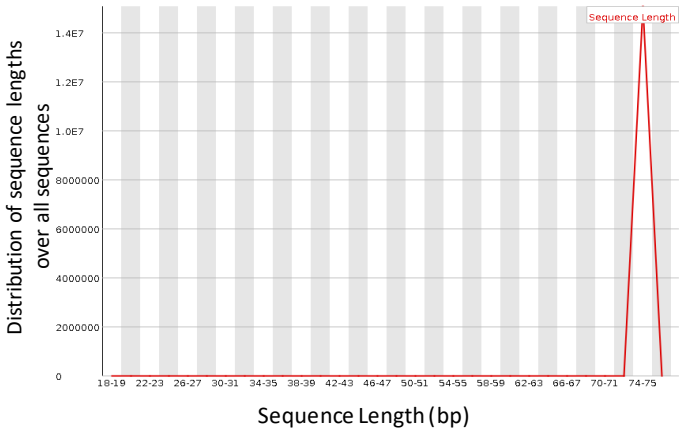
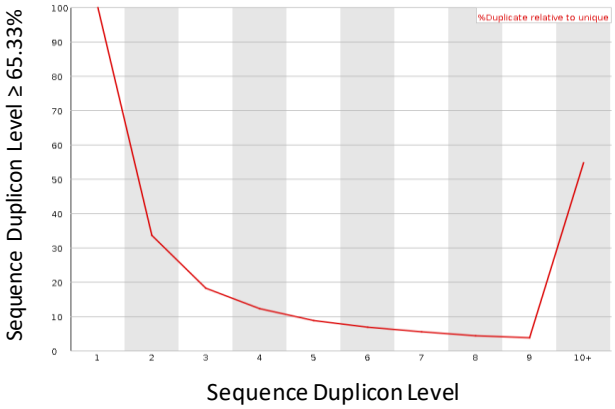
2.4.3.1 Adapter, Quality Trimming and FASTQC Analysis of Data

Adapter sequences flag the reads that contain sequences of interest, adapters must be removed by "Adapter trimming" so that only the relevant part of the read is used for downstream analysis. Adapter trimming was achieved using the Scythe© tool (https://github.com/vsbuffalo/scythe) and "Quality Trimming" was performed using Sickle (https://github.com/najoshi/sickle), reads with Q score <20 were removed. Reads underwent quality control analysis before and after trimming using FastQC© v0.10.1 (Simon Andrews, Babraham Bioinformatics). FastQC aims to identity biases in the data which may originate either in the sequencer or in the starting library material, as these may affect downstream analysis.

FastQC Module	Function
1. Basic Statistics	Simple composition statistics for the file analysed including; The total number of sequences processed; Sequence Length; The overall %GC of all bases in all sequences.
2. Per Base Sequence Quality	Assesses the range of quality values across all bases at each position in the FastQ file. A warning will be issued if the lower quartile for any base is less than 10, or if the median for any base is less than 25. 
3. Per Sequence Quality Scores	Identifies if a subset of sequences has universally low quality values. A warning is raised if the most frequently observed mean quality is below 27 - this equates to a 0.2% error rate. (Failure if error rate=1%). 

4. Per Base Sequence Content	Identifies the proportion of each base position in a file for which each of the four DNA bases has been called. This module issues a warning if the difference between A and T, or G and C is greater than 10% in any position. (Failure if 20%). 
5. Per Base GC Content	Measures the GC content of each base position in a file. This module issues a warning if the GC content of any base strays more than 5% from the mean GC content (Failure if 10%). 

6. Per Sequence GC Content	Measures the GC content across the whole length of each sequence in a file and compares it to a modelled normal distribution of GC content. A warning is raised if the sum of the deviations from the normal distribution represents more than 15% of the reads (Failure if 30%). 
7. Per Base N Content	Calculates the percentage of base calls at each position for which an N (sequencer unable to make a base call) was called. This module raises a warning if any position shows an N content of >5%. (Failure >20%). 

8. Sequence Length Distribution	Assesses the distribution of fragment sizes. Some sequencers can generate reads of varying lengths. This module will raise a warning if all sequences are not the same length. 
9. Duplicate Sequences	Counts the degree of duplication for every sequence in the set and creates a plot showing the relative number of sequences with different degrees of duplication. A low level of duplication may indicate a very high level of coverage of the target sequence, but a high level of duplication is more likely to indicate some kind of enrichment bias (e.g. PCR over amplification). This module will issue a warning if non-unique sequences make up more than 20% of the total. (Failure if 50%). 
10. Overrepresented Sequences	Lists all of the sequence which make up more than 0.1% of the total. If a single sequence is very overrepresented in the set either means that it is highly biologically significant, or indicates that the library is contaminated, or not as diverse as you expected.

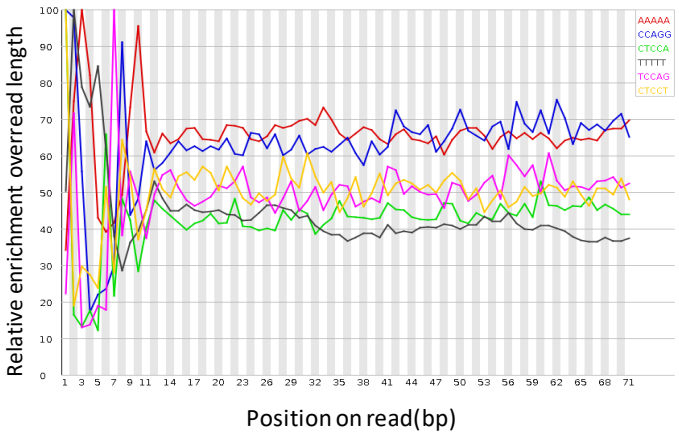
11. Overrepresented Kmers	Counts the enrichment of every 5-mer within the sequence library. It calculates an expected level at which this k-mer should have been seen based on the base content of the library as a whole and then uses the actual count to calculate an observed/expected ratio for that k-mer. The 6 most highly expressed k-mers are plotted. This module will issue a warning if any k-mer is enriched more than 3 fold overall, or more than 5 fold at any individual position. (Failure if 10 fold). 

Table 2.4.1: FastQC Module Summary. FastQC can be used to assess the quality of sequencing data (reads). FASTQ files inputted into the FastQC tool which has 11 analysis modules of which results are outputted into a summary report. Potential biases in the data that may affect analysis can be detected.

2.4.3.2 Concatenation of Data Files

Once FASTQ files for all samples had been trimmed and run through quality control, the FASTQ files from the same sample containing forward and reverse reads were concatenated using the 'zcat' command in linux to produce a single forward and reverse FASTQ file per sample. The concatenated files were then analysed using FastQC again to ensure the

concatenation step did not alter the files. A summary of the quality control programs used and the command lines used to execute their function can be found in Table 2.4.2.

Programme	Function	Command line
zcat	**Concatenates Data**	`zcat my.fastq.gz | wc -l`
Scythe	**Removes adapter sequences**	`path/scythe -a adapter_file.fasta -q solexa -p 0.1 -o trimmed_sequences.fastq sequences.fastq`
Sickle	**Removes low quality reads**	`path/sickle pe -f R1.fastq -r R2.fastq -t sanger -o qtrim.1.fastq -p qtrim.2.fastq -s qtrim.unpaired.fastq -q 20 -l 20`
FastQC	**Quality control of data**	`fastqc path/fastq`

Table 2.4.2: Summary of Programs Used to Trim and Assess Quality of RNA-Seq Read files. The 'zcat' command (Ubuntu Linux operating system version 12.04 LTS) was used to concatenate FASTQ files. Scythe (https://github.com/vsbuffalo/scythe) and Sickle (https://github.com/najoshi/sickle) were used to remove adapters and low quality reads. FastQC analysis was performed to ensure data file processing had not corrupted read files.

2.4.4 Alignment of Reads Using TopHat2

TopHat2 maps splice junctions for RNA-seq reads by aligning reads to the relevant genome using the high-throughput short read aligner Bowtie (http://bowtie-bio.sourceforge.net), mapping results are then analysed to identify splice junctions (Trapnell *et al*., 2012). Tophat2 v2.0.12 (Cole Trapnell, Center for Bioinformatics and Computational Biology, University of Maryland) was used to align the reads to human assembly GRCh37 (http://grch37.ensembl.org/index.html) and produced a single BAM file for each RNA sample sequenced, which can then be used for downstream analysis.

TopHat Arguments	Description
-G <genome_index_base>	The basename of the genome index to be searched.
-p/--num-threads <int>	Use this many threads to align reads. The default is 1.
-o/--output-dir <string>	Sets the name of the directory in which TopHat will write all of its output. The default is "./tophat_out".

TopHat Command Line	tophat -p 5 -G genes.gtf -o .bam genome.fasta R1.fastq R2.fastq

Table 2.4.3: Arguments and Command Line used to run TopHat2 Read Alignment

TopHat output	Description
accepted_hits.bam	A list of read alignments in SAM/BAM format. SAM/BAM is a compact short read alignment format
junctions.bed	A UCSC BED track of junctions reported by TopHat. Each junction consists of two connected BED blocks, where each block is as long as the maximal overhang of any read spanning the junction. The score is the number of alignments spanning the junction.
insertions.bed and deletions.bed	UCSC BED tracks of insertions and deletions reported by TopHat.
Insertions.bed chromLeft	Refers to the last genomic base before the insertion.
Deletions.bed chromLeft	Refers to the first genomic base of the deletion.

Table 2.4.4: TopHat2 Read Aligner Command Line and Output Files

2.4.5 Differential Gene Expression Analysis

The Cufflinks suite (v2.2.1) includes a series of program that enable transcriptome assembly and differential gene expression analysis of RNA-Seq data (Trapnell *et al*., 2012). Cufflinks is made up of multiple programs, 5 of which were used for RNA-Seq analysis in this thesis and are summarised in Table 2.4.3.

Program	Function
Cufflinks	Transcriptome assembly and quantification
Cuffcompare	Compares transcriptome assembly to "reference" or assemblies of other samples
Cuffmerge	Merges all transcriptome assemblies into a "master transcriptome", which is required for differential gene expression analysis
Cuffdiff	Compares expression levels of genes and transcripts
Cuffnorm	Normalises Fragments Per Kilobase Million (FPKM) expression levels

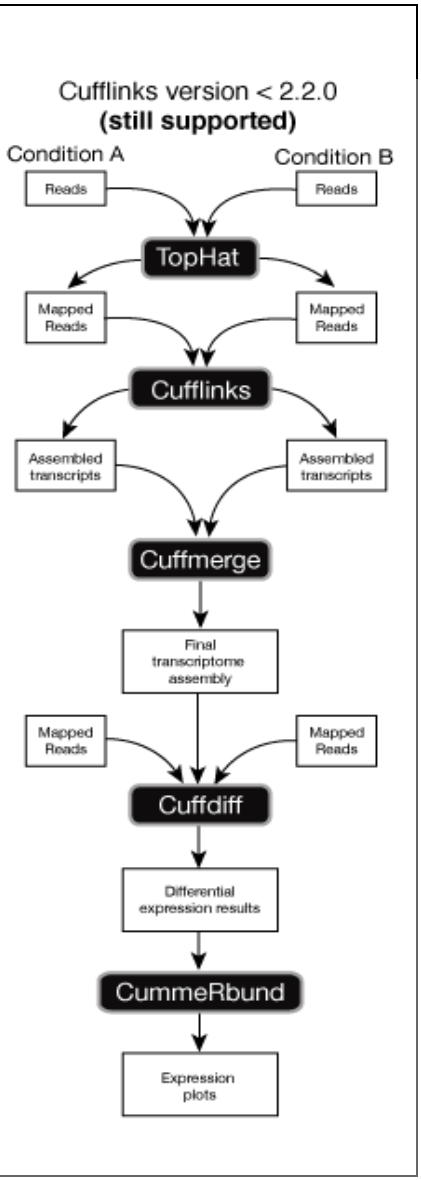


Figure 2.4.2: Summary of the Cufflinks Suite of Tools used for RNA-Seq Analysis and TopHat-Cufflinks Pipeline

In order to identify differentially expressed genes, BAM alignment files were run through Cufflinks for transcriptome assembly. The assemblies were then merged together using Cuffmerge to provide a master transcriptome from which gene and transcript expression could be calculated for each condition. The BAM files, containing the aligned reads, and the merged assembly were then used by Cuffdiff to calculate gene expression levels Fragments Per Kilobase of transcript (FPKM) and test for statistical significance (10% False Discovery

Rate). Cuffdiff outputs were reported as text files and results were graphed using GraphPad PRISM. The command lines used for the differential expression analysis protocol are summarised in Table 2.4.5.

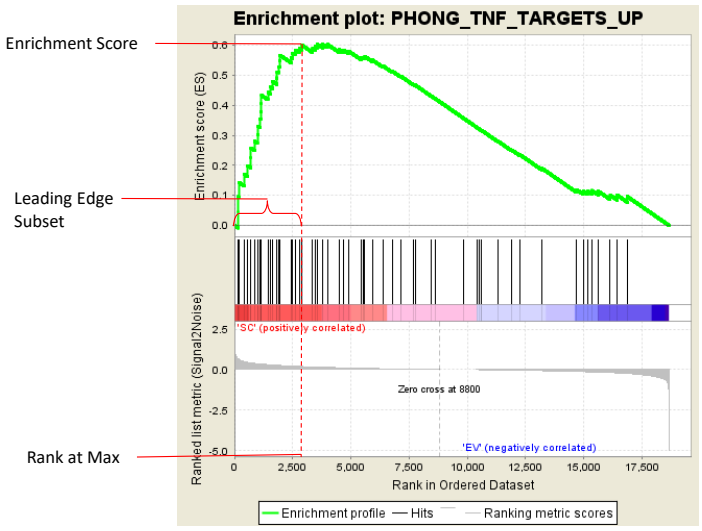
	Analysis Step	Command line
1	Transcriptome assembly using Cufflinks	cufflinks [options] <aligned_reads.(sam/bam)>
2	Merge transcriptomes to generate a reference assembly using Cuffmerge	cuffmerge [options]* <assembly_GTF_list.txt>
3	Quantify and compare gene expression using Cuffdiff	cuffdiff [options]* <transcripts.gtf>

Table 2.4.5: Differential Gene Expression Analysis Steps Using Cufflinks Package

2.4.6 Gene Set Enrichment Analysis

Gene set enrichment analysis (GSEA) is a method that examines gene expression data at the level of gene sets, which are compiled based on published data or co-expression studies (Subramanian *et al*., 2005). The annotated gene sets are organised into the Molecular Signatures Database (MSigDB). GSEA identifies if members of a gene set (S) are randomly distributed throughout a gene list (L) or occur toward the top or bottom of the L. GSEA calculates an Enrichment Score (ES) which is defined as "the degree to which a set S is overrepresented at the extremes (top or bottom) of the entire ranked list L. The magnitude of the increment depends on the correlation of the gene with the phenotype. The enrichment score is the maximum deviation from zero encountered in the random walk; it corresponds to a weighted Kolmogorov–Smirnov-like statistic" (Subramanian *et al*., 2005) GSEA then estimates the statistical significance of the ES and also adjusts the estimated significance for multiple hypothesis testing. Not all genes within a gene set contribute to the ES, the genes that account for the enrichment signal are termed the Leading-Edge Subset. The Leading-Edge Subset genes in high scoring gene sets can highlight biologically relevant

genes. Three statistics are used to define the leading edge subset; Tags, List and Signal. 'Tags' indicates the percentage of genes contributing to the enrichment score. 'List' indicates where in the gene list the enrichment score is attained and 'Signal' combines the previous two statistics to calculate the enrichment signal strength.



Phenotype	uPAR.cls#SC_versus_EV_repos
Upregulated in class	SC
GeneSet	PHONG_TNF_TARGETS_UP
Enrichment Score (ES)	0.6042305
Normalized Enrichment Score (NES)	1.965128
Nominal p-value	0.0
FDR q-value	0.097868316
FWER p-Value	0.087

Figure 2.4.3: GSEA Enrichment Plot and Results Summary. Example of an enrichment plot generated for the pathways (gene sets) tested, GSEA is able to calculate the enrichment score for a given gene set in the dataset analysed. Leading edge genes are outputted separately in html or XML format. FDR = false discover rate; FWER = family wise error rate.

To perform GSEA Cuffnorm first was used to generate FPKM counts, this data was then parsed in two stages so that it was in the correct format for the program. The first parsing script splits genes into separate rows if they occur in the same row, (separated by a ',') and assigns each separated gene (these have the same XLOC id) the same expression value. The script does not process newly discovered genes and does not process genes that occur

multiple times. The second script sums the FPKMs to generate a final single FPKM per gene FPKM per sample. The gene expression used by GSEA will be the sum of all XLOC FPKMs that belong to a gene. The advantage of this is that it is an alternative to averaging the data, using the average may skew the data. The main disadvantage is that genes that had multiple XLOCs assigned to them may by overrepresented as their reads will be counted additional times. However, this issue will apply to all samples that have multiple XLOCs so any effects should be cancelled out during GSEA.

	Analysis Step	Platform/ program	Command
1	Run Cuffnorm to generate normalised FPKM values for individual samples	Linux	`cuffnorm [options] <transcripts.gtf> <sample1_replicate1.sam[,…,sample1_replicateM.sam]>`
2	Remove duplicates from cuffnorm output	Linux (python)	`gene.perXLOC_exp_parser.py`
3	Run parser script to format data	Linux (python)	`expression_table_parser.py`
4	Run GSEA	GSEA	Load expression dataset: gsea_exp_c2.all.txt Load phenotype file: uPAR.cls Set parameters and run GSEA (collapse dataset to gene symbols: false; permutations 1000

Table 2.4.6: Summary of GSEA workflow. Gene expression levels generated using the Cufflinks tool, Cuffnorm, which were then parsed (formatted) for GSEA analysis

A phenotype file is required, detailing the number of phenotypes and number of replicates. GSEA computes the enrichment score, normalised enrichment score, *p* value and false discovery rate (FDR) for each gene set. A report is also generated detailing the number of gene sets enriched in a phenotype (FDR <25%), the number and details of enriched gene sets with a *p* value of less than 1% and 5%.

2.5 Statistical Analyses

All statistical analyses were carried out in GraphPad PRISM version 7.01. Details of specific statistic methods are described.

2.5.1 Analyses of Variance

Tests carried out to identify variance in the mean (parametric) or median (nonparametric) occurring between groups can be categorised based on the number of samples analysed. When comparing two independent samples either a Student's t-test (parametric) or Mann-Whitney test (non-parametric) was used, non-parametric tests were performed when using small datasets (n<20). All tests were carried out as two-tailed, where the null hypothesis is rejected when the value of the test statistic is either sufficiently small or sufficiently large i.e. you are testing the possibility of the relationship in both directions. A one-tailed test only tests the effect in one direction and provides more power to detect an effect in one direction. Either a one-way ANOVA (parametric) or a Kruskal-Wallis test (nonparametric) was carried out when comparing measurements across treatments. Post-hoc tests were conducted to confirm where the differences occurred between the groups. The Tukey's post-hoc test compares all columns to each other whereas a Dunnet's compares columns to a selected control column. A two-way ANOVA was used to compare measurements over time, post-hoc analysis was carried out using the Bonferroni test. Area under the curve (AUC) analysis was used for TEER and ECIS data over time, media was normalised to the media control from each experiment.

2.5.2 Linear regression

Regression analysis was used to model the relationship between protein expression and TEER using a straight line. Linear regression fits a straight line through the data to calculate the best fit value of the slope and intercept. The slope is equal to the change in Y (usually the outcome under investigation) for each unit change in X (usually the exposure variable). The Y intercept is the value of Y when X is equal to zero.

2.5.3 Correlation Analysis

Correlation analysis was used to compute a correlation coefficient (*r*) which is a measure of the strength and direction of a linear relationship between two variables e.g. protein expression vs TEER. Where *x* and y have a strong positive linear correlation (as values for *x* increases, values for *y* also increase) *r* is close to +1. Where *r* is close to -1 this indicates *x* and *y* have a strong negative correlation. Correlations in this thesis are non-normal (non-parametric) datasets therefore the non-parametric version of the statistical tool (Spearman's Correlation) was used.

Chapter 3: The Urokinase Pathway as a Regulator of Airway Epithelial Barrier Properties

3 The Urokinase Pathway as a Regulator of Airway Epithelial Barrier Properties

3.1 Introduction

An improved understanding of the underlying pathways of asthma is needed to develop treatments that target specific asthma phenotypes, particularly in patients with severe asthma where this unmet need is greatest (Bucchieri, Marino Gammazza *et al*. 2015). Asthma is increasingly being viewed as a disease of the epithelium and emphasis is needed for therapies that target these cells and improve the airways' barrier function to prevent penetration of inhaled stimuli across the airway wall (Holgate 2011). As discussed in Chapter 1, airway epithelial cells form a barrier to the outside environment and regulate the mucosal immunity of the airways. Apical junction complexes (AJCs), mucus and airway secretions together form the epithelial barrier. AJCs are made up of TJs and AJs which have been shown to be dysfunctional in asthma (Vermeer, Denker *et al*. 2009, Short, Kasper *et al*. 2016). An intact barrier and functional AJCs are required for regulation of cell polarity, cell-cell contact, movement of ions and macromolecules and to prevent microbes and viruses from crossing from the lumen into the airways (Georas and Rezaee 2014). The asthmatic epithelium is structurally and functionally impaired in asthma which has implications for its barrier function properties (Grainge and Davies 2013).

The airway epithelium in asthma undergoes abnormal repair and is more susceptible to damage from environmental stimuli such as cigarette smoke (Olivera, Boggs *et al*. 2007), rhinovirus (Sajjan, Wang *et al*. 2008) and house dust mite allergens (Tai, Tam *et al*. 2006). Chronic inflammation has been considered a cause of TJ damage and epithelial barrier

disruption (Wittekindt 2017). TJP expression and localisation is regulated by cytokines including TNF-α which modulates intracellular localisation of TJPs (Coyne, Vanhook *et al*. 2002) and type 2 cytokines IL-4 and IL-13 increase paracellular permeability in human bronchial epithelial cells (Saatian, Rezaee *et al*. 2013). Understanding the molecular regulation of TJPs in the lung, including damage during inflammation, may help understand how we can target the epithelium to improve the management and control of asthma (Wittekindt 2017). The paradigm that inflammation causes TJ damage does not account for changes in TJs induced by airway remodelling, furthermore defects in epithelial TJs are maintained in passaged epithelial cells suggesting these changes may be in part be inherent and independent of inflammation (Xiao, Puddicombe *et al*. 2011). It has also been shown that remodelling processes such as basement membrane thickening, epithelial secretion of TGF-β and mucous cell metaplasia are largely driven by mechanical forces caused by bronchoconstriction (Grainge, Lau *et al*. 2011). It is probable that multiple factors alter TJs and contribute to increased epithelial permeability in the airways in asthma, the clinical implications of a defective epithelial barrier are not yet known. Impaired barrier function may lead to over-activation of the immune response and airway inflammation, understanding the mechanisms of epithelial damage in asthma may help evaluate the effects on disease progression (Holgate 2013).

Matrix metalloproteinases (MMPs) are a group of proteases involved in extracellular matrix (ECM) degradation (Smith and Marshall 2010), MMP activity is tightly controlled through gene transcription (e.g. by growth factors and cytokines), activation via proteolytic cleavage and inhibition by tissue inhibitors of metalloproteases (TIMPs) (Vermeer, Denker *et al*. 2009). The protease plasmin is activated by uPAR-uPA interaction, plasmin is required for cleavage and activation of MMPs including MMPs-3, 9 and 12 (Carmeliet, Moons *et al*. 1997). The pro-

inflammatory environment of the asthmatic airway is thought to dysregulate this process resulting in elevated MMP activity, MMP-9 in particular has been implicated in asthma pathology and is elevated in epithelial biopsies from asthma patients (Ohno, Ohtani *et al*. 1997) and induced sputum in severe asthma (Mattos, Lim *et al*. 2002). In addition to ECM degradation MMP-9 is associated with airway remodelling and epithelial damage. MMP-9 treatment in HBEC results in impaired localisation of TJPs (claudin-1 and occluden), altered barrier integrity and detachment-induced cell death and MMP-9 activity is suppressed by azithromycin which promotes epithelial barrier formation (Vermeer, Denker *et al*. 2009; Slater, Torr *et al*. 2016). The regulatory processes upstream of MMP-9 which lead to its dysregulation are not fully understood.

Soluble forms of uPAR modulate MMP-9 and plasmin activity in HBEC as well cellular proliferation and migration, suggesting that uPAR may play a role in epithelial cell homeostasis and airway remodelling. MMP-9 and uPAR have been shown to interact in numerous cancers (Veeravalli and Rao 2012) however their co-expression and possible interaction in airway epithelial cells has not been confirmed.

As discussed in Chapter 1, scuPAR is a soluble form of uPAR which results from cleavage of its GPI anchor (Hoyer-Hansen 1992). uPAR SNPS are associated with lung function (Barton, Koppelman *et al*. 2009) and airway remodelling in asthma (Ierodiakonou, Portelli *et al*. 2016) and elevated scuPAR levels in serum are associated with more severe and nonatopic subphenotypes of asthma (Portelli, Moseley *et al*. 2016). Together these findings suggest that aberrant expression and regulation of scuPAR may have implications on airway structural changes and epithelial function in lung disease (Ierodiakonou, Portelli *et al*. 2016).

Therefore, we hypothesised that altered expression of the uPAR pathway may regulate airway epithelial barrier function and inflammatory cytokine secretion.

Transepidermal water loss (TEWL) is a measure of inside-out barrier function of the epidermal barrier (Georas and Rezaee 2014). There is no equivalent to TEWL to monitor inside-out barrier function of the airway epithelium in asthmatic patients therefore we used two physiologically relevant model systems to investigate whether or not there is a relationship between airway epithelial barrier function and the uPAR pathway. ALI and ECIS were both used to study barrier function in basal and differentiated airway epithelial cells. Both ALI and ECIS allow measurements to be taken in real time and factors can be added to manipulate cell behaviour. The ALI model pushes cells to form a pseudostratified epithelium that develop a transepithelial electrical resistance (TEER), which is marker of TJ formation and barrier function (Blume, 2010). Primary airway epithelial cells can be cultured at an ALI to drive them to differentiate and form a pseudostratified epithelium. ALI cultures display markers of differentiation, including ZO-1 and β tubulin IV, by day 14 and can be successfully cultured for 28 days (Bérubé, Prytherch *et al*. 2010). Cells are seeded on to the porous membranes of a transwell insert, on reaching confluency media is removed from the apical compartment and replaced in the basal compartment only (Yamaya, Finkbeiner *et al*. 1992). The ALI protocol used for this study is discussed in detail in section 3.3.1. Conditions mimic those of the human airways driving cells towards a mucociliary phenotype, forming tight junctions and differentiating to ciliated, basal and secretory cells. Primary airway epithelial cells cultured at ALI share a high degree of similarity with the transcriptional profile and morphological characteristics of *in vivo* primary epithelia (Pezzulo, Starner *et al*. 2011).

We also a used a second model system, ECIS, to study the effects of blocking uPAR on epithelial barrier properties (resistance) and also cell adhesion and spreading properties of HBEC by measuring cellular capacitance. ECIS is non-invasive therefore causes less disturbance to cells, however can only be carried out using submerged undifferentiated cultures. Both techniques have advantages as well as technical drawbacks therefore both were used to provide a comprehensive evaluation of the relationship between uPAR expression and epithelial barrier formation and maintenance. uPAR interacts with multiple ligands and co-receptors including uPA and integrins α3β1 or α5β1, distinct binding sites for these ligands (Figure 3.1.1) enables coordinated regulation of receptor functions such as cell adhesion and signalling (Degryse, Resnati *et al*. 2005; Gårdsvoll, Gilquin *et al*. 2006; Madsen, Ferraris *et al*. 2007). ECIS experiments included 3 blocking antibodies that target distinct uPAR epitopes.

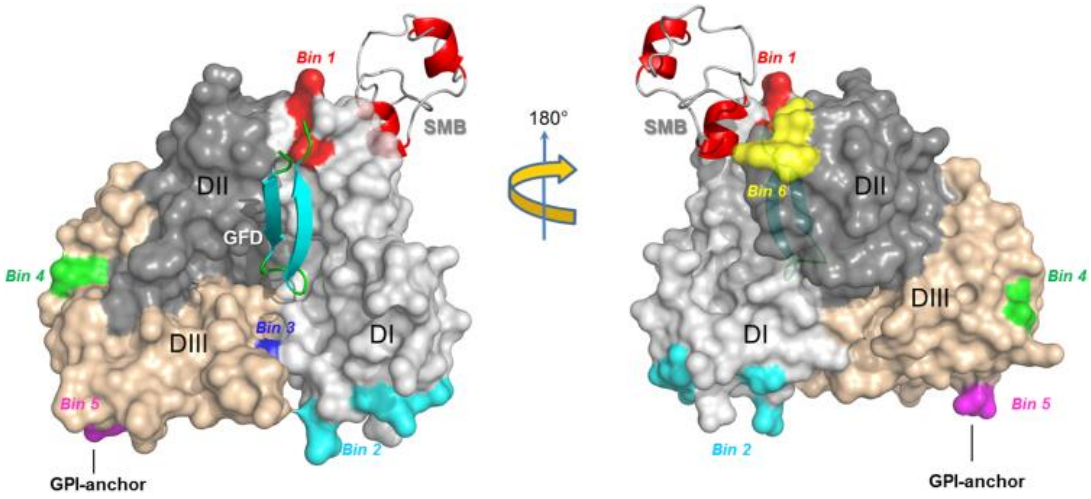


Figure 3.1.1: Topographic landscape on human uPAR for different monoclonal antibody epitope bins. Ly-6/uPAR (LU) domains colour coded; DI (light grey), DII (dark grey) and DIII (wheat). The growth factor like binding domain (GFD) and Somatomedin B domain (SMB) are the binding domains for urokinase (uPA) and vitronectin, respectively. Defined epitope bins are highlighted in red (BIN1), cyan (BIN2), blue (BIN3), green (BIN4), magenta (BIN5) and yellow (BIN6). (Zhao *et al*., 2015)

3.2 Aims

The aim of this current chapter was to provide greater insight into the role of the uPAR-uPA pathway in the formation and maintenance of the bronchial epithelial barrier.

3.2.1 Specific Aims

- Characterise the expression profile of the uPAR pathway in the ALI model of the airway epithelium.
- Assess the relationship between uPAR, uPA, PAI-1 and MMP-9 expression and epithelial barrier function during differentiation and in an established barrier.
- Assess the relationship between the uPAR pathway and barrier function and adhesive properties in undifferentiated cells.
- Assess the effect of blocking specific uPAR epitopes linked to specific uPAR functions on epithelial barrier function and cell adhesion.

3.3 Methods

3.3.1 Air Liquid Interface Culture of Human Bronchial Epithelial Cells

Human bronchial epithelial cells (Lonza® Castleford, UK) were seeded at passage 3 to collagen-coated 6.5mm transwells with 0.4 µm pore polyester inserts (50,000 cells per well) in 200 µl (BEGM). Collagen solution was made up by dissolving PureCol Type 1 Bovine Collagen solution into sterile water at a ratio of 1:100 to make a 30 µg/ml solution. 100 µl of collagen solution was added to each transwell and incubated for 30 minutes at 37 °C, and then aspirated.

2-3 days post seeding once cells had formed a confluent monolayer media was removed from the apical compartment ('airlift'-day 0 ALI). Cells were washed with 200 µl of PBS and BEGM was replaced with bronchial epithelial differentiation medium (BEDM) in the basal compartment only. To prepare BEDM, 2X BEGM was prepared with the exception of retinoic acid and gentamicin, and supplemented with 0.5 % BSA (1.5mg/ml). Dulbecco's Modified Eagle Medium (DMEM) was supplemented with 1% Sodium Pyruvate; 1% Non-essential Amino Acids; 1% Penicillin-Streptomycin-Fungiezone (PSF) and 1% L-glutamate. Retinoic acid was prepared by diluting 50 mg of retinoic acid (molecular weight: 300.44 g/mol) in 1.25 ml of sterile DMSO to give a 0.1 M solution. This solution was diluted in 11.25 ml DMSO to make a 0.01 M solution. 5 µl of the 0.01 M solution were then diluted in 1 ml of BEDM to give a 50 µM solution. 1X BEDM was prepared by mixing DMEM and 2X BEGM 1:1 and spiked with 50 nM of retinoic acid at the time of use. Apical washes were carried out by adding 200 µl of PBS to the apical compartment and incubating for 20 minutes at 37°C. Apical washes and

basolateral supernatants were collected at days 7, 14 and 21 ALI and stored at -°C. An overview of the culture procedure is shown in Figure 3.3.1.

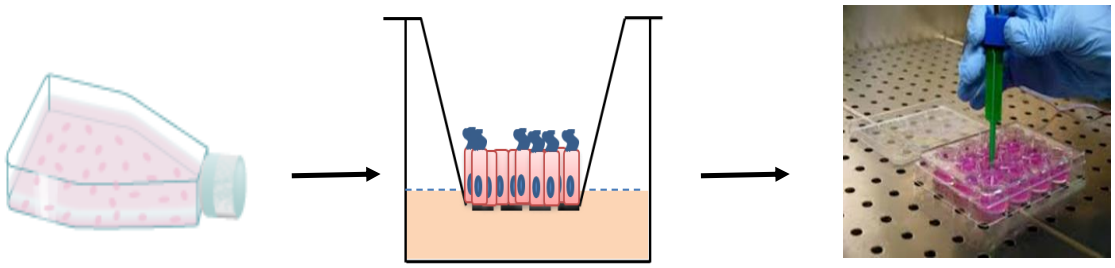


Figure 3.3.1: Air Liquid Interface Procedure. Schematic showing submerged culture and cells under ALI conditions using transwell inserts. Transepithelial electrical resistance (TEER) measurements were recorded and cell supernatants were collected at day 7, 14 and 21 ALI.

3.3.2 Measuring Transepithelial Electrical Resistance

Differentiated airway epithelial cultures develop transepithelial electrical resistance, measurement of TEER can be used to study barrier properties of the airway epithelium and is used as an indirect measure of tight junction formation (Stewart, 2012).

Medium was aspirated from the transwell and replaced with 200 µl and 500 µl in the apical and basolateral compartments, respectively. Cultures were equilibrated at 37°C for 30 minutes before measurement of TEER. TEER was measured using the EVOM2, Epithelial Volt-ohmeter as per manufacturer's instructions (World Precision Instruments, UK). STX2 chopstick electrodes were disinfected with 70% ethanol and washed with PBS and then sterile water, and allowed to equilibrate in BEDM for 30 minutes before use. To measure

background resistance electrode tips were immersed into a well containing media only. This was then repeated for epithelial cultures. Actual resistance was calculated using the equation below:

Actual resistance (Ω/cm^2) = (Measured resistance (Ω) - Control resistance (Ω)) x insert area (cm^2)

3.3.3 Stimulation of ALI Cultures

In order to determine the effect of uPAR activation via uPA and the effect of soluble uPAR differentiated HBEC cultures were stimulated at day 21 ALI with recombinant protein for 4 and 24 hours (soluble uPAR, R&D systems, 1310-SE-010; uPA, R&D systems, 807-UK-100/CF). ALI cultures were stimulated with recombinant soluble-uPAR and recombinant uPA to investigate the effects of these proteins on epithelial barrier properties. Key outcomes included TEER measurements and expression of inflammatory cytokines and chemokines post-stimulation.

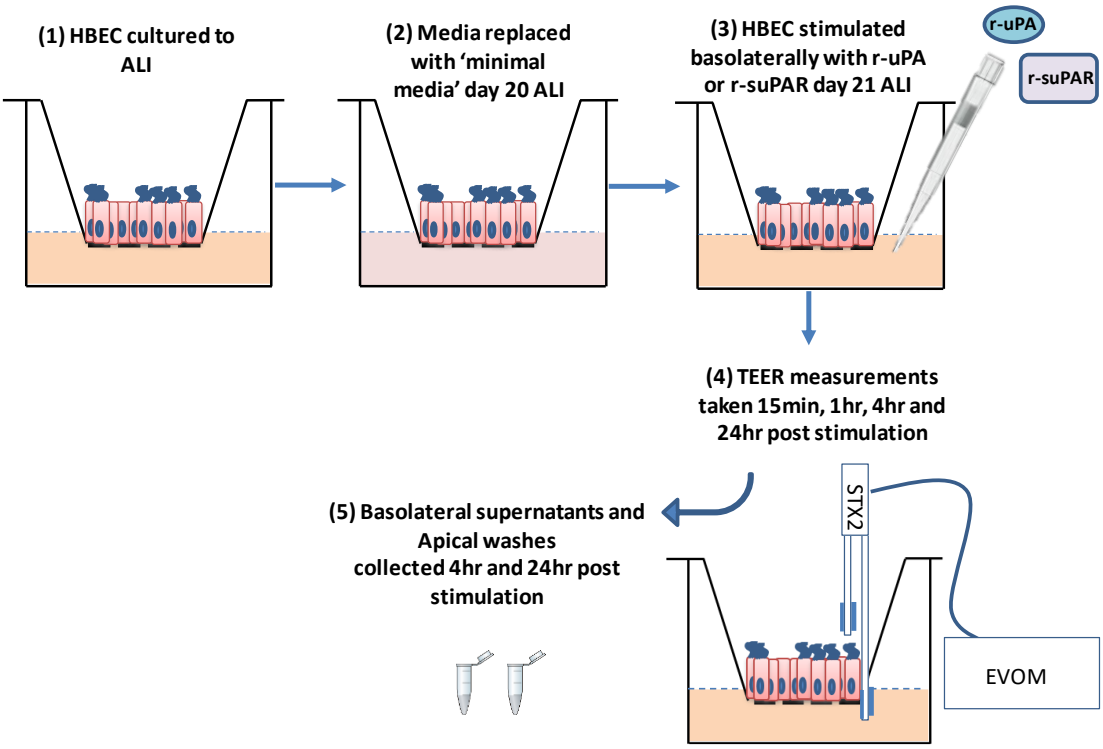


Figure 3.3.2: Stimulation of ALI cultures: Schematic illustrating the procedure used to stimulate ALI cultures at with recombinant urokinase (r-uPA) and recombinant soluble uPAR (r-suPAR). HBEC were cultured at ALI, media was replaced with minimal medium at day 20 and cultures were stimulated basolaterally at day 21 ALI. TEER measurements were taken using STX2 electrode set for the Epithelial Volt/Ohm Meter (EVOM) and apical washes and basolateral supernatants were collected post stimulation.

BEDM medium for ALI cultures was replaced 24 hours prior to stimulation with a 'minimal medium' which was prepared by supplementing bronchial epithelial basal medium (BEBM) with 1% Insulin-Transferrin-Sodium Selenium (ITS) and 1% BSA (Xiao *et al.*, 2011). Cells were then washed with 200 µl PBS and stimulated basolaterally with 1 µg /ml recombinant uPA and suPAR for 24 hours**,** antibodies were prepared in minimal medium**.** TEER readings were taken at 15 minutes, 1 hour, 4 hours and 24 hours post stimulation as described in Section 3.3.2. Basolateral supernatants, apical washes, TEER measurements and RNA were collected at 4 hours and 24 hours post stimulation.

3.3.4 Preparation of Transwell Inserts for Histology of Transwells

Transwells were processed, embedded and sectioned by Histopathology, Queen's Medical Centre. Briefly, the membrane was cut out of the insert and placed in a cassette and processed overnight. Processed cells were then embedded in paraffin wax and sectioned at 4 microns. Sections were mounted onto SuperFrost Ultra Plus® slides and incubated overnight at 55°C and then stored at room temperature until use. Sections were stained using Haemotoxylin and Eosin and Alcian blue staining as described in sections 2.3.5 and 2.3.6, respectively.

3.3.5 Antibody Blocking of uPAR Epitopes

To inhibit specific uPAR binding epitopes and therefore specific functions of uPAR, basal epithelial cultures cells were treated with anti-uPAR clones R3 and R4 and anti-uPAR ATN 658. Prior to seeding, cells were incubated in solution with 1µg/ml of each antibody and IgG1 isotype control for 1 hour. Antibodies and isotype control were diluted to working concentrations in BEGM at the time of use. The antibodies bind to distinct receptor-binding domains, R3, R4 and ATN-658 bind in bins 1, 4 and 5, respectively (see Figure 3.1.1). Cells were then seeded at 1.875 x 10^5 cells/ ml to cell culture arrays for subsequent ECIS experiments.

3.3.6 Electric Cell-substrate Impedance Sensing

Electric Cell-substrate Impedance Sensing is a method that can be used to study characteristics of a cell monolayer (Giaver and Keese, 1993). These include morphological changes, barrier properties and cell locomotion. Cells are cultured on gold electrodes and a

small alternating current is applied (~1uA) resulting in a potential across the electrodes that can be measured. As the cell monolayer changes impedance is affected and these changes are recorded, from this resistance and capacitance are calculated using Ohm's Law.

$$Z = V/I$$

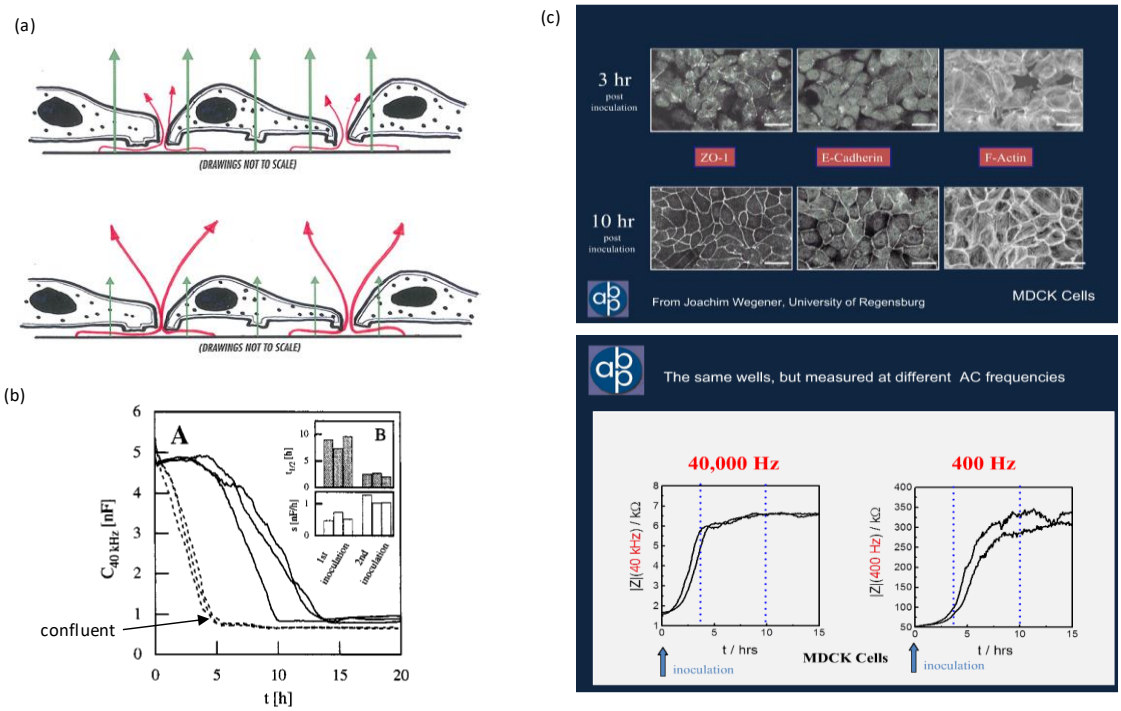


Figure 3.3.3: Electrical Cell-Substrate Impedance Sensing. (a) Cross section of a confluent cells layer where the path of the current is indicated by the arrows. Green arrows indicate current moving capacitively through cell membranes. The current flow moving through the paracellular passage between the cells (the barrier function) is represented by red arrows. (b) Cell capacitance demonstrating cell attachment to electrodes coated with different protein layers. The arrow indicates cells have attached and have formed a confluent layer. (c) Staining for junctional proteins Z0-1, E-Cadherin and structural protein F-actin at 3 h and 10 h post-seeding and impedance measurements from the same wells at 40,000 Hz and 400 Hz. The cell layer is confluent by 3 hours post-seeding, this is conveyed by the plateau in impedance at 40,000 Hz. At 400Hz we see that the formation of barrier function is not completed until 10 hours. (Adapted from http://www.biophysics.com/ecismodel.php and (Wegener *et al*., 2000).

The ECIS instrument measures voltage changes at multiple frequencies. At higher frequencies impedance is affected mostly by cell coverage, more current travels through cells indicating monolayer formation. At low frequencies impedance is affected mainly by changes in spaces between and under cells, more current travels through the gaps between cells giving information regarding barrier formation and permeability (Szulcek *et al*., 2014).

In brief, 8W10E array (IBIDI) wells were treated with 200 µl of 10 mM L-cysteine for 15 minutes at room temperature. Arrays were then washed 3 times with 300 µl of sterile water and coated with collagen by adding 200 µl of PureCol Type 1 Bovine Collagen, 30 µg/ml, and incubating overnight at 37°C. Arrays were then washed 3 times with 300 µl of BEGM and stabilised by adding 400 µl BEGM to each well and connecting the array to the ECIS instrument. Once stabilised the media was aspirated and cells were seeded to the array which was then re-connected to the ECIS instrument and kept at 37°C 5% CO_2. Resistance (measured at 400Hz) and cell capacitance (measured at 32 kHz), which is more sensitive to changes due to cell attachment/spreading, were recorded from 0-72 hours after which cell supernatants were collected and cells were discarded. Cell impedance, resistance and capacitance were normalised to the media control in Microsoft Excel and statistics were carried out using GraphPad Prism as described in section 2.5.

3.4 Results

3.4.1 Bronchial Epithelial Cells Express Epithelial Lineage Markers CK14 and E-Cadherin

HBEC were characterised for basal epithelial markers cytokeratin 14 (CK-14), an intracytoplasmic cytoskeleton protein and E-cadherin, a cell adhesion molecule, using immunofluorescence (see section 2.3.3) to provide initial characterisation of commercially sourced primary cells.

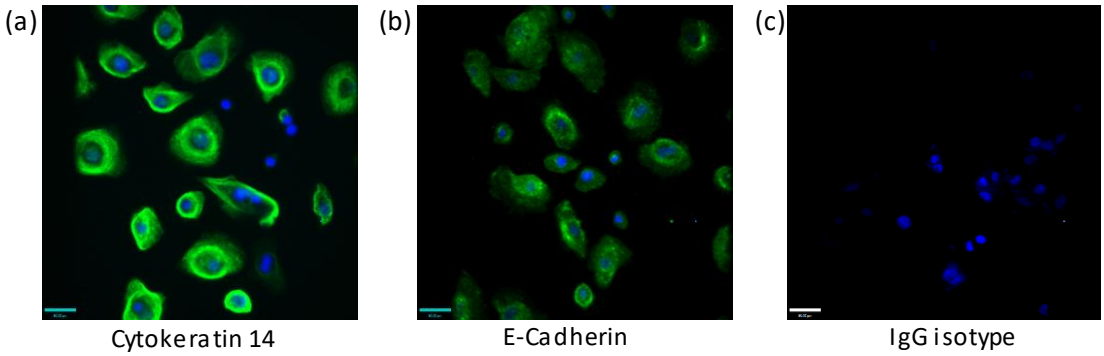


Figure 3.4.1: Characterisation of Primary Human Bronchial Epithelial Cells. Images are representative of primary HBEC cultures stained for epithelial markers using immunofluorescence. (a) CK14 stains basal cell compartments (green); (b) E-cadherin staining is predominantly cytoplasmic (green); (c) IgG1 isotype control. Nuclei are stained blue with DAPI.

Figure 3.4.1 above shows three representative images of CK-14 and E-cadherin staining for four primary HBEC donors. All donors showed positive expression and the same staining pattern for both markers, these results confirm cell populations were of epithelial lineage.

3.4.2 Bronchial Epithelial Cells Cultured at ALI Develop a Characteristic TEER Profile Indicative of Barrier Formation.

To provide insight into the properties of cells at different stages of differentiation we took sequential TEER measurements at days 7, 14 and 21 ALI which were normalised as described in section 3.3.2. A characteristic TEER profile was observed for all donors at ALI providing confidence in the differentiation technique. TEER profiles varied across donors, Figure 3.4.2 shows the combined TEER profile of four HBEC donors. TEER profiles for individual donors can be found in Appendix 2.

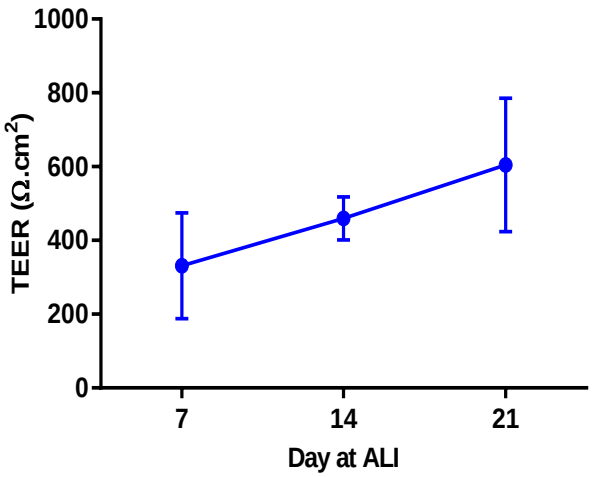


Figure 3.4.2: TEER measurements of HBEC at day 7, 14 and 21 ALI. Four HBEC donors were cultured at ALI for 21 days. TEER measurements were taken at day 7, 14 and 21 ALI using the EVOM voltohmeter (World Precision Instruments). Data represents average TEER ± SEM (*n*=4 different donors).

HBEC cultured at ALI resulted in a TEER value of 332 ± 287 Ω.cm^2 at day 7, 459 ± 117 Ω.cm^2 at day 14 ALI and 604 ± 362 Ω.cm^2 by day 21 ALI. TEER values indicated that all donors reached differentiation by day 14 ALI. TEER profiles showed variation across donors, 3 of the 4 donors cultured demonstrated an increase in resistance from day 7 to 21 (donors 3, 5 and 7). Donor 4 developed a TEER of 541 Ω.cm^2 by day 7 which reduced to 258 Ω.cm$^{2.}$

3.4.3 uPAR Localizes at the Apical and Basal Membrane of Differentiated Bronchial Epithelial Cells

To further assess the differentiation technique histology of differentiated epithelial cell cultures from HBEC donors 2 and 3 was carried out. H&E and Alcian Blue staining were performed to assess morphology and detect the presence of mucus producing goblet cells, immunofluorescence was used to detect the presence of uPAR.

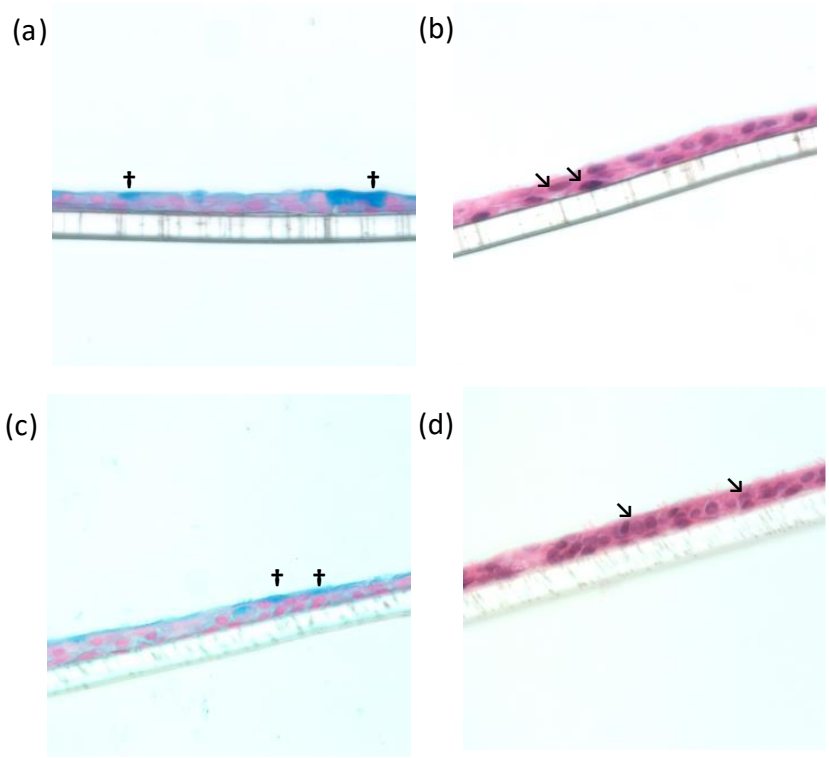


Figure 3.4.3: Primary Human Bronchial Epithelial Cells Cultured at the Air-Liquid Interface. Alcian blue (a and c) and Hematoxylin and eosin (H&E) staining (b and d) of two commercial normal HBEC donors 2 and 3 at passage 3 day 21 ALI (Lonza® Clonetics™) (x40 objective). † highlights goblet cells ↘highlights cilia.

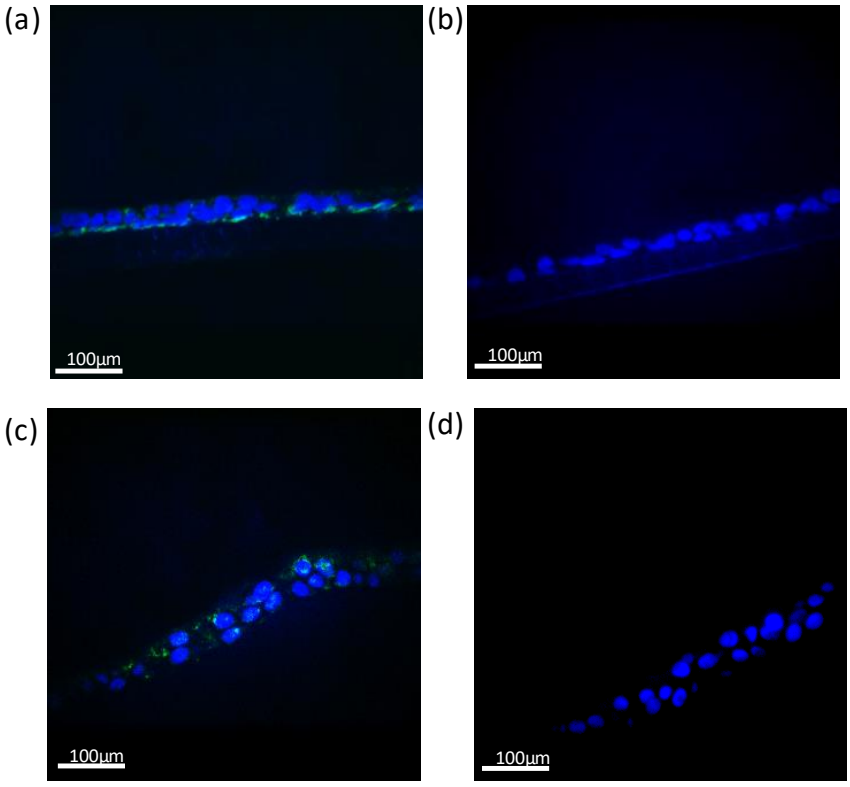


Figure 3.4.4: uPAR expression in Air Liquid Interface Cultures. uPAR expression (a and c) and isotype control (b and d) of two commercial normal HBEC donors 2 and 3 at passage 3 at day 21 ALI (Lonza® Clonetics™). Commercial HBEC donors were stained for uPAR (green) and IgG1 isotype and counterstained with 4',6-diamidino-2-phenylindole (DAPI) (blue) for staining of the nuclei.

Cultures developed a pseudostratified epithelium with the presence of ciliated cells (↘) and of goblet cells (†) (See Figure 3.4.3). These data also confirm the presence of uPAR expression in differentiated bronchial epithelial cells, uPAR was detected at the basal and apical membrane across the cell layer (See Figure 3.4.4).

3.4.4 Expression of the uPAR-uPA Pathway during Bronchial Epithelial Cell Differentiation

To provide insight into the expression of uPA-uPAR pathway during bronchial epithelial cell differentiation and homeostasis scuPAR, uPA, PAI-1 and MMP-9 levels were measured. Basolateral supernatants from four HBEC donors and were collected at days 7, 14 and 21 ALI and proteins were measured using ELISA and Luminex (for methods see 2.3.1 and 2.3.2).

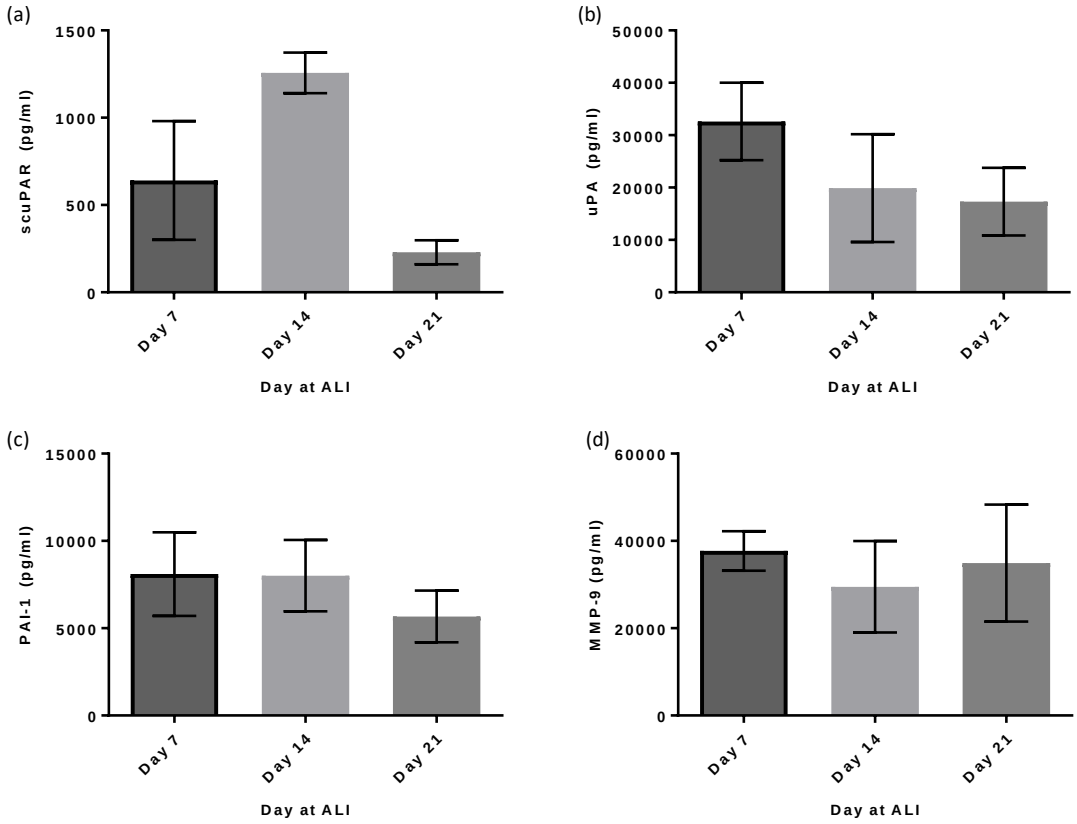


Figure 3.4.5: Expression of uPAR pathway components scuPAR, uPA, PAI-1 and MMP-9, during bronchial epithelial differentiation. (a-d) scuPAR, uPA, PAI-1 and MMP-9 protein (pg/ml) measured in neat basolateral supernatants taken at day 7, 14 and 21 ALI (*n*=4 HBEC donors) using Luminex. scuPAR levels showed the greatest change over the course of differentiation however changes in levels were not significant. FI-bkgd = fluorescence intensity - background; scuPAR = soluble cleaved urokinase plasminogen activator receptor; uPA = urokinase; PAI-1 = plasminogen activator inhibitor-1; MMP-9 = matrix metalloproteinase-9.

scuPAR levels showed a significant difference over the course of ALI (Friedman test, p =0.04). Expression increased 1.8 fold from day 7 to day 14 ALI, levels then saw a considerable reduction at day 21 (fold change 0.16, Friedman test, p = 0.04). MMP-9 and PAI-1 expression were relatively stable across all time points (MMP-9, Friedman test p = 0.9; PAI-1, Friedman test p = 0.7). uPA expression did not significantly differ across the time points however protein levels decreased over the course of differentiation (Friedman test p = 0.2).

3.4.5 scuPAR, uPA and MMP-9 Expression are Negatively Correlated with Epithelial Barrier Function

Having established the expression profiles of uPAR pathway components in the ALI model we then investigated whether or not a relationship existed between protein expression and TEER, the key outcome related to barrier properties in this *in vitro* model. Activity of the uPAR pathway was investigated by measuring scuPAR and uPA and the downstream protease MMP-9. Protein levels were measured by ELISA and were correlated with TEER at days 14 and 21 ALI, correlations were assessed using Spearman's rank coefficient.

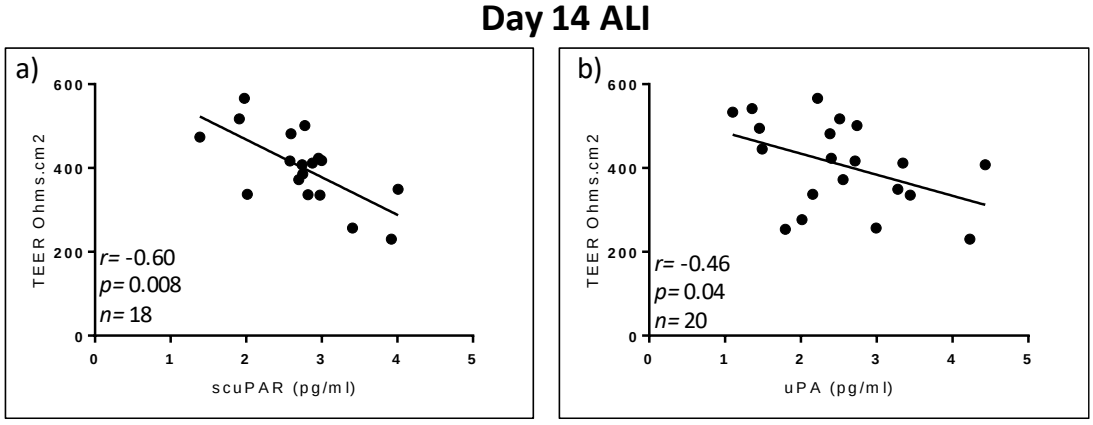


Figure 3.4.6: scuPAR and uPA levels are negatively correlated with TEER in primary human bronchial epithelial cells during differentiation. scuPAR and uPA levels were measured in basolateral supernatants from differentiated HBEC at days 14 ALI. Protein expression was correlated with TEER. (a) scuPAR (pg/ml) vs TEER ($\Omega.cm^2$) at day 14 ALI (p=0.008) (b) uPA (pg/ml) vs TEER ($\Omega.cm^2$) at day 14 ALI (p=0.04). Representative data from HBEC donor 3 where n=individual data points.

	Correlation Coefficient (*r*)			
	Donor 3	**Donor 4**	**Donor 5**	**Donor 6**
scuPAR (pg/ml) v TEER (Ω/cm²)	**-0.60 *** (n=18)	-0.58 (n=10)	**-0.97 *** (n=8)	-0.54 (n=10)
MMP-9 (pg/ml) v TEER (Ω/cm²)	**-0.57 *** (n=22)	0.15 (n=10)	-0.38 (n=8)	-0.25 (n=10)
uPA (pg/ml) v TEER (Ω/cm²)	**-0.46 ***(n=20)	-0.27 (n=11)	**-0.89 *** (n=8)	0.12 (n=10)
scuPAR (pg/ml) v MMP-9 (pg/ml)	**0.78 *** (n=15)	-0.57 (n=7)	-0.6 (n=8)	**0.73 *** (n=10)

Table 3.4.1: Summary table of Spearman Rank Correlation Coeffiecients for scuPAR (pg/ml) v TEER (Ω/cm^2); MMP-9 (pg/ml) v TEER (Ω/cm^2); uPA (pg/ml) v TEER (Ω/cm^2); scuPAR (pg/ml) v MMP-9 (pg/ml) across four HBEC donors. Values in **bold** = $p < 0.05$.

scuPAR and uPA expression negatively correlated with TEER in differentiated HBEC at day 14 ALI (Spearman's Rank Coefficient, p = 0.008 and p = 0.04, respectively). scuPAR and uPA were negatively correlated with TEER in 4 separate HBEC donors, however the observation was significant in only 2 of the donors tested (see Table 3.4.1). These data suggest that elevated expression of scuPAR and the ligand uPA may play a role in regulating epithelial barrier properties.

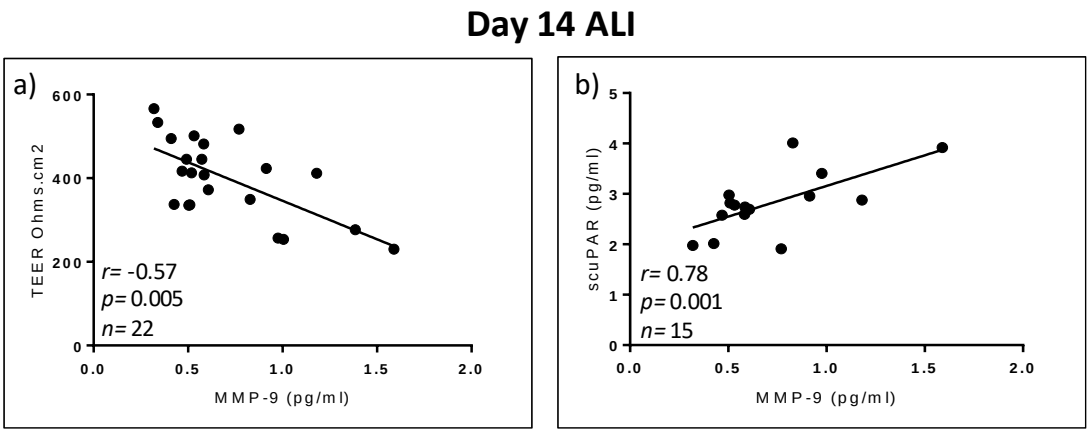


Figure 3.4.7: MMP-9 and scuPAR show coordinated expression in differentiated bronchial epithelial cells and MMP-9 levels negatively correlate with TEER. Correlation between MMP-9 levels in basolateral supernatants of untreated HBEC and TEER/scuPAR levels at day 14 ALI. (a) MMP-9 (pg/ml) vs TEER ($\Omega.cm^2$) day 14 ALI (p = 0.005), (b) MMP-9 (pg/ml) vs scuPAR (pg/ml) day 14 ALI. Data for HBEC donor 3 only where n=individual data points.

Total MMP-9 levels were inversely correlated with TEER at day 14 ALI (p = 0.005, HBEC donor 3, Figure 3.4.7 a), this relationship was observed in 3 out 4 HBEC donors however was statistically significant in donor 3 only (see Table 3.4.1). MMP-9 expression positively correlated with scuPAR expression at the same timepoint (p = 0.001, HBEC donor 3, Figure 3.4.6 b), this relationship was observed in 2 out of 4 HBEC donors. These data suggest that MMP-9 and scuPAR levels are coordinated during differentiation in HBEC and that elevated scuPAR, uPA and MMP-9 expression are negatively correlated with epithelial barrier integrity.

We then investigated the relationship between pathway expression and epithelial barrier function at day 21 ALI. MMP-9, uPA and scuPAR were measured in basolateral supernatants at day 21 and correlated with TEER measurements at the same timepoint.

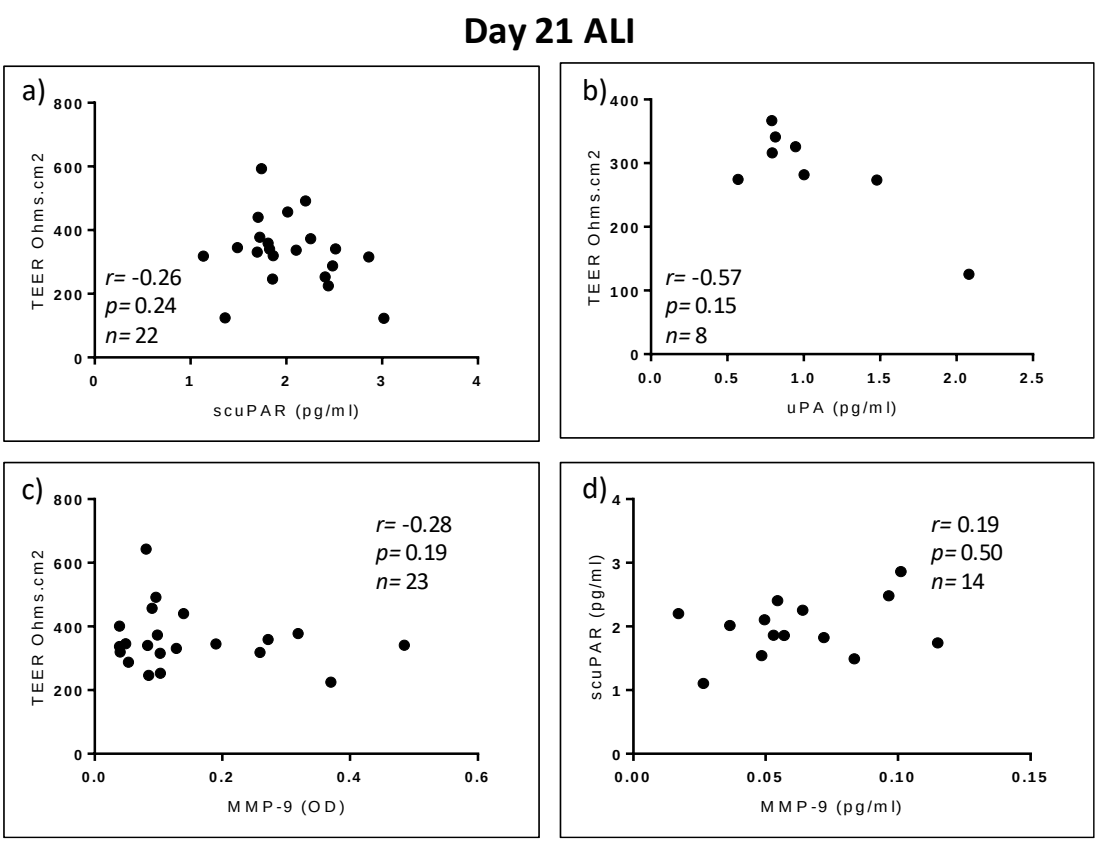


Figure 3.4.8: uPAR pathway expression is not related to barrier function bronchial epithelial cells with an established barrier. Correlation between scuPAR, uPA, MMP-9 levels in basolateral supernatants of untreated HBEC and TEER at day 21 ALI. (a) scuPAR (pg/ml) vs TEER ($\Omega.cm^2$), (b) uPA (pg/ml) vs TEER ($\Omega.cm^2$), (c) MMP-9 (pg/ml) vs TEER ($\Omega.cm^2$), (d) MMP-9 (pg/ml) vs scuPAR (pg/ml). Data for HBEC donor 3 only where *n*=individual data points.

The relationship observed between scuPAR, uPA and MMP-9 expression and TEER at day 14 ALI was not observed at day 21 ALI (see Figure 3.4.8). These data suggest that the uPAR pathway may play a role in barrier formation and not in cells with an established barrier.

3.4.6 Treatment with Recombinant uPA and uPAR does not alter TEER of Differentiated Bronchial Epithelial Cells

To further investigate the relationship between soluble uPAR, uPA and epithelial barrier properties, differentiated epithelial cells from four HBEC donors with an established TEER were treated at day 21 with recombinant uPA and uPAR. Barrier properties were monitored by measuring TEER 15 minutes, 30 minutes, 1 hour, 4 hours and 4 hours post-treatment.

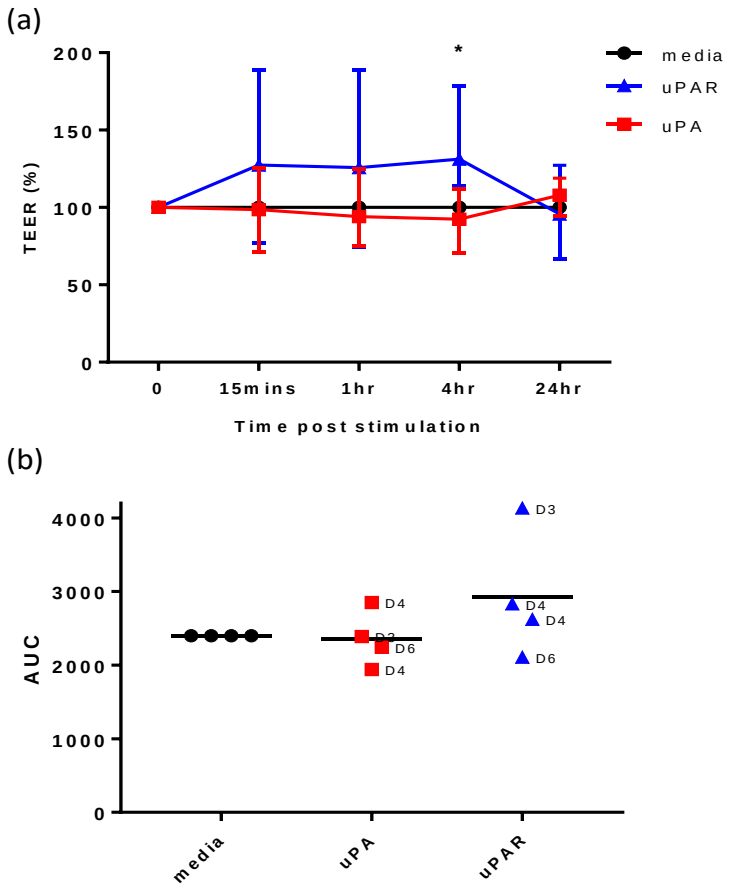


Figure 3.4.9: uPA and uPAR differentially effect bronchial epithelial barrier properties. HBEC (*n*=4) were serum starved for 24 h and stimulated with uPA (1 µg/ml) and uPAR (1 µg/ml) at day 21 ALI. (a) TEER (Ω.cm^2 ±SEM) was measured at 0 min, 15 min, 1 h, 4 h and 24 h post stimulation. uPA (red) vs media control (black), and uPAR (blue) vs media control (TEER measurements normalised to media control, n = 4, median with IQR). TEER in uPA treated HBECs *vs* uPAR treated was statistically different 4 h post stimulation (2way ANOVA, multiple comparisons test). (b) AUC of uPA *vs* media control 0- 24 h post stimulation (red) AUC of uPAR *vs* media control 0- 24 h post stimulation (blue). AUC = area under the curve.

Treatment with uPA resulted in a slight decrease in TEER (not significant), the decrease in resistance was greatest at after 1 hour (-11.9%). Stimulation with uPAR led in an increase in TEER at 1 hour (20%) and 4 hours (16%) which returned to baseline after 24 hours, however these changes were not significant.

3.4.7 Effects of Elevated uPAR on Cytokine Expression in Differentiated HBEC

In order to investigate the effects of the addition of recombinant soluble uPAR on the inflammatory profile of bronchial epithelial cells, 4 HBEC donors were stimulated with recombinant soluble uPAR and apical washes were collected at 4 and 24 hours. The cytokines CCL2, CCL3, CCL4, IL-2, GM-CSF, IL-6, VEGF, TNF alpha, IL-1β, IL-4, IL-12, CCL11, IL-10, IFN-gamma, CCL22, CCL13, IL-17A, CCL26, IL-5, CCL17, IL-8 were measured in the apical washes using Luminex. The cytokines CCL2, CCL3, CCL4, IL-2, IL-6, VEGF and GM-CSF had protein levels within range of the assay, however TNF-α, IL-1β, IL-4, IL-12, CCL11, IL-10, IFN-γ, CCL22, CCL13, IL-17A, CCL26, IL-5, CCL17, IL-8 were not in range (For range of analytes measured see Appendix 3).

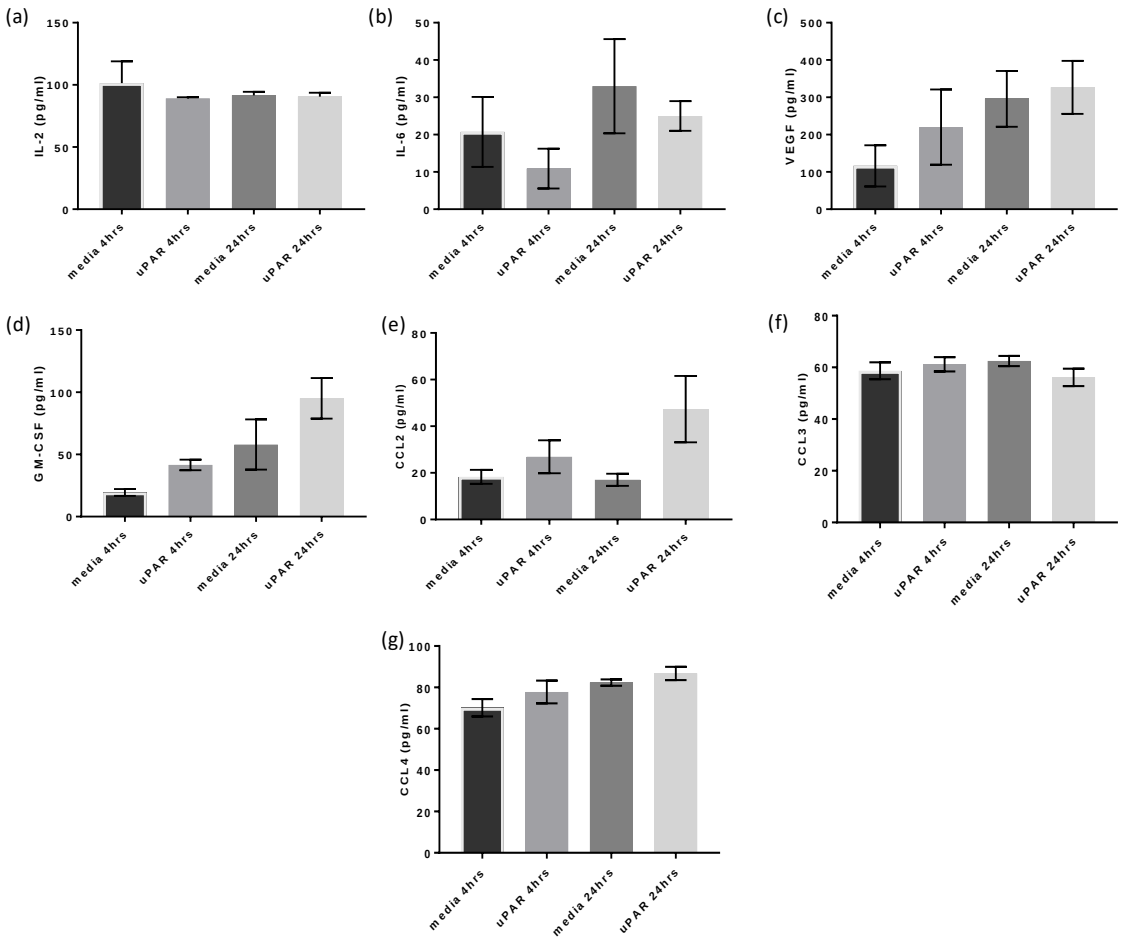


Figure 3.4.10: Secretion of pro-inflammatory cytokines are not altered in differentiated HBEC stimulated with recombinant soluble uPAR. HBEC (*n*=4) were serum starved for 24 hr and stimulated with uPAR (1 µg/ml) at day 21 ALI. Apical washes were collected after 4 hr and 24 hr, (a) CCL2, (b) CCL3, (c) CCL4, (d) IL2, (e) IL6, (f) VEGF and (g) CCL4 GM-CSF protein (% ±SEM) was measured using Luminex. vs media control. IL = interleukin, VEGF = vascular endothelial growth factor, GM-CSF = granulocyte macrophage colony stimulating factor.

Of the cytokines measured, CCL2 and GM-CSF showed slight increases in expression at both time points. IL-6 and VEGF expression were induced after 24 hours and 4 hours, respectively. Changes in expression were not statistically significant. CCL3, CCL4 and IL-2 expression showed no change across both time points.

3.4.8 Investigating the Effects of Blocking uPAR on Barrier Formation in HBEC Using Electric Cell Substrate Impedance Sensing

Expression of scuPAR and pathway components negatively correlate with TEER in differentiated HBEC (see Section 3.4.5). The ECIS model was used to investigate if resistance and capacitance properties in undifferentiated cells correlate with scuPAR and MMP-9 protein expression. We then tested the hypothesis that using therapeutic antibodies to specific epitopes may be beneficial and improve barrier properties, HBEC were treated with antibodies blocking different uPAR-ligand interactions. The receptor was blocked using three antibodies, anti-uPAR R3, anti-uPAR R4 and anti--uPAR ATN-658, each targeting different uPAR epitopes. HBEC (*n*=4) were treated with each antibody and an IgG1 isotype control and were seeded to 8 well arrays, one well contained untreated cells in media only.

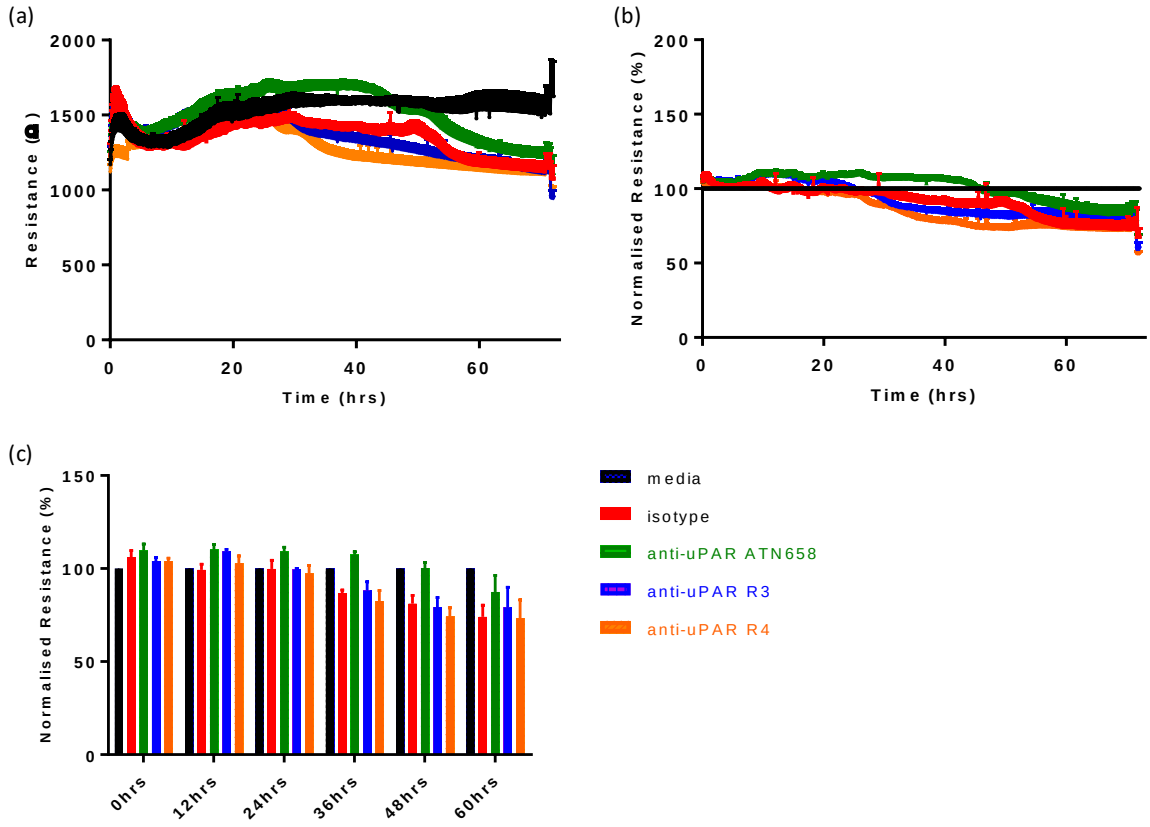


Figure 3.4.11: Cell resistance profiles of HBEC treated with uPAR blocking antibodies. HBEC (*n*=4) were treated with anti-uPAR R3, anti-uPAR R4, anti-uPAR ATN-658 and IgG1 isotype control and resistance

(Ω) was monitored at 400Hz for 72 h using ECIS. (a) Raw resistance traces ±SEM of HBEC treated with monoclonal anti-uPAR R3 (blue), R4 (orange), ATN-658 (green), IgG1 isotype control (red). Media only well (black). (b) Resistance (normalised to media only control well) of HBEC treated with monoclonal anti-uPAR R3 (blue), R4 (orange), ATN-658 (green), IgG1 isotype control (red). Media only well (black). (c) Bar graph showing resistance of treated HBEC at 0, 12, 24, 36, 48 and 60 hr.

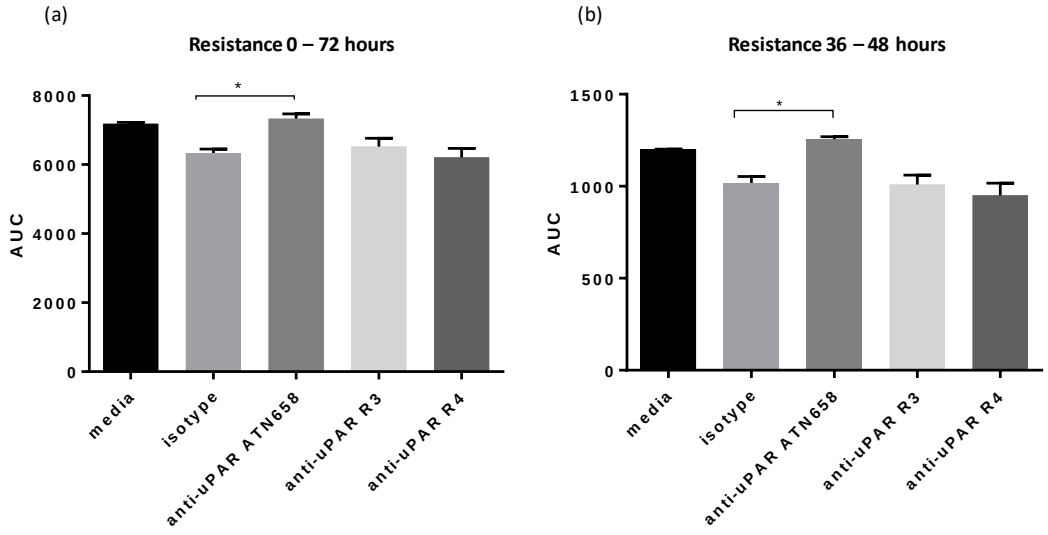


Figure 3.4.12: Treatment with anti-uPAR ATN-658 increases bronchial epithelial barrier function. (a) AUC analysis of HBEC resistance 0-72 h post-treatment. Resistance was greater in HBEC treated with ATN658 *vs* isotype control (Mann Whitney *t*-test, p=0.028). (b) AUC analysis was carried out at 12 hour intervals, resistance at 36-48 h post-treatment was greater in ATN-58 treated cells *vs* isotype control (Mann Whitney *t*-test, *p*=0.028) but not at any other timepoint.

AUC analysis was used to assess the effect of blocking uPAR on bronchial epithelial barrier function (Figure 3.4.11). The addition of anti-uPAR ATN-658 resulted in an increase in resistance (barrier function) when compared to the isotype control (Mann Whitney, *p*=0.028). We then analysed the data at 12 hour intervals to identify if this relationship was continual or intermittent. The effects of anti-uPAR ATN-658 on epithelial resistance were significant at 36-48 hours only (Mann Whitney, *p*=0.028). Treatment with anti-uPAR R3 and anti-uPAR R4 did not have an effect on resistance over 72 hours or at specific time points

when compared to the isotype control. The addition of the IgG1 isotype also appeared to cause a decrease in resistance, this change was not statistically significant. The antibodies used were all mouse IgG1 therefore comparisons were made to the isotype control.

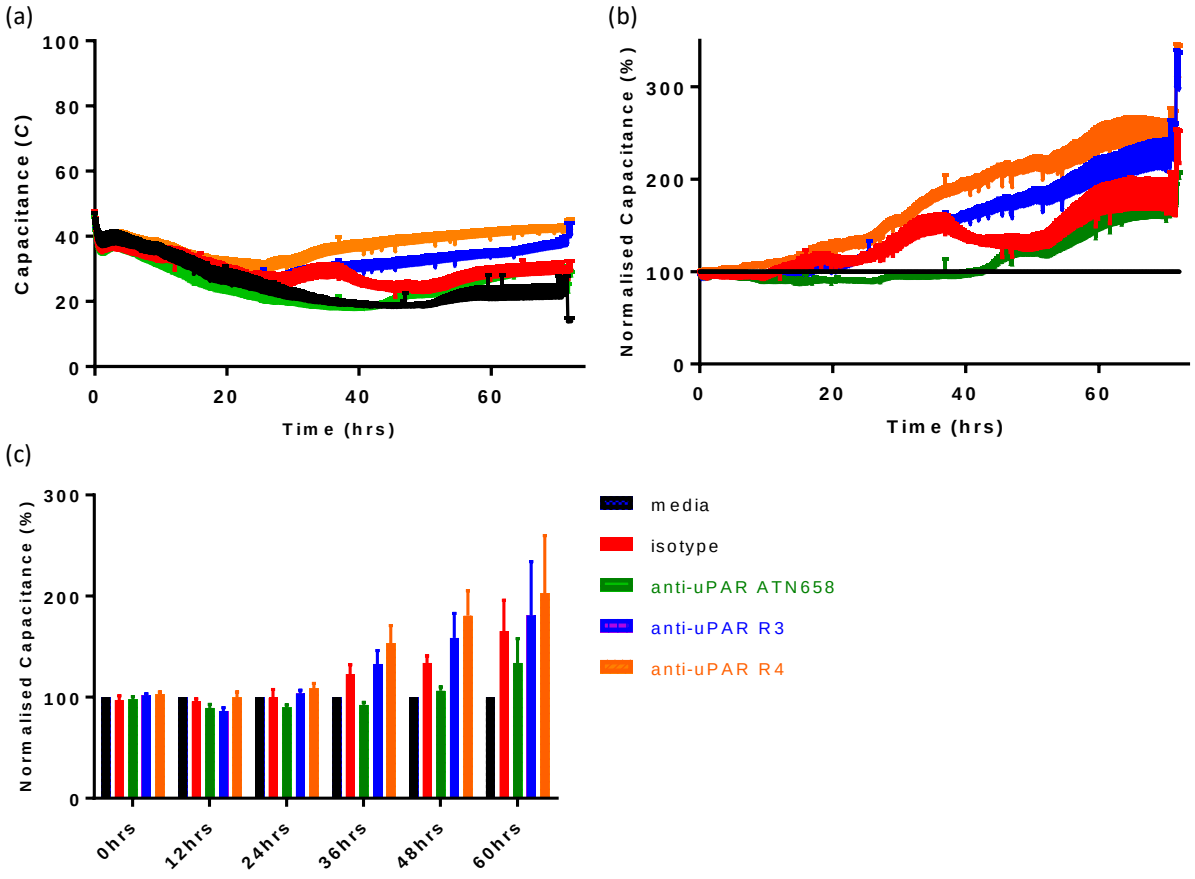


Figure 3.4.13: Cell capacitance profiles of HBEC treated with uPAR blocking antibodies. HBEC (*n*=4) were treated with anti-uPAR R3, R4, ATN-658 and IgG1 isotype control and capacitance (*c*) was monitored at 32 KHz for 72 h. (a) Capacitance ± SEM of HBEC treated with monoclonal anti-uPAR R3 (blue), R4 (orange), ATN-658 (green), IgG1 isotype control (red). Capacitance normalised to media only control well. (b) Bar graph showing the capacitance of treated HBEC at 0, 12, 24, 36, 48 and 60 hr.

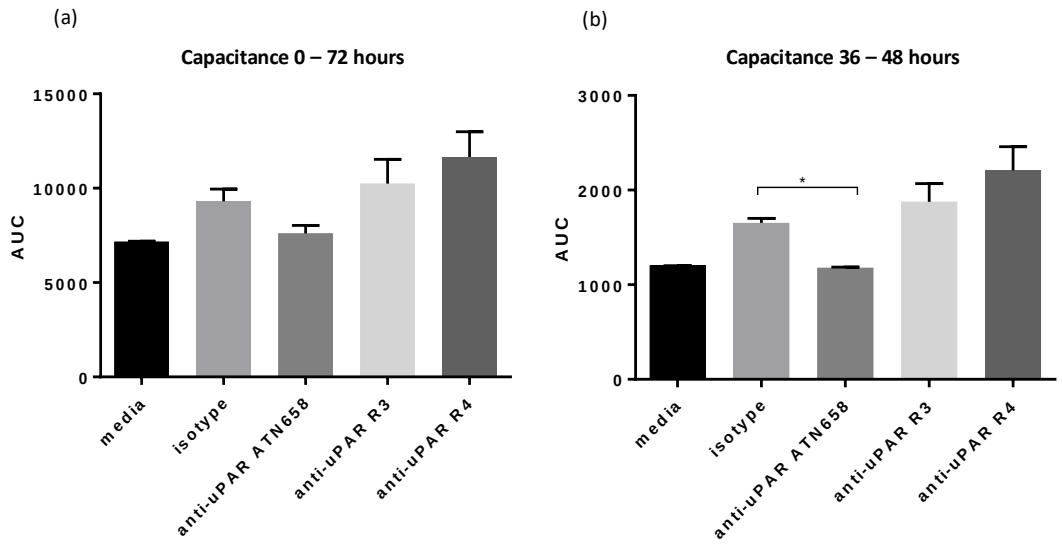


Figure 3.4.14: Bronchial epithelial cells treated with anti-uPAR ATN-658 show reduced cell spreading. (a) AUC analysis of HBEC capacitance 0-72 h post-treatment. ATN-658 caused a drop in cell capacitance whereas R3 and R4 both caused a slight increase (not significant). (d) AUC analysis of capacitance 36-48 h post-treatment. ATN-658 treatment resulted in a significant reduction in cell capacitance which conveys a decrease in cell spreading/ migration at this time point.

Blocking of uPAR with anti-uPAR R3 and anti-uPAR R4 resulted in an increase in cell capacitance however this was not statistically significant. Treatment with anti-uPAR ATN-658 led to a decrease in capacitance, which was significant 36-48 hours post-treatment (anti-uPAR ATN-658 *vs* isotype control, p=0.043). As seen with cell resistance, the addition of the IgG1 isotype also appeared to have an effect on cell capacitance. Again, this change was not statistically significant.

3.4.9 scuPAR Expression Correlates with Barrier Properties of Undifferentiated Epithelial Cells

HBEC were cultured under submerged conditions, resistance and capacitance measurements were taken using ECIS and cell supernatants were collected at 72 hours. scuPAR protein expression was measured using Luminex and total MMP-9 protein expression was measured using ELISA. uPA and PAI-1 and were also measured in the same samples however levels exceeded the detection range of the assay. scuPAR and MMP-9 protein levels were correlated with cell resistance and capacitance at 72 hours (see Figure 3.4.14).

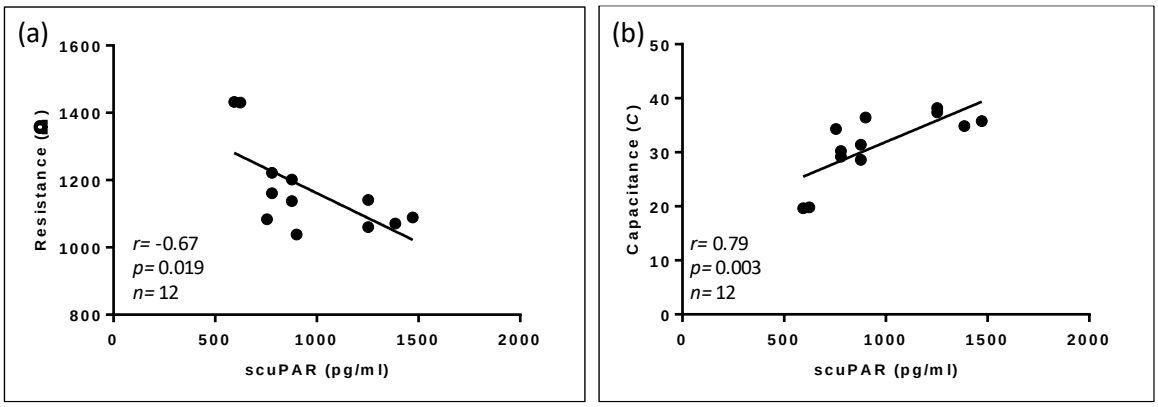


Figure 3.4.15: scuPAR Levels are Correlated with Resistance and Capacitance in Undifferentiated Bronchial Epithelial Cells. Resistance and capacitance properties of HBEC were measured using ECIS for 72 hours. Cell supernatants were collected at 72 hours and scuPAR protein levels were measured using Luminex. scuPAR protein levels inversely correlated with resistance and positively correlated with capacitance**.** (a) scuPAR (pg/ml) *vs* resistance (Ω) (*p*=0.019), (b) scuPAR (pg/ml) *vs* capacitance (Ω) (*p*=0.003). Representative data from HBEC donor 6 where *n*=individual data points.

	Correlation coefficient (*r*)			
	Donor 3	**Donor 4**	**Donor 5**	**Donor 6**
scuPAR v Resistance (Ω)	**-0.67 *** (*n*=12)	-**0.58*** (*n*=12)	-0.25 (*n*=10)	-**0.67*** (*n*=12)
scuPAR v Capacitance (*C*)	**0.66*** (*n*=10)	**0.69*** (n=12)	0.46 (n=12)	**0.79*** (n=12)

Table 3.4.2: Summary table of Spearman Rank Correlation Coeffiecients for scuPAR (pg/ml) v Resistance (Ω) and scuPAR (pg/ml) v Capacitance (*C*) across four HBEC donors. Values in **bold** = $p < 0.05$.

scuPAR protein levels were inversely correlated with resistance (Figure 3.4.14 r= 0.67, p=0.019, n= 12 HBEC donor 6). This relationship was observed across all 4 HBEC donors and was statistically significant in 3 donors. Interestingly, in the same 3 donors scuPAR levels were also positively correlated with cell capacitance (see Figure 3.4.14 and Table 3.4.2).

As shown in section 3.4.5, MMP-9 expression was found to have an inverse correlation with TEER. To test whether MMP-9 levels are related to barrier properties in undifferentiated HBEC, MMP-9 protein was measured in supernatants from HBEC and correlated with cell resistance and capacitance (see Figure 3.4.16). These experiments were conducted using HBEC donors 5 and 6 only due to limited sample.

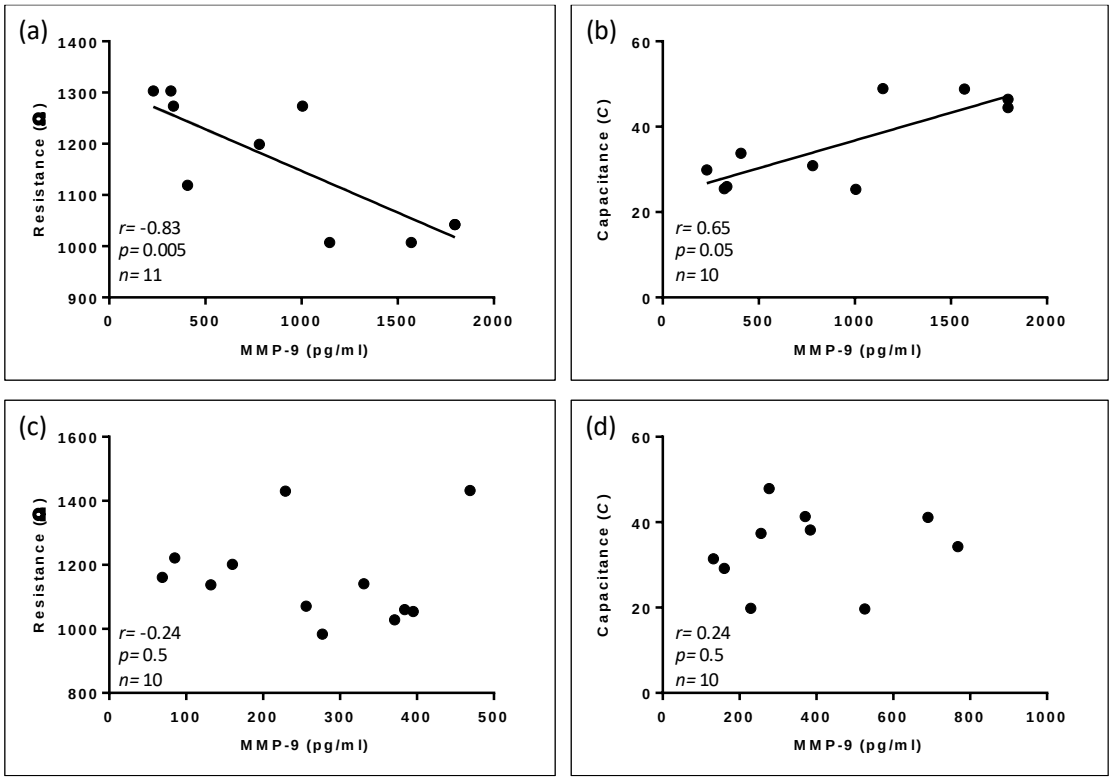


Figure 3.4.16: MMP-9 correlate with cell spreading in bronchial epithelial cells. Resistance and capacitance properties of HBEC were measured using ECIS for 72 hours. Cell supernatants were collected at 72 hours and MMP-9 protein levels for HBEC donors 5 and 6 were measured using ELISA. MMP-9 protein levels inversely correlated with resistance and positively correlated with capacitance**.** (a) MMP-9 (pg/ml) *vs* resistance (Ω) (*p*=0.005), HBEC donor 6, (b) MMP-9 (pg/ml) *vs* capacitance (*C*) (*p*=0.05) HBEC donor 6, (c) MMP-9 (pg/ml) *vs* resistance (Ω) (*p*=0.5 ns) HBEC donor 5, (d) MMP-9 (pg/ml) *vs* capacitance (*C*) (*p*=0.5 ns) HBEC donor 5. Data from HBEC donor 5 and 6 where *n*=individual data points.

MMP-9 expression was negatively correlated with cell resistance (HBEC donor 6, *r*-0.83, *p*=0.005, *n*=11, HBEC donor 5, *r*-0.24, *p*=0.05, *n*=10), and positively correlated with cell capacitance (HBEC donor 6, *r* 0.65, *p*=0.005, *n*=11, HBEC donor 5, *r* 0.24, *p*=0.5, *n*=10). However, correlations were significant in one of the 2 HBEC donors used for these experiments.

3.5 Discussion

The aims of this chapter were to i) Determine an expression profile of the uPA-uPAR pathway in an epithelial differentiation model; ii) Identify a relationship between the uPA-uPAR pathway and barrier formation in two independent models; iii) Identify the direct effect of pathway activation (via uPA and scuPAR) on barrier properties and the inflammatory profile of the cells and; iv) Provide proof of concept that we can block uPAR function for potential therapeutic benefit, i.e. to improve bronchial epithelial barrier function. Overall, we showed that scuPAR levels are greatest at day 14 ALI and that levels of uPA, PAI-1 and MMP-9 are relatively stable over the course of differentiation. We found that elevated scuPAR, MMP-9 and uPA expression negatively correlate with epithelial barrier properties and that scuPAR and uPA correlate with MMP-9 expression. Pathway activation via the addition of soluble uPAR to differentiated HBEC did not alter the expression of inflammatory cytokines and led to a slight increase in epithelial resistance, which was not statistically significant. Interestingly, in basal submerged cells blocking α5β1-uPAR interaction with ATN-658 led to an increase in epithelial resistance. ATN-658 also attenuated cell spreading in bronchial epithelial cells, inhibition of uPA-uPAR interaction with anti-uPAR R3 and R4 did not significantly alter barrier properties or cell adhesion/ spreading.

The development of *in vitro* models such as the ALI and ECIS have helped in our understanding of the contribution of epithelial barrier dysfunction in the development of chronic lung diseases (Blume, 2010). The ALI model has been used to investigate the localization, expression and function of proteins in the epithelium (Faura Tellez *et al*., 2016), to understand how TJPs are regulated and disrupted in asthma (Hackett *et al*., 2013, Hardyman *et al*., 2013) and to study compounds that may restore bronchial barrier function

(Slater *et al*., 2016). The ECIS technique has also been key in translational research on barrier function and also cell-matrix contact (Heijink *et al*., 2010a). Heijink *et al* have demonstrated how the ECIS model can provide insight into the underlying mechanism of allergic asthma (Heijink *et al*., 2010b). Both techniques serve as physiological models to study airway epithelial physiology. HBEC cultured at ALI in this thesis demonstrated the presence of goblet and ciliated cells and TEER measurements typical of this cell type (Stewart *et al*., 2012d). We also confirmed the presence of uPAR in differentiated HBEC using immunofluorescence.

We have shown that MMP-9 as well as the uPAR-uPA-PA1-1 axis regulate TJPs and epithelial barrier function. The uPAR pathway was characterised for expression of scuPAR, uPA, PAI-1 and MMP-9 at different stages of ALI. HBEC form a differentiated layer within 14-21 days ALI (Parker *et al*., 2010), we therefore related day 14 ALI to 'barrier formation/ differentiation' and day 21 to 'barrier established/ differentiated'. Protein levels were relatively stable over time with the exception of scuPAR expression which significantly decreased from day 14 to day 21 ALI. We found that elevated expression of scuPAR, uPA and MMP-9 are inversely correlated with epithelial barrier integrity at day 14 ALI and that scuPAR and uPA levels correlate with those of MMP-9. These effects are no longer significant by day 21, furthermore the addition of uPA and uPAR did not alter TEER in HBEC with an established barrier (day 21 ALI) suggesting the potential regulatory role played by scuPAR occurs during barrier formation (day 14 ALI). Together our findings suggest that elevated uPAR pathway activity correlates with MMP-9 expression and impairs bronchial epithelial barrier integrity.

The ECIS model was then used to investigate the effect of blocking uPAR on the barrier and adhesion properties of HBEC, three anti-uPAR antibodies were used that bind to distinct epitopes. Anti-uPAR ATN-658 binds in bin 5 in domain 3 and inhibits binding with integrin

α5β1. uPAR-α5β1 binding has been shown to activate MMP-9 via the ERK signalling pathway (Wei *et al*., 2007). Anti-uPAR R3 binds bin 1 in domain 2 and inhibits binding with uPA and anti-uPAR R4 binds in bin 4 in domain 3 (Zhao *et al*., 2015), both antibodies inhibit uPA-uPAR interaction. Anti-uPAR R3 and R4 did not alter resistance in HBEC suggesting that inhibition of uPA-uPAR binding in domain 2 and blocking ligands interacting with bin 4 do not have an effect on the ability of the receptor to regulate barrier properties of the cell. ATN-658 however resulted in an increase in resistance, this supports the hypothesis that elevated levels and activity of uPAR augment barrier function and provide evidence that the receptor may be acting via α5β1 integrin. It remains unclear whether effects are mediated by scuPAR or muPAR or both forms of the receptor as domain 3 is intact in both forms. Although inhibition of uPA-uPAR inhibition by R3 did not alter barrier properties in this model, uPA correlated with TEER and MMP-9 in HBEC at ALI, suggesting uPA interaction may still be important in regulating epithelial tight junctions.

An inverse relationship between scuPAR, uPA, and MMP-9 protein levels and resistance was also observed in the ECIS model, scuPAR showing the strongest correlation. Interestingly levels of the receptors' inhibitor, PAI-1, positively correlated with resistance. Using ECIS we also investigated the relationship between the uPAR pathway and cell capacitance, which translates to adhesive and proliferative properties of cells, depending on cell type and the time point at which capacitance is measured (Wegener *et al*., 2000). uPAR interacts with the ECM protein vitronectin to regulate cell adhesion, spreading and proliferation (Pirazzoli *et al*., 2013; Liu *et al*., 2014a). scuPAR and MMP-9 expression positively correlate with cell capacitance at 72 hours post-seeding, suggesting increased expression promotes cell migration and spreading. These findings are in line with previous studies in cancer cells where uPAR has been shown to promote cell migration via interaction with ECM (Noh *et al*., 2013b).

As with resistance, PAI-1 showed the opposite relationship to the receptor and levels were negatively correlated with capacitance suggesting PAI-1 may attenuate cell migration in this system. The second observation when treating HBEC with ATN-658 was that the antibody led to a reduction in cell capacitance. ATN-658 has been shown to inhibit cell migration and proliferation in cancer cells (Rabbani *et al*., 2010) and is currently in Phase 1 clinical trial in cancer patients. This effect was seen at 36-48 hours, by this time point cells have attached and are actively proliferating, spreading and migrating which suggests that inhibition of uPAR by ATN-658 may attenuate these processes.

A number of inflammatory cytokines have been associated with epithelial barrier function and the uPA-uPAR pathway has been shown to regulate innate immune cells e.g. neutrophils and macrophages and levels of inflammatory cytokines and IL8, IL-10 and TNF-α are correlated with uPAR in sputum from asthma and COPD patients (Xiao *et al*., 2005b). To investigate the relationship between uPAR and epithelial cytokine production HBEC donors cultured at ALI were challenged with soluble uPAR and inflammatory cytokines were measured in cell supernatants. The addition of uPAR led to a decrease in IL-6 and increase in VEGF and GM-CSF secretion, however changes were not statistically significant. There was no effect on IL-2, CCL2, CCL3 and CCL4 in response to stimulation with uPAR. Certain cytokines could not be measured as they were not in range of the assay (TNF-α, IL-1β, IL-4, IL-12, CCL11, IL-10, IFN-γ, CCL22, CCL13, IL-17A, CCL26, IL-5, CCL17, IL-8). Both membrane and soluble uPAR play a role in expression in cytokine expression in disease. uPAR and uPA KO mice glioblastomas have decreased levels of GM-CSF (Raghu *et al*., 2012), and suPAR induces IL-4 and TGF-β in cancer cells (Hu *et al*., 2014). Elevating suPAR does not account for the possible role uPA or muPAR in regulating cytokine expression and may in part explain why suPAR alone does not alter cytokine expression. Further investigation of uPAR-cytokine

interaction is needed and should take into account potential roles played by different receptor forms.

In conclusion, this chapter has identified that the elevated expression of the urokinase plasminogen activator pathway is negatively correlated with epithelial barrier integrity, using two independent model systems. Inhibition of uPAR-integrin binding with ATN-658 increases resistance in bronchial epithelial cells and attenuates cell migration and spreading. scuPAR and MMP-9 are both elevated in asthma and have been associated with airway remodelling, our findings are limited to HBEC from healthy donors and should be investigated further in patient cells and clinically relevant samples. These data further implicate uPAR in bronchial epithelial homeostasis and provide proof of concept that targeting uPAR may be a therapeutic approach for lung diseases with a compromised epithelial layer.

Chapter 4: uPAR Expression in Bronchial Epithelial Cells Cultured from Asthma Patients and Healthy Controls

4 uPAR Expression in Bronchial Epithelial Cells Cultured from Asthma Patients and Healthy Controls

4.1 Introduction

uPAR is associated with airway epithelial cell homeostasis (Portelli *et al*., 2015) and protein levels are elevated in induced sputum (Xiao *et al*., 2005b) and bronchial epithelial biopsies from asthma patients (Stewart *et al*., 2012b). Serum scuPAR levels are elevated in a severe and nonatopic asthma phenotype, this study also found that uPAR expression was higher in the *lamina propria* (indicating inflammatory cells) and airway smooth muscle cells in asthma patients compared to healthy controls (Portelli *et al*., 2016). The relative contribution of the lung environment and intrinsic differences in the epithelium in asthma leading to elevated uPAR levels and the effects on airway epithelial homeostasis are not fully understood.

Expression profiling studies have proved powerful in detecting disease mechanisms underlying asthma (endotypes) and potential drug targets (Wesolowska-Andersen and Seibold, 2015). Well characterised study populations are required for these studies to enable findings to be translated to clinical outcomes. Woodruff *et al* identified a 'Th2 high' subset of asthma patients using microarray profiling, the subset was based on the expression of three epithelial genes: *CLCA1* (Chloride Channel Accessory 1), *POSTN* (Periostin), and *SERPINB2* (Serpin family B member 2) which were also shown to be induced by IL-13 (Woodruff *et al*., 2007). Microarray analysis was also used to combine the Th2 biomarker FeNO (forced exhaled nitric oxide) and bronchial epithelial gene expression to cluster asthma patients and identified multiple subgroups with Th2 inflammation with distinct endotypes

(Modena *et al*., 2014). RNA sequencing is now replacing microarray technology as it offers a more sensitive and accurate measurement of gene expression and is increasingly being used to study changes in airway cells in asthma. Yick *et al* compared the transcriptional profile of bronchial biopsies taken from asthma patients and healthy controls (Yick *et al*., 2013). 46 genes were differentially expressed and gene networks were associated with cell morphology, movement and development. Expression of Th2 signature genes, *POSTN*, *CLCA1* and *SERPINB2,* were elevated in asthma compared to controls, however only periostin was significantly differentially expressed. Another study investigated the effects of IL-13 (type 2 cytokine) on gene expression and methylation in epithelial cells from asthma patients, this study identified 8,524 IL-13 responsive gene transcripts of which 1,590 genes were near one or more differentially methylated CpG site (DMC) (Nicodemus-Johnson *et al*., 2016b). Overall this study showed that IL-13 induced changes in DNA methylation patterns in cultured HBEC were significantly enriched near asthma associated genes (e.g. *CCL26*, *POSTN* and *SERPINB2*). The same group integrated genome-wide, DNA methylation and whole transcriptome data from freshly isolated HBEC from 74 asthma patients and 41 non-asthmatic subjects. 638 genes were differentially expressed and 40,892 CpG sites were differentially methylated between asthmatics and non-asthmatics. DMCs but not differentially expressed genes exhibited clustering in co-expression modules and enrichment for eQTLs highlighting the need to further investigate asthma-associated epigenetic changes in the airway epithelium (Nicodemus-Johnson *et al*., 2016a).

Transcriptomics studies have made considerable progress in elucidating how bronchial epithelial genetics and epigenetics contribute to asthma disease onset and progression, and provide a hypothesis free approach to linking gene expression patterns to clinical phenotypes (Modena *et al*., 2014). However, the aforementioned studies have several limitations.

Analysis of whole biopsies enables the contribution of components of the airway wall to be assessed however cannot be translated to the contribution of individual cell types to disease. Secondly, biopsy specimens are limited to more central locations of the airways and so exploration of gene expression of the peripheral airways in severe asthma may prove difficult (Yick *et al*., 2013). Methylation studies in cells from patients with established disease may be affected by the disease itself, may reflect changes in response to the environment or may be affected by medication (Nicodemus-Johnson *et al*., 2016b). The largest airway epithelial RNA-Seq analysis to date was conducted in freshly isolated brush samples, a caveat of this approach is that cells may incur damage and stress as a result of the bronchoscopy process which may confound the findings e.g. injury may alter the inflammatory profile in these cells (Campbell *et al*., 1993).

We therefore sought to investigate differences between cultured HBEC from moderate to severe asthma patients and healthy controls using RNA Sequencing, uPAR (*PLAUR*) gene and isoform expression was explored in these analyses. The rationale of investigating gene expression in cultured HBEC was to identify gene signatures that may be altered and retained in the airway epithelium in asthma and to identify potentially novel pathways and genes that alter epithelial function in asthma.

4.2 Aims

The overall aim of this chapter was to investigate gene expression patterns in cultured bronchial epithelial cells isolated from the airways of moderate to severe asthma patients and healthy control subjects.

4.2.1 Specific aims

- Identify novel genes and pathways that are differentially expressed in epithelial cells isolated and cultured from the airways of asthma and control subjects.
- Specifically determine if total *PLAUR* and splice isoform expression is different in these cultured cells from cases and controls.
- Assess the relative expression and activity of the uPA-uPAR pathway in the bronchial epithelium in asthma.

4.3 Methods

4.3.1 Patient Recruitment

Moderate to severe asthma patients and healthy control subjects were recruited from Nottingham University Hospitals and Glenfield Hospital, Leicester, UK and by local advertising.

For subjects recruited from Glenfield Hospital, Leicester asthma was defined according to GINA (Global Initiative for Asthma) guidelines. Subject characterisation included demographics, spirometry, allergen skin prick tests, sputum induction, methacholine bronchial challenge, nasal brushings, and bronchoscopy. The study was approved by the Leicestershire ethics committees, and all patients gave their written informed consent (Woodman *et al*., 2013). This study was conducted in accordance with the amended Declaration of Helsinki. The Leicestershire, Rutland, and Northamptonshire ethics committee (ethics reference 4977/project approval number 6347) approved the protocol, and written informed consent was obtained from all patients. Subjects from Nottingham were recruited under the "Azithromycin in Asthma" (AZA) study and the "Small airways characterisation study" (SMAC). AZA and SMAC received favourable ethical approval from the NHS National Research Ethics Service (NRES) East Midlands committee in June 2011 (reference 11/EM/0062) and 23 March 2012 (reference 12/EM/0059). Patients with moderate to severe asthma were recruited (BTS step 3-5 (BTS/SIGN, 2016)) and all patients gave written informed consent. Subject characterisation included demographics, past medical history, spirometry, exhaled nitric oxide and bronchoscopy.

4.3.2 Isolation of Bronchial Epithelial Cells from Bronchoscopy

Human bronchial epithelial cells obtained from bronchial brushings from asthma patients and healthy controls were collected via bronchoscopy (City Hospital Nottingham and Glenfield Hospital Leicester, UK). Patients were consented for bronchoscopy. The bronchoscope (EVISEXERAII (BF-1T180)) (Olympus©, UK) was entered through the nasal cavity and passed down to the larynx where lignocaine was delivered through the scope to further suppress cough, and then was progressed down the trachea and bronchi. When the scope had reached the target area i.e. right bronchus intermedius, brush samples were obtained by passing a sheathed 3.0 mm diameter cytology brush down the bronchoscope. The brush was pushed out and cells were collected with a back and forth motion. Two brushes samples were obtained from the same location per subject and samples were pooled. The brushes were kept in 5 ml of BEGM in a 15 ml falcon tube. All of the media was then transferred to one well of a 12 well plate and cells were classed as passage 0. 150 µl cell suspension from the processed brush sample was cytospun and stained with haemotoxylin and eosin (H&E) to establish relative cell populations. Washes and biopsies were also collected from the patient, biopsies were sent for histopathology. Details of all the primary brush cells from asthma and control patients used in this thesis are summarised in Figure 4.3.1.

Asthma Donor	Gender	Age	FEV_1pp
1	-	-	-
2	Male	31	100
3	-	-	-
4	-	-	-
5	-	-	-
6	-	-	-
7	Female	51	50
8	Male	59	86
9	-	-	-
10	-	-	-
11	-	-	
12	Male	-	
13	Female	-	63
14	-	-	-
15	-	-	-
16	Female	-	100
17	-	-	59
18	Male	57	87
19	-	-	92
20	Male	59	103
21	-	-	78
.	-	-	-
23	-	-	79
24	Female	64	63
25	Male	64	54
26	Male	63	80
27	Female	58	90
28	Female	19	67
29	Female	37	90
30	Female	62	112
31	Female	62	76
32	Female	-	-
33	Female	52	67
34	Female	62	67
35	Female	21	81

Control Donor	Gender	Age	FEV_1pp
1	-	-	103
2	-	-	106
3	-	-	101
4	-	-	106
5	-	-	95
6	Male	24	-
7	Male	63	-
8	Female	27	-
9	Male	40	-
10	Female	20	-
11	Male	47	-
12	Female	30	-
13	Male	51	-
14	Male	23	109
15	Male	49	91
16	Male	64	113
17	Male	29	109
18	-	-	82

Table 4.3.1: Asthma and Healthy Control HBEC donor information. Asthma patients (*n*=35) and healthy controls (*n*=18) were recruited across two centres. Gender, Age and FEV_1pp (Forced Expiratory Volume in 1 second as a percent of predicted) were collected. '-' denotes where data was not available.

4.3.3 Cell Culture and RNA Isolation

Cells were thawed at passage 2/3 to a T75 cell culture flask and cultured in BEGM as described in section 2.1.2. Flasks were coated with collagen, collagen solution was made up by dissolving PureCol Type 1 Bovine Collagen solution into sterile water at a ratio of 1:100 to make a 30 μg/ml solution. 5 ml of collagen solution was added to the flask and incubated for 30 minutes at 37°C, and then aspirated prior to cell seeding. Media was changed every 2-3 days and RNA was harvested when cells had reached 80% confluency and RNA isolation was performed as described in section 2.2.1

4.3.4 RNA Sequencing

RNA QC, sequencing and analysis methods are described in detail in section 2.4 of this thesis. Briefly, RNA was assessed using RIN analysis (section 2.4.1) and library preparation and sequencing was performed by the Genome Analysis Facility (GAF), Genomics Coordination Centre (GCC) University Medical Centre Groningen (section 2.4.2.1). Read data was aligned to the human assembly GRCh37 using TopHat2 (section 2.4.4) and differential expression analysis and pathway analysis were completed using the Cufflinks and GSEA tools, respectively (sections 2.4.5 and 2.4.6).

4.3.5 Measuring Plasmin Activity in HBEC Supernatants

Plasmin activity was measured in supernatants from cultured HBEC isolated from asthma patients and healthy control subjects. The AFC Plasmin Assay Kit (SensoLyte® AS-72124) enables the measurement of plasmin activity using a fluorogenic substrate which releases the fluorophore AFC (7-amido-4-trifluoromethylcoumarin). Upon plasmin cleavage AFC

emits a yellow-green fluorescence, which can be quantified at excitation/emission=380 nm/500 nm. In brief, plasmin substrate was diluted in 2X assay buffer (50 µl plasmin substrate added to 4.95 ml assay buffer). 50 µl of cell supernatant was added to a well of a 96 well plate. A positive control (purified active plasmin) and a substrate control (deionized water) were included. The plate was pre-incubated for 10 minutes at the assay temperature (room temperature). The enzymatic reaction was then run by adding 50 µl of plasmin substrate solution into each well, reagents were mixed by gently shaking the plate for 30 seconds. Fluorescence was measured at 30, 60, 90, 120 and 150 minutes at Ex/Em=380 nm/500 nm.

4.4 Results

4.4.1 Subject Demographics

Demographics of the 33 asthma and 18 healthy control subjects are summarised in Table 4.4.1. Data for age, gender, lung function (FEV_1, FEV_1/FVC), asthma severity (BTS/GINA), atopy, blood eosinophil levels and serum IgE levels was collected.

	Asthma	Control
Subject *n*	33	18
Age- mean ±SD	53 ±14	39 ±16
Gender (% female)	61	25
FEV_1 (% predicted) ±SD	79 ±17	101 ±10
FEV_1 /FVC ±SD	79 ±8	68 ±11
BTS/ GINA >3 (% moderate/ severe asthma)	91	-
Atopy (% at least one positive indication)	50	0
Mean blood eosinophils ($x10^9$/L) ±SD	0.48 ± 0.49	0.13 ±0.07
Mean serum IgE (kU/L) ±SD	620 ±1371	52 ±72

Table 4.4.1: Demographics for Asthma and Control Subjects Used in RNA-Seq Analysis. Data are presented as mean±SD with the number of individuals with data (%). FEV_1 = forced expiratory volume in 1 sec; FVC = forced vital capacity.

4.4.2 Morphology and Characterisation of Primary Brush HBEC

HBEC from asthma and healthy patients in this chapter were collected via bronchial brushings (as described in section 4.3.2). Figure 4.4.2 shows a representative image of HBEC in submerged culture that were collected via brushing the airways. Cells from all donors were cultured under the same conditions and RNA and supernatants were collected from passage 2/3 HBEC.

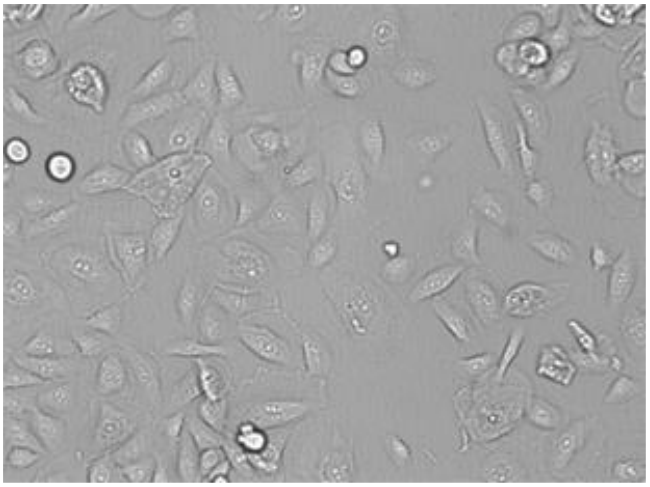


Figure 4.4.1: Representative Image of Primary Bronchial Epithelial Cells (passage 3) Isolated from Bronchoscopy Brushes. Under submerged conditions, cells exhibit cobblestone appearance typical of epithelial morphology.

Cells were characterised for the epithelial marker CK-14 using immunofluorescence (see Section 2.3.3). Figure 4.4.3 demonstrates that asthma and healthy donor cells obtained via brushing express the airway epithelial marker cytokeratin (CK-14).

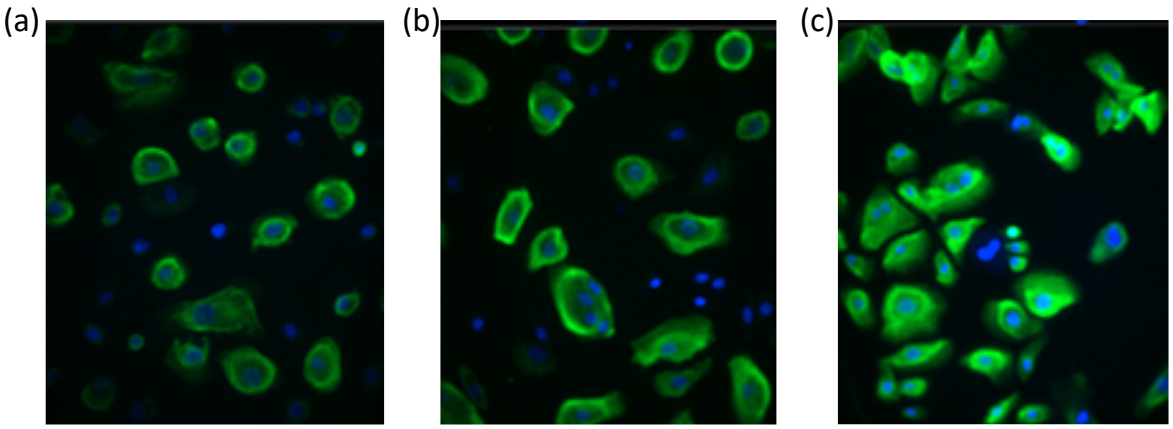


Figure 4.4.2: Characterisation of Primary HBEC Cultured from Asthma and Healthy Patients. HBEC isolated from bronchial brushes were cultured to passage 2-3, (a) Control subject, (b) Asthma patient 1, (c) Asthma patient 2 exhibit epithelial morphology and positive staining for CK-14. Nuclei Stained with 4',6-diamidino-2-phenylindole (DAPI) (blue).

4.5 Whole Transcriptome Analysis of Primary Cultured HBEC from Asthma and Control Subjects

HBEC cultured from brush samples taken from asthma patients (*n*=33) and healthy controls (*n*=18) were harvested at passage 2 or 3 for RNA and quality was assessed using RIN analysis. RNA sequencing was performed using the Illumina HiSeq 2500 to generate FASTQ files containing paired end 75 base pair reads for all samples. Files containing raw reads were concatenated to create single R1 (forward strand) and R2 (reverse strand) files. R1 and R2 files were then trimmed to remove adapters and quality trimmed to remove reads with phred score < 20.

Trimmed read files were aligned to the human genome build Gr37 release 75 using Tophat2. The Cufflinks package was used carry out differential gene expression analysis and to generate gene expression values (FPKM) for all genes detected in each sample. Gene set enrichment analysis was also used to identify differentially regulated pathways in epithelial cells from asthma patients compared to controls.

4.5.1 RNA Quality Control Analysis

RIN analysis quantification of RNA was assessed using the bioagilent analyser to assess whether RNA samples were suitable for RNA sequencing or not (see section 2.4.1 for methods). RIN analysis identified samples scored 9> and were suitable for sequencing. Due to insufficient sample RIN analysis was not performed for asthma donor 29.

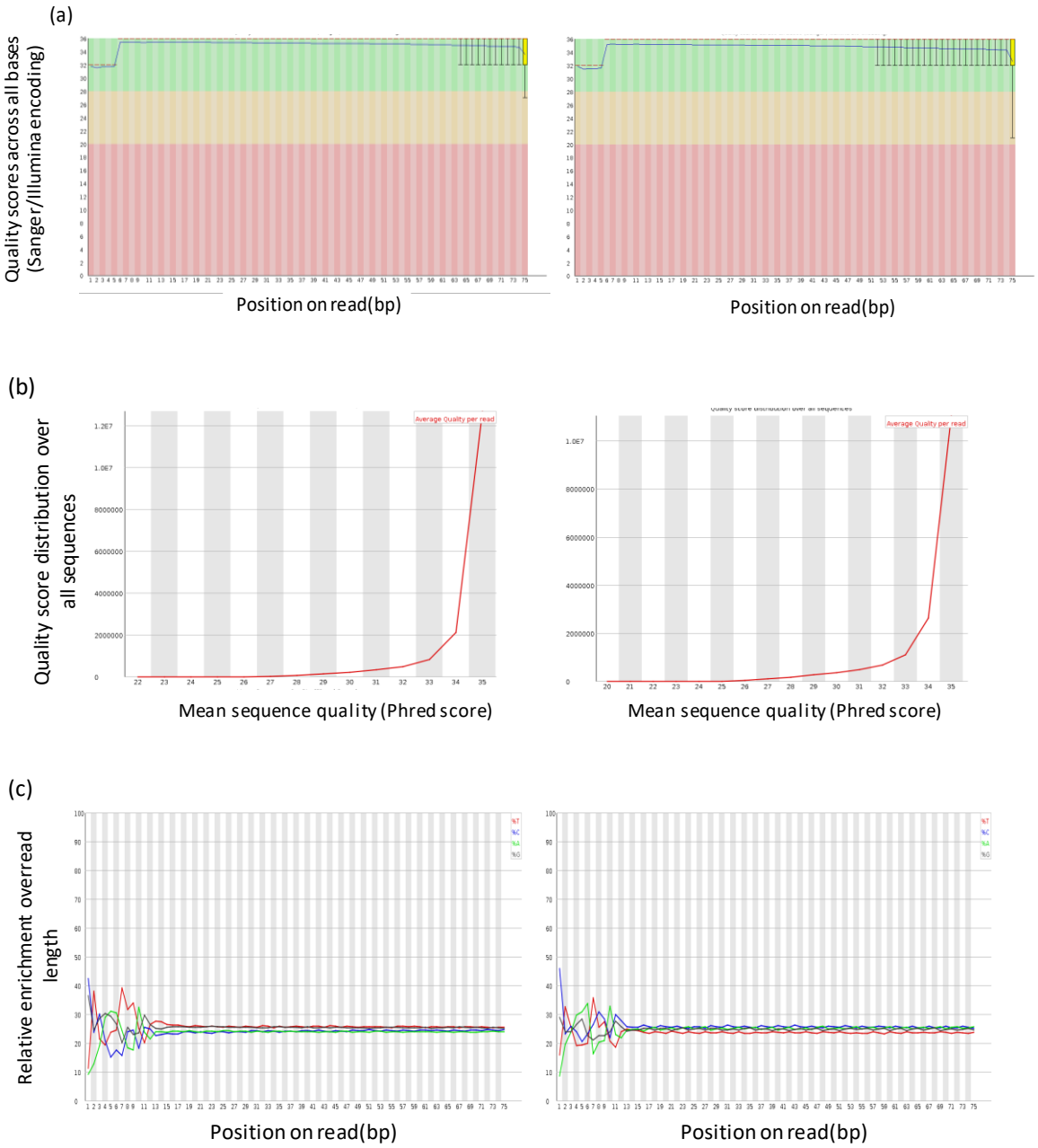
Asthma Donor	RIN score	Concentration (ng/µl)
1	10	586.9
2	10	236.1
3	10	231.7
4	10	317.7
5	10	353.1
6	10	437.6
7	10	402.9
8	9	783.2
9	10	521.1
10	10	595.3
11	10	112.5
12	9	559.7
13	10	559.2
14	10	179.9
15	10	456.7
16	10	420.1
17	10	193.3
18	10	175.1
19	10	129.4
20	10	590.3
21	9	177.8
22	10	204.3
23	10	308.7
24	10	456.1
25	10	89.4
26	10	154.7
27	10	612.2
28	10	129.3
29		
30	10	279.7
31	10	128.1
32	10	195.7
33	10	577.1

Control Donor	RIN score	Concentration (ng/µl)
1	9	599.3
2	10	607.9
3	10	294.3
4	10	589.1
5	10	214.6
6	9	309.8
7	10	573.4
8	10	533.5
9	10	513.8
10	10	627.3
11	10	304.9
12	10	218.9
13	10	377.9
14	10	109.5
15	10	383.1
16	9	307.8
17	10	529.9
18	10	210.6

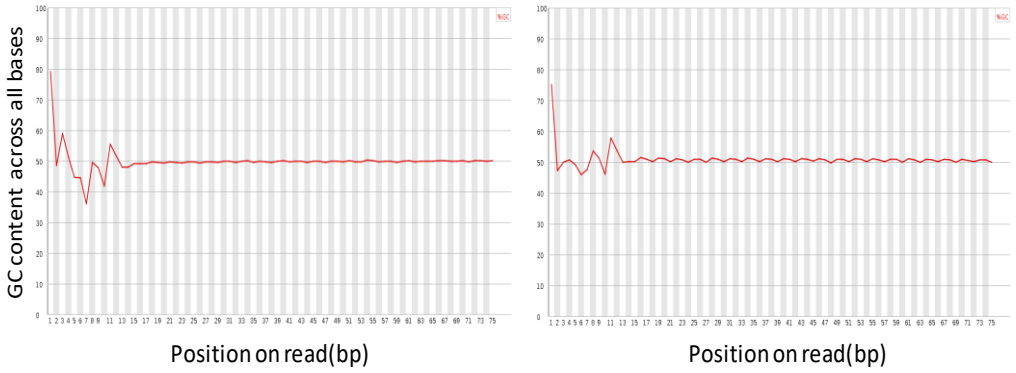
Table 4.5.1: RNA Integrity Analysis (RIN) and Concentration of RNA isolated from HBEC Isolated from Asthma Patients and Healthy Subjects. All samples achieved a RIN score of 9> and concentrations that were suitable for RNA sequencing.

4.5.2 Trimming, Quality Control and Alignment of Sequencing Data

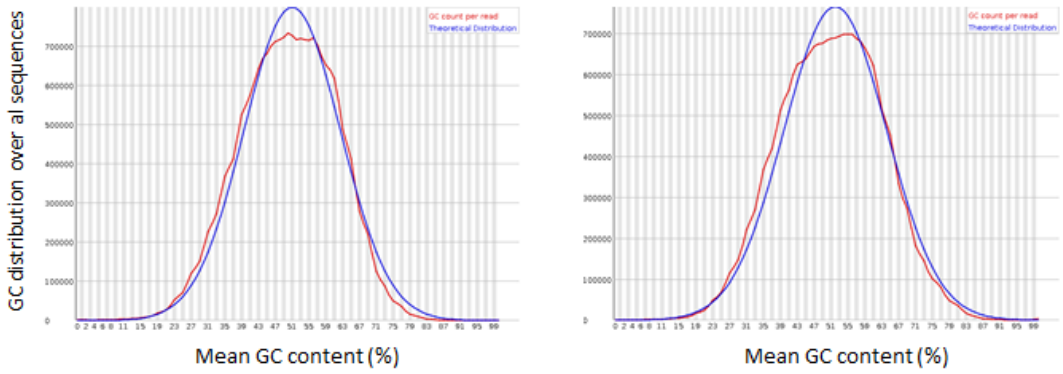
Sequencing data (reads) were processed as described in 2.4.3 and assessed for quality using the FastQC tool as described in section 2.4.3.1. Representative graphs for FastQC analysis for forward and reverse concatenated read files are shown below in Figure 4.5.2.



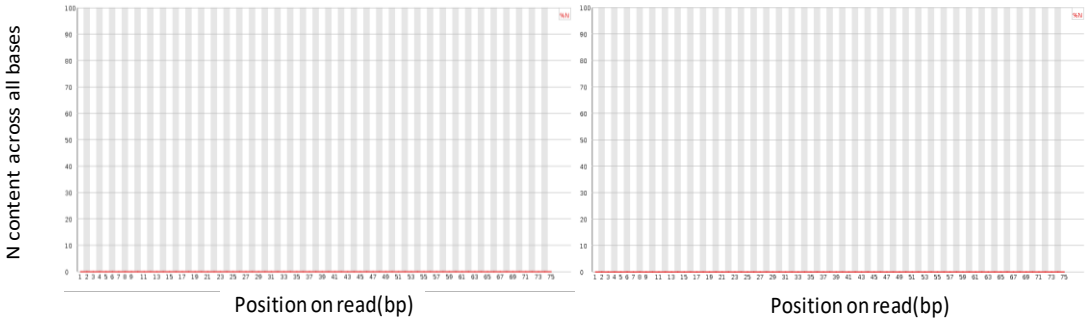
(d)


GC content across all bases
Position on read(bp)
Position on read(bp)

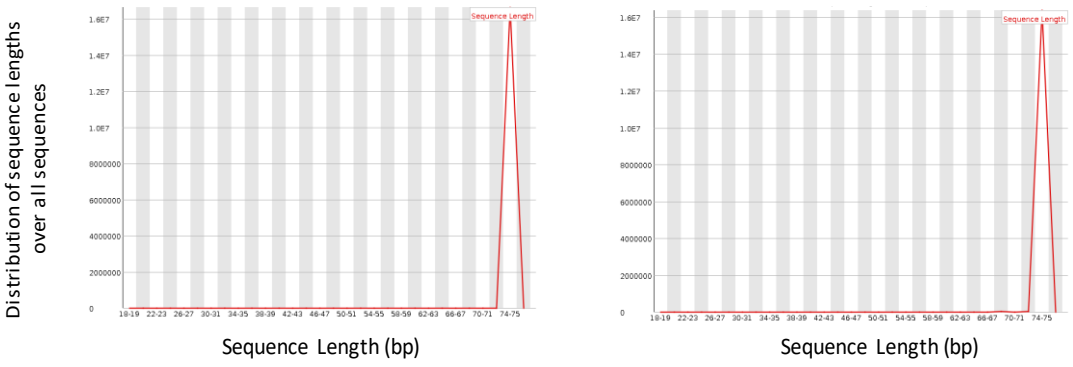
(e)


GC distribution over al sequences
Mean GC content (%)
Mean GC content (%)

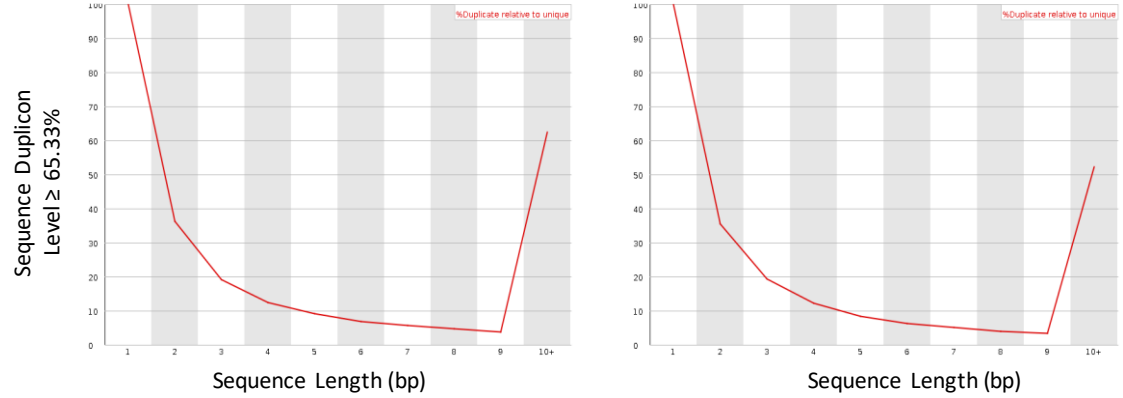
(f)


N content across all bases
Position on read(bp)
Position on read(bp)

(g)


Distribution of sequence lengths over all sequences
Sequence Length (bp)
Sequence Length (bp)

(h)



(i)

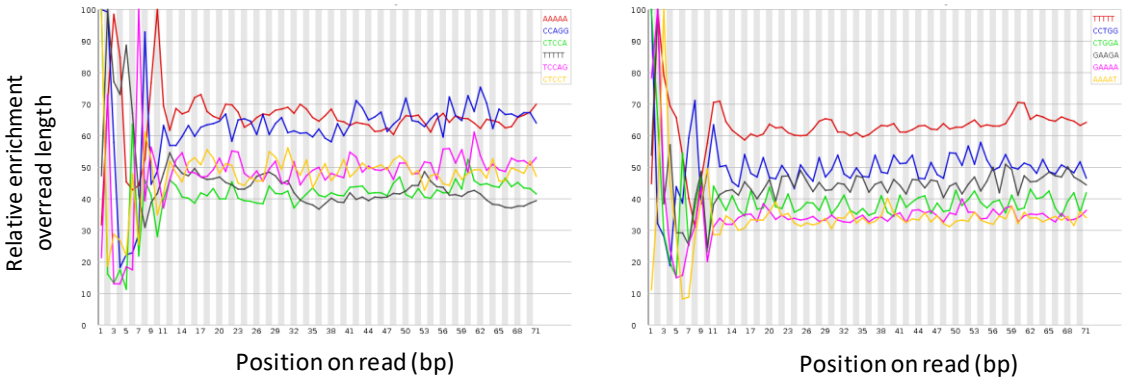


Figure 4.5.1: FastQC Confirmed Read Files Containing Sequencing Data are Suitable for Downstream Analysis. All parameters measured passed quality control analysis (a) Per base quality assessment showed that all reads met q score >20, read quality was poorest at the end of the read which is typical of sequencing data. (b) Per sequence mean quality score = >27. (c) Per base sequence content = <20% (d) Per base GC content = <10% (e) Per sequence GC content 15-30% (f) Per base N content = 0 (failure = >20%) (g) Sequence length distribution analysis did not identify read sequences of varying lengths (h) Duplicate sequences = <20% (i) Overrepresented Kmers = <10 fold. Read 1 files (R1, forward reads) and Read 2 files (R2, reverse reads) are shown on the left and right, respectively.

Paired end reads were aligned to the human genome build Gr37 using the TopHat alignment software tool. The alignment rate and number of paired end reads aligned for each sample are summarised in Figure 4.5.1. The average read depth was 16,521,259 PE reads (read depth ranged from 10,361,312- 19,395,273 PE reads). The effects of differences in sequencing depth are minimized by normalisation methods (Conesa *et al*., 2016).

Asthma Donor	Total PE reads	Alignment rate (%)
1	17,324,629	97.8
2	18,303,527	97.3
3	17,915,831	96.5
4	18,232,269	97.4
5	18,355,045	97.6
6	16,489,582	96.8
7	16,872,275	97.5
8	12,506,419	97.5
9	14,675,273	97.1
10	16,659,442	96.6
11	17,367,706	97.6
12	16,038,550	96.6
13	16,479,407	97.1
14	18,684,553	95.1
15	17,178,046	97.3
16	17,056,909	97.0
17	17,940,975	96.9
18	16,828,235	97.4
19	14,807,550	97.5
20	15,029,318	97.5
21	16,720,944	96.9
22	17,566,035	97.5
23	15,842,931	97.2
24	14,875,653	97.4
25	16,682,937	96.7
26	15,008,445	93.9
27	17,289,252	97.3
28	17,241,314	97.3
29	13,681,492	92.9
30	17,382,993	94.0
31	16,480,592	97.3
32	17,607,014	97.0
33	15,675,049	97.3

Control Donor	Total PE reads	Alignment rate (%)
1	15,698,701	97.7
2	16,976,363	96.9
3	18,582,151	96.8
4	17,137,065	97.1
5	15,685,255	96.9
6	14,875,653	97.4
7	17,783,536	96.8
8	17,193,467	97.2
9	16,034,270	96.8
10	16,453,023	97.3
11	16,014,587	96.7
12	15,282,905	96.6
13	17,096,134	96.8
14	19,395,273	97.3
15	13,168,186	97.0
16	17,075,479	97.0
17	18,860,359	96.9
18	10,361,312	97.3

Table 4.5.2: Alignment Rate and Read Depth of Asthma and Control Samples Used for RNA-Seq Analysis. Alignment scores ranged from 92.9-97.8% indicating a high proportion of reads were mapped for all samples. Read depth achieved from sequencing was sufficient for differential gene expression analysis.

4.5.3 Differential Gene Expression Analysis

The Cuffdiff tool from the Cufflinks package was used to calculate mean FPKM values for all genes identified in RNA from asthma and control subjects. Table 4.5.3 lists the genes that were differentially expressed in order of significance (FDR) as well as the fold change and the locus of each gene. FPKM values were log transformed prior to differential expression analysis therefore fold changes presented as log2.

GENE	LOCUS	ASTHMA (FPKM)	HEALTHY (FPKM)	log2 (FOLD CHANGE)	FDR (q value)
SPRR3	1:152973927-152976395	21.10	56.89	1.43	0.02
DISP1	1:222988363-223179337	9.23	23.18	1.33	0.02
PTCH2	1:45265732-45308735	14.36	0.10	-7.14	0.02
GAS5	1:173832385-173872687	215.89	470.97	1.13	0.02
IMMP1L	11:31391365-31531192	52.25	14.45	-1.85	0.02
RAB3IL1	11:61664732-61687741	0.55	2.57	2.22	0.02
CHD4	12:6679116-6723297	48.32	100.36	1.05	0.02
NOS1	12:117645946-117889975	2.35	1.09	-1.11	0.02
ANKRD10	13:111530886-111567433	14.31	8.54	-0.75	0.02
SNRPN,SNURF	15:25068793-25492435	171.04	76.87	-1.15	0.02
PAQR5	15:69591241-69740768	16.66	1.01	-4.05	0.02
TJP1	15:29991570-30261068	88.76	45.77	-0.96	0.02
MSLN	16:810745-818928	14.83	6.77	-1.13	0.02
TMC5	16:19421817-19510435	0.82	6.58	3.01	0.02
SLC9A3R1	17:72666716-72765492	166.42	66.57	-1.32	0.02
KRT13	17:39657230-39662020	9.82	28.05	1.51	0.02
CLHC1	2:55400155-55496627	2.26	10.60	2.23	0.02
PPIL3	2:201735629-201768655	44.96	17.71	-1.34	0.02
TIGD1	2:233412778-233547491	0.54	71.23	7.05	0.02
MIR663A	20:26167555-26232162	5.94	249.23	5.39	0.02
ADA,Z97053.1	20:43160425-43280874	229.82	20.59	-3.48	0.02
TANGO2	22:20004536-20058066	18.64	9.10	-1.03	0.02
APOL1	22:36649053-36663857	34.39	19.53	-0.82	0.02
DERL3	22:24129149-24181315	0.98	0.33	-1.58	0.02
CXCL5	4:74861358-74864496	11.65	5.38	-1.11	0.02
DDR1	6:30844197-30868754	365.56	263.92	-0.47	0.02
SYNGAP1,ZBTB9	6:33378175-33425369	51.20	10.06	-2.35	0.02
ANLN	7:36363762-36493459	30.89	15.21	-1.02	0.02
CCDC180	9:99918851-100140806	0.28	5.17	4.19	0.02
COL5A1	9:137533618-137736686	1.02	2.68	1.39	0.02
RP11-258C19.4	X:53122891-53200096	0.94	0.30	-1.66	0.02
OPHN1	X:67262185-67653755	17.38	1.60	-3.44	0.02
TOP2A	17:38544767-38574212	12.21	7.03	-0.80	0.04
THBD	20:23022332-23030854	20.81	32.39	0.64	0.04
SPINK7	5:147647742-147763346	0.47	2.16	2.20	0.04
HLA-S	6:31349850-31350065	2775.18	0.00	-inf	0.04
CEA,CEACAM5,CEACAM6	19:42212503-42290801	15.05	25.03	0.73	0.05
IFITM1,IFITM2	11:307630-315475	158.12	93.02	-0.77	0.05
FNBP4	11:47738063-47789172	169.11	109.33	-0.63	0.05
DYSF	2:71680468-71913898	7.60	13.01	0.78	0.05
SAMHD1	20:35504523-35580246	8.84	4.97	-0.83	0.08
CDK1	10:62494099-62555340	10.93	5.99	-0.87	0.09
SEPT4	17:56597197-56769416	0.44	0.78	0.84	0.09
B3GNT8	19:41931263-41934635	75.80	136.32	0.85	0.09
IL18R1,IL1RL1	2:102927961-103015218	21.17	10.40	-1.03	0.09
CRCT1	1:152486977-152488486	20.52	39.28	0.94	0.10
HLA-DPB1	6:33032345-33054978	1.03	0.35	-1.54	0.10
HLA-DPA1	6:33032345-33054978	1.78	0.62	-1.53	0.10

Table 4.5.3: Genes Differentially Expressed in the Epithelium in Asthma. 48 genes were differentially expressed in cultured HBEC from asthma patients (*n*=33) compared to healthy controls (*n*=18). *Genes

<50bp apart within a given loci are assigned to the same locus and listed together. (FDR < 10%). FDR = false discovery rate (equivalent to the *q* value/ corrected *p* value); Inf = infinity (indicates the gene is 'switched' on).

48 genes were identified as differentially expressed (DE) (FDR <10%) in epithelial cells from asthma patients compared to controls 40 of which met FDR <5%. *TIGD1* (Tigger Transposable Element Derived 1, fold change (FC) -7.05), *MIR663A* (MicroRNA 663a, FC -5.39), *CCDC180* (Coiled-Coil Domain Containing 180, FC -4.19) and *TMC5 (*Transmembrane Channel Like 5, FC -*3.01*) were the most downregulated genes based on FDR and fold change. Genes with the greatest increase in expression were *PTCH2* (Patched 2, FC 7.14), *PAQR5* (Progestin and AdipoQ Receptor Family Member 5, FC 4.05), *ADA* (Adenosine Deaminase, FC 5.16), *OPHN1* (Oligophrenin 1, FC 3.44). The *HLA-S* pseudogene was 'switched on' in asthma cells, these changes are considered rare but can be detected in DE analysis.

DE genes that have previously been associated with asthma include *TJP1* (tight junction protein 1/ zona occluden 1, FC 0.96), *NOS1* (Nitric Oxide Synthase 1, FC 1.11), *IL1RL1* (Interleukin 1 Receptor Like 1, FC 1.03), *IL18R1* (Interleukin 18 Receptor 1 FC 1.03), *CXCL5* (C-X-C Motif Chemokine Ligand 5, FC 1.11) *HLA-DPB1* (Major Histocompatibility Complex, Class II, DP Beta 1, FC 1.54) and *HLA-DPA1* (Major Histocompatibility Complex, Class II, DP Alpha 1, FC 1.53). DE genes for structural proteins in the lung comprised of *KRT13* (Keratin 13, FC -1.51), *COL5A1* (collagen type V alpha 1 chain, FC -1.39) and *ANLN* (anillin actin binding protein, FC -1.02). Expression of type 2 signature genes *POSTN* (FC 0.16), *SERPINB2* (FC -0.23) and *CLCA1* (FC 1.2) were not significantly differentially expressed. To understand the collective effect of changes in gene expression and the biological relevance of observed fold changes in airway epithelial cells in asthma patients, pathway analysis was performed.

4.5.4 Pathway Analysis Using Gene Set Enrichment Analysis

GSEA was performed using normalised FPKM values generated using Cuffnorm (see section 1.6.6). Pathways or "gene sets" are identified as up or downregulated based on the enrichment of genes in a given phenotype. An initial analysis was conducted using the Hallmark (H) database containing 50 gene sets that summarise and represent specific well-defined biological states or processes (Liberzon *et al*., 2015). Hallmark gene sets are derived from multiple "founder sets" and undergo computational processing to assign biological themes to overlapping gene sets and identify expression data. A second and more in-depth analysis was performed using the Curated database (C2) which comprises of 4729 gene sets collected by online pathway databases, PubMed publications, microarray studies and MYC Target Gene Database at (Johns Hopkins University School of Medicine) (Subramanian *et al*., 2005). The enrichment score (ES) indicates the change in expression of a given gene set and is calculated from the 'Signal' statistic. This is generated using the 'Tag' and 'List' value which indicate the percentage of genes contributing to the ES and where in the list the ES is attained. The results from the H and C2 database analyses are summarised in Tables 4.5.2 and 4.5.3, this thesis focuses on the most statistically significant results and a cut-off of the 20 most altered gene sets (pathways) was chosen.

4.5.4.1 Pathway Analysis Using the Hallmark database

Table 4.5.4 summarises details of the pathways altered in cultured bronchial epithelial cells in asthma based on analyses using the GSEA Hallmark database.

(a)

GENE SET	SIZE	ES	NES	NOM p-value	FDR q-value	FWER p-value	RANK AT MAX	LEADING EDGE		
E2F TARGETS	199	0.62	2.65	0	0	0	2314	tags=50%,	list=12%,	signal=56%
INTERFERON ALPHA RESPONSE	94	0.68	2.57	0	0	0	3611	tags=73%,	list=19%,	signal=91%
G2M CHECKPOINT	199	0.58	2.48	0	0	0	3273	tags=53%,	list=18%,	signal=63%
INTERFERON GAMMA RESPONSE	197	0.57	2.42	0	0	0	3611	tags=54%,	list=19%,	signal=66%
CHOLESTEROL HOMEOSTASIS	73	0.56	2.07	0	0	0	3334	tags=51%,	list=18%,	signal=62%
MITOTIC SPINDLE	199	0.48	2.05	0	0	0	3876	tags=38%,	list=21%,	signal=47%
TGF BETA SIGNALING	54	0.45	1.57	0.01	0.01	0.09	5614	tags=50%,	list=30%,	signal=71%
FATTY ACID METABOLISM	158	0.37	1.52	0.00	0.03	0.17	5361	tags=45%,	list=29%,	signal=63%
TNFA SIGNALING VIA NFKB	199	0.35	1.49	0.00	0.03	0.22	4413	tags=39%,	list=24%,	signal=50%
BILE ACID METABOLISM	112	0.37	1.47	0.01	0.03	0.28	2625	tags=28%,	list=14%,	signal=32%
REACTIVE OXIGEN SPECIES PATHWAY	47	0.44	1.47	0.03	0.03	0.30	4214	tags=45%,	list=23%,	signal=58%
MTORC1 SIGNALING	199	0.35	1.47	0.01	0.03	0.30	4792	tags=39%,	list=26%,	signal=52%
DNA REPAIR	143	0.35	1.43	0.01	0.04	0.42	4129	tags=36%,	list=22%,	signal=46%
OXIDATIVE PHOSPHORYLATION	199	0.32	1.38	0.01	0.07	0.59	5269	tags=38%,	list=28%,	signal=53%
ALLOGRAFT REJECTION	200	0.32	1.37	0.02	0.07	0.62	5588	tags=41%,	list=30%,	signal=58%
COMPLEMENT	196	0.32	1.36	0.01	0.07	0.66	4590	tags=33%,	list=25%,	signal=44%
EPITHELIAL MESENCHYMAL TRANSITION	199	0.32	1.35	0.02	0.07	0.68	4827	tags=37%,	list=26%,	signal=50%
SPERMATOGENESIS	133	0.34	1.35	0.03	0.07	0.69	4127	tags=29%,	list=22%,	signal=37%
APOPTOSIS	160	0.32	1.35	0.03	0.06	0.70	5013	tags=34%,	list=27%,	signal=46%
ESTROGEN RESPONSE LATE	199	0.30	1.28	0.03	0.11	0.88	4939	tags=37%,	list=27%,	signal=49%
XENOBIOTIC METABOLISM	199	0.30	1.28	0.05	0.11	0.89	2553	tags=20%,	list=14%,	signal=23%
MYC TARGETS V1	199	0.30	1.25	0.06	0.13	0.93	4781	tags=33%,	list=26%,	signal=44%
PI3K AKT MTOR SIGNALING	105	0.32	1.23	0.11	0.15	0.96	5529	tags=42%,	list=30%,	signal=59%
ADIPOGENESIS	196	0.29	1.21	0.09	0.17	0.98	6219	tags=39%,	list=33%,	signal=58%
IL2 STAT5 SIGNALING	199	0.28	1.18	0.12	0.22	1.00	4586	tags=35%,	list=25%,	signal=46%

(b)

GENE SET	SIZE	ES	NES	NOM p-value	FDR q-value	FWER p-value	RANK AT MAX	LEADING EDGE		
MYC TARGETS V2	58	-0.47	-1.82	0.00	0.01	0.01	3577	tags=47%	list=19%	signal=57%
HEDGEHOG SIGNALING	36	-0.43	-1.47	0.04	0.05	0.11	2664	tags=36%	list=14%	signal=42%

Table 4.5.4: “Hallmark” Pathways Regulated in The Bronchial Epithelium in Asthma. GSEA was performed using the Hallmark Database to identify pathways regulated by HBEC from asthma patients (FDR <25%). (a) 25 pathways were upregulated. (b) 2 pathways were downregulated (b) in HBEC cultured from asthma subjects compared to healthy controls. ES = enrichment score; NES = normalised enrichment score; NOM = nominal; FDR = false discovery rate; FWER = family wise error rate.

Using the hallmark database, 25 out of 50 gene sets were significantly upregulated and 2 gene sets were downregulated in asthma samples (FDR<25%). The most upregulated pathway consisted of genes targeted by the E2F transcription factor (NES 2.65), important in cell proliferation. Immune and signalling processes that have been identified in asthma previously include TGFβ and TNFα signalling, and the complement pathway. Genes related to epithelial mesenchymal transition and reactive oxygen species pathways were also upregulated in cultured asthma HBEC. Interestingly pathway activity of developmental and metabolic processes such as adipogenesis and fatty acid metabolism are increased in asthma cells, less known is known about the contribution of these processes in asthma. The pathways shown to be downregulated were MYC targets and hedgehog signalling which regulate cell cycle progression and differentiation.

4.5.4.2 Pathway Analysis Using the Curated Database

Table 4.5.5 provides a summary of details of the pathways altered in cultured bronchial epithelial cells in asthma based on analyses using the GSEA Curated database.

(a)

GENE SET	SIZE	ES	NES	NOM p-value	FDR q-value	FWER p-value	RANK AT MAX	LEADING EDGE		
CERVICAL_CANCER_PROLIFERATION_CLUSTER	137	0.71	2.89	0	0	0	2167	tags=68%,	list=12%,	signal=76%
BREAST_CANCER_GRADE_1_VS_3_UP	146	0.70	2.86	0	0	0	2167	tags=58%,	list=12%,	signal=65%
EGFR_SIGNALING_24HR_DN	244	0.65	2.80	0	0	0	3315	tags=61%,	list=18%,	signal=73%
LARGE_TO_SMALL_PRE_BII_LYMPHOCYTE_UP	160	0.67	2.78	0	0	0	3220	tags=61%,	list=17%,	signal=73%
DOXORUBICIN_RESISTANCE_UP	53	0.79	2.77	0	0	0	3219	tags=89%,	list=17%,	signal=107%
EARLY_T_LYMPHOCYTE_UP	102	0.71	2.76	0	0	0	2167	tags=64%,	list=12%,	signal=72%
PEDIATRIC_CANCER_MARKERS	115	0.69	2.75	0	0	0	2888	tags=64%,	list=16%,	signal=76%
CELL_CYCLE_GENES_IN_IR_RESPONSE_24HR	123	0.68	2.74	0	0	0	4150	tags=74%,	list=22%,	signal=95%
ESTRADIOL_RESPONSE_24HR_UP	316	0.61	2.72	0	0	0	3295	tags=56%,	list=18%,	signal=67%
OLIGODENDROCYTE_DIFFERENTIATION_UP	554	0.58	2.70	0	0	0	3037	tags=50%,	list=16%,	signal=58%
NORMAL_QUIESCENT_VS_NORMAL_DIVIDING_DN	86	0.71	2.70	0	0	0	2605	tags=62%,	list=14%,	signal=71%
CYCLING_GENES	143	0.67	2.69	0	0	0	4331	tags=76%,	list=23%,	signal=98%
NRAS_SIGNALING_DN	72	0.72	2.67	0	0	0	3219	tags=78%,	list=17%,	signal=94%
IL6_DEPRIVATION_DN	98	0.70	2.67	0	0	0	3283	tags=74%,	list=18%,	signal=90%
ADIPOGENESIS_3	101	0.69	2.66	0	0	0	3273	tags=68%,	list=18%,	signal=82%
DNA_REPLICATION	185	0.63	2.65	0	0	0	4522	tags=63%,	list=24%,	signal=82%
CML_DIVIDING_VS_NORMAL_QUIESCENT_UP	178	0.63	2.62	0	0	0	3284	tags=55%,	list=18%,	signal=66%
CELL_CYCLE_GENES_IN_IR_RESPONSE_6HR	82	0.70	2.62	0	0	0	4150	tags=78%,	list=22%,	signal=100%
MULTIPLE_MYELOMA_PR_UP	44	0.79	2.61	0	0	0	3089	tags=82%,	list=17%,	signal=98%
CELL_CYCLE_MITOTIC	308	0.59	2.61	0	0	0	4150	tags=56%,	list=22%,	signal=71%

(b)

GENE SET	SIZE	ES	NES	NOM p-value	FDR q-value	FWER p-value	RANK AT MAX	LEADING EDGE		
GENDER_EFFECT_UP*	9	-0.98	-2.36	0.00	0.00	0.00	300	tags=100%	list=2%	signal=102%
TRETINOIN_RESPONSE*	12	-0.76	-1.97	0.00	0.19	0.41	2110	tags=58%,	list=11%	signal=66%

Table 4.5.5: "Curated" Pathways Regulated in The Bronchial Epithelium in Asthma. A second more comprehensive analysis was conducted using the Curated Pathways Database to identify pathways regulated in HBEC from asthma patients (FDR <25%). (a) 846 pathways were upregulated (a) and 2 pathways were downregulated in HBEC cultured from asthma subjects compared to healthy controls. Pathways representing genes that are up or down regulated under certain conditions, or genes that are altered after a time point, specify this in the name. ES = enrichment score; NES = normalised enrichment score; NOM = nominal; FDR = false discovery rate; FWER = family wise error rate;. IR = ionizing radiation; PR = proliferation

GSEA identified 846 out of 4723 gene sets that were upregulated in asthma and 2 downregulated gene sets (FDR<25%). The most enriched pathway was the cervical cancer proliferation cluster (NES 2.89), which includes genes involved in cell cycle progression and cell growth. Other pathways upregulated involve cell proliferation, immune processes,

signalling as well development and differentiation. The “gender effect up” was downregulated in asthma HBEC (NES -0.98), this pathway consists of genes related to gender-associated differences in disease. The “tretanoin response” pathway involves genes that regulate cell death and differentiation, these genes are downregulated in cultured epithelial cells from asthma patients. Analysis conducted using the hallmark and curated database have identified pathways that have been associated with asthma pathobiology as well as novel pathways that may further explain altered epithelial function in asthma.

4.5.5 Expression of the uPAR Pathway Genes in Asthma Subjects compared to Healthy Control Subjects

uPAR pathway genes were not identified as differentially expressed by Cuffdiff in cultured epithelial cells from asthma patients compared to healthy controls. To investigate mRNA expression of uPAR (*PLAUR*), uPA (*PLAU*), PAI-1 (*SERPINE1*) and MMP-9 (*MMP9*) across all subjects, normalised FPKM values for asthma and control HBEC donors were generated using Cuffnorm and analysed in GraphPad Prism.

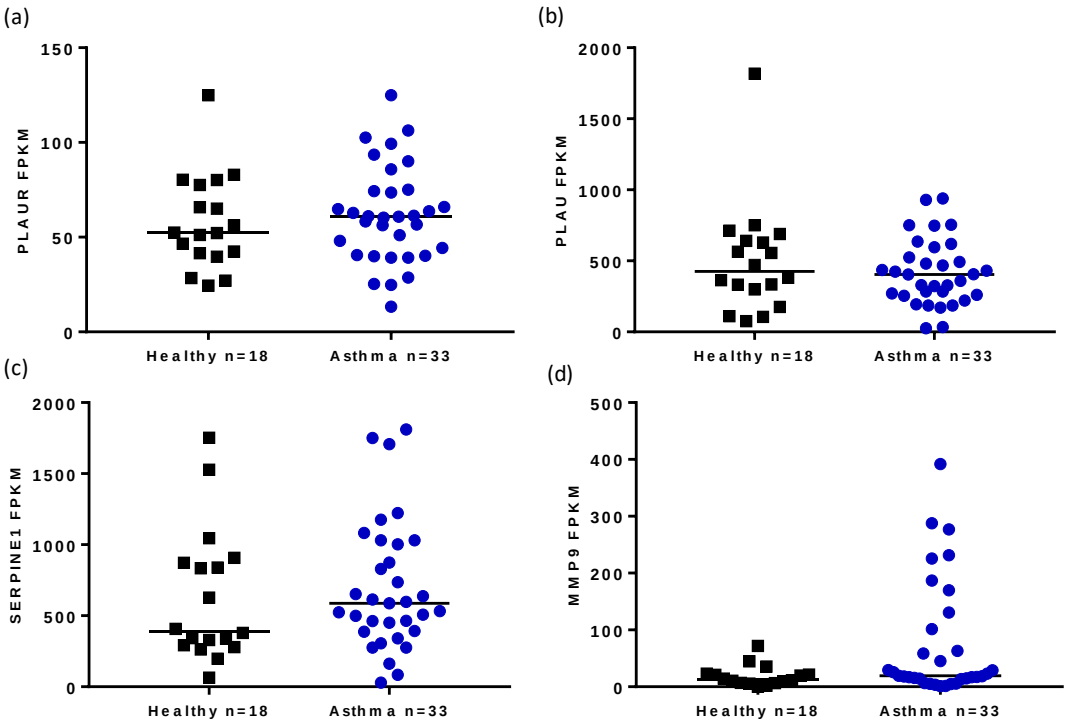


Figure 4.5.2: uPAR Pathway Genes Are Not Differentially Expressed in Cultured Epithelial Cells from Asthma Patients: Whole transcripome analysis of cultured HBEC from asthma (*n*=33) and control (*n*=18) subjects was performed using RNA-Seq. uPAR (*PLAUR*), uPA (*PLAU*), PAI-1 (*SERPINE1*) and MMP-9 (*MMP9*) median expression levels in asthma subjects *vs* controls were compared using a Mann-Whitney two-tailed *t*-test. a) *PLAUR*, asthma (A) FPKM = 60.76, control (C) FPKM = 52.35, p = 0.6; b) *PLAUR*, A FPKM= 404.7, C FPKM = 426, p = 0.54; c) *SERPINE1*, A FPKM = 586.8, C FPKM = 393.3, p = 0.39; d) *MMP9*, A FPKM = 19.38, C = 12.91, p = 0.10).

PLAUR, *SERPINE1* and *MMP9* mRNA expression were elevated in asthma subjects compared to healthy controls however the differences in expression were not statistically significant. (*PLAUR*, Mann Whitney two-tailed *t*-test, asthma median 60.76 *vs* healthy median 52.35 FPKM, p = 0.6; *SERPINE1*, Mann Whitney two-tailed *t*-test, asthma median 586.8 *vs* healthy median 393.3 FPKM, p = 0.39; *MMP9*, Mann Whitney two-tailed *t*-test, asthma median 19.38 *vs* healthy median 12.91 FPKM, p = 0.10). *PLAU* expression was slightly elevated in controls (*PLAU*, Mann Whitney two-tailed *t*-test, asthma median = 404.7 *vs* healthy median = 426 FPKM, p = 0.54).

4.5.6 Analysis of PLAUR Expression in the Epithelium in Asthma using Gene Expression Omnibus

PLAUR mRNA was investigated in epithelial cells isolated from asthma patients in two independent studies. Publicly available expression data was used to extract gene expression values for PLAUR from freshly isolated HBEC using the Woodruff *et al* microarray study (Woodruff *et al*., 2007) and a more recent RNA-Seq analysis (Nicodemus-Johnson *et al*., 2016a). Analyses were carried out in asthma subjects and healthy controls and expression data was obtained from GEO (Gene Expression Omnibus, www.ncbi.nlm.nih.gov/geo).

Microarray analysis was carried out in airway epithelial brushings for 42 asthma subjects and 28 healthy controls (GE0 accession number: GSE4302) using the Affymetrix Human Genome U133 Plus 2.0 Array (PLAUR probe I.D's 210845, 214866, 211924). RNA-Seq analysis was performed in 64 asthmatic and 31 healthy subjects using the Illumina HiSeq2000. PLAUR mRNA expression in these subjects is shown in Figure 4.5.4.

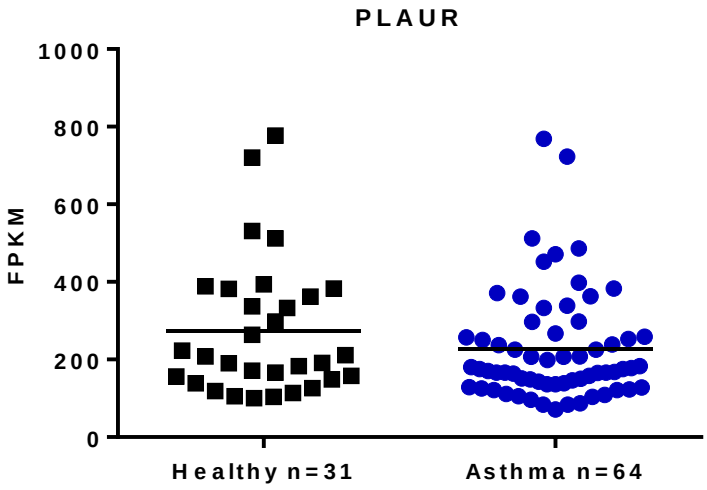


Figure 4.5.3: RNA-Seq Analysis of *PLAUR* mRNA Expression in Freshly Isolated HBEC from Asthmatics and Healthy Controls. Freshly isolated HBEC from asthma (*n*=64) and control (*n*=31) subjects were harvested for RNA and whole transcriptome analysis was performed using RNA-Seq. PLAUR mRNA was not differentially expressed in asthma patients (Mann-Whitney *t*-test, healthy median 208 FPKM vs asthma median 175 FPKM, *p*=0.21).

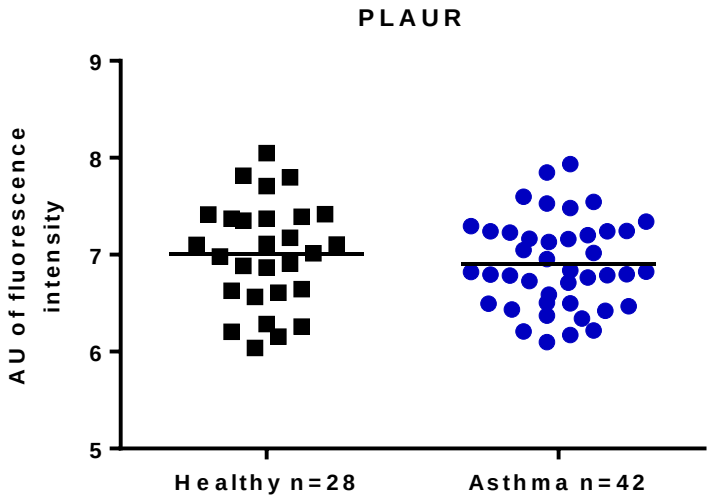


Figure 4.5.4: Microarray Analysis of PLAUR mRNA Expression in Freshly Isolated Bronchial Epithelial Cells from Asthma Subjects. Epithelial brush samples were obtained from 42 asthma patients and 28 healthy individuals for gene expression profiling using microarray (Affymetrix Human Genome U133 Plus 2.0 Array). PLAUR expression was not significantly altered in asthma HBEC (Mann-Whitney t-test, healthy median 7.05 vs asthma median 6.82, *p*=0.37).

RNA-Seq analysis did not identify a significant difference in *PLAUR* mRNA expression in asthma HBEC compared to healthy individuals (Figure 4.5.4). *PLAUR* expression ranged from 71 to 769 FPKM in asthma subjects which was similar to expression in healthy controls (31 to 777 FPKM). FPKM values in freshly isolated cells were 2.8 fold higher than in cultured epithelial cells in asthma (freshly isolated HBEC median 175, cultured HBEC median 60.7) and almost 4 fold higher in control HBEC (freshly isolated HBEC median 205, cultured HBEC median 52.4), suggesting basal PLAUR expression in the bronchial epithelium decreases in

passaged cells. Furthermore, microarray analysis also found the PLAUR expression was not elevated in HBEC from asthma patients (Figure 4.5.5).

4.6 Expression and Activity of the uPA-uPAR Pathway in the Bronchial Epithelium in Asthma

4.6.1 qPCR Analysis of PLAUR Expression in Primary Cultured HBEC from Asthma and Control Subjects

uPAR (PLAUR) has been shown to be elevated in the airway epithelium in asthma biopsies, and membrane PLAUR (mPLAUR) and soluble-spliced PLAUR (ssPLAUR) have each been shown to regulate cellular processes in HBEC. To further explore the expression of PLAUR variants in the bronchial epithelium in asthma, total PLAUR, mPLAUR and ssPLAUR mRNA expression was measured in RNA harvested from confluent cultures of passage 2/3 HBEC from asthma patients and healthy control subjects. RNA isolation and cDNA synthesis were performed as described in sections 2.2.1 and 2.2.4 and gene expression was measured using Taqman qPCR, for methods and primer sequences see section 2.2.5.

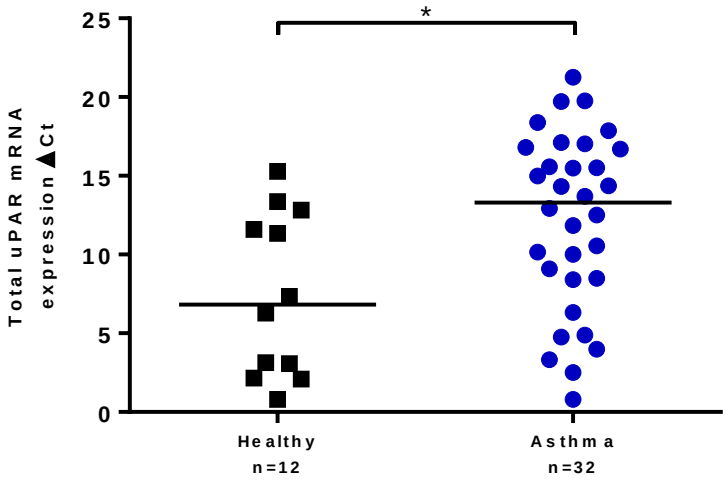


Figure 4.6.1: Total PLAUR mRNA Levels are Elevated in Cultured HBEC Isolated from Asthma Patients compared to Healthy Controls. Total PLAUR expression was measured in epithelial cells isolated via bronchial brushing from asthma (*n*=32/33) and healthy control subjects (*n*=12/18). HBEC were cultured using BEGM and harvested at passage 2/3 for RNA. RNA extraction and complementary DNA synthesis as described in sections 2.2.1 and 2.2.4 and section 2.3.5. qPCR reactions were performed in triplicate, expression was quantified using the ΔCT method. Median and individual data are shown. *p<0.05.

Total *PLAUR* mRNA levels were significantly elevated in cultured HBEC from asthma patients (*n*=32) compared to healthy subjects (*n*=12) (Mann Whitney *t*-test, asthma median 13.31 *vs* healthy median 6.82 ΔCT, *p*=0.011). The assay was not detected (no CT value) in 6 control subjects and 1 asthma subject, the data for these individuals is not presented.

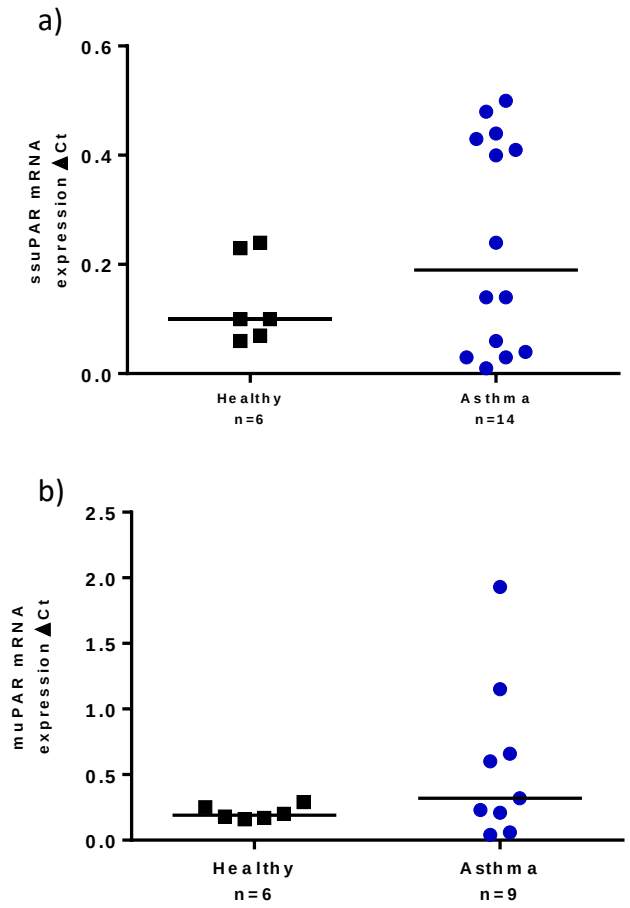


Figure 4.6.2: Soluble-spliced *PLAUR* and Membrane *PLAUR* Levels Are Not Significantly Altered in Cultured Bronchial Epithelial Cells from Asthma Patients Compared to Healthy Subjects. a) ssPLAUR and b) mPLAUR mRNA expression was assessed in cultured airway epithelial cells. Median and individual data are shown. Both PLAUR variants were elevated in asthma subjects however this change was not significant. ssPLAUR was detected in 6/ 18 control subjects and 14/ 33 asthma subjects and mPLAUR was measured in 6/18 control subjects and 9/33 asthma subjects. HPRT1 was measured in all samples (data not shown) suggesting the PLAUR assays could not efficiently detect these variants.

ssPLAUR mRNA expression was elevated in asthma patients (*n*=14) compared to healthy subjects (*n*=6), however this was not significantly different (Mann-Whitney *t*-test, asthma median 0.19 *vs* healthy median 0.10 ΔCT, p = 0.53). mPLAUR levels were also elevated in asthma (*n*=9) vs healthy controls (*n*=6) (Mann-Whitney *t*-test, asthma median 0.32 *vs* healthy median 0.19 ΔCT, p = 0.22). These data are difficult to interpret as ssPLAUR and mPLAUR

were detected in 6 out of 18 control subjects and 9/33 and 14/33 asthma subjects, respectively. HPRT1 mRNA levels were detected in all HBEC samples, therefore it is likely that sample preparation was not optimal for the ssPLAUR and mPLAUR assays.

PLAUR mRNA expression measured in asthma and control HBEC using RT-PCR (ΔCT) were correlated with FPKM values. ΔCT and FPKM were positively correlated in asthma and control bronchial epithelial cells (r=0.33, p=0.03, n=42). The correlation observed highlights differences in ΔCT and FPKM from the same individuals. This may be due to differences in sample preparation, for example library preparation for RNA-sequencing. Another explanation may be that additional transcripts are detected when using the *PLAUR* qPCR assay compared to RNA-Seq quantification, or vice versa.

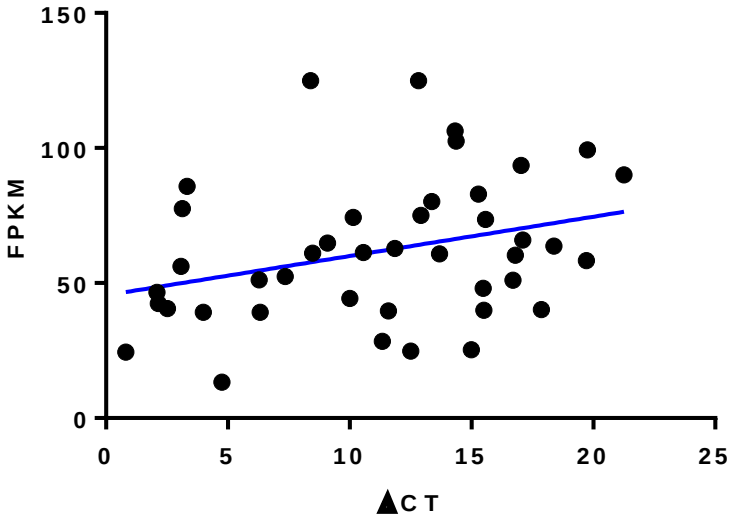


Figure 4.6.3: Correlation of PLAUR ΔCT *vs* FPKM in Primary Epithelial Cells. qPCR and RNA-Sequencing (for methods see section 2.3.5 and 2.6.2) were used to measure PLAUR mRNA in cultured HBEC isolated from asthma patients and healthy control subjects (n=42). ΔCT and FPKM were positively correlated (r=0.33, p=0.03).

4.6.2 Protein Expression of uPAR Pathway Components in the Bronchial Epithelium in Asthma

Elevated scuPAR, uPA, PAI-1 and MMP-9 protein levels have been detected in asthma. Cultured HBEC isolated from asthma and healthy control patients were cultured to passage 2/3 under submerged conditions, cell supernatants were collected for protein analysis. scuPAR, uPA, PAI-1 and MMP-9 protein levels were measured using the Luminex Multiplex assay (as described Section 2.4.2) in order to determine whether levels of secreted protein are altered in HBEC from asthma subjects compared to healthy controls.

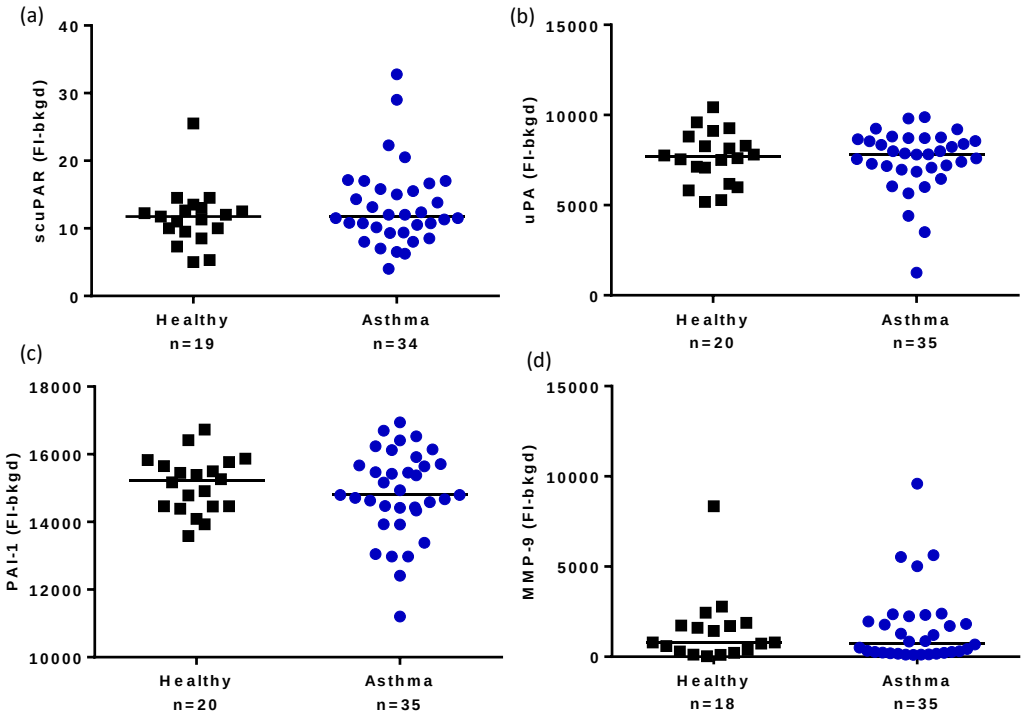


Figure 4.6.4: uPAR Pathway Proteins are not elevated in Cultured Epithelial Cells from Asthma Subjects. Cell supernatants were collected from cultured HBEC (passage 2/3) isolated from asthma and healthy control subjects. Levels of scuPAR, uPA, PAI-1 and MMP-9 were measured in supernatants using Luminex. Levels of secreted protein did not differ in cultured asthma HBEC when compared to HBEC from healthy controls. (Mann-Whitney *t*-test scuPAR p=0.44; MMP-9 p=0.99; uPA p=0.9; PAI-1 p=0.65) Median and individual data are shown.

scuPAR, MMP-9, uPA and PAI-1 levels were not statistically different in HBEC cell supernatants from asthma subjects compared to healthy controls (Mann-Whitney *t*-test, scuPAR asthma median *n*=34, healthy median *n*=19, *p*=0.44; MMP-9 asthma median *n*=32, healthy median *n*=18, *p*=0.99; uPA asthma median *n*=35, healthy median *n*=20, *p*=0.9; PAI-1 asthma median *n*=35 healthy *n*=20, *p*=0.65). These findings suggest that altered expression of uPAR pathway components in asthma may arise from another cell type (e.g. immune cells in sputum) or that expression in passaged epithelial cells returns to basal levels.

To assess cell associated proteolytic activities such as MMP-9 activation and ECM proteolysis, cell supernatants were collected as described previously and plasmin activity was assessed. Plasmin activity was monitored for 150 minutes in asthma (*n*=10) and control subjects (*n*=6). Plasmin activity was elevated overall in supernatants from asthma subjects however this change was not significant (asthma median 166.2 O.D (range 45.9-320.3), healthy control median 131.5 O.D (range 39.03-213.1)), see Figure 4.6.5. uPA is a protease required for plasmin activation, uPA secretion was not elevated in asthma HBEC which may in part explain these data.

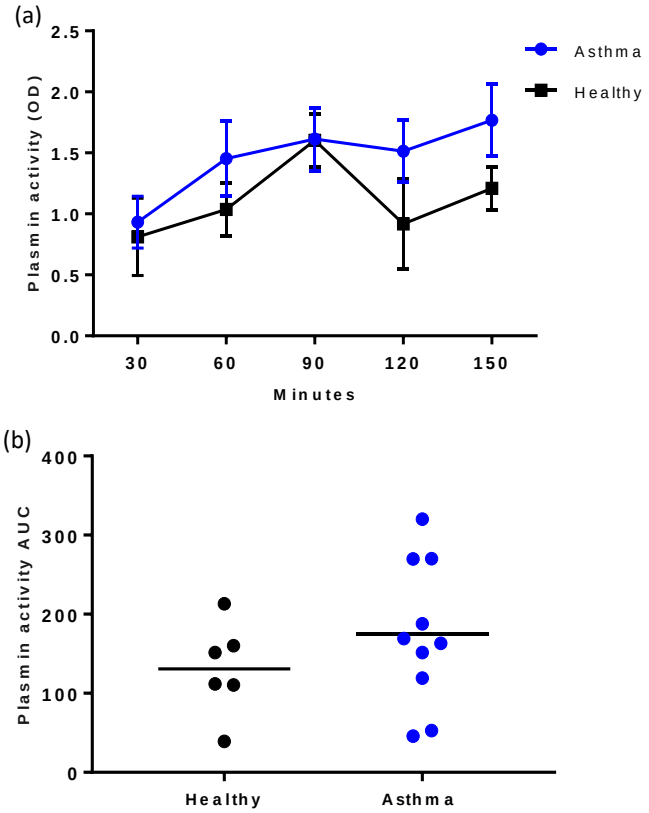


Figure 4.6.5: Plasmin Activity in Cultured Bronchial Epithelial Cells is Moderately Elevated in Asthma. HBEC brush samples from asthma and healthy individual were cultured to passage 2-3. a) A fluorometric assay was used to quantify plasmin activity in cell supernatants, plasmin activity was elevated in asthma subjects however this was not statistically significant (Two Way Anova, p=0.39). b) Area under the curve (AUC) in asthma (n=10) and control subjects (n=6), Mann-Whitney t-test, asthma median 166.2 OD *vs* control median 131.5 O.D, p=0.22.

To investigate the relationship between the expression of uPAR pathway components, scuPAR, MMP-9, uPA and PAI-1 levels in cell supernatants from asthma and healthy HBEC were correlated and assessed using Spearman's rank correlation coefficient (see Figure 4.6.6).

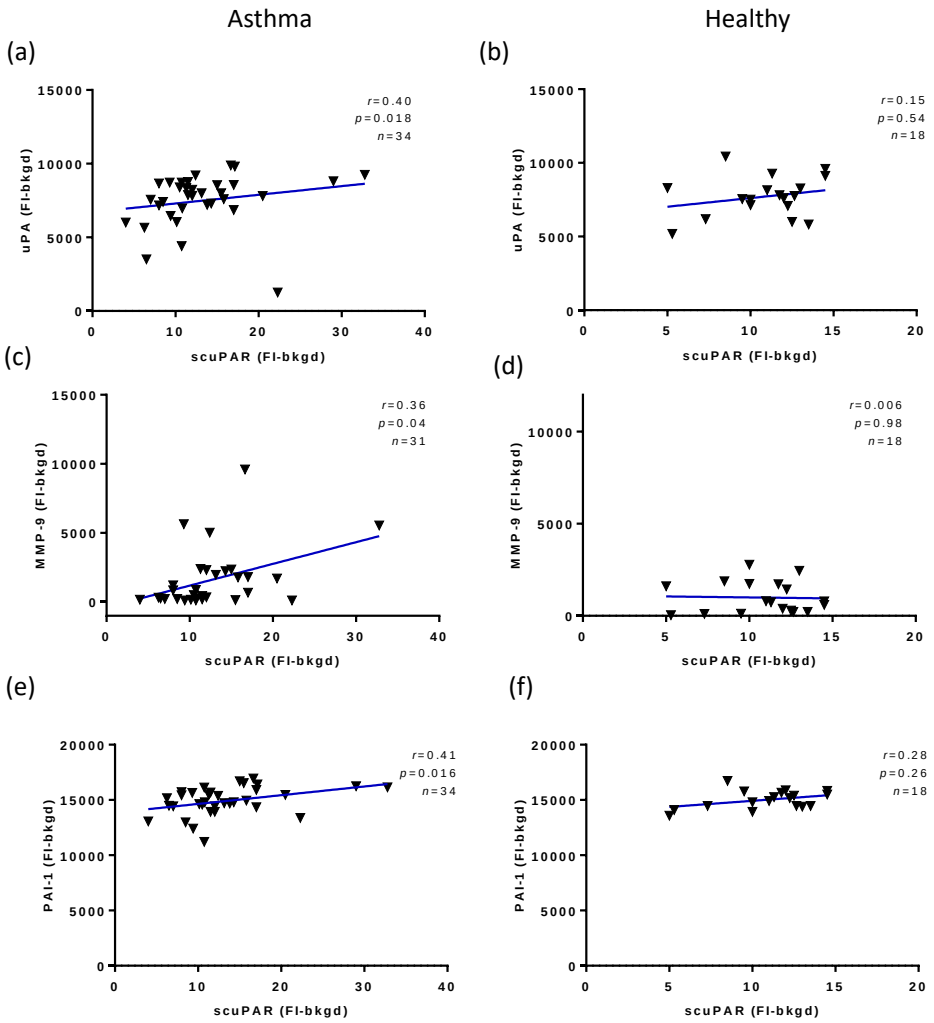


Figure 4.6.6: scuPAR Expression Correlates with MMP-9, uPA and PAI-1 levels in the Bronchial Epithelium in Asthma. Supernatants from cultured HBEC brush samples from asthma and healthy individuals (passage 2-3) were collected and levels of scuPAR (soluble-cleaved uPAR) uPA (urokinase), MMP-9 (matrix metalloproteinase 9) and PAI-1 (plasminogen activator inhibitor 1). scuPAR levels were positively correlated with MMP-9, uPA and PAI-1 in cells from asthma patients, protein levels did not correlate in control subject cells.

scuPAR expression positively correlated with uPA, MMP-9 and PAI-1 in asthma subjects. This relationship was not observed in samples from healthy control cells (asthma: scuPAR *vs*. MMP-9 p=0.04; scuPAR *vs* PAI-1 p=0.016; uPA *vs*. scuPAR p=0.018; healthy controls: scuPAR *vs* MMP-9 p=0.98; scuPAR *vs* PAI-1 p=0.26; uPA *vs*. scuPAR p=0.54).

4.7 Discussion

In this chapter, we aimed to investigate gene and protein expression in cultured bronchial epithelial cells isolated from the airways of moderate to severe asthma patients and healthy control subjects. The key aims were to i) Identify novel genes and pathways that are differentially expressed in epithelial cells isolated and cultured from the airways of asthma and control subjects; ii) Specifically determine if total *PLAUR* and splice isoform expression is different in these cultured cells from cases and controls; and to iii) Assess the relative expression and activity of the uPA-uPAR pathway in the bronchial epithelium in asthma. RNA-Seq analysis identified 48 differentially expressed genes in epithelial cells isolated from asthma subjects, some of which have been associated with asthma, and GSEA pathway analysis identified processes that may be dysregulated in the asthmatic epithelium. qPCR and protein analysis did not identify altered uPAR pathway activity in asthma cells but did show that total PLAUR levels are elevated in cultured asthma HBEC.

As discussed at the beginning of this chapter, transcriptomics studies have been pivotal in our understanding of the genetic and epigenetic landscape of the epithelium in asthma. We conducted RNA-Seq analysis in cultured bronchial epithelial cells to identify changes in gene expression which may represent more permanent alterations in the epithelium. DE analysis identified 48 differentially expressed genes (FDR <10%), the genes with the greatest increase in expression in asthma HBEC were *PTCH2* (FC 7.14), PAQR5 (FC 4.05), *ADA* (Adenosine Deaminase, FC 5.16) and *OPHN1* (FC 3.44). The PAQR5 steroid binding receptor regulates cilia beat frequency in ciliated cells in the fallopian tube and is expressed in liver and lung in mice suggesting a role in these tissues (Nutu *et al*., 2007). *PTCH2* is a regulator of hedgehog signalling which is required for cell development and differentiation (Rahnama *et al*., 2004),

and *OPHNI1* is associated with cell adhesion and migration in cancer (Goto *et al*., 2014). The *ADA* gene regulates T cell activity (Ohta and Sitkovsky, 2014) and IL-13 induced suppression of *ADA* in COPD correlates with reduced FEV_1 suggesting this gene may play a role in lung function (Maneechotesuwan *et al*., 2016). *HLA-S* is a pseudogene, pseudogenes are thought to be conserved in the genome but their function is not clear (Shina 2009).

TIGD1 (FC -7.05), *MIR663A* (FC -5.39), *CCDC180* (FC -4.19) and *TMC5* (FC -3.01) were the most downregulated genes in asthma subjects. *TIGD1* belongs to a family of DNA-mediated transposons in humans, the exact function of this gene is not known, DNA transposons are involved in genome evolution however are generally thought to be inactive in humans (Reilly *et al*., 2013). Downregulation of the micro RNA *MIR663A* is associated with increased cell proliferation and invasion in non-small cell lung cancer (Zhang *et al*., 2016) and *CCDC180* is a coiled-coil domain-containing protein, many of which regulate gene expression, associated between this SNP and the inflammatory disorder Behcet's disease (Fei *et al*., 2009). *TMC5* is thought to code membrane proteins that form transmembrane channels and is a marker in several cancers (Zhan *et al*., 2015). A group of structural genes, *KRT13*, *ANLN* and *COL5A1* were also downregulated in asthma epithelial cells. *ANLN* is associated with cell migration and cytokinesis and *KRT13* and *COL5A1* encode keratin and collagen proteins**.** In summary, cultured bronchial epithelial cells isolated from asthma subjects' exhibit reduced expression of genes that regulate cell division and cytoskeletal changes, gene transcription and malignancy and elevated expression of cell proliferation, migration and signalling genes. Further investigation of the genes identified may aid in our understanding of abnormal repair and regeneration of the epithelium in asthma.

We also identified genes previously linked with asthma that were upregulated in cultured epithelial cells from asthma patients, including *IL1RL1* and *IL18R1*. The *IL1RL1/IL18R1* locus has been associated with asthma (Moffatt *et al*., 2010; Ramasamy *et al*., 2012; Gordon *et al*., 2016), *IL1RL1* encodes the ST2 receptor which is elevated in serum in asthma (Oshikawa *et al*., 2001). *TJP1* encodes the tight junction protein ZO-1, the present analysis has found that expression is elevated in asthma HBEC however reduced expression of ZO-1 has been shown in atopic asthma and is related to impaired epithelial barrier function (de Boer *et al*., 2008). The role of *TJP1* in epithelial barrier function is not fully understood, investigation of protein localisation as well as expression is needed to assess how altered expression impacts on epithelial barrier properties (Vermeer *et al*., 2009). *NOS1* (neuronal NOS) is expressed constitutively in the airway epithelium and *NOS1* gene variants are associated with asthma risk and lung function however the role of this protein in asthma pathology is unclear (Gao *et al*., 2000; Grasemann, 2001; Vareille et al., 2011). Expression of the chemokine *CXCL5* and antigen receptors *HLA-DPA1* and *HLA-DPB1* were also elevated in asthmatic epithelial cells. CXCL5 regulates neutrophil trafficking and expression levels are elevated in acute asthma exacerbations (Qiu *et al*., 2007; Koltsova and Ley, 2010) (Koltsova and Ley, 2010), *HLA-DPA1* and *HLA-DPB1* variants are associated with paediatric asthma (Noguchi *et al*., 2011). The genes identified provide insight into the processes that may be inherently altered in the bronchial epithelium in asthma and serve as potential targets in asthma management. Expression of type 2 signature genes were not differentially expressed in cultured HBEC; *POSTN* and *CLCA1* were elevated (*POSTN* FC 0.16 and *CLCA1* FC 1.2) whereas *SERPINB2* expression was slightly reduced (FC -0.23). Validation and functional analysis of differentially expressed genes is needed to conclude how altered gene expression and pathway activity affect epithelial function in asthma.

GSEA pathway analysis was carried out using two databases, the hallmark and curated databases consisting of 50 and 4723 gene sets, respectively. 37 gene sets from the hallmark database were significantly upregulated and 2 gene sets were downregulated in asthma samples. The most upregulated pathway consisted of E2F transcription factor targets genes, suggesting altered regulation cell division and proliferation. TGF-β and TNF-α signalling, EMT and reactive oxygen species pathways were also upregulated which may represent a pro-remodelling and inflammatory phenotype. Upregulation of developmental and metabolic processes such as adipogenesis and fatty acid metabolism in asthma cells may serve as interesting pathway to target, although less known is known about the contribution of these processes in asthma. MYC target genes and hedgehog signalling which regulate cell cycle progression and differentiation, were downregulated in cultured epithelial cells.

A more comprehensive analysis was completed using the curated database, 846 pathway gene sets were upregulated in asthma and 2 were significantly downregulated. The cervical cancer proliferation cluster, which regulates cell cycle progression and cell growth, showed the greatest upregulation in asthma cells. Downregulation of the tretanoin response pathway which regulates cell death differentiation, further emphasis altered homeostasis in airway epithelial cells from asthma subjects. Genes related to gender-associated differences in disease were downregulated in asthma HBEC, this gene set shares genes with developmental processes which may be less active in basal epithelial cells. Although many of the pathways identified have been derived from cancer-associated studies, the genes involved may regulate these processes in other cell types and tissues. Analyses conducted using the hallmark and curated database have identified pathways regulating cell proliferation, immune processes, signalling as well development and differentiation.

Having identified differentially expressed genes and pathways, we then assessed the relative expression and activity of the uPA-uPAR pathway in the bronchial epithelium in asthma. Total *PLAUR* (uPAR) mRNA expression was elevated in asthma HBEC however this increase was only significant when quantified using qPCR. m*PLAUR* and ss*PLAUR* expression was not altered in asthma subjects, data however was difficult to interpret as both variants were not detected in all subjects, this may be due to low abundance of these in cultured primary HBEC. These data suggest that elevated uPAR expression in the bronchial epithelium, as shown *in vivo* (Stewart and Sayers, 2009), is retained in cultured epithelial cells. Total *PLAUR* gene expression values from qPCR and RNA-Seq analysis were positively correlated (r=0.33, p=0.03), correlation data highlights discordance between qPCR and RNA-Seq data. This may be due to sample preparation and also differences in sensitivity and the number of transcripts detected, which may explain why whole transcriptome analysis did not identify uPAR as differentially expressed in asthma cells. Separate microarray and RNA-Seq studies also showed that uPAR expression was not elevated in asthma subjects when compared to healthy controls (see section 4.5.6), however study populations for these analyses included mild asthma patients whereas our analysis included moderate to severe asthmatics. There is evidence that elevated uPAR is related to severe non-atopic asthma (Portelli *et al*., 2016), our findings provide further evidence that uPAR levels play a role in severe asthma.

We did not observe differences in protein expression or activity of uPAR pathway components in epithelial cells cultured from asthma patients. HBEC from asthma patients and control subjects had similar levels of scuPAR, uPA, PAI-1 and MMP-9 in cell supernatants, plasmin activity was elevated in asthma cells however this was not significant. scuPAR expression is also regulated by proteases that cleave the receptor which may not be expressed or active in passaged basal cells. Elevated scuPAR in asthma has been observed in

sputum and serum in asthma (Xiao *et al*., 2005a; Portelli *et al*., 2015), these samples may retain elevated scuPAR whereas this may be lost in cultured cells. uPA, PAI-1 and MMP-9 have also been shown to be elevated in sputum (Xiao *et al*., 2005a), the source of increased levels of these proteins may be immune cells rather the airway epithelium. Furthermore, these proteins are elevated in response to tissue injury (Crosby and Waters, 2010), in cultured undifferentiated cells expression may return to basal levels. Interestingly, levels of these pathway proteins were positively correlated in asthma patients and not in healthy individuals. MMP-9 levels correlate with uPA, PAI-1 and uPAR in vascular disorders and liver malignancies suggesting their co-expression may be important in disease (Inuzuka *et al*., 2000; Schneiderman et al., 1998).

In summary, we have identified genes and pathways with altered expression in cultured airway epithelial cells and have characterised the uPAR pathways in these cells. Previous gene expression studies of the epithelium in asthma have sequenced endobronchial biopsy samples and freshly isolated epithelial cells, (Yick *et al*., 2013; Nicodemus-Johnson *et al*., 2016a) however no studies to date have performed whole transcriptome analysis using passaged cells. A key strength of our model is that the genes and pathways identified are likely to signify inherent changes that underlie epithelial dysfunction, as opposed to acute changes in response to tissue injury. This is also a possible limitation as genes involved in these responses are central in understanding disease progression. Future studies comparing the expression of freshly isolated and cultured cells from the same patients could identify pathways that continue to be active and may in turn lead to altered structure and function of the epithelium. A second limitation is that we used an analysis pipeline different to those used in previous expression studies therefore it is difficult to directly compare results. There is no optimal pipeline and different software tools normalise and process data differently

which can have an effect on the results (Conesa *et al*., 2016). We chose to use analyses software suitable for heterogeneous datasets and with normalisation methods that help overcome variability in read depth as seen with our samples. Further study of these genes is needed to determine whether pathways can be targeted therapeutically in asthma. Our investigation of the uPAR pathway found that HBEC from asthma patients do not exhibit increased pathway activity, as observed *in vitro* (Xiao *et al*., 2005b), however pathway components are highly correlated in HBEC from asthma subjects suggesting they may be co-expressed. We also found that total *PLAUR* levels were increased in asthma patients compared to controls, *PLAUR* levels are elevated in bronchial biopsies in asthma (Stewart and Sayers, 2009), our data strongly suggest that elevated expression of uPAR is retained in cultured cells. There is increasing evidence that uPAR is player in airway remodelling and that there is aberrant pathway activity in asthma (Portelli *et al*., 2015), particularly severe subtypes.

Chapter 5: Whole Transcriptome Analysis of Human Bronchial Epithelial Cells Engineered to Overexpress uPAR Variants

5 Whole Transcriptome Analysis of Human Bronchial Epithelial Cells Engineered to Overexpress uPAR Variants

5.1 Introduction

uPAR is a regulator of cell homeostasis and there is emerging evidence that this receptor regulates airway epithelial function and that pathway activity is dysregulated in asthma. Elevated protein expression of uPAR has been observed in sputum, serum and epithelial biopsies from asthma patients (Xiao *et al*., 2005a; Portelli *et al*., 2014; Stewart *et al*., 2012a). Expression of uPA, PAI-2 (*SERPINB2*), PAI-1 and plasmin are altered in asthma suggesting that the pathway is dysregulated.

Multiple isoforms of uPAR are expressed in HBEC (Stewart and Sayers, 2009) and cleavage of the receptor results in soluble forms of the receptor, it is not known whether specific forms of the receptor are differentially expressed in asthma. Overexpression of the soluble and membrane bound receptor in bronchial epithelial cells results in altered cell proliferation, migration and protease activity, importantly different receptor variants differentially regulate these processes suggesting that certain variants drive a distinct phenotype. Different uPAR isoforms are expressed and have been shown to have distinct roles in HBEC. The membrane and soluble forms are able to perform different functions due to interaction with different ligands and signalling pathways (Ferraris *et al*., 2014, Portelli *et al*., 2015).

	muPAR	scuPAR	ssuPAR
Proliferation	No effect	Increase	Increase
Migration	Decrease	Decrease	No effect
Apoptosis	No effect	No effect	No effect
uPA	No effect	Increase	No effect
suPAR	Increase	Increase	No effect
Plasmin	Decrease	Increase	Decrease
VEGF	No effect	No effect	No effect
Total MMP9	Increase	Increase	No effect
Active MMP9	Increase	No effect	No effect

Table 5.1.1: Summary of the Effects on Cell Expression Profiles Due to Genetic Manipulation. MMP-9, matrix metalloproteinase-9; muPAR, membrane-bound urokinase plasminogen activator receptor; scuPAR, soluble cleaved urokinase plasminogen activator receptor; ssuPAR, soluble spliced urokinase plasminogen activator receptor; suPAR, soluble urokinase plasminogen activator; uPA, urokinase plasminogen activator; VEGF, vascular endothelial growth factor (Portelli et al., 2015). .

In this chapter, we took the RNA from HBEC that had been engineered to overexpress uPAR variants; membrane uPAR (muPAR), soluble spliced variant (ssuPAR) and the soluble cleaved variant (scuPAR). Generation and quality control of engineered cells was conducted by Dr Michael Portelli and Dr Ceri Stewart (Portelli *et al*., 2015; Portelli, 2013). To further our understanding of the effects of elevated uPAR in bronchial epithelial cell function whole transcriptome analysis was carried out using RNA-Sequencing and differential gene expression and pathway analysis were performed.

RNA-Seq technology enables the study of global gene expression of different phenotypes/ conditions and is an accurate method of detecting changes in expression of genes and individual isoforms. RNA-seq is a powerful method that can be used to identify pathways underlying disease states and provide insight into disease mechanisms ultimately leading to novel drug targets.

5.2 Aims

The overall aim of this chapter was to determine the effect of elevated membrane uPAR (muPAR), soluble spliced uPAR (ssuPAR) and soluble cleaved uPAR (scuPAR) on bronchial epithelial cell function and to identify novel pathways influenced by these uPAR variants.

5.2.1 Specific aims

- Identify genes differentially expressed in human bronchial epithelial cells engineered to overexpress muPAR, ssuPAR and scuPAR
- Identify pathways regulated by these uPAR variants using Gene Set Enrichment Analysis
- Identify uPAR isoforms expressed by human bronchial epithelial cells

5.3 Methods

5.3.1 Transfecting Human Bronchial Epithelial Cells

In order to investigate the effects of elevated levels of uPAR variants on bronchial epithelial cell function HBEC were transfected with overexpression plasmids (pcDNA3™) containing three uPAR variants: pcDNA3-soluble cleaved (scuPAR), pcDNA3-soluble-spliced (ssuPAR), pcDNA3-membrane (muPAR) and pcDNA3-empty vector control. pcDNA3-muPAR, pcDNA3-ssuPAR and pcDNA3-scuPAR constructs were designed and tested by the Ian Sayers' Group (Stewart and Sayers, 2009; Portelli *et al*., 2015; Portelli, 2013). Transient transfections of human bronchial epithelial cells were carried out by Dr Michael Portelli using the lipid based transfection reagent FuGENE® 6 (Promega, UK) (Uyttersprot *et al*., 1998) where the liposome+DNA complex moves into the cell by either endocytosis or fusion with the plasma membrane via lipid moieties of the liposome. FuGENE® 6 was selected based on its very high transfection efficiency, low cytotoxicity and ability to function equally well in the presence or absence of serum. HBEC were seeded at passage 4 to 6-well plates, transfections were carried out according to the manufacturer's instructions when cells achieved 50-80% confluence. Briefly, the FuGENE®6 Transfection Reagent was first diluted in BEGM, followed by a 5 minute incubation. Plasmid DNA was then added at an experiment specific ratio, allowed to complex with the FuGENE® 6 for 15 minutes and then added to the cells. HBEC were harvested for RNA 24 hours post-transfection.

5.3.2 RNA Sequencing

RNA-Seq whole transcriptome analysis was performed to measure the changes of gene expression in HBEC engineered to overexpress ssuPAR, scuPAR and muPAR. RNA QC and sequencing, differential gene expression analysis and GSEA pathway analysis are described in the section 2.4. RNA QC results and sample details are detailed in this chapter. All bioinformatics analyses were carried out using the Ubuntu Linux operating system version 12.04 LTS, with the exception of PCA analysis which was performed using R version 3.3.1 (The R Foundation for Statistical Computing). Principle component analysis and rank product analysis were performed using this dataset. A detailed description of differential gene expression analysis methods are described in section 2.4.5.

5.3.3 Principle Component Analysis

Principle component analysis (PCA) can be used to analyse gene expression data and to assess noisy, high dimensional data (Yeung and Ruzzo, 2001). PCA is a statistical technique used to identify the underlying variables in a dataset, or *principle components*. PCA was used to assess how adapter and quality trimming impacted on variability between donor replicates. The first step was to create a FPKM matrix, FPKM values were generated from Cuffnorm (see section 2.4.5). To build the matrix the first row must be shifted left as this is the preferred format. Gene names may have duplicated therefore were replaced by a numerical value and the document was saved as a .txt file. Secondly a colour matrix is generated to inform the programme to assign colours to the samples, this document is also stored as a .txt file. PCA analysis was carried out in R studio © R version 3.3.1, 2D and 3D

plots were generated for both untrimmed and trimmed read files. Command lines are summarised in Table 5.3.1.

PCA	Command Line
2D Plots	> setwd("D:/PhD/Lab Book/RNA seq data/PCA") > PCA_raw=read.table("trim_genespca.fpkm_table.txt", header = T) > pca <- prcomp(PCA_raw, center=TRUE, scale=TRUE) > PC1=pca$rotation[,1] > PC2=pca$rotation[,2] > PC3=pca$rotation[,3] > Colour_pca=read.table("colour_Matrix.txt", header = T) > View(Colour_pca) > colormat=Colour_pca$treatment > plot(PC1, PC2, col=colormat, pch=16) > plot(PC1, PC3, col=colormat, pch=16) > plot(PC2, PC3, col=colormat, pch=16)
3D Plots	>setwd("D:/PhD/Lab Book/RNA seq data/PCA") > PCA_raw=read.table("trim_genespca.fpkm_table.txt", header = T) > pca <- prcomp(PCA_raw, center=TRUE, scale=TRUE) > library(rgl) > Colour_pca=read.table("colour_Matrix.txt", header = T) > View(Colour_pca) > colormat=Colour_pca$treatment > plot3d(pca$rotation[,1], pca$rotation[,2], pca$rotation[,3], xlab = "PC1", ylab = "PC2", zlab = "PC3", col=colormat, size=10) > text3d(pca$rotation[,1], pca$rotation[,2], pca$rotation[,3]+0.1, rownames(pca$rotation))

Table 5.3.1: Command Lines Used to Perform Principal Component Analysis in R. 2D and 3D PCA plots were generated in R.

5.3.4 Rank Product Analysis

Rank Product Analysis (RPA) is a technique for identifying differentially expressed genes and calculates rank products from replicate experiments in order to identify up-regulated and down-regulated genes under one condition compared to another e.g. control *vs* treatment. The RPA algorithm is an alternative to differential gene expression analysis and is not limited by 'noisy' data sets i.e. datasets with a high degree of variability between biological replicates (Laing and Smith, 2010). RPA is a non-parametric method that identifies genes that are

consistently highly ranked among replicates, the program makes the following assumption; 1. Relevant expression changes affect only a minority of genes; 2. Measurements are independent between replicate arrays (applicable to microarray data only); 3. Most changes are independent of each other and 4. Measurement variance is about equal for all genes (Breitling *et al*., 2004). RPA was conducted in R studio © R version 3.2.2.

Analysis Step	Command line
1. Build RankProd program	>source("https://bioconductor.org/biocLite.R") >biocLite("RankProd") >library(RankProd)

2. Read exprssion data	EVvM_df <- read.csv("EVvM.csv")
	row.names(EVvM_df) <- EVvM_df[,1]
	EVvM_df[,1] <- NULL
	# prepare labels file
	n1 <- 4
	n2 <- 4
	cl <- rep(c(0,1),c(n1,n2))

3. Run analysis	EVvM<-RP(EVvM_df,cl,num.perm = 100, logged=TRUE,na.rm = FALSE, plot=TRUE) # get the top genes (all data in this case) EVvM_r<-topGene(EVvM, cutoff=1, method="pval",logged=TRUE, logbase=2,gene.names=row.names(EVvM_df)) method="pval",logged=TRUE, logbase=2,gene.names =row.names(MEDvEV_df))
4. Write the results out	write.csv(EVvM_r$Table1,"EVvM_r_UP.csv") write.csv(EVvM_r$Table2,"EVvM_r_DOWN.csv")

Table 5.3.2: Command Lines used for RankProd Analysis. RankProd was built using the biocLite installer (https://www.bioconductor.org/install/). Gene expression data generated using Cuffnorm was inputted into the program. Results were outputted according to “up” and “down” regulated genes for each comparison made.

5.3.5 Splice Variant Analysis

SpliceGrapher is a Python package that predicts splice-graphs using alignment data and transcript assemblies produced in Cufflinks (see Section 4.5.3) which are used as 'gene models'. The software identifies splice junctions and enables visualisation of splice variants for a given transcript (Rogers *et al*., 2012). SpliceGrapher version 0.2 was used for splice variant analysis.

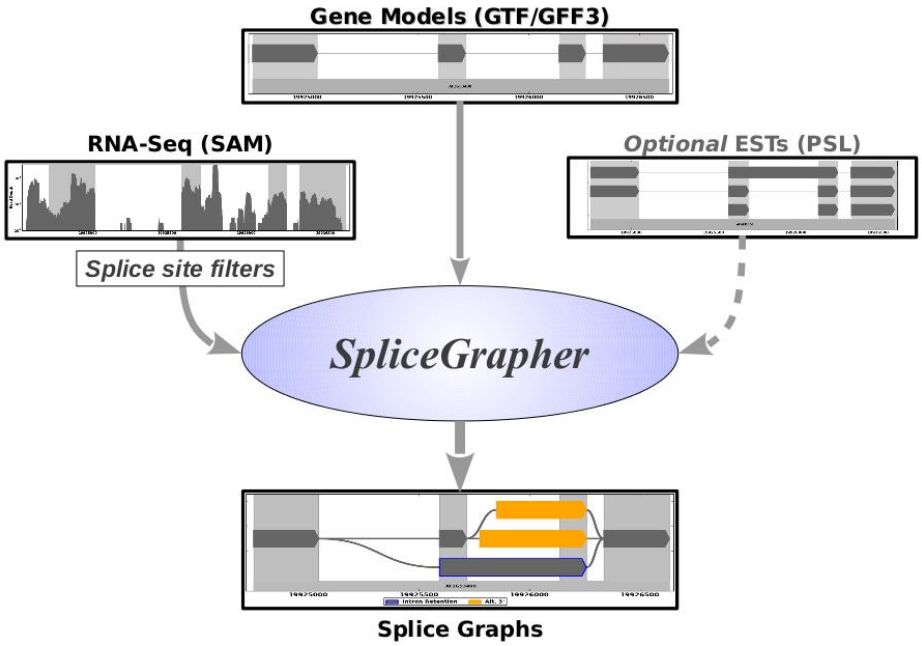


Figure 5.3.1: SpliceGrapher Analysis Pipeline. GTF files containing transcript assemblies or SAM alignment files can be used to identify and graph splice variants present for a given dataset (splicegrapher.sourceforge.net). SAM = Sequence Alignment Map; GTF = Gene transfer format; GFF = General feature format; ESTs = Expressed sequence tag; PSL = Profile scripting language.

SpliceGraphs were generated by first converting the merged assembly file from a .gtf to a .gff3 file (>convert_models.py .gtf --gff3=.gff3 (convert merged .gtf file to gff3 format)). A gene model was then generated for the human genome hg19, this would be used to compare with the assembly generated form the RNA-seq data (>gene_model_to_splicegraph.py -m

hg19_genes.gff3 -d hg19_annotation -S -a –n). A configuration file was then generated that would be used to plot the splice graphs (>plotter.py .cfg (plots splice variants at specified loci).

	[SinglePlotConfig] legend = True output_file = gene.png shrink_introns = True
	[GeneModelGraph] plot_type = gene file_format = gene_model source_file = .gff3 gene_name = XLOC_id relative_size = 0.1 title_string = Predicted gene Isoforms Assembly
	[CuffmergePrediction] relative_size = 2.0 plot_type = isoforms source_file =.gff title_string = Predicted gene Isoforms Assembly background = False iso_labels = True

Figure 5.3.2: Format of Configuration File Used by SpliceGrapher. The configuration file specifies the parameters used (default settings were used) and informs the programme where to extract data for the gene or loci of interest.

Cuffcompare was used to compare the transcripts in donor 1 and donor 2 with the reference genome (build GR37) using the following command:

	Analysis Step	Command line
	Transcriptome comparison using Cuffompare	cuffcompare [options] <query.gtf> -r <referencegr37.gtf>

Cuffcompare summarises the variants detected in each donor (denoted by a 'TCONS' tracking ID), the table also highlights which known variant (denoted 'ENST' Ensembl transcript ID) variants correspond with. TCONS designated a 'j' symbol are potentially novel variants as they have alternative splice junctions to the known variants.

5.4 Results

5.4.1 RNA Integrity Number Analysis

RIN analysis and quantification of RNA was performed using the bioagilent analyser. All samples scored a RIN 8> indicating samples were of satisfactory quality for sequencing. Samples with the lowest scores (sample 10, RIN 8.7; sample 14, RIN 8.0) achieved good sequencing depth and read alignment rate, as shown in Table 5.4.2.

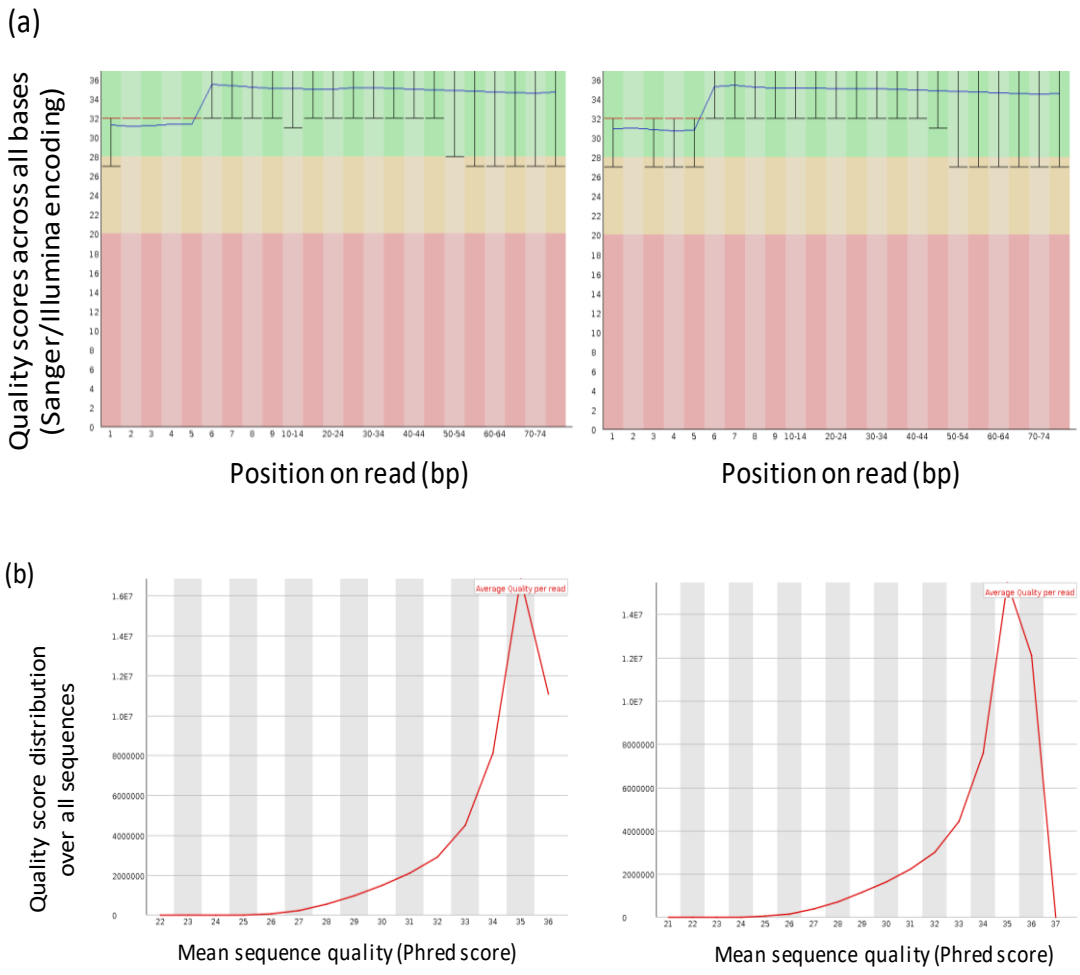
Sample no.	Description	RIN score 2	Qubit conc (ng/µl)
1	Donor 1a media	9.4	619
2	Donor 1a empty vector	9.1	655
3	Donor 1a muPAR	9.1	628
4	Donor 1a scuPAR	9.1	649
5	Donor 1a ssuPAR	9.2	611
6	Donor 1b media	9.2	492
7	Donor 1b empty vector	9.4	462
8	Donor 1b muPAR	9.1	402
9	Donor 1b scuPAR	9.7	424
10	Donor 1b ssuPAR	8.7	473
11	Donor 2a media	9.5	661
12	Donor 2a empty vector	9.4	697
13	Donor 2a muPAR	9.7	547
14	Donor 2a scuPAR	8.0	637
15	Donor 2a ssuPAR	9.9	685
16	Donor 2b media	10	670
17	Donor 2b empty vector	9.8	705
18	Donor 2b muPAR	9.9	648
19	Donor 2b scuPAR	9.9	709
20	Donor 2b ssuPAR	9.9	605

Table 5.4.1: RIN analysis and concentration of RNA samples. The table summarises the RIN scores and concentrations of samples used for analysis. ‘Donor 1a’ and ‘Donor 1b’ and ‘Donor 2a’ and ‘Donor 2b’

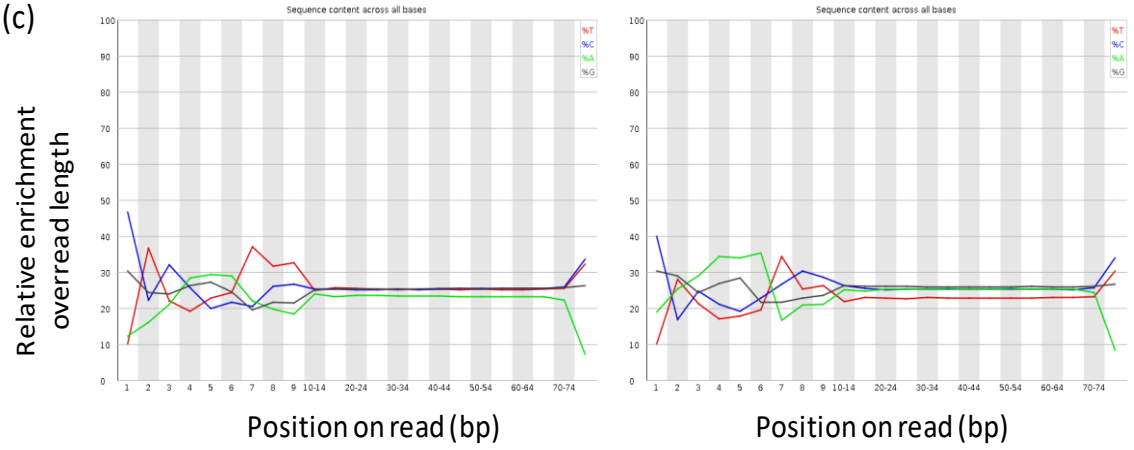
refer to technical replicates from the same HBEC donor. 'muPAR', 'ssuPAR' and 'scuPAR' refer to the form of uPAR HBEC were engineered to overexpress. 'Media' and 'empty vector' refer to HBEC media and empty vector controls, respectively. muPAR = membrane uPAR; scuPAR = soluble cleaved uPAR; ssuPAR = soluble-spliced uPAR.

5.4.2 Sequencing Data Quality Control Analysis

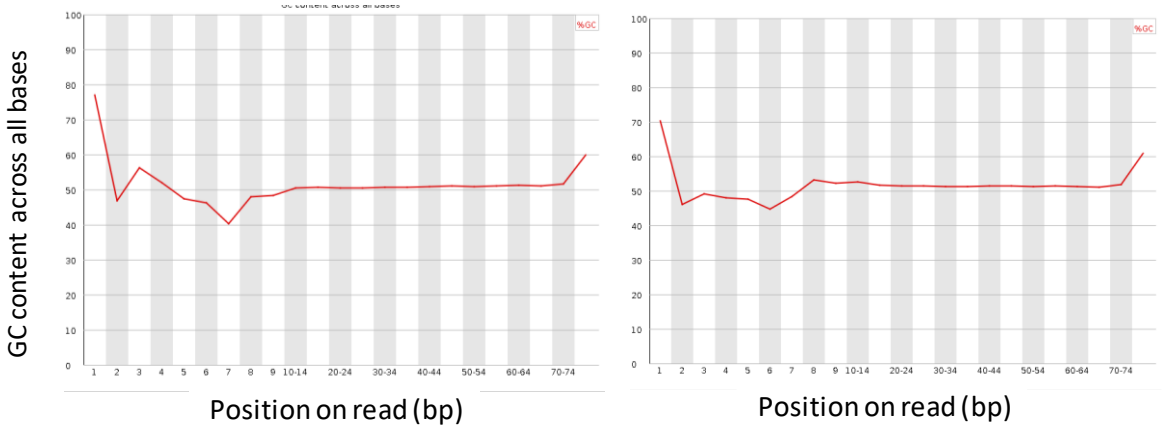
Assessment of sequencing data was performed using FastQC, principle component analysis and TopHat. Trimmed reads were used for downstream analysis. Sequencing data (reads) were processed as described in section and assessed for quality using the FastQC tool as described in section 2.4.3.1. Representative graphs for FastQC analysis for forward and reverse concatenated read files are shown below in Figure 5.4.1.



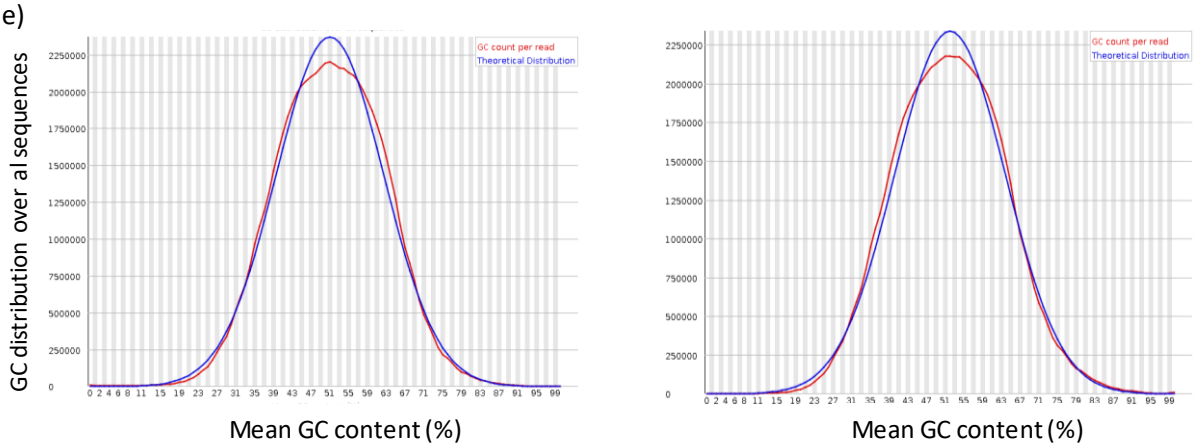
(c)


Sequence content across all bases
%T
%C
%A
%G
Relative enrichment overread length
Position on read (bp)
Sequence content across all bases
%T
%C
%A
%G
Position on read (bp)

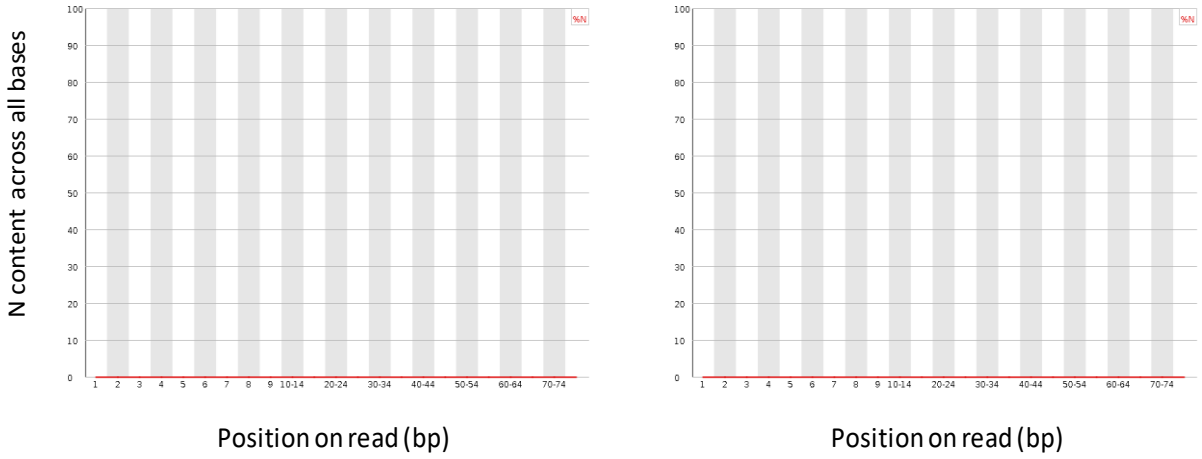
(d)


%GC
GC content across all bases
Position on read (bp)
%GC
Position on read (bp)

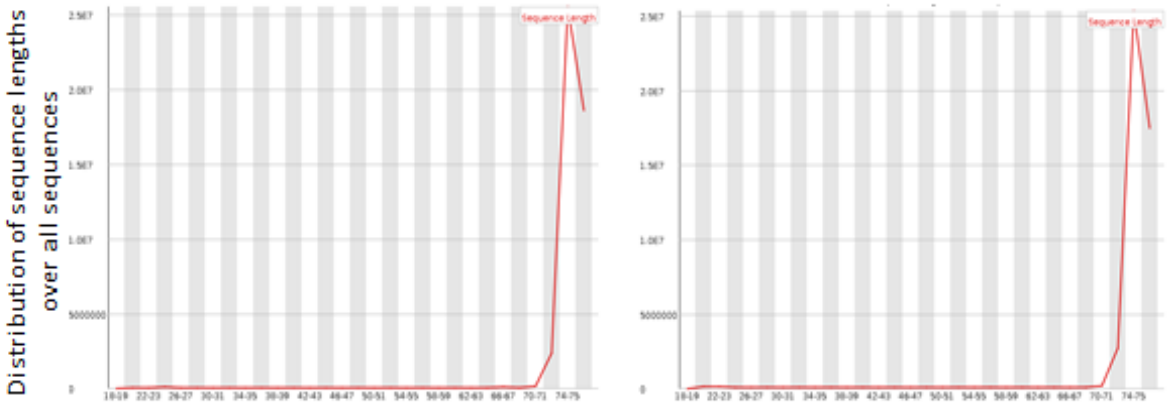
(e)


GC count per read
Theoretical Distribution
GC distribution over al sequences
Mean GC content (%)
GC count per read
Theoretical Distribution
Mean GC content (%)

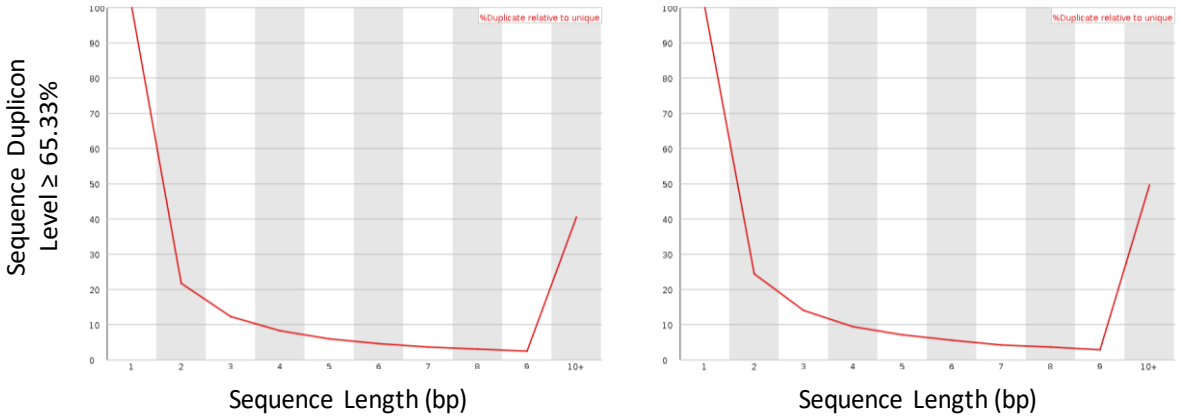
(f)


N content across all bases
%N
Position on read (bp)
%N
Position on read (bp)

(g)


Distribution of sequence lengths over all sequences
Sequence Length
Sequence Length

(h)


Sequence Duplicon Level ≥ 65.33%
%Duplicate relative to unique
Sequence Length (bp)
%Duplicate relative to unique
Sequence Length (bp)

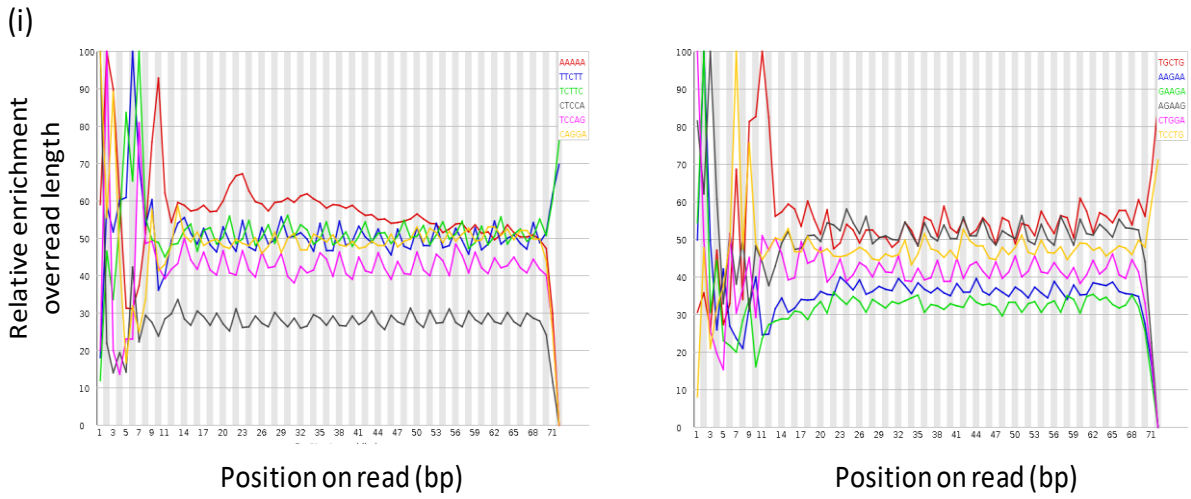


Figure 5.4.1: FastQC Confirmed Read Files Containing Sequencing Data are Suitable for Downstream Analysis. All parameters measured passed quality control analysis (a) Per base quality assessment showed that all reads met q score >20, read quality was poorest at the end of the read which is typical of sequencing data. (b) Per sequence mean quality score = >27. (c) Per base sequence content = <20% (d) Per base GC content = <10% (e) Per sequence GC content 15-30% (f) Per base N content = 0 (failure = >20%) (g) Sequence length distribution analysis did not identify read sequences of varying lengths (h) Duplicate sequences = <20% (i) Overrepresented Kmers = <10 fold. Read 1 files (R1, forward reads) and Read 2 files (R2, reverse reads) are shown on the left and right, respectively.

5.4.3 Principle Component Analysis

PCA was carried out on gene expression data for all samples using both untrimmed data (raw reads) and trimmed data (adapter and quality trimmed reads) to assess how trimming affected the variability of the data. Figure 5.4.2 shows 3D PCA plots for raw untrimmed data, samples 8 and 16 are notably variable in comparison to the rest of the dataset. The remaining samples show a great degree of overlap, read data was therefore trimmed.

Untrimmed Read Data

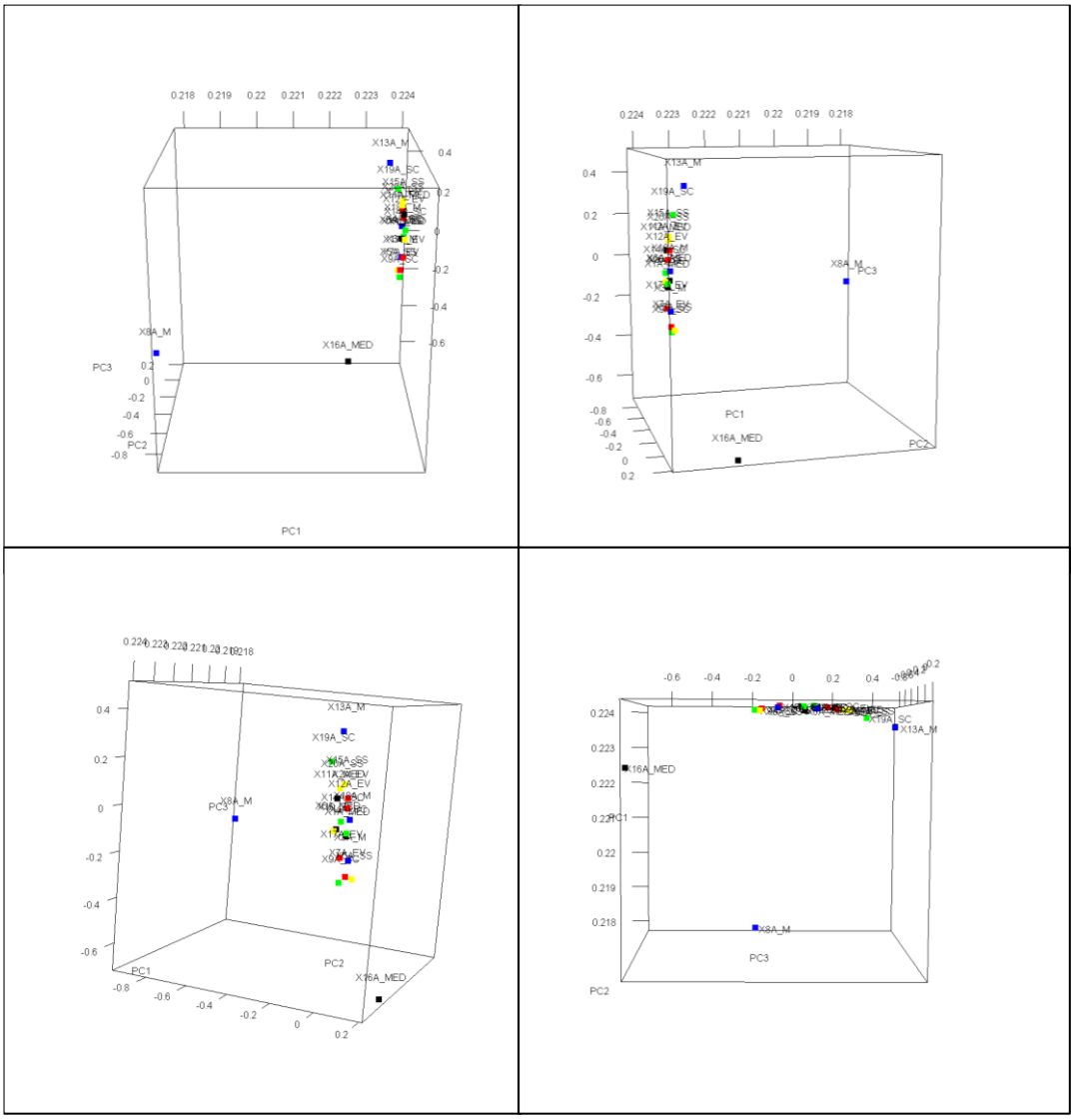


Figure 5.4.2: Principle Component Analysis of Raw Untrimmed Reads Show Highlights Overlap Between Conditions. 3D Principle component analysis of gene expression (FPKM) values generated from raw reads to assess data quality and reduced noise. Replicates have been assigned the same colour: media=black, empty vector= red, muPAR=blue, ssuPAR=yellow, scuPAR= green.

Trimmed Read Data

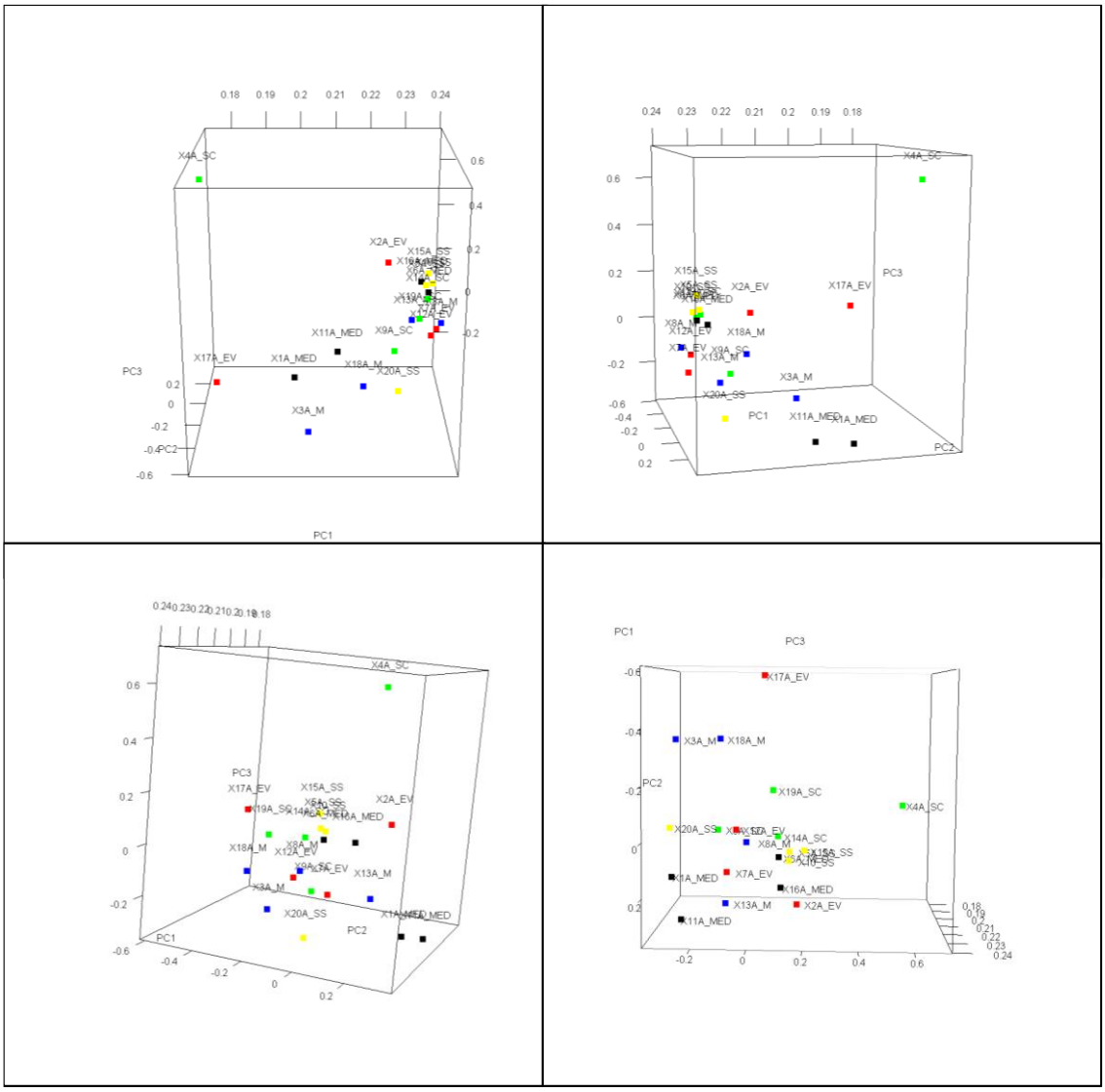


Figure 5.4.3: Trimming of Read Data Improves Grouping of Replicate Samples. Principle component analysis of gene expression (FPKM) values generated from trimmed reads was performed to assess if read trimming improved data quality and reduced noise. 3D PCA plots of showing all dimensions simultaneously indicate that trimmed readings show some degree of clustering within replicates and that scales of variances are reduced compared to raw data (see Figure 5.4.2). Replicates have been assigned the same colour: media=black, empty vector= red, muPAR=blue, ssuPAR=yellow, scuPAR= green.

Paired end (PE) reads were then aligned to the human genome build Gr37 using the TopHat alignment software. The alignment rate and number of paired end reads aligned for each sample are summarised below. Alignment rate ranged from 93.2- 95.1% and read depth 41.3

– 60.7 million PE read, this read depth is sufficient for differential expression profiling (Liu *et al*., 2014b).

Sample no.	Description	Reads aligned (%)	Read Depth
1	Donor 1a media	95.1	45,071,368
2	Donor 1a empty vector	94.8	56,455,713
3	Donor 1a muPAR	94.2	57,918,593
4	Donor 1a scuPAR	94.5	41,336,063
5	Donor 1a ssuPAR	94.4	45,971,861
6	Donor 1b media	95.1	54,943,592
7	Donor 1b empty vector	94.7	54,707,645
8	Donor 1b muPAR	93.2	54,612,630
9	Donor 1b scuPAR	94.8	57,421,050
10	Donor 1b ssuPAR	95.1	54,518,610
11	Donor 2a media	94.7	54,065,360
12	Donor 2a empty vector	95	57,099,912
13	Donor 2a muPAR	95	58,786,185
14	Donor 2a scuPAR	94.9	60,746,928
15	Donor 2a ssuPAR	94.9	60,090,053
16	Donor 2b media	94.9	58,399,173
17	Donor 2b empty vector	93.9	52,285,907
18	Donor 2b muPAR	95	50,234,531
19	Donor 2b scuPAR	95	56,076,035
20	Donor 2b ssuPAR	95	58,536,731

Table 5.4.2: Alignment Rate and Read Depth of Samples used for RNA-Seq analysis. Alignment rate and read depth values were generated using TopHat. 'Donor 1a' and 'Donor 1b' and 'Donor 2a' and 'Donor 2b' refer to technical replicates from the same HBEC donors. 'muPAR', 'ssuPAR' and 'scuPAR' refer to the form of uPAR HBEC were engineered to overexpress. 'Media' and 'empty vector' refer to HBEC media only and empty vector controls, respectively. muPAR = membrane uPAR; scuPAR = soluble cleaved uPAR; ssuPAR = soluble-spliced uPAR.

5.4.4 Multiple PLAUR Splice Variants are Expressed in the Bronchial Epithelium

To identify *PLAUR* (uPAR) transcripts expressed in the bronchial epithelium and to determine their abundance RNA from two HBEC were sequenced using whole transcriptome analysis. The Splicegrapher and Cuffcompare tools (see section 5.3.5 for methods) were used to compare the transcripts in donor 1 and donor 2 with the reference genome (build GR37).

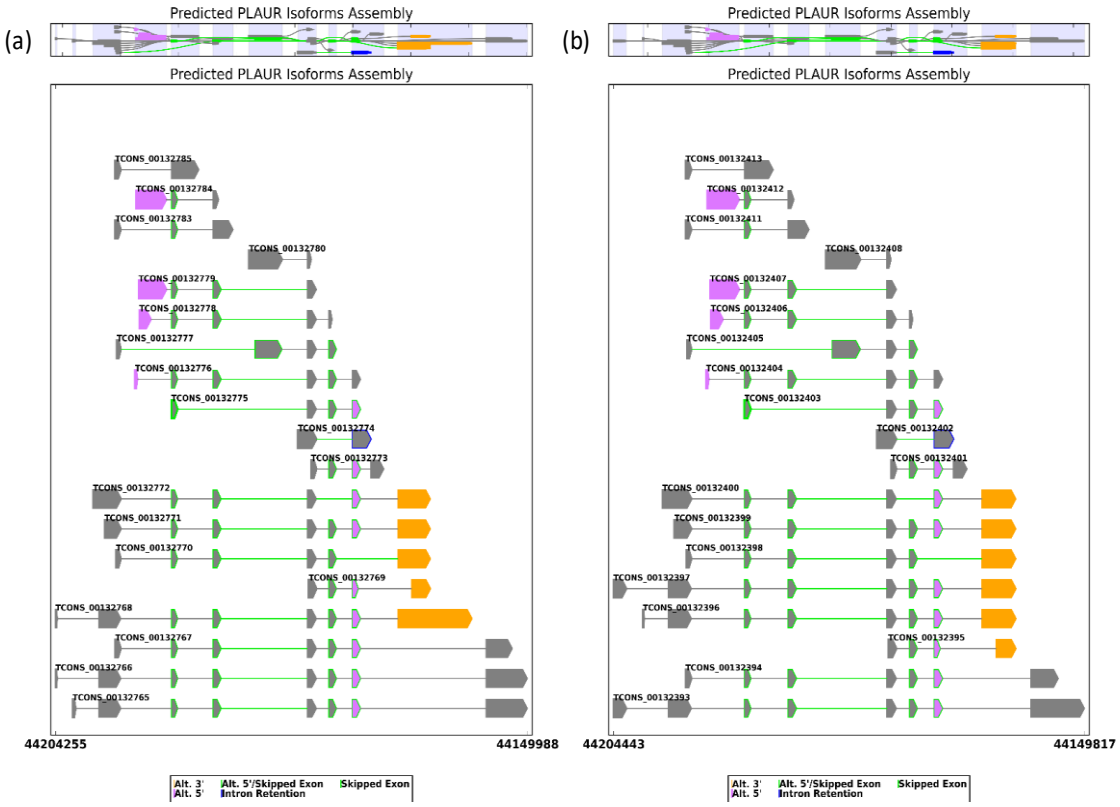
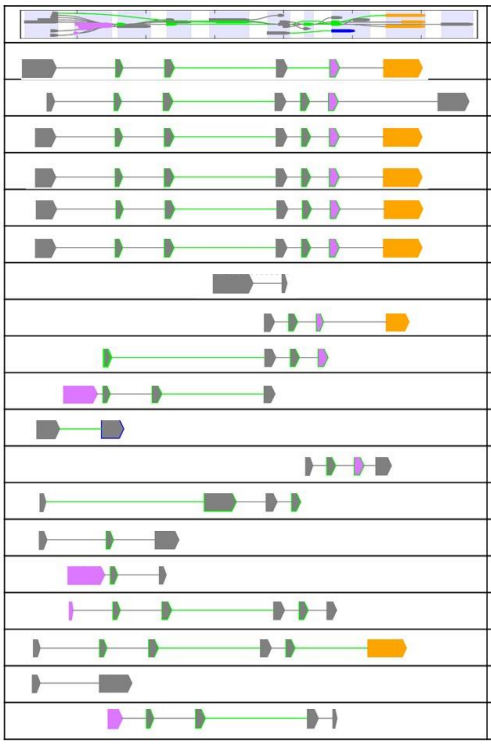


Figure 5.4.4: *PLAUR* Splice Variants Identified in Two HBEC Donors using Splicegrapher. RNA-Seq analysis was performed using two primary HBEC donors (a) HBEC donor 1 and (b) HBEC donor 2. Splicegrapher and Cuffcompare were used to perform splice-analysis. 19 splice variants were identified in each donor.

19 PLAUR splice variants were identified in both HBEC donors and were each assigned a 'TCONS' id. Cuffnorm and Cuffcompare were used to calculate transcript abundance and

identify the known variants the transcripts correspond with. Details including percentage abundance in HBEC donors 1 and 2 are shown in Figure 5.4.5. The full-length isoform of uPAR was predominantly expressed by both HBEC donors.



PLAUR Ensembl ID	HBEC Donor 1	%	HBEC Donor 2	%
ENST00000221264	TCONS_00132772	0.77	TCONS_00132400	0.78
ENST00000339082	TCONS_00132767	14.24	TCONS_00132394	10.84
ENST00000340093	TCONS_00132765*	0	TCONS_00132393*	0.49
ENST00000340093	TCONS_00132766*	1.67	TCONS_00132396*	0
ENST00000340093	TCONS_00132768*	0.5	TCONS_00132397*	0
ENST00000340093	TCONS_00132771	63.01	TCONS_00132399	72.71
ENST00000593396	TCONS_00132780	1.04	TCONS_00132408	0.67
ENST00000593447	TCONS_00132769	1.8	TCONS_00132395	2.61
ENST00000593714	TCONS_00132775	0.64	TCONS_00132403	0.58
ENST00000593939	TCONS_00132779	0.49	TCONS_00132407	0.03
ENST00000594364	TCONS_00132774	0.38	TCONS_00132402	0.2
ENST00000595038	TCONS_00132773	0.71	TCONS_00132401	0.66
ENST00000597107	TCONS_00132777	0.09	TCONS_00132405	0.28
ENST00000598875	TCONS_00132783	0.17	TCONS_00132411	0.43
ENST00000599546	TCONS_00132784	0.12	TCONS_00132412	0.1
ENST00000599892	TCONS_00132776	12.2	TCONS_00132404	6.32
ENST00000601723	TCONS_00132770	1.62	TCONS_00132398	3.03
ENST00000601876	TCONS_00132785	0.16	TCONS_00132413	0.26
ENST00000602141	TCONS_00132778	0.13	TCONS_00132406	0

ENST00000340093 PLAUR isoform 1 - full length isoform
ENST00000339082 PLAUR isoform 2 - soluble isoform
ENST00000601723 PLAUR isoform 4 - truncated full length isoform
ENST00000599892 PLAUR isoform X4 - truncated full length isoform

Figure 5.4.5: *PLAUR* Isoform Expression in Two HBEC Donors Using RNA Seq. Structure and abundance of known and potentially novel *PLAUR* isoforms in two human bronchial epithelial cell donors illustrating heterogeneity in expression levels. Percentage abundances (% FPKM) were calculated for each donor, isoforms. Transcripts for full length and soluble *PLAUR* were identified at similar abundancies. FPKM; fragments per kilobase of transcript per million mapped reads.

5.4.5 Differential Gene Expression Analysis Using the Cuffdiff Tool

The Cufflinks tool Cuffdiff was used to identify genes differentially expressed in HBEC overexpressing uPAR variants in order to further understand receptor function and identify potentially novel functions. HBEC (*n*=4) were cultured to 80% confluence and transiently

transfected with pcDNA3™ vectors to overexpress muPAR, ssuPAR, scuPAR and an empty vector control (Portelli *et al.*, 2015). RNA was sequenced and differential gene expression analysis was performed as described in section 2.4.5. Overexpression of muPAR, ssuPAR and scuPAR resulted in differential gene expression of 15, 20 and 13 genes, respectively (<10% FDR).

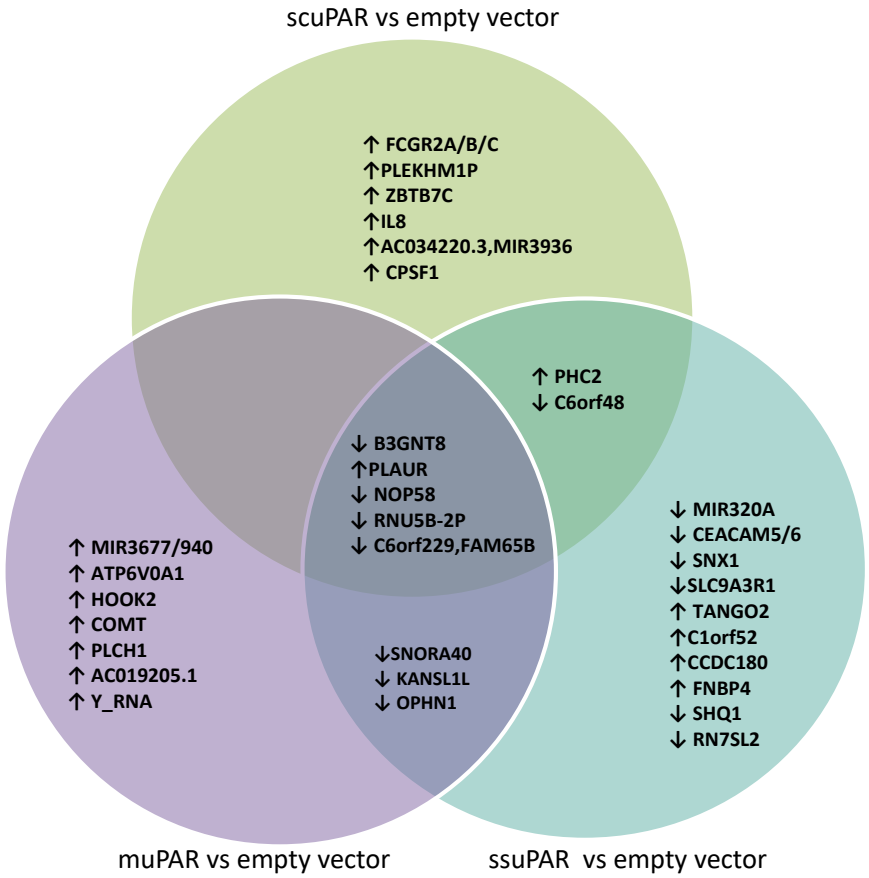


Figure 5.4.6: Venn Diagram of Differentially Expressed Genes in uPAR overexpressing Bronchial Epithelial Cells (FDR <10%; HBEC *n* = 4). Human Bronchial Epithelial Cells were transfected with overexpression vectors containing either membrane uPAR (muPAR), soluble-cleaved uPAR (scuPAR) and soluble-spliced uPAR (ssuPAR) or an empty vector ($pcDNA_3$) control. Whole transcriptome analysis of engineered cells to identify receptor function. Venn analysis was performed to identify genes distinctly and commonly regulated by uPAR variants. ↑↓indicate the direction of change of expression.

Cuffdiff assigns a test status for all genes based on the quality of read alignment and the number of fragments at the locus. For analysis of ssuPAR transfected HBEC against empty vector control cells for 16, 513 genes were tested. 16,115 and 16,513 genes were tested for differential expression compared to the empty vector control for muPAR and scuPAR transfected HBEC, respectively. Tables 5.4.3 provides a summary of the function and fold changes of genes differentially expressed as a result of elevated ssuPAR in HBEC.

Soluble-spliced uPAR

Gene	Gene name	log2 (fold change)	FDR	Gene function
PHC2	Polyhomeotic Homolog 2	1.11	0.05	Responsible for the stable inheritance of gene activity in Drosophila
SNORA40	Small Nucleolar RNA, H/ACA Box 40	-5.39	0.05	RNA processing
FNBP4	Formin Binding Protein 4	3.06	0.05	Binds Formin, a protein involved in adheren junction formation
SNX1	Sorting Nexin 1	-0.89	0.05	Regulates expression of EGFR, P2RY1 and PAR-1
C15orf52	Chromosome 15 open reading frame 52	1.82	0.05	Associated with Pancreatic ductal adenocarcinoma
SLC9A3R1	SLC9A3 Regulator 1	1.10	0.05	Scaffold protein involved in TJ organization
CEACAM5/6	Carcinoembryonic Antigen Related Cell Adhesion Molecule	-1.43	0.05	Cell adhesion molecule. May regulate differentiation, apoptosis, and cell polarity
B3GNT8	Beta-1,3-N-acetylglucosaminyltransferase 8	-2.23	0.05	Reduces tumorigenicity of gastric cancer in mice
PLAUR	Urokinase plasminogen activator receptor	4.63	0.05	Receptor for urokinase plasminogen activator
NOP58	NOP58 Ribonucleoprotein	-1.84	0.05	Small nuclear RNA (snoRNAs)
KANSL1L	KAT8 Regulatory NSL Complex Subunit 1 Like	-4.56	0.05	Shown to have histone acetyltransferase (HAT) activity
TANGO2	Transport And Golgi Organization 2 Homolog	1.57	0.05	Protein loading in the endoplasmic reticulum Prostate cancer suscetibility
RNU5B-2P	RNA, U5B Small Nuclear 2	-5.85	0.05	Pseudogene
C6orf48	Chromosome 6 Open Reading Frame 48	-1.58	0.05	Uncharacterised protein
*1. C6orf229 2. FAM65B	Chromosome 6 Open Reading Frame 229. Family With Sequence Similarity 65 Member B	-8.45	0.05	Uncharacterised protein. Required for hearing, Involved in skeletal muscle development
MIR320A	MicroRNA 320a	-10.46	0.05	Tumour suppressive gene, regulates proliferation and apoptosis
CCDC180	Coiled-Coil Domain Containing 180	2.92	0.05	Uncharacterised protein
OPHN1	Oligophrenin 1	2.07	0.05	Stimulates GTP hydrolysis of members of the Rho family, which regulate cell migration and morphogenesis
RN7SL2	RNA, 7SL, Cytoplasmic 2	-0.68	0.08	Mediates cotranslational insertion of secretory proteins into the lumen of the endoplasmic reticulum
SHQ1	SHQ1, H/ACA Ribonucleoprotein Assembly Factor	-0.97	0.08	Ribosomal RNA processing

Table 5.4.3: Genes and Regulatory RNAs Regulated by Soluble-Spliced uPAR. Human bronchial epithelial cells (n=4) were engineered to overexpress ssuPAR and gene expression was quantified suing RNA-Seq whole transcriptome analysis. Differential gene expression (DE) analysis using Cuffdiff calculated the log2 fold change and false discovery rate (FDR) for genes measured and identified 20 DE genes (FDR <10%) compared to the empty vector control.

20 genes were differentially expressed in HBEC overexpressing ssuPAR compared to empty vector control cells. The largest number of genes encode proteins and regulatory RNA species involved in gene transcription and post translational regulation (*PHC2*, *SNORA40*, *NOP58*, *RNU5B-2P*, *KANSL1L* (Smith *et al*., 2005) *SHQ1* (Nallar *et al*., 2011) and *RN7SL2*. The second largest group of genes are associated with malignancies, specifically pancreatic cancer (*C15orf52)* (Giulietti *et al*., 2016)), prostate cancer (*TANGO2)* (Karyadi *et al*., 2017) and breast cancer (*B3GNT8, C6orf48***)** (Pan *et al*., 2012), and *MIR320a* is a potential tumour suppressive gene (Xie *et al*., 2017). *FNBP4, SLC9A3R1* were both upregulated and have been implicated in barrier function (Castellani *et al*., 2012).

There were also a number of genes which regulate specific cell processes, *SNX1* regulates EGFR degradation and may affect receptor signalling (Chin *et al*., 2001) and *CEACAM5* and *OPHN1* regulate cell adhesion and migration (Goto *et al*., 2014). *CCDC180* and *FAM65B* are associated with inflammatory syndromes (Fei *et al*., 2009), *FAM65B* promotes T cell proliferation and contributes to liver inflammation (Petros *et al*., 2017, Froehlich *et al*., 2016).

Membrane uPAR

Gene	Gene name	log2 (fold change)	FDR	Gene function
SNORA40	Small Nucleolar RNA, H/ACA Box 40	-6.32	0.06	Small Nucleolar RNA
MIR3677/940	MicroRNA677/940	5.59	0.06	Non-coding RNA. miR-940 shown to regulate cell cytoskeleton and cell migration
ATP6V0A1	ATPase H+ Transporting V0 Subunit A1	1.41	0.06	Enzyme that mediates acidification of eukaryotic intracellular organelles.
*1.HOOK2 2.RTBDN	1.Hook Microtubule-Tethering Protein 2 2. Retbindin	2.13	0.06	1. Cytosolic coiled-coil proteins which attaches to microtubules. 2. Shares homology with riboflavin binding proteins
B3GNT8	Beta-1,3-N-acetylglucosaminyltransferase 8	-2.25	0.06	Reduces tumorigenicity of gastric cancer in mice
PLAUR	Urokinase plasminogen activator receptor	3.74	0.06	Receptor for urokinase plasminogen activator
NOP58	NOP58 Ribonucleoprotein	-1.66	0.06	Small nuclear RNA (snoRNAs)
KANSL1L	KAT8 Regulatory NSL Complex Subunit 1 Like	-4.47	0.06	Shown to have histone acetyltransferase (HAT) activity
COMT	catechol-O-methyltransferase	2.19	0.06	Metabolism of catecholamines
RNU5B-2P	RNA, U5B Small Nuclear 2	-6.22	0.06	Pseudogene
PLCH1	Phospholipase C Eta 1	8.05	0.06	Member of the PLC-eta family of the phosphoinositide-specific phospholipase C (PLC) superfamily
AC019205.1	n/a	5.62	0.06	Non-coding sequence
*1.C6orf229 2.FAM65B	Chromosome 6 Open Reading Frame 229. Family With Sequence Similarity 65 Member B	-8.14	0.06	1. Uncharacterised protein. 2. Required for hearing, Involved in skeletal muscle development
Y_RNA	n/a	7.33	0.06	Non-coding RNA
OPHN1	Oligophrenin 1	-1.42	0.06	Stimulates GTP hydrolysis of members of the Rho family, which regulate cell migration and morphogenesis

Table 5.4.4: Genes and Regulatory RNAs Regulated by Membrane uPAR. Human bronchial epithelial cells (n=4) were engineered to overexpress muPAR, whole transcriptome analysis was performed to identify muPAR function. Differential gene expression analysis using Cuffdiff calculated the log2 fold change and false discovery rate (FDR) for genes measured and identified 15 DE genes (FDR <10%) compared to the empty vector control.

Overexpression of muPAR in HBEC resulted in differential expression of 15 genes, two of the loci identified contained two genes within 50bp of one another. *NOP58, KANSL1L, RNU5B-2P, SNORA40* were downregulated in muPAR and ssuPAR overexpressing cells. Expression of *B3GNT8*, *C6orf48*, *OPHN1* and *FAM65B* were also dysregulated in both phenotypes. Expression of the transcriptional regulators *MIR3677* and *YRNA* (Zhang *et al*., 2011) were upregulated in muPAR transfected cells. *COMT* and *PLCH1* are both associated with malignancies and expression was elevated (Zhang *et al*., 2013, Tan and Chen, 2014). HOOK2 is involved in centrosome regulation and may be upregulated in cell division. ATP6V0A1 is a regulator of airway acidification (Fischer and Widdicombe, 2006).

Soluble-cleaved uPAR

Gene	Gene name	log2 (fold change)	FDR	Gene function
FCGR2A/B/C	Fc Fragment Of IgG Receptor Ii	2.24	0.06	Immunoglobulin Fc receptor genes, involved phagocytosis and clearing of immune complexes
PHC2	Polyhomeotic Homolog 2	1.05	0.06	Responsible for the stable inheritance of gene activity in Drosophila
PLEKHM1P	Pleckstrin Homology And RUN Domain Containing M1 Pseudogene 1	1.43	0.06	Pseudogene
ZBTB7C	Zinc Finger And BTB Domain Containing 7C	2.21	0.06	Uncharacterised protein
B3GNT8	Beta-1,3-N-acetylglucosaminyltransferase 8	-1.93	0.06	Reduces tumorigenicity of gastric cancer in mice
PLAUR	urokinase plasminogen activator receptor	5.20	0.06	Receptor for urokinase plasminogen activator
NOP58	NOP58 Ribonucleoprotein	-1.77	0.06	Small nuclear RNA (snoRNAs)
RNU5B-2P	RNA, U5B Small Nuclear 2	-5.75	0.06	Pseudogene
IL8	Interleukin 8	1.73	0.06	Neutrophil activation, mediates inflammatory response
*1. AC034220.3 2. MIR3936	1. Known processed transcript. 2. microRNA 3936	3.59	0.06	2. post-transcriptional regulation of gene expression
C6orf48	Chromosome 6 Open Reading Frame 48	-1.56	0.06	Uncharacterised protein
*1. C6orf229 2. FAM65B	1. Chromosome 6 Open Reading Frame 229. 2. Family With Sequence Similarity 65 Member B	-6.77	0.06	1. Uncharacterised protein. 2. Required for hearing, Involved in skeletal muscle development
CPSF1	Cleavage And Polyadenylation Specific Factor 1	2.67	0.06	3-prime processing of pre-mRNAs

Table 5.4.5: Genes and Regulatory RNAs Regulated by Soluble-Cleaved uPAR.. Human bronchial epithelial cells (n=4) were engineered to overexpress ssuPAR, whole transcriptome analysis was performed to identify scuPAR function. Differential gene expression analysis using Cuffdiff calculated the log2 fold change and false discovery rate (FDR) for genes measured and identified 13 DE genes (FDR <10%) compared to the empty vector control.

RNA-Seq analysis identified 14 genes differentially expressed by epithelial cells with elevated scuPAR. *PHC2, NOP58, RNU5B-2P* regulate gene expression and *B3GNT8* were differentially expressed in muPAR and ssuPAR overexpressing cells. The pseudogene *PLEKHM1P* was upregulated, *ZBTB7C* regulates MMP-9 expression in mice, *FCGR2A* is required for antigen recognition and phagocytosis and IL-8 also regulates immune processes and is a pro-inflammatory cytokine (Strieter, 2002).

5.4.6 Differential Gene Expression Analysis using Rank Product Analysis

RNA-Seq data was also analysed using Rank Product Analysis (RPA) to identify differentially expressed genes (Laing and Smith, 2010). FPKM values generated using the Cuffnorm tool (see section 2.4.5) were analysed as described in section 2.4.6. The total number of genes upregulated by scuPAR, ssuPAR and muPAR variants in bronchial epithelial cells are shown in Figure 5.4.8.

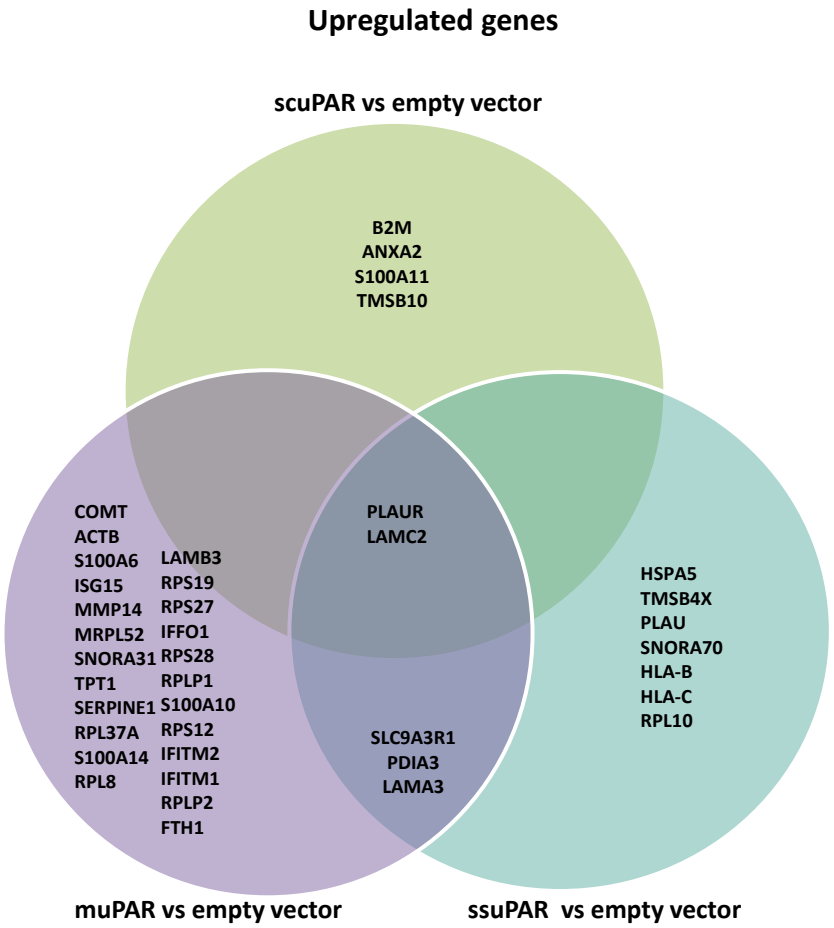


Figure 5.4.7: Rank product Analysis of Genes Upregulated by uPAR Variants. RNA-Seq was performed to investigate changes in global gene expression of human bronchial epithelial cells (*n*=4) overexpressing membrane uPAR, soluble-spliced uPAR and membrane uPAR. Rank product analysis was used to identify differentially expressed genes (FDR <10%), *PLAUR* the gene encoding uPAR was upregulated in all variants.

RPA identified 29 genes upregulated by muPAR, 12 genes upregulated by ssuPAR and 6 by scuPAR compared to the empty vector control (FDR <10%). 2 genes were significantly upregulated in all conditions, *PLAUR* and *LAM2* (laminin 2). *SLC9A3R1*, *PDIA3* and *LAMA3* were elevated in ssuPAR and muPAR cells. Cuffdiff analysis also identified *COMT* as a gene upregulated by muPAR. Interestingly *PLAU* (urokinase) was upregulated in ssuPAR overexpressing HBEC and muPAR induced expression of *SERPINE1* (PAI-1), these changes in expression may serve as feedback mechanisms. muPAR overexpression also led to increased expression of ribosome biogenesis genes (*RPL37A, RPL8, RPS19, RPS27, RPS28, RPLP1, RPS12, RPLP2*), interferon response (*IFITM2, IFITM1*) and damage response (*S100A6, S100A10, S100A14*). ssuPAR increase in *HLA-B* and *HLA-C* and scuPAR increases *B2M* suggesting soluble forms may play a role in antigen presentation.

Downregulated

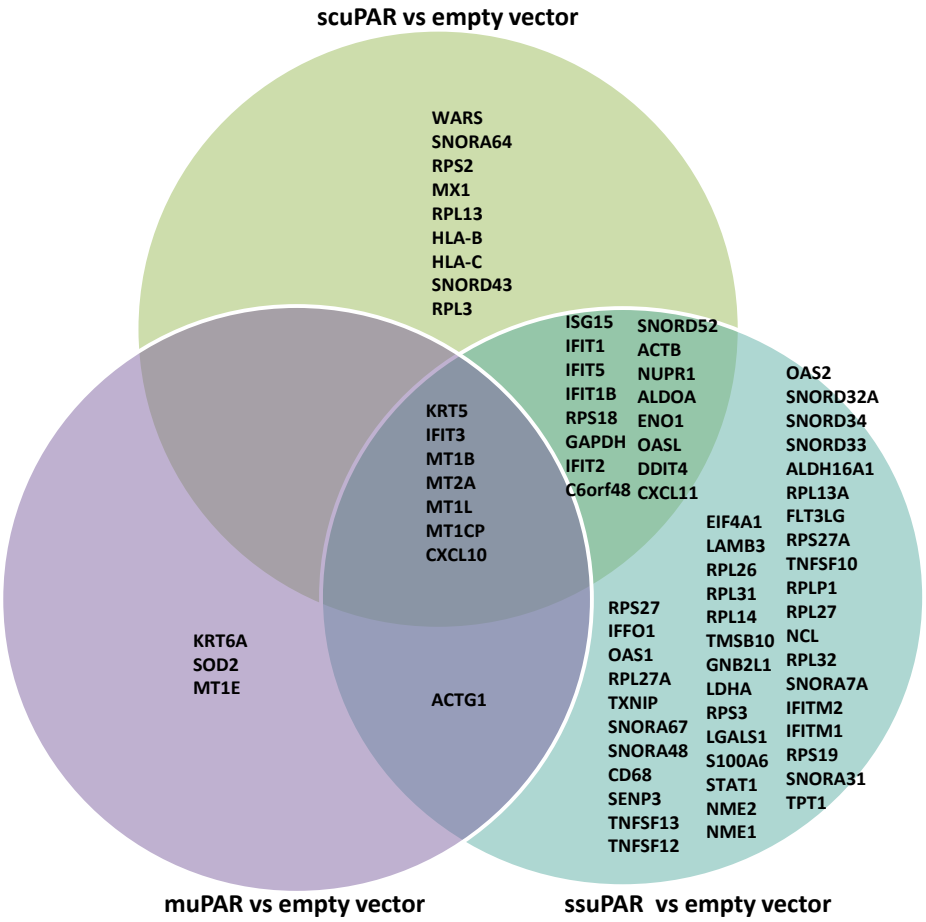


Figure 5.4.8: Rank product Analysis of Genes Downregulated by uPAR Variants. RNA-Seq was performed to investigate changes in global gene expression of human bronchial epithelial cells (*n*=4) overexpressing membrane uPAR, soluble-spliced uPAR and membrane uPAR. Rank product analysis was used to identify differentially expressed genes (FDR <10%).

32 genes were downregulated by scuPAR, 11 genes by muPAR and 67 by ssuPAR. Genes downregulated by all variants included *KRT5*, MT genes, *IFIT3* and *CXCL10* suggesting common functions related to ECM, viral response, immune regulation and response to oxidative stress. *HLA-B* and *HLA-C* were upregulated by ssuPAR and downregulated by scuPAR, suggesting these receptor variants may share gene targets however have opposing effects. ssuPAR also led to downregulation of small nuclear RNAs and Tumour Necrosis Factor Superfamily Members.

5.4.7 Identification of Cellular Pathways Regulated by uPAR using Gene Set Enrichment Analysis

In order to identify processes with altered activity as a result of elevated uPAR levels, gene set enrichment analysis was performed using ssuPAR, scuPAR or muPAR transfected bronchial epithelial cells. GSEA enables the investigation of the collective effect of changes in gene expression and the biological relevance of observed fold changes, for detailed methods see section 2.4.6. The enrichment score (ES) indicates the change in expression of a given gene set and is calculated from the 'Signal' statistic. This is generated using the 'Tag' and 'List' value which indicate the percentage of genes contributing to the ES and where in the list the ES is attained. Venn analysis was used to identify pathways that are regulated by one or more receptor variant.

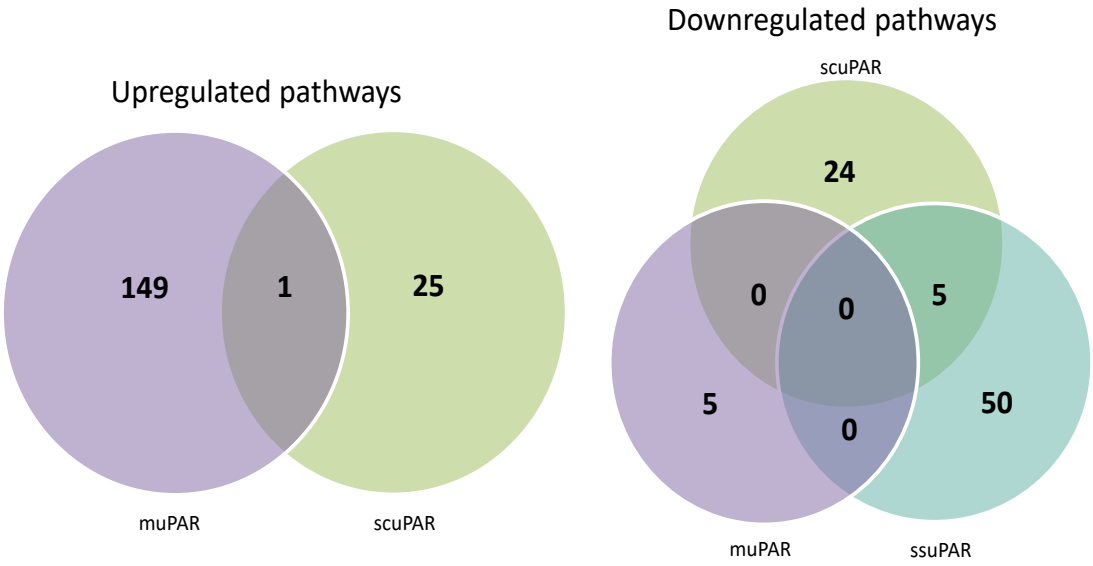


Figure 5.4.9: Gene Set Enrichment Analysis of Pathways Regulated by muPAR, ssuPAR and scuPAR. The GSEA database of gene sets represents pathways involved in specific cellular functions. GSEA was used to examine gene expression data from bronchial epithelial cells overexpressing variants of uPAR in order to identify pathways that are up and downregulated (FDR < 25%).

Upregulated pathways (25% FDR)

(a)

scuPAR	SIZE	ES	NES	NOM p-value	FDR q-value	FWER p-value	RANK AT MAX	LEADING EDGE		
Transiently induced by EGF	217	0.53	2.03	<0.001	0.03	0.03	4118	tags=45%	list=22%	signal=57%
TNF targets up	63	0.61	1.98	<0.001	0.04	0.08	3549	tags=49%	list=19%	signal=61%
Photodynamic therapy stress up	792	0.46	1.96	<0.001	0.04	0.10	5095	tags=47%	list=27%	signal=63%
HRAS oncogenic signature	250	0.48	1.92	<0.001	0.06	0.20	4887	tags=50%	list=26%	signal=67%
Epithelial differentiation module	69	0.58	1.90	<0.001	0.07	0.27	4642	tags=55%	list=25%	signal=73%

(b)

muPAR	SIZE	ES	NES	NOM p-value	FDR q-value	FWER p-value	RANK AT MAX	LEADING EDGE		
Kegg Ribosome	88	0.77	2.80	<0.001	<0.001	<0.001	2996	tags=86%	list=16%	signal=102%
Peptide chain elongation	102	0.74	2.71	<0.001	<0.001	<0.001	3872	tags=85%	list=21%	signal=107%
Cotranslational protein targeting to membrane	126	0.70	2.67	<0.001	<0.001	<0.001	3872	tags=78%	list=21%	signal=97%
Influenza viral RNA transcription and replication	118	0.70	2.64	<0.001	<0.001	<0.001	3369	tags=75%	list=18%	signal=91%
3 UTR mediated translational regulation	123	0.69	2.62	<0.001	<0.001	<0.001	3872	tags=76%	list=21%	signal=95%

Table 5.4.6: GSEA was performed using the Hallmark Database to identify pathways regulated by uPAR in HBEC (FDR <25%). 150 pathways were upregulated muPAR, 26 by scuPAR and 0 pathways were significantly upregulated by ssuPAR (a) 5 most upregulated pathways in scuPAR and muPAR overexpressing cells. a) details of b) details of. ES = enrichment score; NES = normalised enrichment score; NOM = nominal; FDR = false discovery rate; FWER = family wise error rate.

149 pathways were upregulated muPAR and 26 by scuPAR in bronchial epithelial cells, ssuPAR did not significantly upregulate any pathways. We focused to the 5 most upregulated pathways for each condition, scuPAR resulted in upregulation of genes targeted by EGF and TNF suggesting this form may interact with EGF and TNF signalling. scuPAR also upregulated genes related to cell division, growth and epithelial differentiation. muPAR upregulated genes involved in ribosome biogenesis, transcription and protein translation. Both variants increased expression of genes downregulated by E-cadherin, suggesting they interfere with E-cadherin signalling (pathway ID: CDH1_TARGETS_3_DN). E-Cadherin signalling plays a key role in regulating the epithelial barrier and is associated with EMT.

.

Downregulated pathways (25% FDR)

(a)

ssuPAR	SIZE	ES	NES	NOM p-value	FDR q-value	FWER p-value	RANK AT MAX	LEADING EDGE		
IFNA response	31	-0.75616	2.11	<0.001	<0.001	<0.001	2638	tags=74%,	list=14%,	signal=86%
Interferon response genes	67	-0.64	-2.05	<0.001	<0.001	0.001	4204	tags=66%	list=23%	signal=84%
IRF3 targets up	15	-0.83591	-1.98	<0.001	0.003	0.009	1598	tags=53%	list=9%	signal=58%
Neoplastic transformation up	73	-0.60216	-1.94	<0.001	0.007	0.036	2581	tags=38%	list=14%	signal=44%
Interferon response	23	-0.73076	-1.93	<0.001	0.008	0.047	2837	tags=61%	list=15%	signal=72%

(b)

scuPAR	SIZE	ES	NES	NOM p-value	FDR q-value	FWER p-value	RANK AT MAX	LEADING EDGE		
NRAS signalling down	72	-0.58	2.01	<0.001	0.09	0.1	5020	tags=58%	list=27%	signal=80%
IL6 deprivation down	98	-0.54	-1.98	<0.001	0.07	0.16	5187	tags=60%	list=28%	signal=83%
Anemia pathway	21	-0.72	-1.92	<0.001	0.13	0.37	4306	tags=71%	list=23%	signal=93%
Multiple myeloma up	44	-0.61	-1.92	<0.001	0.10	0.38	5134	tags=59%	list=28%	signal=81%
Cell cycle genes in IR response	82	-0.53	-1.89	<0.001	0.12	0.51	5141	tags=62%	list=28%	signal=85%

(c)

muPAR	SIZE	ES	NES	NOM p-value	FDR q-value	FWER p-value	RANK AT MAX	LEADING EDGE		
HS GAG biosynthesis	31	-0.66	2.10	<0.001	0.11	0.08	2445	tags=35%	list=13%	signal=41%
Chondroitin sulfate/ dermatan sulfate metabolism	47	-0.57	-2.03	<0.001	0.17	0.23	2445	tags=34%	list=13%	signal=39%
Chondroitin sulfate biosynthesis	19	-0.71	-2.00	0.002	0.18	0.34	2309	tags=42%	list=12%	signal=48%
Heparan sulfate/Heparin HS GAG metabolism	52	-0.55	-1.94	<0.001	0.23	0.53	2445	tags=29%	list=13%	signal=33%
Response to methotrexate up	22	-0.66	-1.94	<0.001	0.21	0.64	67	tags=9%	list=0%	signal=9%

Table 5.4.7: Pathways downregulated by uPAR variants. GSEA was performed using the Hallmark Database to identify pathways regulated by uPAR in HBEC (FDR <25%). 5 pathways were upregulated muPAR, 29 by scuPAR and 55 by ssuPAR (a) 5 most upregulated pathways in ssuPAR, scuPAR and muPAR overexpressing cells. a) details of b) details of. ES = enrichment score; NES = normalised enrichment score; NOM = nominal; FDR = false discovery rate; FWER = family wise error rate.

muPAR downregulated 5 pathways, suggesting this receptor form mainly activates gene transcription (upregulated 150 pathways). ssuPAR had opposite effects and downregulated 50 pathways compared to 0 upregulated pathways. scuPAR led to the enrichment of 29 pathways. As previously mentioned, we focused to the 5 most altered pathways as they contain genes with the greatest enrichment. ssuPAR downregulated pathways related interferon response suggesting a role in viral response. scuPAR overexpression increases expression of genes suppressed by IL6 and NRAS signalling and cell cycle genes. muPAR downregulated pathways involved in Heparin sulphate and Chondroitin sulphate biosynthesis and metabolism. 5 pathways were downregulated by both soluble forms of the receptor, these contained genes involved in the anemia pathway, upregulated in myeloma, response to ECM damage, interferon signalling and systemic lupus erythematosus.

5.4.8 Validation of RNA-Sequencing Using Real-Time PCR

In order to validate RNA-Seq the combined data from differential gene expression, rank product and gene set enrichment analyses were used. Validation was performed using qPCR and is necessary to validate sequencing (Fang and Cui, 2011). The genes selected for validation were significantly differentially expressed in at least 3 out 4 replicates based on either Cuffdiff or Rank Product analysis and belonged to a pathway significantly altered due to overexpression of muPAR, scuPAR or ssuPAR. qPCR validation was performed using the RNA samples used for sequencing, a summary of the genes selected for validation for each variant are summarised in Figure 5.4.10.

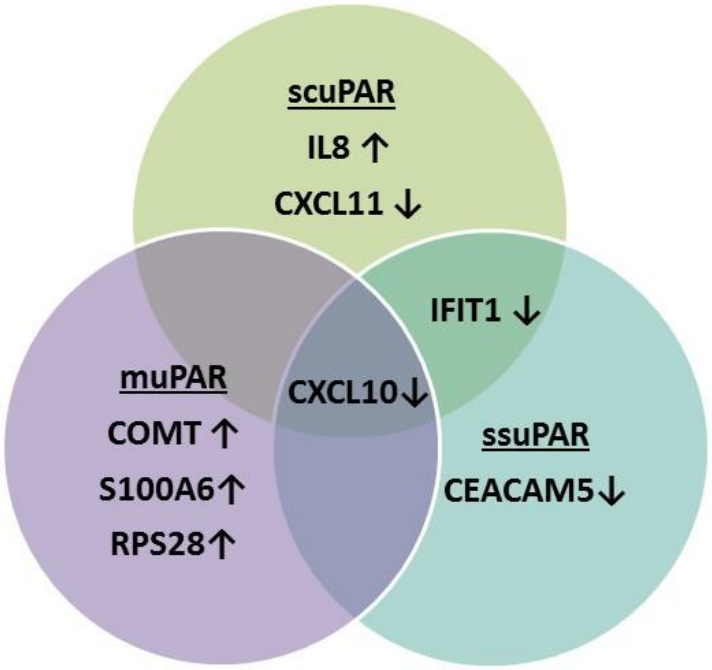
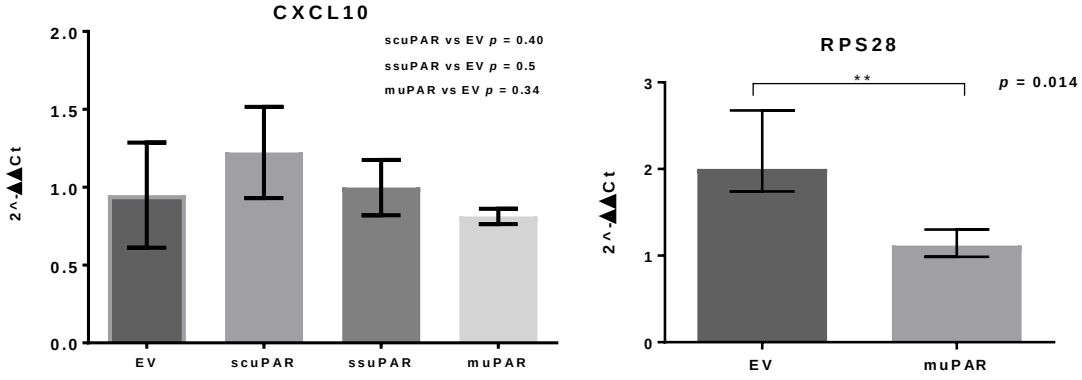


Figure 5.4.10: RNA-Seq Validation Genes. Whole transcriptome analysis was performed for human bronchial epithelial cells engineered to overexpress soluble cleaved uPAR (scuPAR), soluble-spliced uPAR (ssuPAR) and membrane uPAR (muPAR) using RNA-Seq analysis. 8 genes were selected to validate RNA-Sequencing based on differential gene expression and pathway analyses. The genes selected were identified as statistically differentially expressed by either Cuffdiff or Rank Product Analysis and were present in gene sets of pathways regulated by uPAR variants. ↑↓indicate the direction of change of expression.



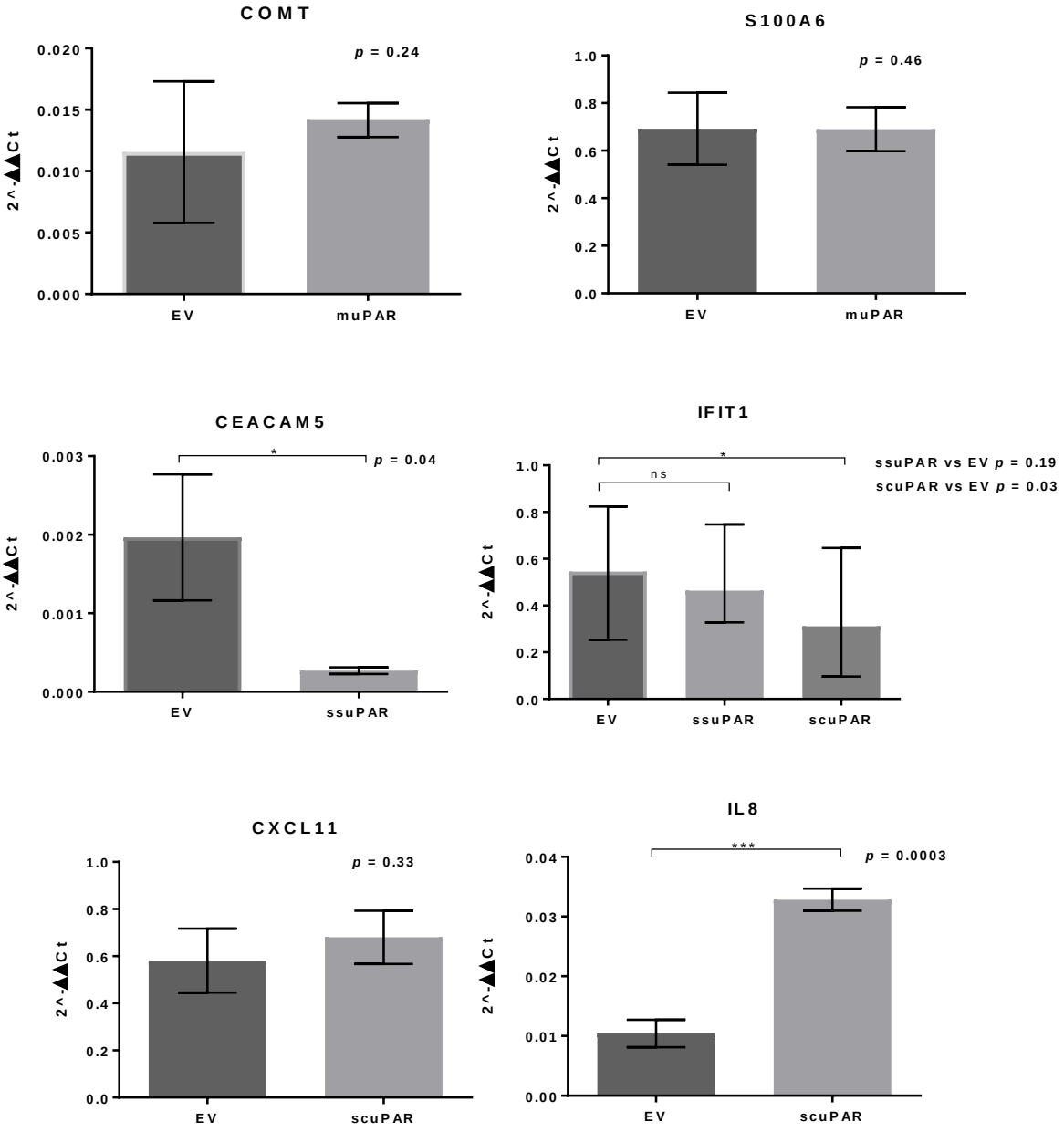


Figure 5.4.11: RNA-seq validation. qPCR was used to quantify the relative expression of CXCL10, CXCL11, IFIT1 and IL8 in HBEC overexpressing scuPAR vs empty vector; CXCL10, CEACAM5 and IFIT1 in HBEC overexpressing ssuPAR vs empty vector; and CXCL10, RPS28, COMT and S100A6 in HBEC overexpressing muPAR vs empty vector (*n*=4 ±SEM). HPRT1 reference gene was also measured in all samples.

CXCL10, CXCL11, IFIT1, CEACAM5, COMT, S100A6, RPS28 and IL8 gene expression were measured using qPCR and levels were compared in the respective uPAR variants and empty vector control using a Mann-Whitney one tailed *t*-test. Of these genes IL-8, CXCL11, IFIT1 and CEACAM5 showed similar patterns of expression as observed in the RNA-Seq analysis

$2^{-\Delta\Delta Ct}$ vs FPKM	*r*	*p*	sig.
CXCL10	0.63	<0.0001	Y
IL8	0.91	<0.0001	Y
CXCL11	0.46	0.04	Y
IFIT1	0.86	<0.0001	Y
CEACAM5	0.67	0.0015	Y
COMT	0.39	0.20	N
S100A6	-0.20	0.47	N
RPS28	-0.49	0.08	N

Table 5.4.8: Correlation Analysis of Target Gene Expression qPCR *vs* FPKM values. In order to compare gene expression values measured by qPCR ($2^{-\Delta\Delta Ct}$) with RNA-Seq (FPKM), values for the genes listed were measured in identical RNA samples were correlated using Spearman's rank co-efficient.

CXCL10, IL-8, CXCL11, IFIT1, CEACAM5 $2^{-\Delta\Delta Ct}$ and FPKM values were significantly positively correlated highlighting that both qPCR and RNA-Seq complement one another for these genes. COMT $2^{-\Delta\Delta Ct}$ and FPKM values were also positively correlated however this was not statistically significant, S100A6 and RPS28 values were negatively correlated indicating potential differences in mRNA detection by qPCR compared to RNA-Seq analysis.

(a)

FPKM vs PLAUR FPKM	*r*	*p*	sig.
CXCL10	-0.66	0.006	Y
IL8	0.53	0.01	Y
CXCL11	0.49	0.11	N
IFIT1	-0.59	0.02	Y
CEACAM5	-0.14	0.62	N
COMT	0.52	0.20	N
S100A6	0.76	0.006	Y
RPS28	0.54	0.17	N

(b)

$2^{-\Delta\Delta Ct}$ vs PLAUR FPKM	*r*	*p*	sig.
CXCL10	-0.47	0.0035	Y
IL8	0.55	0.02	Y
CXCL11	0.09	0.69	N
IFIT1	-0.48	0.0043	Y
CEACAM5	-0.55	0.015	Y
COMT	0.07	0.80	N
S100A6	0.20	0.48	N
RPS28	0.53	0.16	N

Table 5.4.9: Correlation Analysis of Target Gene Expression *vs PLAUR* expression. In order to compare the relationship between target genes and *PLAUR* mRNA expression, (a) 2^-ΔΔCt and (b) FPKM values of target genes were correlated with *PLAUR* FPKM values.

Correlation analysis of target gene expression with PLAUR expression was performed to assess the relationships observed from differential gene expression analysis i.e. positive *r* will correspond with an increase in expression whereas a negative *r* will correspond with a decrease in expression as a result of elevated PLAUR expressed by HBEC. CXCL10, IL-8 and IFIT1 correlations with PLAUR levels corresponded with findings from RNA-Seq differential gene expression analysis. CEACAM5, CXCL11 COMT, S100A6 and RPS28 were not significantly correlated with PLAUR expression with the exception of CEACAM5 when correlating 2^-ΔΔCt.

5.5 Discussion

The overall aim of this chapter was to investigate the effects of elevated muPAR, ssuPAR and scuPAR on bronchial epithelial cell function. Work presented in this thesis and findings from previous studies have demonstrated that uPAR expression is elevated in the bronchial epithelium in asthma (Stewart *et al*., 2012a). scuPAR is elevated in serum in asthma and levels have been associated with tissue remodelling and EMT (Wang *et al*., 2013; Portelli *et al*., 2015). muPAR, ssuPAR and scuPAR have each been shown to differentially regulate cellular functions in HBEC and soluble forms promote a pro-remodelling phenotype, elevating cell proliferation and MMP-9 activity (Portelli *et al*., 2015). Key aims of this chapter were to i) Identify genes differentially expressed in human bronchial epithelial cells engineered to overexpress muPAR, ssuPAR and scuPAR ii) Identify pathways regulated by these uPAR variants using Gene Set Enrichment Analysis and to iii) Identify uPAR isoforms expressed by human bronchial epithelial cells. PLAUR expression was significantly upregulated in all cells engineered to overexpress the different variants. Two separate analyses identified 52 genes regulated by scuPAR, 102 by ssuPAR and 62 by muPAR. Pathway analysis found that scuPAR regulated genes associated with IL-6 and TNF-α cytokine signalling and also NRAS signalling pathways. muPAR largely upregulated genes required for transcription and translation. ssuPAR predominantly suppressed gene expression and targeted genes related to interferon response.

Cuffdiff analysis identified 15 genes regulated by membrane bound uPAR, 7 of which were specifically elevated by muPAR. *MIR3677* and *YRNA* code are potential transcriptional regulators (Zhang, Langley *et al*. 2011), *COMT* and *PLCH1* are associated with cancer and (Zhang, Hua *et al*. 2013; Tan and Chen 2014) *HOOK2* is involved in centrosome regulation

and *ATP6V0A1* regulates airway acidification which has been shown to be important for airway defence (Fischer and Widdicombe 2006). muPAR interacts with numerous ligands (e.g. uPA), integrins and GPCRs (Smith and Marshall, 2010), the targets identified may be downstream of these pathways and therefore enable muPAR to regulate cell division (*HOOK2, COMT, PLCH1*) and extracellular pH (*ATP6V0A1*). Pathway analysis found that muPAR upregulated transcriptional regulation (Moheimani *et al*., 2016) and also protein translation pathways, which may serve as a mechanism for regulating cell division and growth, processes already associated with uPAR (Noh *et al*., 2013a). The pathways suppressed by muPAR were related to synthesis of proteoglycans required for intercellular and ECM interaction, reduced expression of these molecules may alter cell adhesion properties in epithelial cells (Shannon *et al*., 2003). Rank product analysis identified that *SERPINE1*, the gene encoding PAI-1, and MMP-14 expression are elevated by muPAR. Both proteins are associated with the ECM and are elevated in asthma (Moheimani *et al*., 2016). Expression of a large number of ribosomal proteins were elevated which complemented pathway analyses findings that ribosome biogenesis was the most upregulated pathway.

scuPAR increased the expression of the cytokine IL-8, the zinc finger gene ZBTB7C and the IgG receptor fragment FCGR2A as well as numerous pseudogenes. scuPAR expression strongly correlated with IL-8 levels, IL-8 recruits and activates neutrophils and (Pease and Sabroe, 2002) and is elevated in BALF from asthma patients (Nocker *et al*., 1996). These proteins have been shown to correlate in disease, IL-8 and uPAR levels correlate in colorectal cancer (Terada *et al*., 2005), and scuPAR may promote airway inflammation via the induction of IL-8. ZBTB7C regulates MMP-9 expression in mice and (Jeon *et al*., 2016), data presented in this thesis showed that scuPAR may act via MMP-9 to regulate epithelial barrier function, scuPAR induction of ZBTB7C may be required to regulate MMP-9 activity. FCGR2A belongs

to a family of antigen presenting receptors, the role of these receptors are not fully understood, increased expression may have implications for airway inflammation (Wu *et al*., 2014). Rank product analysis identified B2M is induced by scuPAR, a cleaved fragment of this protein is secreted by airway epithelial cells and has antimicrobial activity and recruits monocytes to induce an immune response (Chiou *et al*., 2016). Pathway analysis also revealed that scuPAR upregulated genes associated with remodelling and inflammation, including EGF pathway, epithelial differentiation genes and TNF-α pathway genes.

ssuPAR is predominantly a suppressor of gene expression. Cuffdiff identified a number of downregulated genes including *SNX1* which is needed to internalize EGFR (Chin *et al*., 2001), SNX1 suppression may contribute to increased EGFR expression, EGFR is elevated asthma and is related to epithelial barrier function (Heijink *et al*., 2010b). Interestingly, rank product analysis found that *PLAU* the gene encoding uPA, is upregulated by ssuPAR which may serve as a feedback mechanism to augment uPAR receptor signalling. A large number of interferon response genes were downregulated by ssuPAR, pathway analysis also showed that ssuPAR suppressed interferon pathway targets. Elevated ssuPAR levels may dampen the immune response to viral infections in the lungs (Vareille *et al*., 2011), increasing susceptibility to infection and exacerbation (Kloepfer and Gern, 2010).

In addition to receptor specific functions, genes regulated by multiple receptor forms were also identified. muPAR and scuPAR induce genes suppressed by E-cadherin, and may contribute to disruption of E-cadherin signalling which has been shown to promote Th2 cell recruitment in allergic asthma via EGFR signalling (Heijink *et al*., 2007). Rank product analysis found that all variants reduced expression of metallothionein proteins which act as free radical scavengers (Kumari 1998) and have anti-inflammatory properties in OVA-induced

mice (Inoue *et al*., 2009). Furthermore, both soluble forms of uPAR downregulated genes involved in ECM modulation. Overlapping and specialised functions of uPAR isoforms have been identified and provide novel insight into the mechanisms underlying altered bronchial epithelial structure and function resulting from elevated uPAR.

A limitation of the study is that PLAUR expression levels indicate intra and inter-donor variability in transfected HBEC which may account for the relatively low number of differentially expressed genes identified using the Cuffdiff analysis. Primary cells are a physiological model but can give rise to heterogenous results, inter donor variability may have resulted from differences in transfection efficiency. Variation can introduce bias in gene expression analysis, to address this reads were quality trimmed to improve the accuracy of read alignment and transcript assembly. Furthermore, we used two independent methods, Rank Product Analysis and Cuffdiff, to confirm that PLAUR was indeed upregulated as result of genetic modification. Genes identified in the separate analyses showed little overlap with the exception of *PLAUR,* Rankproduct uses a ranking method whereas Cuffdiff quantifies average expression across all replicates. Subsequent GSEA analysis identified pathways with genes from both the Cuffdiff and Rankprod analysis suggesting that both analysis methods were appropriate and also highlights the need to analyse RNAseq data using different pipelines to obtain meaningful results. Future work requires analysis of protein networks to determine how proteins identified in DE analysis are related, although this is partly achieved through GSEA.

In summary, this study has shown that the effects of elevated uPAR expression on bronchial epithelial function are complex and different receptor isoforms are likely to drive distinct phenotypes. muPAR induced pathways support the role of uPAR as regulator of cell

proliferation and migration and findings provide novel insight into the mechanisms underlying these functions. scuPAR and ssuPAR function is far beyond that of a decoy receptor. these analyses demonstrate the importance of these uPAR variants in airway inflammation, barrier regulation via E-cadherin signalling and the epithelial response to virus infections.

Chapter 6: Genetic Association Study of Asthma Related Phenotypes at Chromosome 19q13 (*PLAUR*)

6 Genetic association study of asthma related phenotypes at chromosome 19q13 (*PLAUR*)

6.1 Introduction

Asthma is a complex genetic disorder thought to involve multiple genes, with expression influenced by both genetic and environmental factors (Rava, 2015). Linkage analysis and more recently genome-wide association studies (GWAS) have been powerful tools in identifying genomic regions and genetic variants associated with disease (Ober, 2016). Genomic approaches have proven to be instrumental in our understanding of asthma genetics and have led to the identification of over a hundred genes that have been associated with asthma (Thomsen, 2015).

Genome-wide analyses of particular asthma phenotypes have been conducted to identify pathogenetic mechanism, for example a GWAS of childhood asthma with severe exacerbations identified *CDHR3* as an asthma susceptibility gene (Cadherin Related Family Member 3) (Bønnelykke *et al*., 2014). A separate study investigating moderate-severe asthma confirmed previously identified signals at 17q21 and *IL1RL1* loci and findings were suggestive for loci, *C5orf56* and *CD83* (Wan *et al*., 2012). GWAS of refined asthma phenotypes e.g. childhood onset and asthma with allergic rhinitis, have identified overlapping and distinct genetic loci and may lead to the identification of specific genetic risk factors (Portelli and Sayers, 2016).

SNPs spanning the urokinase plasminogen activator receptor (*PLAUR* or uPAR) were associated with asthma susceptibility, BHR and plasma uPAR levels through

linkage/association analyses (Barton *et al*., 2009) and baseline lung function in smokers (Stewart, 2009). Barton *et al* conducted linkage and association analyses using 587 white asthma families spanning 14.4 mega base pairs (Mbps) on 19q13. 46 families from Nottingham (UK) and 341 families from Southampton (UK) were recruited on the basis of 2 siblings with a current physician diagnosis of asthma, 200 families from the Netherlands were recruited by using probands with asthma. Linkage and association analyses was performed using microsatellite markers spanning region on 19q13, the region then underwent fine mapping using haplotype tagging SNPs. 18 *PLAUR* SNPs were tested for the association with asthma, BHR, FEV_1, plasma uPAR levels and rate of annual FEV_1 decline in subjects with asthma. The study identified 2 SNPs, rs4493171 (5' region) and rs2239372 (intron 3), that showed modest association with asthma and had the same direction of effect in two cohorts (Nottingham and Dutch). Analyses of the BHR phenotype identified rs2239372 in all 3 cohorts, and rs4493171 Southampton and Nottingham populations. rs2356338 (5' region) and rs4493171 were associated with FEV_1 in the Nottingham and Dutch, and Southampton and Nottingham cohorts. rs2239372, rs2356338, and rs4493171 showed an association with plasma uPAR levels in the Nottingham cohort, providing the link between uPAR protein and asthma risk alleles

.

SNP	Allele	MAF (GBR/CEU)	Location (hg19)	Location in PLAUR	Association with Asthma and airway remodelling
rs2239372	A	0.49	44162954	Intron 3	Atopy, ↑serum PLAUR, Asthma risk [1] [2] eQTL for expression levels in blood
rs2302524	C	0.16	44156472	Exon 6 (Lys220Arg)	Asthma risk, Accelerated lung function decline [1] Decreases baseline lung function [2] Basal epithelial proliferation [3] eQTL for expression levels in blood
rs4251953	A	0.057	44151525	3'UTR/intron	Accelerated decline in lung function [1] [2] eQTL for expression levels in blood
rs4803648	T	0.22	44145543	3'UTR	Asthma risk, Accelerated decline in lung function [1] [2] Basal epithelial proliferation [3] eQTL for expression levels in blood
rs4493171	T	0.23	44184856	5'UTR	↓ Asthma risk, ↓serum PLAUR [1] [2] Collage III deposition [3] eQTL for expression levels in blood
rs2356338	T	0.32	44174971	5'UTR	↑ Asthma risk, accelerated lung function decline, increased serum soluble cleaved uPAR [1] [2] Basal epithelial proliferation [3]
rs4760	C	0.16	44153100	Exon 7 (Leu317Pro)	mRNA eQTL in peripheral blood [4]

Table 6.1.1: *PLAUR* SNPs Reproducibly Associated with Asthma Risk, Lung Function and PLAUR Levels. PLAUR SNP associations with asthma related phenotypes have been identified in multiple studies, [1] (Barton 2009), [2] (Stewart 2009), [3] (Ierodiakanou 2016). UTR = Untranslated region; eQTL = Expression quantitative trait loci; LD = Linkage disequilibrium; CEU = Northern and Western European (population code); GBR = British in England and Scotland; MAF = Minor allele frequency.

PLAUR SNPs were tested for association with lung function in smokers, rs2302524 and rs2283628 were associated with FEV_1 (lower and higher, respectively) and 5' SNPs rs740587, rs11668247 and rs344779 were associated with increased FEV_1/VC providing evidence that *PLAUR* influences baseline lung function in smokers (Stewart *et al*., 2009). In a separate study the relationship between 22 previously investigated *PLAUR* SNPs and markers of airway remodelling were investigated (Ierodiakonou *et al*., 2016a). 11 SNPs analysed were associated with one or more outcomes including: AHR, basal epithelial proliferation, basement membrane thickness and collagen III deposition. Of these 11 SNPs, seven had previously been associated with asthma, four with lung function decline in asthma and eight

showed an association with basal epithelial proliferation (Ki67). These data identifying a potential role for *PLAUR* in epithelial homeostasis. A summary of *PLAUR* SNP associations with asthma, *PLAUR* levels and lung function can be found in Table 6.1.1.

In this chapter, we set out to investigate the relationship between polymorphisms in the *PLAUR* gene and clinical and immunological features of asthma as well as airway remodelling features. The traits analysed included lung function (FEV_1 and FEV_1/FVC), atopy, serum IgE levels and blood eosinophils in moderate to severe asthma patients. Lung function measurements can serve as indicators of the state of airway remodelling (Chae *et al*., 2011). Total IgE serves as a biomarker for atopic asthma, allergen-specific IgE is used to specify which allergen the individual is sensitized, we focused to total IgE for these analyses (Szefler *et al*., 2012). Atopic status is also an important determinant for atopic asthma and blood eosinophils can identify patients with type 2 asthma phenotype(s) and higher counts often correlate with frequency of exacerbations in asthma (Carr *et al*., 2016).

6.2 Aims

The aim of this chapter was to define the relative contribution of genetic polymorphisms spanning the *PLAUR* gene to the clinical features and presentation of asthma using a novel cohort of moderate to severe asthma patients from the Genetics of Asthma Severity and Phenotypes (GASP) study.

6.2.1 Specific Aims

- Investigate association between *PLAUR* SNPs and FEV_1, FEV_1/FVC, Atopy, Total serum IgE levels and Blood Eosinophils in severe asthma patients.
- Investigate if *PLAUR* SNPs previously associated with asthma and related phenotypes are identified in this study.

6.3 Methods

Genetic association studies presented in this thesis were completed in collaboration with Neil Bennett, Ionna Ntall, Nick Shrine and Louise Wain, University of Leicester, UK.

6.3.1 Study Population and Patient Recruitment

2,885 patients with asthma were recruited across UK specialist centres as part of the Genetics of Asthma Severity and Phenotypes (GASP) study. Subjects were recruited in two batches, HALLUKBVAX (Batch 1) and UoNAX (Batch 2). The recruitment centres and number of individuals recruited from each centre are listed in the table below. From the original 2,885 patients recruited, data from 2,536 patients were used for association analysis. Ethics approval was provided by individual study centres during study recruitment.

Centre	Total number of patients recruited	Total number of patients used in analysis
Belfast	100	93
Birmingham	43	42
Cumbria	33	30
Nottingham	574	506
Leicester	318	284
Glasgow	651	617
Manchester	829	678
Southampton	337	286
Total	2885	2536

Table 6.3.1: Summary of UK Recruitment Centres for Genotyped Samples. Table includes the total numbers of asthma patients recruited and the final number of patient samples with genotyping data. Belfast, Birmingham, Glasgow, Manchester, Southampton (Wan *et al*., 2012). Nottingham University Hospitals (5 cohorts: Nottingham asthma families (Barton SJ, 2009), Nottingham Gedling (Wain *et al*., 2014), Nottingham asthma, Nottingham city asthma and Nottingham cell bank), Leicester Glenfield Hospital (3 cohorts: Gabriel (Moffatt *et al*., 2010), Leicester asthma and Roche.

6.3.2 Isolation of DNA, Genotyping and Quality Control of Sample Data

DNA extraction from 1ml blood was outsourced to Source Biosciences (Nottingham, UK). Genotyping of patient samples was outsourced to Affymetrix INC. (Santa Clara, California). Two genotyping runs were performed using two Affymetrix chips; UK BiLEVE (Wain 2015), and the UK Biobank Affymetrix chip (ukbiobank.ac.uk). The custom Affymetrix Axiom array was designed to measure variants associated with lung function and respiratory disease and rare coding variation. The Affymetrix chips shared 95% of reference SNPs and 820,967 SNPs were measured in total across both chips, see Table 6.3.2

Category	Number of Markers
Markers of specific interest	
Alzheimer's Disease	803
ApoE	1,147
Autoimmune/Inflammatory	258
Blood Phenotypes	2,545
Cancer common variants	343
Cardiometabolic	377
eQTL	17,115
Fingerprint	262
HLA	7,348
KIR	1,546
Lung function phenotypes	8,645
Common mitochondrial DNA variants	180
Neurological disease	19,791
NHGRI GWAS catalog	8,136
Pharmacogenetics/ADME	2,037
Tags for Neanderthal ancestry	11,057
Y chromosome markers	807
Rare variants in cancer predisposition genes	6,543
Rare variants in cardiac disease predisposition genes	1,710
Rare, possibly disease causing, mutations	13,729
CNV regions for development delay, neuropsychiatric disorders and lung function	2,639
Rare coding variants	
Protein truncating variants	30,581
Other rare coding variants	80,581
Genome-wide coverage	
Genome-wide coverage for common variants	348,569
Genome-wide coverage for low frequency variants	280,838
Total number of markers	820,967

Table 6.3.2: The Essential Components of the Genotyping Arrays (both UKBiLEVE and UK Biobank)

Each genotyping batch underwent quality control to check for outliers in explanatory variables (age, gender and height), duplicated entries, incorrect matches between genotype and phenotype data, and outright missing genotype or phenotype data for an individual. Following initial quality control, 2,536 samples remained for further analysis.

6.3.3 Clinical Measures for Asthma Traits

Patient phenotype data was collected by respective centres, FEV_1 (in litres) and FEV_1/FVC were measured from spirometry (the best of three satisfactory attempts in line with ATS/ERS requirements) (BTS 2005). Atopy was defined as – At least one "atopy" test from the following; one or more positive skin prick test and/or "doctor diagnosed" atopy from questionnaire. Total serum IgE levels were reported in number of kilounits per litre (kU/L) and blood eosinophil count in cells per litre ($x10^9$/L). Subjects broadly represent a moderate to severe asthma population (BTS/GINA 3-5), severity was determined by lung function FEV_1 < 80% and a corresponding reduction in FEV_1/FVC and medication.

Phenotype	Subjects with data
Age	2,241
Gender	2,534
GINA/BTS score	2,536
Mean FEV_1 (% predicted)	1,765
Mean FEV_1/FVC (%)	1,888
Mean Serum IgE (kU/L)	1,377
Mean Blood Eosinophils ($x10^9$/L)	969
Atopic (with ≥ 1 positive test)	1,561

Table 6.3.3: Number of Patients Included in Genetic Analyses of Traits. Number of individuals with data for the traits analysed from 2,536 subjects that had genotyping data which passed quality control.

6.3.4 Association Testing

Association data for each phenotype was generated using the open-source whole genome association analysis toolset PLINK with an additive genetic model (Purcell *et al*., 2007). The distribution of the data was analysed and total serum IgE and blood eosinophils values were log transformed prior to association testing. FEV_1, FEV_1/FVC, total serum IgE and blood eosinophils followed a linear regression model, while atopy utilised logistic regression as a binary variable. Explanatory variables (age, height, gender, the ten principal components of ancestry and batch) were used to correct for each of the phenotypes tested. The corresponding explanatory variables for the traits analysed (response variable) are summarised in Table 6.3.4.

Response variable	Explanatory variables
FEV_1	height, age, age^2, gender, ancestry principal components, batch
FEV_1/FVC	height, age, age^2, gender, ancestry principal components, batch
log10 (Blood eosinophils)	age, gender, ancestry principal components, batch
log10 (Total IgE)	age, gender, ancestry principal components, batch

Table 6.3.4: Explanatory Variables used to Correct for Traits

6.3.4.1 Visualisation of Region Based Association Signals

The online tool LocusZoom (Pruim, 2010) (Version 1.1) was used to plot the resulting association data for the locus for PLAUR +/- 50Kb using the human genome build hg19. SNPs

for each phenotype were then explored within the Asthma UK Genetics of Severe Asthma (AUGOSA) GWAS dataset of 933 subjects with asthma and 3,346 healthy controls and with asthma severity in a separate moderate-severe cohort (Wan, 2012).

6.3.5 Power Calculations

Power calculations were carried out in QUANTO © Version 1.2.4 for association studies of continual ((FEV_1, FEV_1/FVC, log10(serum IgE) and log10(blood eosinophils)) and binary (Atopy) traits in the cohorts of non-related individuals. Power calculations were carried out using the following steps:

Parameters	Continuous data	Binary data
Outcome/Design	➢ Continuous, Independent Individuals	➢ Disease, Case-Control (unmatched)
Hypothesis	➢ Gene only	➢ Gene only
Gene G	➢ SNP 'minor allele frequency' inserted ➢ Additive model selected	➢ SNP 'minor allele frequency' inserted ➢ Log additive model selected
Outcome model	➢ Mean value and standard deviation for the trait analysed were introduced ➢ The tab 'main effect' was selected and the beta value for the trait were inputted	➢ The tab 'genetic effect' was selected and the beta value for the trait were inputted
Power	➢ Sample size was inputted and an acceptable error rate of 0.05 set	
	➢ The calculator button was pressed to run the calculation	

Table 6.3.5: Quanto Parameters used for Power Calculations for Association Analyses of Continual and Binary Traits.

6.4 Results

6.4.1 Subject Demographics

Demographics of the 2,536 subjects genotyped and included in trait analysis are summarised in Table 6.4.1. Data for age, gender and asthma severity (BTS/GINA) was collected for >88% subjects, 61% of subjects had data for atopy, and 70% and 74% had data for FEV_1 and FEV_1/FVC, respectively.

Subject Demographics (n=2,536)	Value
Age - mean (SD)	48 (16)
Gender (% female)	64
FEV_1 (%Predicted) (SD)	77.2 (23.4)
FEV_1/FVC (SD)	0.69 (0.14)
Smoking (%) • Never • Ever • Current	 58.4 23.4 18.2
BTS/GINA >3 (% moderate/severe asthma)	87.2
Atopy (% at least one positive indication)	68.5
Mean Blood Eosinophils ($x10^9$/L)	0.31 (0.41)
Mean Serum IgE (kU/L)	407 (748.7)

Table 6.4.1: Demographics for the Final Study Population of Asthma Subjects used in Genetic Analyses. SD = standard deviation; BTS = British Thoracic Society; GINA = Global Initiative for Asthma.

6.4.2 Quality Control of Sample Data

Quality Control was carried out by Ionna Ntall, University of Leicester (Wain, Shrine *et al*. 2015). Data was checked for outlying values in explanatory variables, gender mismatches

and duplicates. The tables below summarise the number of individuals remaining in the analysis after quality control checks had been completed.

	Batch 1		Batch 2	
	Number removed	Number remaining	Number removed	Number remaining
Initial sample set	-	744	-	2172
Genotype failures	0	744	73	2098
Sex mismatches	16	728	45	2053
Heterozygosity outliers	17	711	62	1991
Call rate outliers	0	711	1	1990
Duplicates/related individuals	17	694	62	1928
Ancestry outliers	9	685	38	1890

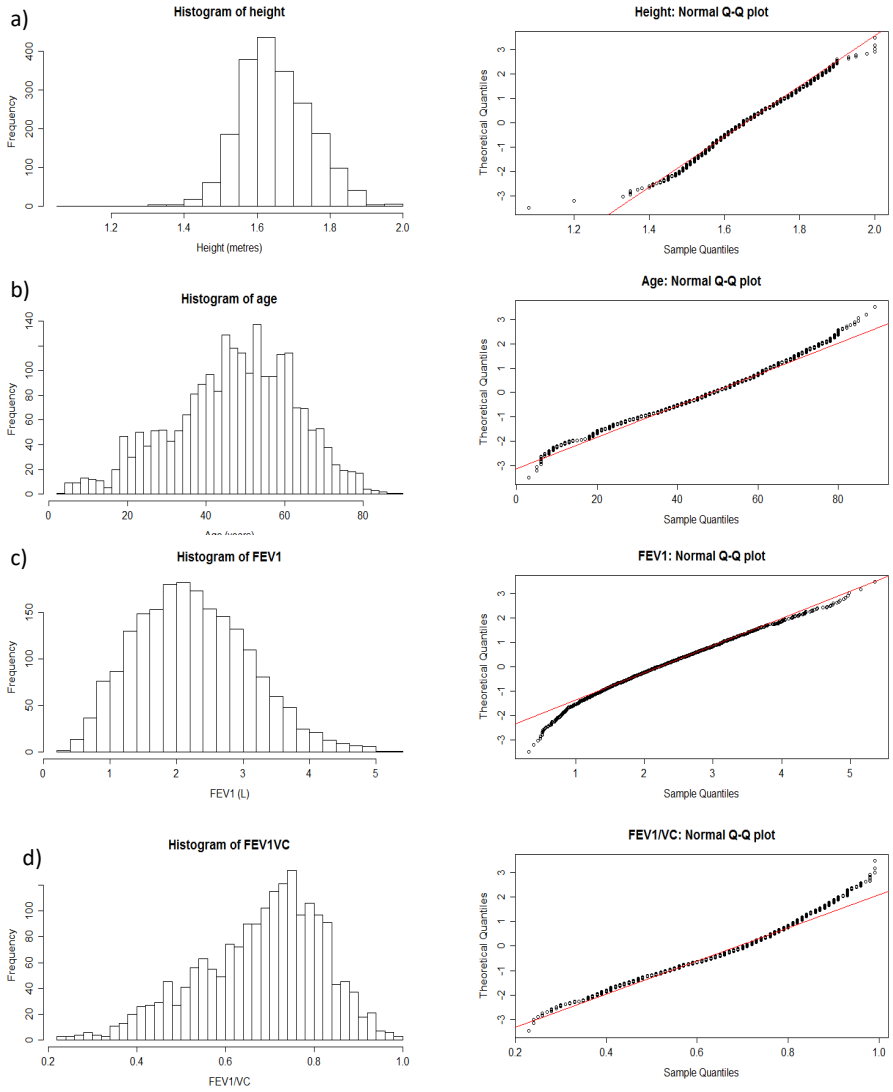
Table 6.4.2: Number of Individuals Removed from Batch 1 and Batch 2 after Quality Control for Explanatory Variables, Gender Mismatches and Duplicates

	Number removed	Number remaining
Batch 1 + Batch 2	-	2575
Batch 1 related outliers	12	2563
Duplicate/related pairs	14	2549
Batch 2 further sex mismatches	2	2547
Genotyped but no phenotype data available	5	2542
Genotyped but to be discarded as these are controls per recruiting centres	3	2539
Genotyped but to be discarded as these are duplicates per recruiting centres	3	2536

Table 6.4.3: Number of Individuals Removed from Batch 1 and Batch 2 after Quality Control for Genotype Data

6.4.2.1 Distribution of Subject Data

Samples unsuitable for downstream analysis were removed from the dataset and to test for evidence of systematic bias (from unrecognized population structure, analytical approach, genotyping artefacts, etc.), quantile-quantile (Q-Q) plots were used to characterize the extent to which the observed distribution of subject data followed the expected (null) distribution.



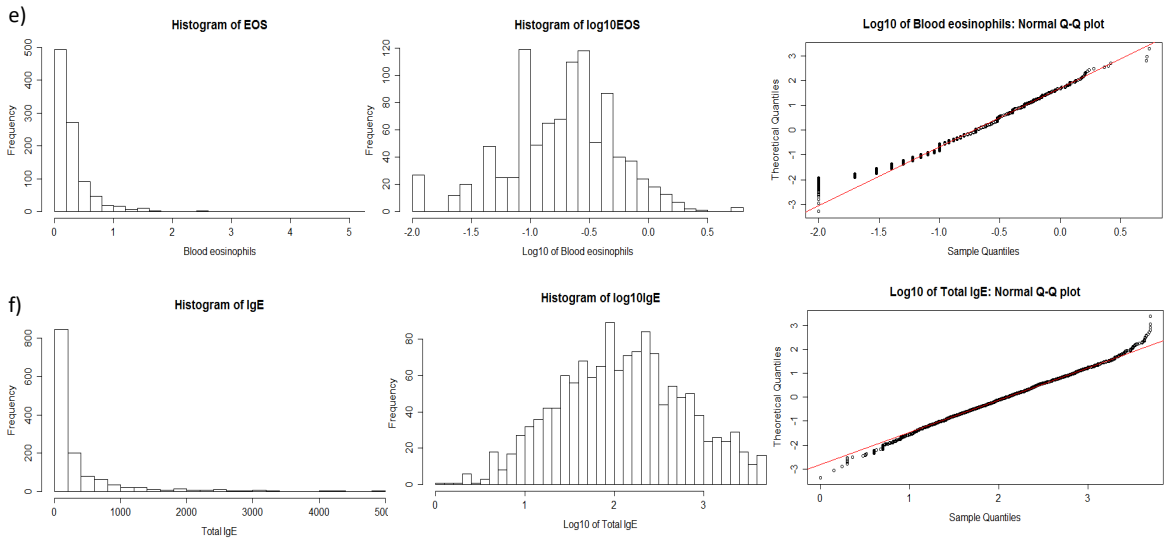


Figure 6.4.1: Data for Traits Measured Show a Normal Distribution. Histograms and Normal Q-Q plots showing the distribution of data for (a) height, (b) age, (c) FEV_1, (d) FEV_1/FVC, (e) Blood Eosinophils and log10 Blood Eosinophils, (f) IgE and log10 IgE. Data for blood eosinophils and IgE were transformed (log10) to achieve normal distribution. Histograms display the number of individuals (frequency, y axis) for each continuous variables (x axis). QQ plots provide a visual comparison of the sample quantiles to the corresponding theoretical quantiles

.

Height, age, FEV_1 and FEV_1/FVC were normally distributed. Data for EOS and IgE were logged to achieve a normal distribution. (Atopic status is a binary (and not a continuous) variable therefore cannot have a normal distribution). Normal Q-Q plots for the traits measured exhibit straight lines highlighting data follows the assumed distribution (see Figure 6.5.4.).

6.4.2.2 Quality Control of SNP Genotyping

Q-Q plots of observed P-values versus expected P-values were generated for FEV_1, FEV_1/FVC, log10 blood eosinophils and log10 total serum IgE.

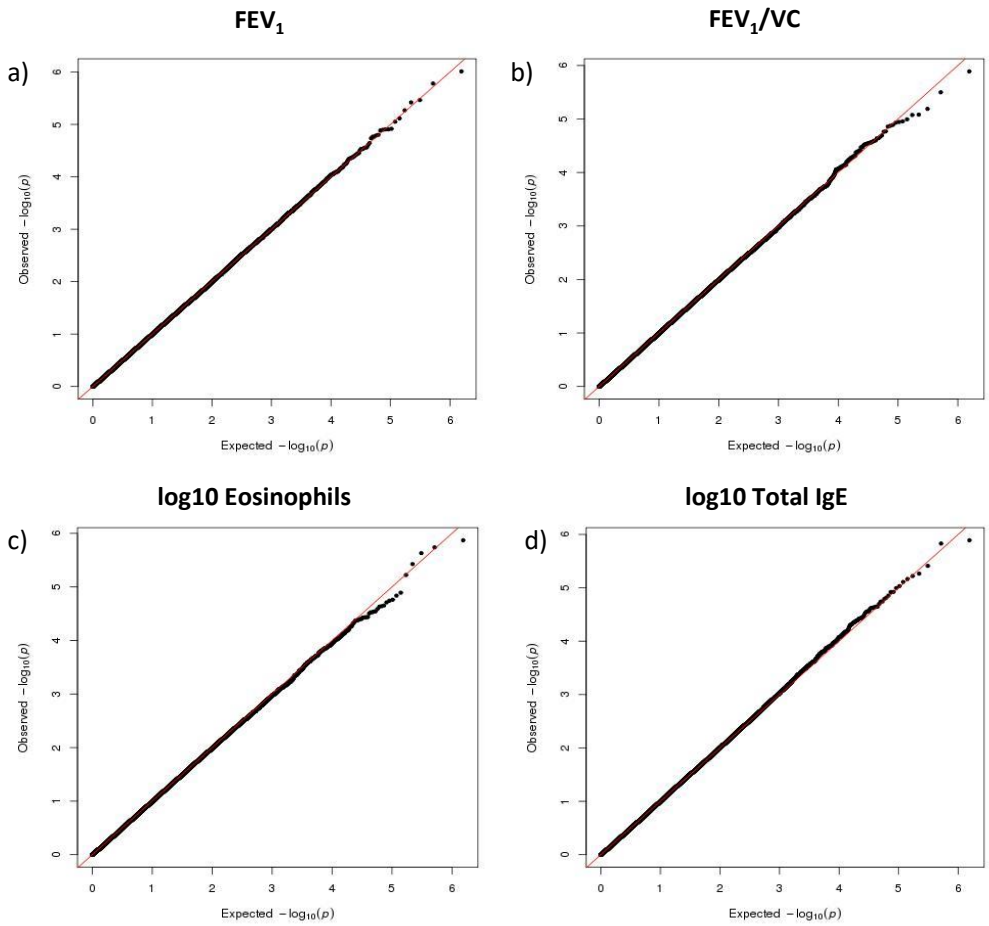


Figure 6.4.2: SNPs across Whole Genome. Q-Q plot of Observed P-values vs Expected P-values for (a) FEV_1, (b) FEV_1/FVC, (c) log10 Eosinophils and (d) log10 Total IgE.

Plots generated straight lines matching X=Y, deviations from the line represent the small number of true associations among thousands of unassociated SNPs. Q-Q plot of observed P-values versus expected P-values for FEV_1, FEV_1/FVC, log10 blood eosinophils and log10 total serum IgE demonstrate that the data follows the assumed distribution (distribution of observed *p* values were plotted against distribution of theoretical *p* values).

6.4.2.3 Estimates of Lambda (Genomic Inflation Factor)

To investigate if there are any systematic biases that may be present in our association results the genomic inflation factor, also known as lambda gc (λgc), was calculated. λgc is defined as the median of the resulting chi-squared test statistics divided by the expected median of the chi-squared distribution. Data that follows the normal chi-squared distribution, the expected λgc value is 1. If the λgc value is greater than 1, then this may be evidence for some systematic bias that needs to be corrected in your analysis (de Bakker, Ferreira *et al*. 2008).

	Estimate	Standard error
FEV_1	0.9959	$7.746x10^{-6}$
FEV_1/FVC	0.9907	$9.004x10^{-6}$
log10(EOS)	0.9882	$8.811x10^{-6}$
log10(IgE)	0.9984	$1.203x10^{-5}$

Table 6.4.4: Summary of Lambda Values for FEV1, FEV1/FVC, log10 EOS and log10 IgE

As shown in Table 6.4.6 the lambda values were close to 1 supporting the conclusion that we had not introduced any systematic biases.

6.4.3 Association of *PLAUR* Polymorphisms with FEV_1, FEV_1/FVC, Blood Eosinophils, Serum IgE and Atopy

As described in section 6.3.4, association data was generated using PLINK with an additive genetic model and association plots were generated using Locus Zoom. For each of the measured phenotypes, no polymorphisms at chromosome 19:44050246−44274498 met genome wide significance ($p<5x10-8$). The Bonferroni correction is an approach to correct for multiple testing, the alpha value from $\alpha = 0.05$ is adjusted so that $\alpha = (0.05/k)$ where k is the number of statistical tests conducted (i.e. the number of polymorphisms in the region). No SNPs at the *PLAUR* locus met the refined threshold for the phenotypes tested (FEV_1 and FEV_1/FVC, 97 polymorphisms, $p < 5.15 x10-4$; log10 EOS, 92 SNPs, $p < 5.43 x10-4$; log10 IgE, 95 SNPs, $p < 5.26 x 10-4$; Atopy, 90 SNPs, $p < 5.56 x 10-4$). We therefore report SNPs meeting nominal significance ($p < 0.05$) across the phenotypes tested. Association plots and summary tables for the 10 most significant SNPs for FEV_1, FEV_1/FVC, log10 EOS, log10 IgE and atopy are shown in Figure 6.5.1 to Figure 6.5.5.

6.4.3.1 Association of chr19q13 SNPs with FEV_1

Data for FEV_1 was collected for 1,765 subjects, 97 SNPs were tested for association with FEV_1 at chr19:44050246−44274498 and were plotted across the region (Figure 6.4.3 and Table 6.4.5).

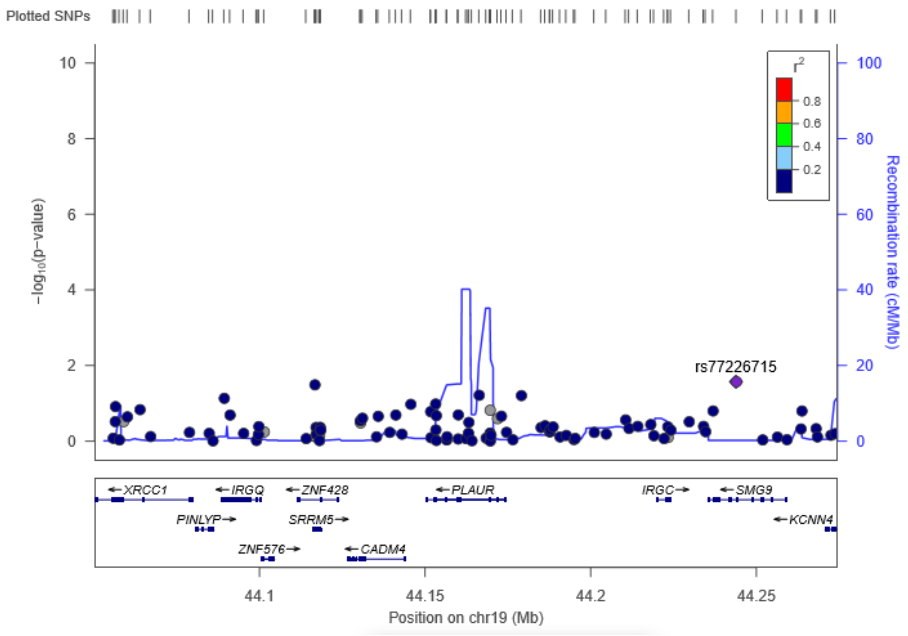


Figure 6.4.3: rs77226715 and rs201742640 Show Moderate Association with FEV_1. Association plot of PLAUR SNPs with FEV_1 in moderate to severe asthma patients. Upper panel: pairwise r^2 (derived from HAPMAP) between the lead SNP and the SNPs in its flanking regions are shown together with the association P-value. cM = centimorgan; Mb = megabase; *XRCC1* = X-Ray Repair Cross Complementing 1 gene; *PINLYP* = Phospholipase A2 Inhibitor And LY6/PLAUR Domain Containing gene; *IRGQ* = Immunity Related GTPase Q gene; *ZNF576* = Zinc Finger Protein 576 gene; *SRRM5* = Serine/Arginine Repetitive Matrix 5 gene; *CADM4* = Cell Adhesion Molecule 4; *PLAUR* = Urokinase plasminogen activator receptor gene; *IRGC* = Immunity Related GTPase Cinema gene; *SMG9* = SMG9, Nonsense Mediated MRNA Decay Factor; *KCNN4* = Potassium Calcium-Activated Channel Subfamily N Member 4 gene.

SNP	Base Pair Position	n	BETA	OR	SE	P-value	Minor Allele	Major Allele	GENO	MAC	MAF
rs77226715	44243834	1994	-0.34	0.71	0.15	0.03	A	G	0/55/2478	55	0.01
rs201742640	44116609	1431	-0.99	0.37	0.46	0.03	A	C	0/6/1860	6	0.00
rs4251842	44166187	1996	0.12	1.13	0.06	0.06	C	A	13/288/2231	314	0.06
rs73044790	44178928	1995	0.08	1.08	0.04	0.06	T	C	63/656/1814	782	0.15
rs77595924	44089240	1935	0.14	1.15	0.08	0.07	T	C	1/238/2232	240	0.05
rs140046361	44153044	563	1.47	4.36	0.91	0.10	G	A	0/1/663	1	0.00

Table 6.4.5: Association Results of *PLAUR* SNPs with FEV_1. rs77226715 and rs201742640 met p=< 0.05. n = Number of individuals included in genetic association testing of phenotype; BETA = Beta value of phenotype; OR = odds ratio yielded by genetic association testing of phenotype = exp(BETA.assoc); SE = Standard error for BETA; GENO = Genotype breakdown: homozygous minor allele/heterozygous/heterozygous minor allele; MAC = minor allele count; MAF = minor allele frequency.

Of the 97 SNPs tested two SNPs, rs77226715 (A/G, n=1994, BETA=-0.34, MAF= 0.01, p=0.03) and rs201742640 (A/C, n=1431, BETA=-0.99, MAF= 0.0016, p=0.03), showed moderate association with reduced FEV_1 in this study cohort.

6.4.3.2 Association of chr19q13 SNPs with FEV_1/FVC

Data for FEV_1/FVC was collected for 1,888 subjects, 97 SNPs were tested for association results with FEV_1/FVC at chr19:44050246−44274498 (Figure 6.4.4 and Table 6.4.6).

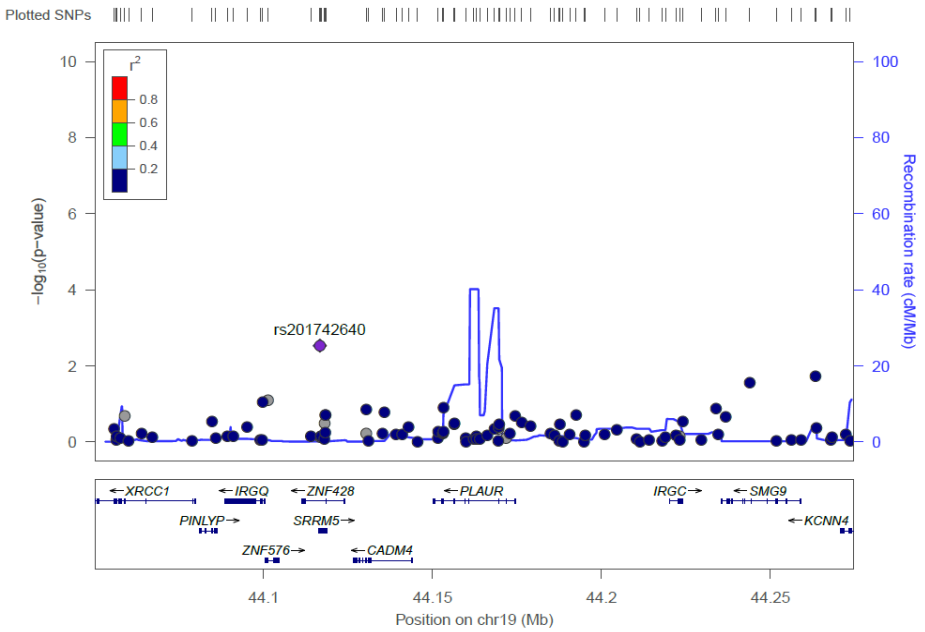


Figure 6.4.4: Lack of association between *PLAUR* SNPs and FEV_1/FVC. Association plot of *PLAUR* SNPs with FEV_1/FVC in moderate to severe asthma patients. Upper panel: pairwise r^2 (derived from HAPMAP) between the lead SNP and the SNPs in its flanking regions are shown together with the association P-value. cM = centimorgan; Mb = megabase; *XRCC1* = X-Ray Repair Cross Complementing 1 gene; *PINLYP* = Phospholipase A2 Inhibitor And LY6/PLAUR Domain Containing gene; *IRGQ* = Immunity Related GTPase Q gene; *ZNF576* = Zinc Finger Protein 576 gene; *SRRM5* = Serine/Arginine Repetitive Matrix 5 gene; *CADM4* = Cell Adhesion Molecule 4; *PLAUR* = Urokinase plasminogen activator receptor gene; *IRGC* = Immunity Related GTPase Cinema gene; *SMG9* = SMG9, Nonsense Mediated MRNA Decay Factor; *KCNN4* = Potassium Calcium-Activated Channel Subfamily N Member 4 gene.

SNP	Base Pair Position	n	BETA	OR	SE	P-value	Minor Allele	Major Allele	GENO	MAC	MAF
rs201742640	44116609	1314	-1.44	0.24	0.48	0.003	A	C	0/6/1860	6	0.00
rs145704690	44101297	1850	1.76	5.78	1.00	0.08	T	C	0/1/2534	1	0.00

Table 6.4.6: Association Results of *PLAUR* SNPs with FEV_1/FVC. rs201742640 met p=< 0.05. n = Number of individuals included in genetic association testing of phenotype; BETA = Beta value of phenotype; OR = odds ratio yielded by genetic association testing of phenotype = exp(BETA.assoc); SE = Standard error for BETA; GENO = Genotype breakdown: homozygous minor allele/heterozygous/heterozygous minor allele; MAC = minor allele count; MAF = minor allele frequency.

One SNP, rs201742640 (A/C, n=1314, BETA=-1.44, MAF=0.0016, p=0.003), showed moderate association with reduced FEV_1/FVC in this study cohort, rs201742640 was also associated with reduced FEV_1.

6.4.3.3 Association of chr19q13 SNPs with Blood Eosinophil Count

Subject data for blood eosinophils was collected from 969 individuals, 92 SNPs were tested for association results with log10(blood eosinophils) at chr19:44050246−44274498.

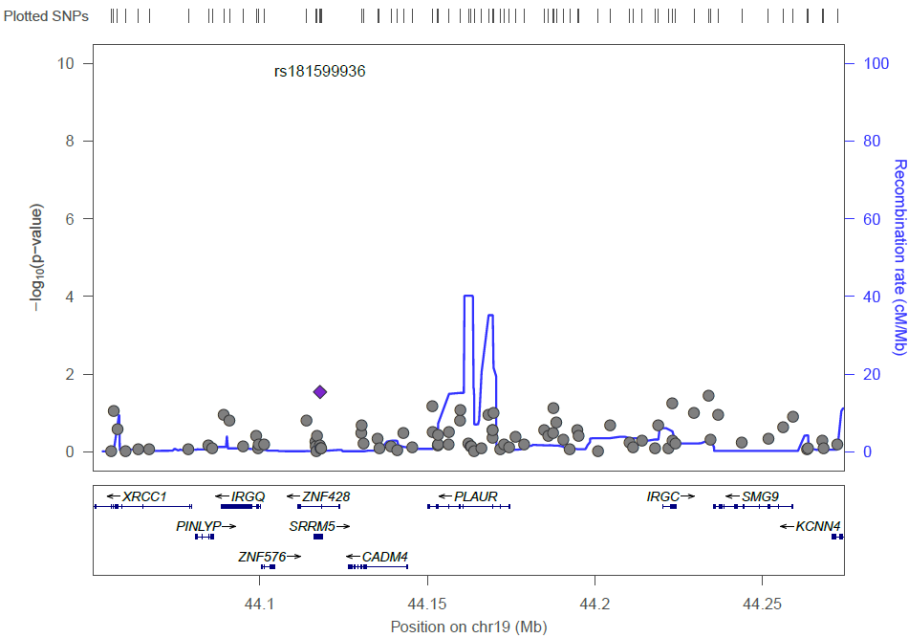


Figure 6.4.5: Lack of association between *PLAUR* SNPs and blood eosinophils. Association plot of *PLAUR* SNPs with log10(blood eosinophils) in moderate to severe asthma patients. Upper panel: pairwise r^2 (derived from HAPMAP) between the lead SNP and the SNPs in its flanking regions are shown together with the association P-value. cM = centimorgan; Mb = megabase; *XRCC1* = X-Ray Repair Cross Complementing 1 gene; *PINLYP* = Phospholipase A2 Inhibitor And LY6/PLAUR Domain Containing gene; *IRGQ* = Immunity Related GTPase Q gene; *ZNF576* = Zinc Finger Protein 576 gene; *SRRM5* = Serine/Arginine Repetitive Matrix 5 gene; *CADM4* = Cell Adhesion Molecule 4; *PLAUR* = Urokinase plasminogen activator receptor gene; *IRGC* = Immunity Related GTPase Cinema gene; *SMG9* = SMG9, Nonsense Mediated MRNA Decay Factor; *KCNN4* = Potassium Calcium-Activated Channel Subfamily N Member 4 gene.

SNP	Base Pair Position	n	BETA	OR	SE	P-value	Minor Allele	Major Allele	GENO	MAC	MAF
rs181599936	44117985	966	-1.26	0.28	0.58	0.03	A	G	0/5/2529	5	0.00
rs4251953	44151525	965	-0.18	0.83	0.10	0.07	T	C	11/266/2256	288	0.06
rs4251882	44159876	966	-0.17	0.85	0.10	0.09	A	G	11/267/2256	289	0.06
rs4251831	44169738	964	0.08	1.08	0.05	0.10	G	C	234/1021/1276	1489	0.29

Table 6.4.7: Association results of *PLAUR* SNPs with blood eosinophils. rs181599936 met p=< 0.05. n = Number of individuals included in genetic association testing of phenotype; BETA = Beta value of phenotype; OR = odds ratio yielded by genetic association testing of phenotype = exp(BETA.assoc); SE = Standard error for BETA; GENO = Genotype breakdown: homozygous minor allele/heterozygous/heterozygous minor allele; MAC = minor allele count; MAF = minor allele frequency.

The SNP, rs181599936 (A/G, n=966, BETA=-1.26, MAF=0.0009, p=0.03), showed moderate association with reduced blood eosinophil count.

6.4.3.4 Association of chr19q13 SNPs with Serum IgE Levels

Data for serum IgE was collected for 1,377 individuals, values you were transformed (log10) and 95 SNPs were tested for association results with log10(IgE) at chr19:44050246−44274498.

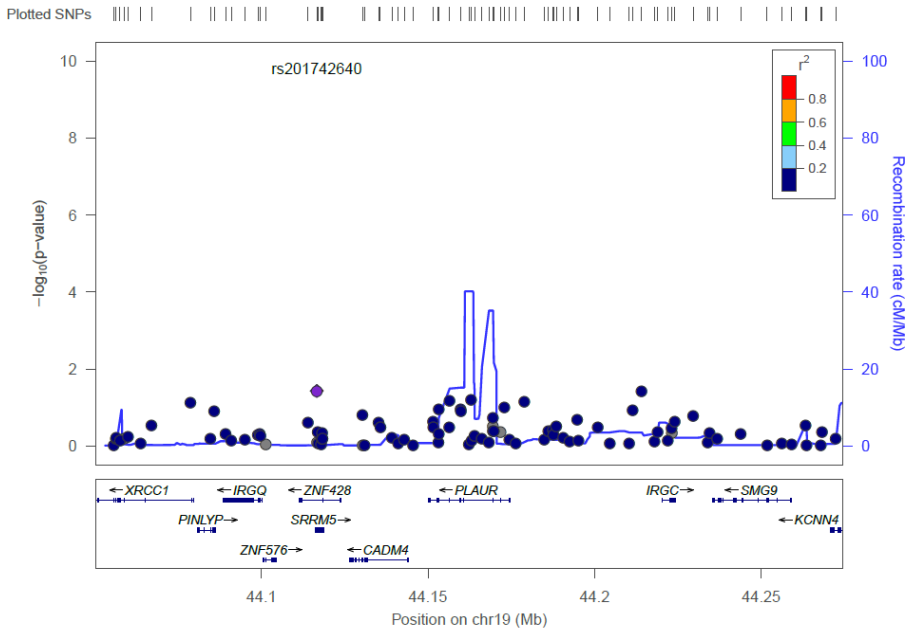


Figure 6.4.6: Lack of association between *PLAUR* SNPs and serum IgE. Association plot of *PLAUR* SNPs with log10(IgE) in moderate to severe asthma patients. Upper panel: pairwise r^2 (derived from HAPMAP) between the lead SNP and the SNPs in its flanking regions are shown together with the association P-value. cM = centimorgan; Mb = megabase; *XRCC1* = X-Ray Repair Cross Complementing 1 gene; *PINLYP* = Phospholipase A2 Inhibitor And LY6/PLAUR Domain Containing gene; *IRGQ* = Immunity Related GTPase Q gene; *ZNF576* = Zinc Finger Protein 576 gene; *SRRM5* = Serine/Arginine Repetitive Matrix 5 gene; *CADM4* = Cell Adhesion Molecule 4; *PLAUR* = Urokinase plasminogen activator receptor gene; *IRGC* = Immunity Related GTPase Cinema gene; *SMG9* = SMG9, Nonsense Mediated MRNA Decay Factor; *KCNN4* = Potassium Calcium-Activated Channel Subfamily N Member 4 gene.

SNP	Base Pair Position	n	BETA	OR	SE	P-value	Minor Allele	Major Allele	GENO	MAC	MAF
rs201742640	44116609	1115	0.92	2.51	0.44	0.04	A	C	0/6/1860	6	0.00
rs2239372	44162954	1370	0.07	1.07	0.04	0.06	G	A	594/1299/634	2487	0.49
rs2302524	44156472	1371	0.10	1.10	0.05	0.07	C	T	68/683/1780	819	0.16
rs73044790	44178928	1373	0.10	1.10	0.05	0.07	T	C	63/656/1814	782	0.15
rs344782	44172890	1373	0.06	1.07	0.04	0.10	A	C	542/1271/722	2355	0.46

Table 6.4.8:: Association results of *PLAUR* SNPs with serum IgE. rs201742640 met p=< 0.05. n = Number of individuals included in genetic association testing of phenotype; BETA = Beta value of phenotype; OR = odds ratio yielded by genetic association testing of phenotype = exp(BETA.assoc); SE = Standard error for BETA; GENO = Genotype breakdown: homozygous minor allele/heterozygous/heterozygous minor allele; MAC = minor allele count; MAF = minor allele frequency.

The SNP rs201742640 (A/C, n=1115, BETA=0.92, MAF=0.0016, p=0.04), showed moderate association with increased serum IgE. rs201742640 was also associated with reduced FEV_1 and FEV_1/FVC.

6.4.3.5 Association of chr19q13 SNPs with Atopy

Atopic status (with ≥1 positive test) was confirmed for 1,561 individuals, 90 SNPs were tested for association results with atopy at chr19:44050246−44274498.

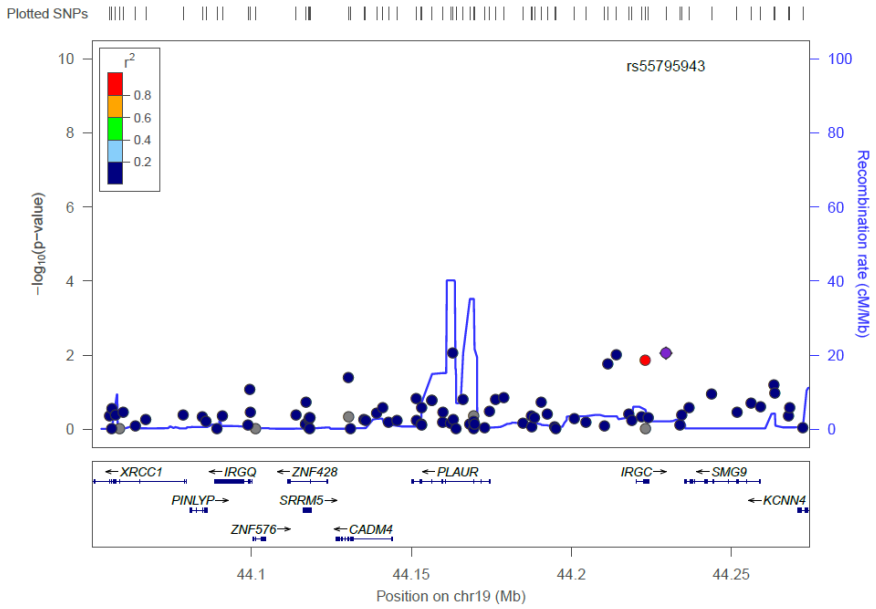


Figure 6.4.7: Lack of association between *PLAUR* SNPs and atopy. Association plot of *PLAUR* SNPs with atopy in moderate to severe asthma patients. Upper panel: pairwise r^2 (derived from HAPMAP) between the lead SNP and the SNPs in its flanking regions are shown together with the association P-value. cM = centimorgan; Mb = megabase; *XRCC1* = X-Ray Repair Cross Complementing 1 gene; *PINLYP* = Phospholipase A2 Inhibitor And LY6/PLAUR Domain Containing gene; *IRGQ* = Immunity Related GTPase Q gene; *ZNF576* = Zinc Finger Protein 576 gene; *SRRM5* = Serine/Arginine Repetitive Matrix 5 gene; *CADM4* = Cell Adhesion Molecule 4; *PLAUR* = Urokinase plasminogen activator receptor gene; *IRGC* = Immunity Related GTPase Cinema gene; *SMG9* = SMG9, Nonsense Mediated MRNA Decay Factor; *KCNN4* = Potassium Calcium-Activated Channel Subfamily N Member 4 gene.

SNP	Base Pair Position	n	BETA	OR	SE	P-value	Minor Allele	Major Allele	GENO	MAC	MAF
rs55795943	44229567	1554	-0.98	0.38	0.37	0.01	T	C	0/103/2428	103	0.02
rs2239372	44162954	1554	-0.21	0.81	0.08	0.01	G	A	594/1299/634	2487	0.49
rs380442	44214054	1546	0.34	1.40	0.13	0.01	A	C	28/397/2092	453	0.09
rs11555891	44223113	1559	-0.88	0.42	0.36	0.01	A	G	0/103/2432	103	0.02
rs366489	44211390	1557	0.31	1.36	0.13	0.02	G	T	27/406/2099	460	0.09
Affx-15999158	44079591	1559	1.61	5.02	0.78	0.04	A	C	0/11/2525	11	0.00
rs147390796	44130315	1559	1.77	5.85	0.86	0.04	T	C	0/11/2525	11	0.00
rs73048635	44263319	1554	-0.31	0.73	0.17	0.06	C	T	12/353/2166	377	0.07
rs116968052	44099538	1559	-0.55	0.58	0.32	0.08	T	C	0/98/2437	98	0.02

Table 6.4.9: Association results of *PLAUR* SNPs with atopy. rs55795943, rs2239372, rs11555891 (decreased risk) rs380442, rs366489 and rs147390796 (increased risk) met p=< 0.05. n = Number of individuals included in genetic association testing of phenotype; BETA = Beta value of phenotype; OR = odds ratio yielded by genetic association testing of phenotype = exp(BETA.assoc); SE = Standard error for BETA; GENO = Genotype breakdown: homozygous minor allele/heterozygous/heterozygous minor allele; MAC = minor allele count; MAF = minor allele frequency.

rs55795943 (T/C, n=1554, BETA=-0.98, MAF=0.02, p=0.01), rs2239372 (G/A, n=1554, BETA=-0.21, MAF=0.49, p=0.01), rs11555891 (A/G, n=1559, BETA=-0.99, MAF=0.02, p=0.01) were associated with decreased risk. rs380442 (A/C, n=1557, BETA=0.34, MAF=0.09, p=0.01), rs366489 (G/T, n=1557, BETA=0.31, MAF=0.09, p=0.02) and rs147390796 (T/C, n=1559, BETA=1.77, MAF=0.002, p=0.04) were positively associated with atopy in this cohort. rs2239372 has previously been associated with atopy, serum PLAUR levels and asthma risk (see Table 6.1.1).

6.4.4 Association with Previously Reported Loci

In order to validate the datasets a look-up for association for previously reported loci from the literature was conducted for atopy, IgE, FEV_1 and eosinophils.

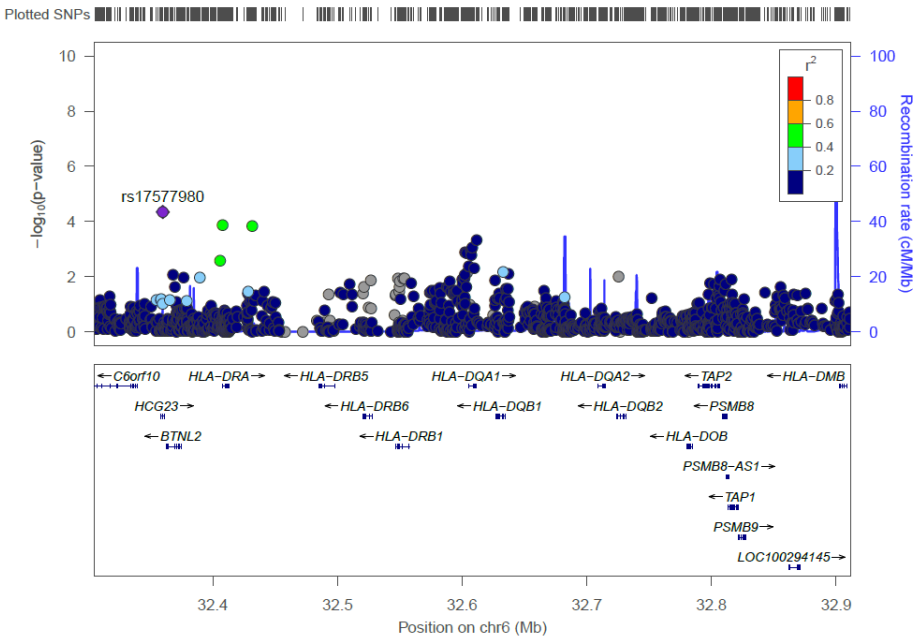


Figure 6.4.8: Polymorphisms Across the HLA Genomic Loci are Associated with Atopy: Upper panel: pairwise r^2 (derived from HAPMAP) between the lead SNP and the SNPs in its flanking regions are shown together with the association P-value. cM = centimorgan; Mb = megabase.

The current study identified an association between SNPs across several HLA genes and atopy. The HLA region has been identified as an asthma susceptibility locus and is associated allergy (Ober and Vercelli, 2011, Moffatt *et al*., 2007).

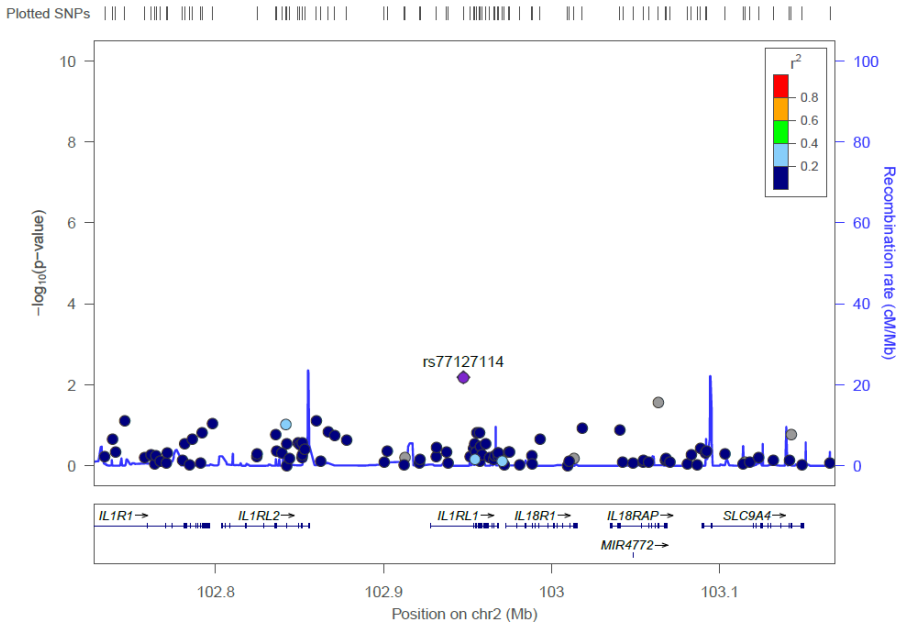


Figure 6.4.9: *IL1RL1* Association with Blood Eosinophil Counts. Upper panel: pairwise r^2 (derived from HAPMAP) between the lead SNP and the SNPs in its flanking regions are shown together with the association P-value. cM = centimorgan; Mb = megabase.

The *IL1RL1* region on 2q12 has previously been associated with blood eosinophil counts in asthma (Ober and Vercelli, 2011) which has been replicated in this study. This gene encodes the ST2 receptor for the asthma susceptibility gene *IL33*.

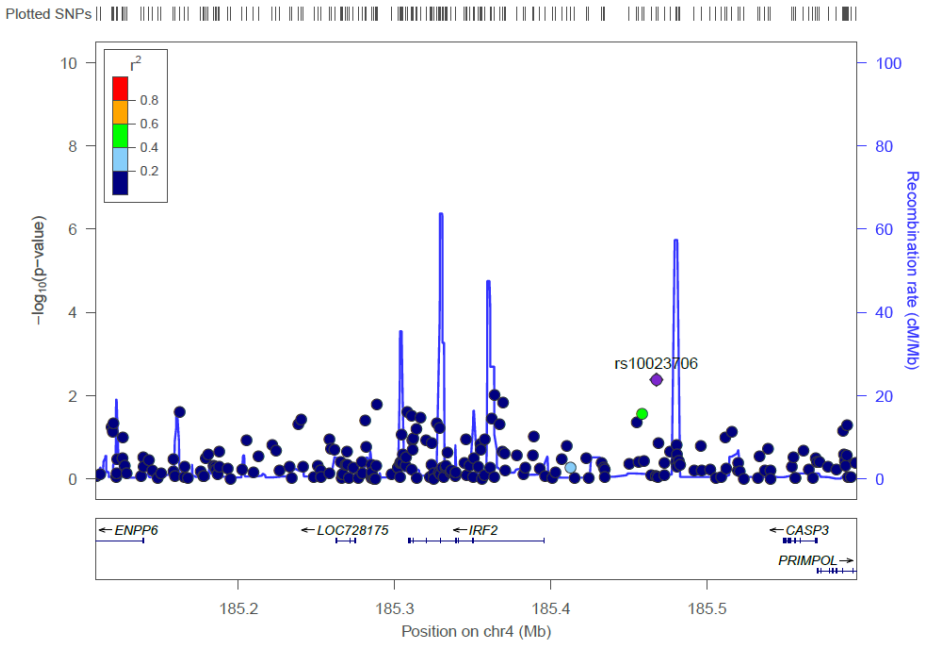


Figure 6.4.10: *IRF2* Association with Forced Expiratory Volume in 1 second. Upper panel: pairwise r^2 (derived from HAPMAP) between the lead SNP and the SNPs in its flanking regions are shown together with the association P-value. cM = centimorgan; Mb = megabase.

IRF2 gene polymorphisms were associated with lung function (FEV_1), which has been shown in asthma and general populations (Li *et al*., 2013).

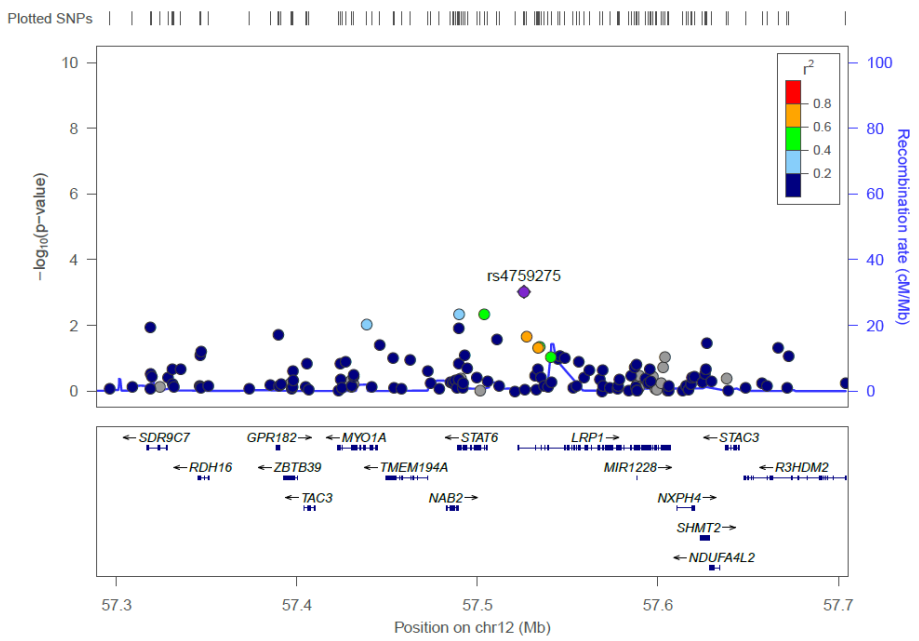


Figure 6.4.11: STAT6 Association with Total Serum IgE, Upper panel: pairwise r^2 (derived from HAPMAP) between the lead SNP and the SNPs in its flanking regions are shown together with the association P-value. cM = centimorgan; Mb = megabase.

Polymorphisms in the *STAT6* gene were shown to be associated with total serum IgE levels in this study and has been previously reported in a GWAS of total serum IgE was conducted in 7,087 asthma cases and 7,667 controls.

6.5 Discussion

PLAUR has been identified as an asthma susceptibility gene through linkage and association analysis (Barton, Koppelman *et al*. 2009), polymorphisms have also been associated with baseline lung function, serum PLAUR levels and epithelial proliferation (Stewart 2009, Portelli, Stewart *et al*. 2015, Ierodiakonou, Portelli *et al*. 2016). The overall aim of this chapter was to define the relative contribution of SNPs spanning *PLAUR* to the clinical features and presentation of asthma using a novel cohort of moderate to severe asthma patients from the GASP study (population enriched for moderate-severe asthma).

The specific aims were to i) investigate the association between *PLAUR* SNPs and FEV_1, FEV_1/FVC, Atopy, Total serum IgE levels and Blood Eosinophils in severe asthma patients and to ii) investigate if *PLAUR* SNPs which have been previously associated with asthma and related phenotypes are identified in this study. Overall, we did not find polymorphisms that were significantly associated with the traits measured however we did identify 3 SNPs that met baseline significance with atopy (*p* value <0.05, MAF >0.05), these were rs2239372 (intron 3), rs380442 (5'UTR), rs366489 (5'UTR), findings are summarised in Table 6.5.1. This analysis did not identify an association between *PLAUR* genetic variants and FEV_1, FEV_1/FVC, blood eosinophil levels or serum IgE levels.

SNP	Allele	MAF (GBR/CEU)	Location (hg19)	Location	Evidence/ SNP summary
rs2239372	A	0.49	44162954	Intron 3	Atopy, serum PLAUR levels, asthma risk [1] [2] eQTL for expression levels in blood GASP: ↓ Atopy (p=0.01) and ↑ Serum IgE (p=0.06)
rs380442	A	0.09	44214054	5' UTR	GASP: ↑ Atopy (p=0.01)
rs366489	G	0.09	44211390	5'UTR	GASP: ↑ Atopy (p=0.02)
***rs2302524**	C	0.16	44156472	Exon 6 (Lys220Arg)	Asthma risk, accelerated lung function decline [1] Baseline lung function [2] Basal epithelial proliferation [3] eQTL for expression levels in blood GASP: ↑ Serum IgE (p=0.07)
***rs4251953**	A	0.057	44151525	3'UTR	Accelerated decline in lung function [1] [2] LD with 15 PLAUR SNPs. eQTL for expression levels in blood GASP: ↓ Blood Eosinophils (p=0.07)
***rs4803648**	A	0.22	44145543	3'UTR	Asthma risk, Accelerated decline in lung function [1] [2] LD with 5 PLAUR SNPs eQTL for expression levels in blood GASP: ↑ FEV_1 (p=0.11)

Table 6.5.1: Summary of *PLAUR* SNP Associations Identified from GASP Study. Table includes SNPs that met baseline significance (p <0.05, MAF >0.05). SNPs denoted with a '*' did not meet p <0.05 but were within the top 10 most significantly associated SNPs for the phenotype tested, these SNPs were found to be associated with asthma related phenotypes in previous association studies (see Table 6.1.1).

It is important to compare the study population with others to assess the validity of the cohort used. A comparison of the study cohort used for these analyses with other study cohorts is summarised in Table 6.5.2. Study 1 refers to the European U-BIOPRED (Unbiased BIOmarkers in PREDiction of respiratory disease outcomes) adult severe asthma cohort (Shaw, Sousa *et al*. 2015). Liang *et al* studied methylation in asthma patients based on IgE levels (Study 2) (Liang, Willis-Owen *et al*. 2015). Price *et al* used records from 130,546 asthma patients to identify variables that may be used to predict asthma exacerbations (Study 3) (Price, Wilson *et al*. 2016). The GASP cohort showed similar characteristics to study 1 with regards to subject age, gender, lung function and eosinophils, with serum IgE levels from study 2 and the proportion of smokers/ non-smokers from study 3.

	GASP	Study 1	Study 2	Study 3
Subject *n*	2536	311	355	130,547
Age - mean (SD)	48 (16)	51.01 (0.8)	28 (2–61)	48.8 (17.4)
Gender (% female)	64	66	48.5	65.9
FEV_1 (%Predicted) (SD)	77.2 (23.4)	67. (1.26)	-	-
FEV_1/FVC (SD)	0.69 (0.14)	0.64 (0.01)	-	-
Smoking (%)				
-Never	58.4	100	-	55.7
-Ever	23.4	-	-	25.5
-Current	18.2	-	12.7	18.8
BTS/GINA >3 (% moderate/severe asthma)	87.2	100	-	-
Atopy (% at least one positive indication)	68.5	78.3	-	-
Mean Blood Eosinophils ($x10^9$/L)	0.31 (0.41)	0.2 (0.3)	0.4 (0.38)	0.2 (1.2, 3.5)
Mean Serum IgE	407 (1-5000) ku/L	119.5 (45−342) IU·mL−1	320 (1-4999) IU/L	-

Table 6.5.2: Comparison of GASP Study Population Demographics with Other UK Asthma Study Cohorts. Study 1 = severe asthma patients recruited for the U-BIOPRED (Unbiased BIOmarkers in PREDiction of respiratory disease outcomes) study (Shaw, Sousa *et al*. 2015); Study 2 = asthma patients assessed For serum IgE levels (Liang, Willis-Owen *et al*. 2015); and Study 3 = asthma cohort used to predict asthma exacerbations (Price, Wilson *et al*. 2016). '-' data not available. Data presented with SD (standard deviation) or range; ku/L = kilo units per litre; IU-Ml-1 = international units per ml; IU/L = international units per litre.

Table 6.5.2 is a comparison of the GASP study cohort with the subjects used in the Barton *et al* linkage and association study which identified *PLAUR* SNPs that were associated with lung function, asthma risk and atopy (see Table 6.1.1). Our data does not support a significant role for *PLAUR* SNPs in contributing to lung function, IgE levels, eosinophil count or atopy in asthma. The differences in study design and in the population used, for example the GASP cohort is enriched for severe asthma patients, may in part account for the lack of association observed in these analyses. Another limitation of this study is the absence of an independent replication sample.

	GASP	Study 4 Nottingham			Study 4 Southampton			
		Pedigrees	Sibling 1	Sibling 2	Pedigrees	Sibling 1	Sibling 2	Controls
Subject *n*	2536	184	46	46	1508	341	328	184
Age - mean (SD)	48 (16)	27.8 (17.0)	15.2 (8.8)	13.0 (9.8)	24.6 (15.2)	13.0 (3.4)	9.9 (3.1)	42.3 (10.6)
Gender (% female)	64	27.8 (17.0)	15.2 (8.8)	13.0 (9.8)	24.6 (15.2)	13.0 (3.4)	9.9 (3.1)	42.3 (10.6)
FEV_1 (%Predicted) (SD)	77.2 (23.4)	ND	100.35 (19.79)	101.26 (14.69)	98.05 (14.96)	94.74 (14.88)	95.62 (14.71)	ND
FEV_1/FVC (SD)	0.69 (0.14)	ND	0.88 (0.66)	0.88 (0.87)	ND	ND	ND	ND
Doctor-diagnosed asthma (%)	100	ND	100	100	60.1	100	100	0

Table 6.5.3: Comparison of GASP Study Population Demographics with Asthma Families used for Linkage and Association Analyses of Chromosome 19q13.1-3.

Trait	SNP	MAF	GASP Cohort Power Calculation
Atopy	rs2239372	0.49	99%
	rs380442	0.09	99%
	rs366489	0.09	99%

Table 6.5.4: Power Calculations for Association Analyses of *PLAUR* SNPs associated with atopy ($p<0.05$, MAF >0.05). Calculations tests whether quality controlled genotyping data is powered to detect variation in levels of phenotypes tested due to changes in SNP genotype via association tests. MAF=Minor Allele Frequency for the analysed population.

The present analysis did not identify an association with the FEV_1, FEV_1/FVC, blood eosinophil levels or serum IgE levels, which may have been due to insufficient power. 8 of the *PLAUR* SNPs associations identified in this study (p <0.05), including some which have been associated with asthma related traits, had a MAF <0.05 and associations are likely to be driven by low numbers (see Table 6.5.4). However, power calculations for rs2239372 (atopy), rs380442 (atopy) and rs366489 (atopy) identified a >99% power statistic for these SNPs. Association analyses were carried out using the additive model, this model has reasonable power to detect both additive and dominant effects, but it is important to note that it may be underpowered to detect some recessive effects (Bush 2012).

The current genetic analysis of *PLAUR* SNPs did not show that *PLAUR* is associated with lung function, IgE or eosinophil levels and showed nominal association with atopy in a severe asthma population, however power analysis suggests that sample sizes for the traits measured were underpowered.

Chapter 7: General Discussion

7 General Discussion

7.1 Hypothesis and Aims

The main hypothesis of this thesis was that elevated expression of the urokinase plasminogen activator receptor in the bronchial epithelium in asthma results in altered bronchial epithelial function which contributes to disease. The overall aim of this project was to characterise the expression of uPAR and key interacting proteins in the bronchial epithelium and to investigate the effects of elevated uPAR expression on bronchial epithelial cell function. In asthma, chronic damage of the epithelium is thought to play a role in airway remodelling (Davies, 2009) and epithelial cells exhibit impaired signalling and repair processes (Roth *et al*., 2012). Structural changes to the epithelium include increased fragility and permeability which may increase susceptibility to environmental stimuli and inappropriate immune cell activation (Davies, 2014). The exact mechanisms of how epithelial damage may contribute to airway hyper-responsiveness are not known (Bai and Knight, 2005).

uPAR levels are elevated in a number of airway diseases including asthma and expression is associated with disease severity (Grove *et al*., 2014, Wang *et al*., 2013, Stewart *et al*., 2012, Chu *et al*., 2006, Portelli *et al*., 2016). Multiple forms of the receptor, including membrane-bound and soluble variants, are expressed by the airway epithelium and have been shown to regulate proteolytic activity and cell proliferation in HBEC (Portelli *et al*., 2015). Genetics studies have identified *PLAUR* SNPs associated with asthma susceptibility, uPAR levels and lung function (Barton *et al*., 2009) and elevated levels are associated with non-atopic severe subphenotype of asthma (Portelli *et al*., 2016). Together these observations provide

accumulating evidence that elevated uPAR levels may contribute to airway remodelling in respiratory disease, particularly in a subset of asthma. Whether elevated uPAR levels are retained in the airway epithelium in asthma or increased in response to signalling, injury or inflammation remains unclear. Furthermore, the role of different receptor forms in HBEC function are not fully understood.

Therefore, the main aims of the thesis were to:

- Characterise the expression profile of the uPAR and key interacting proteins in the ALI model of the airway epithelium and to investigate the role of the uPAR-uPA pathway in the formation and maintenance of a bronchial epithelial barrier.
- Investigate gene expression patterns in cultured bronchial epithelial cells isolated from the airways of moderate to severe asthma patients and healthy control subjects and assess the relative expression and activity of the uPA-uPAR pathway in these cells.
- Determine the effect of elevated membrane uPAR (muPAR), a soluble-spliced variant (ssuPAR) and a soluble cleaved variant (scuPAR) on bronchial epithelial cell homeostasis using whole transcriptome analysis.
- Define the relative contribution of genetic polymorphisms spanning the PLAUR gene to clinical features of asthma including FEV_1, FEV_1/FVC, atopy, total serum IgE levels and blood eosinophils, as a means to understand the role of uPAR in this specific group of moderate to severe asthma patients.

7.2 Main Findings

The current data show that uPAR is differentially expressed during bronchial epithelial cell differentiation and that peak expression of uPAR correlates with epithelial barrier properties of the forming epithelial layer. uPAR expression correlated with ligand and downstream effectors including uPA and MMP-9, respectively. The potential role of uPAR as a modulator of epithelial barrier properties was replicated using an alternative technique, ECIS. These observations lead to the hypothesis that elevated uPAR expression as is seen in the epithelium of asthma patients may attenuate barrier function. Blocking specific uPAR epitopes improved epithelial barrier properties providing proof of concept that targeting uPAR may be a therapeutic approach in asthma. I have also shown that uPAR gene expression is elevated in airway epithelial cells from asthma patients compared to healthy subjects. Cells were cultured indicating altered expression of uPAR may be an intrinsic feature of these cells and that increased uPAR expression may play a role in epithelial homeostasis in asthma. Transcriptomic analysis confirmed that elevated expression of multiple uPAR isoforms alters HBEC function and gene expression patterns indicated that isoforms have distinct as well as overlapping roles in these cells. Soluble forms of uPAR were found to regulate and interact with a number of cell signalling pathways involved in cell growth and repair and immune regulation and the membrane bound receptor largely affected molecules involved in ECM interaction. This analysis provides insight into the potential mechanisms driven by elevated uPAR expression in the epithelium in asthma. The mechanisms for complex diseases such as asthma can be investigated using GWAS. In a population enriched for severe asthma we did not identify an association between *PLAUR* genetic variants and clinical features of asthma. Over 350 *PLAUR* SNPs were tested and were not associated with lung function measures (FEV_1 and FEV_1/FVC), atopy, IgE or blood eosinophil counts.

Barrier function studies presented in this thesis suggest a potential mechanism that elevated scuPAR impairs epithelial barrier function and acts via MMP-9 (Slater *et al*., 2016) and for the first time demonstrates that blocking uPAR increases epithelial barrier integrity. scuPAR and MMP-9 expression are associated with airway remodelling (Bégin and Nadeau, 2014, Wang *et al*., 2013) which is argued to contribute to the development of structural changes to the epithelium in asthma (Holgate, 2008). The epithelial barrier is defective in asthma and exhibits abnormal TJ expression (Grainge and Davies, 2013), a compromised barrier may allow the passage of allergens and stimuli across the barrier contributing to BHR in asthma (Holgate, 2008). The observation that elevated scuPAR may result in defective epithelial barrier properties and that blocking the receptor enhances barrier function could have clinical implications in asthma and other respiratory diseases. Anti-uPAR ATN-658 inhibits cell proliferation and migration in pancreatic cancer and acts by specifically blocking uPAR-a5β1 binding (Rabbani *et al*., 2010), in HBEC this monoclonal antibody enhances barrier properties and attenuates cell migration. uPAR regulation of epithelial barrier properties and also adhesion properties may involve signalling via integrins initiated by interaction with both scuPAR and muPAR. Both receptor forms interact with the same ligands and scuPAR can block muPAR binding its ligands (Montuori *et al*., 2016, Smith and Marshall, 2010). The current study and others show that the role of scuPAR is beyond that of a simple decoy receptor and that altered expression in asthma has implications for epithelial function.

This thesis identified that total uPAR mRNA levels are elevated in bronchial epithelial cells isolated from asthma patients compared to healthy subjects. Expression of uPAR and plasminogen pathway components are also elevated in inflammatory cells in sputum in asthma (Xiao *et al*., 2005) and are induced in response to bronchoconstriction (Chu *et al*., 2006). This novel finding supports the hypothesis that elevated uPAR expression in the

bronchial epithelium may play a role in asthma (Stewart *et al*., 2012). RNA-Seq analysis of cultured asthma HBEC identified genes previously implicated in asthma including *IL1RL1, IL18R1, NOS1, CXCL5, HLA-DPA1, HLA-DPB1* and *TJP1* which were elevated in asthma cells. *IL1RL1, IL18R1* and *HLA* loci have been identified as asthma susceptibility loci (Moffatt *et al*., 2010) and *CXCL5* is elevated during acute exacerbations (Koltsova and Ley, 2010), the current study has found that the expression of genes associated with asthma are intrinsically altered in the asthmatic epithelium. *TJP1* expression is reduced in atopic asthma and reduced TJ expression contributes to a defective epithelial barrier (de Boer *et al*., 2008; Davies, 2014). The finding in the current study that *TJP1* is elevated in cultured epithelial cells from asthma patients contradicts these findings however supports the notion that TJ expression is altered in asthma (Davies, 2014). Th2 signature genes *POSTN, SERPINB2* and *CLCA1* were not differentially expressed in cultured asthma HBEC. Similar studies profiling freshly isolated epithelial cells have found that these genes are elevated in asthma and serve as a signature for IL-13 driven type 2 inflammation (Woodruff *et al*., 2007; Nicodemus-Johnson *et al*., 2016). An explanation may be that this signature is not retained in cultured cells as they have been removed from the inflammatory environment of the airways. Differential gene expression analysis found that genes encoding proteins required for cell division and gene transcription were downregulated in asthma and genes associated with cell proliferation, migration and cell signalling were elevated. Overall, more pathways were enriched, upregulated pathways were related to cell proliferation, immune processes, signalling as well development and differentiation. Our findings support the hypothesis that epithelial repair and regeneration as well as cross-talk with immune cells are aberrant in asthma (Roth et al., 2012; Barnig and Levy, 2015). Differences in *PLAUR* expression levels measured by RNA-Seq and qPCR likely due to the detection of different isoforms and also differences in normalisation methods

between the two techniques. Previous data showing uPAR expression is elevated in the epithelium suggest that elevated levels may play a role in disease (Portelli et al., 2016).

Global gene expression changes in HBEC engineered to overexpress different receptor forms were investigated using RNA-Seq. Two methods collectively identified 52 genes regulated by scuPAR, 102 by ssuPAR and 62 by muPAR. Pathway analysis provides evidence that ssuPAR primarily acts by suppressing gene expression and acts on interferon response pathways, suggesting a possible role for this receptor in the epithelium during viral infections. Reduced expression of interferons is likely to predispose to allergy and asthma (Kloepfer and Gern, 2010), elevated ssuPAR may therefore contribute to exacerbation via suppression of viral response genes. scuPAR regulates pathways related to pro-inflammatory signalling and elevated levels of scuPAR may promote neutrophil recruitment and activation via induction of IL-8. Although muPAR-enriched pathways consisted of gene transcription and translation and downregulated pathways were related to heparin (HS) and chondroitin sulfate (CS) synthesis. Downregulation of these genes is likely to interfere signalling which occurs via cell-ECM and cell-cell interaction necessary for cell homeostasis (Schuger et al., 1996; Shannon et al., 2003).

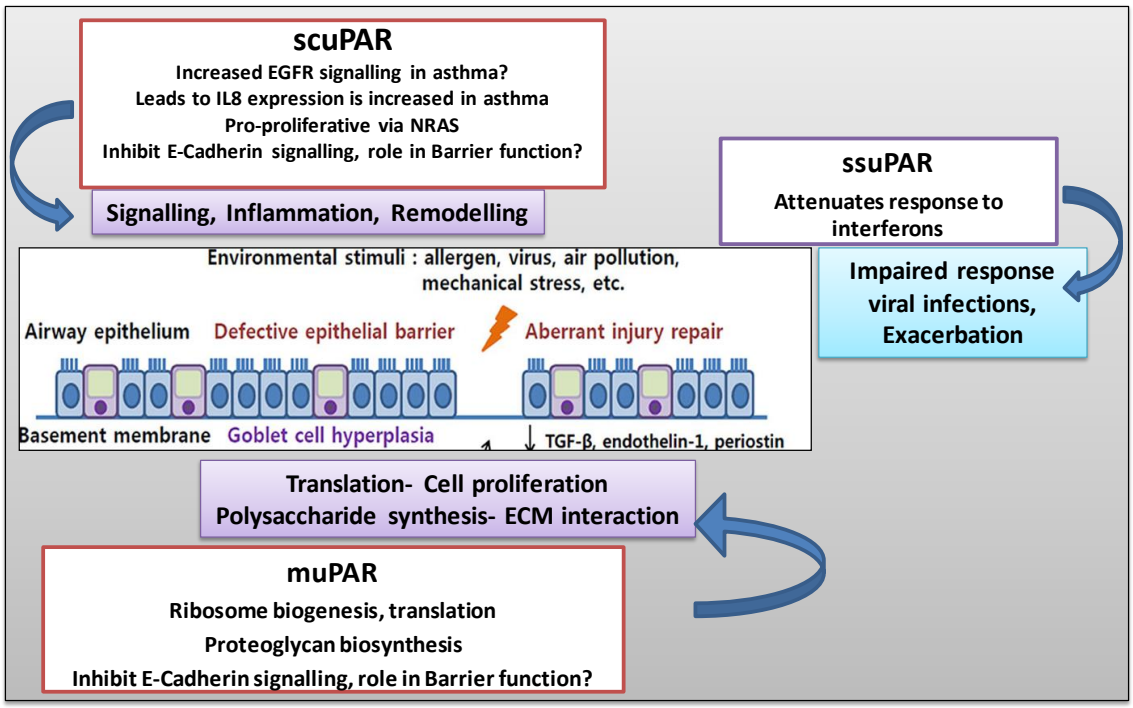


Figure 7.2.1: Summary of Novel Functions Regulated by uPAR in the Bronchial Epithelium based in RNA-Seq whole transcriptome analysis. IL-8 = interleukin 8; EGFR = Epidermal growth factor receptor; NRAS = Neuroblastoma RAS Viral Oncogene

Both muPAR and scuPAR suppress genes inhibited by the tight junction protein E-Cadherin which may have implications for epithelial barrier function (Heijink *et al*., 2007). Interestingly, functions downregulated by both soluble forms of uPAR were related to inflammatory and blood disorders. Soluble uPAR has been proposed as a biomarker for systemic lupus erythematosus and anemia (Enocsson *et al*., 2015), the effects of uPAR on blood cells are not fully understood. In summary, RNA-Seq not only identified potential novel functions of uPAR but also identified pathways which may be regulated by multiple forms of the receptor. Elevated uPAR levels may initiate inappropriate signalling and cell activity that may underlie some of the functional and structural changes in the epithelium that we see in asthma (see Figure 7.2.1). Regarding the methodology used, our findings highlight the strength of using multiple analysis tools to dissect patterns in complex gene expression data. Sequencing technologies provide a powerful tool to identify global changes in gene

expression to help identify gene function however findings ultimately require further study in relevant biological models.

A fundamental question regarding uPAR expression in the airway epithelium in asthma remains unclear- are elevated levels a result of genetic or environmental factors or a combination of both? *PLAUR* SNPs in the 5' region of the gene have been associated with serum/ plasma uPAR levels (Barton *et al*., 2009) as well as asthma risk and lung function. In a novel cohort enriched for severe asthma patients (GASP), *PLAUR* genetic polymorphisms were tested for association with asthma presentation as well as clinical features of asthma (FEV_1, FEV_1/FVC, Atopy, Total serum IgE levels and Blood Eosinophils). *PLAUR* variants previously associated with asthma and with serum/ plasma uPAR levels were also investigated in the analyses. This study did not identify polymorphisms significantly associated with traits measured and does not show clear evidence that genetics drive the presentation of these clinical measure within the asthma population tested. Although our findings provide relatively weak genetic evidence, elevated *PLAUR* expression is associated with asthma that presents as severe and non-atopic (Portelli *et al*., 2016), these findings warrant further investigation of *PLAUR* variants in suitably designed and well characterised populations.

7.3 Limitations of the Study

The initial observation of the relationship between uPAR and epithelial resistance was identified in differentiated ALI cultures. A limitation of the current study was that experiments blocking uPAR were not performed using basal undifferentiated cells. However,

ALI-barrier function and ECIS-blocking experiments identified the same trends in four primary HBEC donors and methods are able to quantify bronchial epithelial resistance. A second limitation is that blocking antibodies were used to suppress uPAR activity, whereas gene knockdown may serve as a more precise method. However, blocking specific epitopes meant we could identify key ligand interactions. A third limitation is that initial studies used healthy cells therefore results may not be directly translated to epithelial dysfunction in asthma. Another criticism of the study design may be that *in vitro* cell culture methods were used rather than *in vivo* models such us the lung explant, which better represents the complex environment of the lung. As our study focused to the role of uPAR in bronchial epithelial function both the ALI and ECIS models were considered appropriate.

When studying gene expression in epithelial cells from asthma patients a possible limitation is that cells were cultured (passage 2/3) whereas other studies have used freshly isolated cells or biopsy samples. As a result, our analyses may not capture changes in gene expression induced by the environment of the asthmatic airway (e.g. genes induced by inflammation, tissue injury, and environmental stimuli) and those specific to specialised differentiated cells. Cultured cells were used to identify inherent changes in epithelial function which may provide insight into the underlying biology of asthma. Furthermore, freshly isolated cells may incur damage as a result of the bronchoscopy procedure activating pathways associated with inflammation and injury. A drawback of next generation sequencing is that various biases can be introduced during sample preparation, transcript quantification and differential gene expression analysis. To overcome this, it is common practice to use quality control tools such as FastQC to assess read quality. Problematic sequencing data was trimmed to remove adaptor sequences and low quality reads to improve mapping. Transcript quantification and differential gene expression analysis were carried out using Cufflinks which, like other

programmes, normalizes raw read counts to remove possible biases. RNA-Seq and qPCR found PLAUR levels to be elevated in asthma HBEC compared to healthy controls, this was significant only when measured by PCR. RNA-Seq provides an absolute quantification of gene expression compared to relative expression as measured by qPCR. Reasons for a lack of correlation between RNA-Seq and qPCR can result from differences in normalisation methods, FPKM values are log transformed to overcome biases in the data.

When validating genes regulated by ssuPAR, scuPAR and muPAR we also found that a number of genes identified in RNA-Seq in analysis did not show the same pattern of expression when quantified using qPCR. For this dataset, the most notable limitation was inter and intra donor variation, to address this issue PCA analysis was performed using data from raw reads and trimmed reads. Trimming the reads greatly improved the quality of the data, furthermore two methods were used to identify DE genes. As a result, we were able to validate differentially expressed genes for each receptor variant. A common approach to identifying gene function is by silencing gene expression, uPAR however is elevated in the airways in asthma therefore the genes for different uPAR variants were overexpressed in epithelial cells to mimic what may be occurring physiologically.

Our investigation of *PLAUR* genetic associations with asthma and clinical features related to asthma was limited by a number of factors. Firstly, power calculations highlighted that association analysis may have been underpowered for the SNPs tested. Lack of power may result in false negatives (type II error). This may explain why *PLAUR* SNPs that have been previously associated with the clinical traits tested did not meet statistical significance in our analysis. A second limitation is that results were not investigated in an independent population, therefore we cannot comment on the reproducibility of these analyses.

7.4 Future Directions

Future work will focus towards the key question, “can uPAR be targeted to improve barrier properties of the epithelium in asthma?”. Functional studies using asthma cells cultured at air liquid interface will enable a better assessment of the relationship between uPAR and epithelial barrier function in disease. Cultured cells have been shown to exhibit impaired barrier function and altered tight junction expression *in vitro* (Xiao *et al*., 2011). Further characterisation of the uPAR-uPA pathway in asthmatic airway epithelial cells in response to allergens such as HDM and RV-16 and also blocking via specific antibodies such as ATN-658 will better conclude whether this pathway can be targeted to improve barrier function. This work will also require investigation of the effects of uPAR pathway activity on proteolytic enzymes such as MMP-9 and also on TJP expression and localization. Clinically, the effects of an impaired epithelial barrier are not known however it may play a role in allergic sensitization and virus-induced exacerbation (Rowe and Gill, 2017). In light of our findings that elevated ssuPAR may suppress genes induced in response to viral infections, the role of ssuPAR in barrier function should also be explored.

RNA-Seq analysis identifying uPAR function in HBEC requires further validation, the potential regulation of certain signalling pathways and cellular processes must be investigated before a conclusion can be drawn on the function of the different receptor types. scuPAR increased TNF-α and IL-6 signalling and also IL-8 expression, co-culture assays with immune cells would allow the effects of elevated signalling on inflammatory cells to be investigated. muPAR regulation of proteoglycan molecules may play role in regulating cell adhesion, a process uPAR has been long associated with, this may have more relevance in cancer biology however will ultimately add to our understanding of uPAR function in the epithelium. Finally,

pathway analysis provided evidence that soluble-spliced uPAR may interfere with the epithelium's ability to respond to viral infections. Further investigation of the relationship between ssuPAR expression and viral response genes in normal and disease airway epithelial cells is needed. Additional bioinformatics analysis is also required to determine whether phenotypes driven by elevated uPAR are also present in the epithelium in asthma or asthma subtypes. Validation of RNA-Seq differential gene expression and pathway analysis of cultured patient epithelial cells must be completed as findings from the current study are only preliminary. Future studies should also incorporate genetic, epigenetic and proteomic analysis of matched epithelial cells that are freshly isolated and cultured, to identify the key pathways that are inherently altered in asthma and underlie epithelial dysfunction.

7.5 Final Conclusion

The findings presented in this thesis provide further evidence that expression of the urokinase plasminogen activator receptor in the bronchial epithelium in asthma is elevated and that aberrant expression is associated with barrier function and airway remodelling, which are recognised as key drivers of asthma pathogenesis (Davies, 2009, Georas and Rezaee, 2014). Elevated expression of uPAR in asthma has previously been described, our observation that elevated levels are retained in the epithelium is novel and importantly suggests that uPAR expression is inherently altered in these cells. It is likely that uPAR function in 'normal' cells maintains bronchial epithelial barrier function and repair, and may also play a role in the regulation of immune cells in the airways. The current *in vitro* data argue that increased scuPAR expression impairs barrier integrity of the epithelium and that the pathway may act via MMP-9, which has been shown to modulate TJPs (Vermeer *et al*.,

2009). This study has also demonstrated for the first time that blocking uPAR increases epithelial resistance and that this may act via suppression of α5β1 integrin signalling.

Increased expression may result from both genetic and environmental factors. Expression of soluble-cleaved uPAR is a marker of various inflammatory disorders (Enocsson *et al*., 2015), in asthma the pro-inflammatory and proteolytic environment of the airways may play a role in elevated levels of soluble forms. Although we did not observe a relationship between *PLAUR* SNPs and asthma features in a severe asthma population, polymorphisms have shown association with asthma, atopy and lung function in linkage association analyses (Barton *et al*., 2009). RNA-Seq analysis of cultured epithelial cells from moderate to severe asthma patients has also provided insight into the mechanisms underlying epithelial dysfunction. More novel pathways include those that regulate fatty acid metabolism, it has been hypothesised that fatty acids contribute to inflammation in asthma (Wendell *et al*., 2014). Genes related to EMT, TGF-β and EGFR signalling were upregulated in cultured asthma HBEC and have been associated with airway remodelling in asthma.

In conclusion, the work presented in this thesis supports the hypothesis that elevated uPAR impairs bronchial epithelial cell function, promotes airway remodelling and is potential therapeutic target in asthma.

8 Appendices

8.1 Appendix 1: Materials and Reagents

General Materials (list)

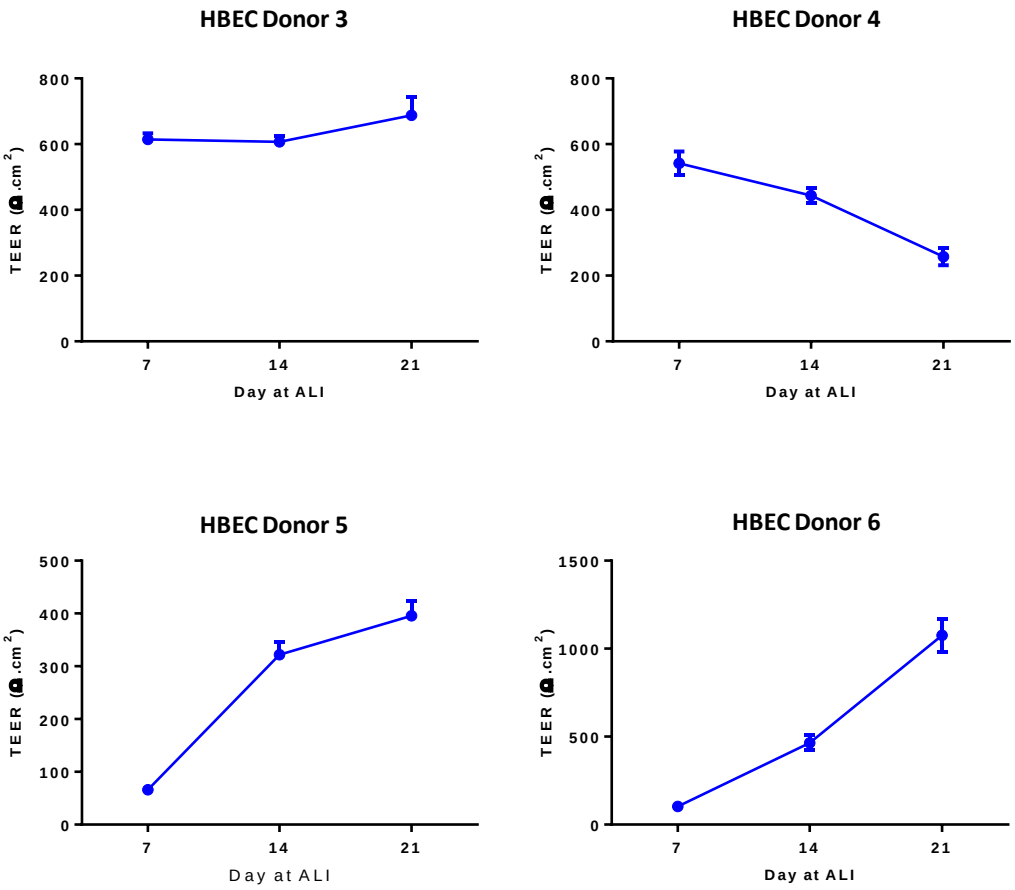
Item	Supplier
1Kb+ DNA ladder	ThermoFisher, 10787-018
Agarose	Invitrogen, 16500500
Agilent QPCR 96-Well plates	Netascientific, 410021
Agilent Mx4000 8-Cap Strips	Netascientific, 410024
Ampicillin	Sigma-Aldrich, A-9518
Bioanalyzer 2100	Agilent
Bio-Plex 200	BioRad
Bovine Serum Albumin (BSA)	Millipore, 820452
DEPC treated water	ThermoFisher, 750024
Dimethyl Sulphoxide (DMSO)	Sigma, 1304
dNTPs	Bioline, BIO 39026
Endotoxin Free Water	Sigma-Aldrich, 2107
Eosin	Sigma-Aldrich, HT110316
Ethanol	University of Nootingham Stores, LH-M0120E
Ethidium Bromide	ThermoFisher, 15585-011
Flexstation 3 microplate reader	Molecular Devices
Gene Genius Gel Doc system	Syngene
GenElute Mammalian Total RNA Purification Kit	Sigma-Aldrich, RTN70
Glycerol	ThermoFisher, BPE299-1
Goat anti Mouse Ig FITC secondary	Sigma-Aldrich, F0257
Goat Serum	Sigma-Aldrich, G6767
Haemotoxylin	Sigma-Aldrich, 51275
Histoclear	ThermoFisher, H/0472/17
House Dust Mite (Dermatophagoides pteronyssinus)	Greer Labs, XPB70D3A25
Human MMP-9 Duoset ELISA	R&D Systems, DY911
Human uPA Duoset ELISA	R&D Systems, DY1310
Human uPAR Duoset ELISA	R&D Systems, DY807
Improvision Spinning Disk Confocal Microscope	Zeiss
Isopropanol	BDH, 10224
Item	Supplier

LB Agar, Miller	ThermoFisher, BPE1425-500
LB Broth, Miller	ThermoFisher, BPE1426-500
MAX Efficiency® DH5αTM T1R Competent Cells	ThermoFisher, 12297-016
Mouse anti 1B10 fibroblast monoclonal IgM	Abcam, AB11333
Mouse anti Cytokeratin 14 monoclonal IgG	Chemicon, MAB3232
Mouse anti Human E-Cadherin (clone 67A4) monoclonal IgG	Millipore, MAB3199Z
Mouse Anti-uPAR Clone R3	ThermoFisher, MON R-3-02
Mouse Anti-uPAR Clone R4	ThermoFisher, MON R-4-02
Mouse IgG1 isotype	Sigma, M7894
Mouse IgM isotype	Abcam, AB18400
Mx3005P qPCR System	Agilent
Nanodrop 2000c UV/IV Spectrophotometer	Thermo Scientific
Orange G dye	Sigma-Aldrich, O-1625
Plasmin Activity Assay Kit	AS-72124
Platinum Taq High Fidelity DNA polymerase	ThermoFisher, 11304-011
PrimeG Thermal Cycler	Techne
QIAPrep® Spin Miniprep Kit	Qiagen, 27106
Recombinant Human uPAR Protein	R&D Systems, 807-UK-100
Recombinant human urokinase Protein	R&D Systems 1310-SE-010
RNase Away	ThermoFisher, 10594063
RNase-Free DNase Set	Qiagen
Gallenkamp Heated Orbital Incubator	Sanyo
SensoLyte® AFC Plasmin Activity Assay Kit	Eurogentec, AS-72124
ß-mercaptoethanol	Sigma-Aldrich, M6250
Sulphuric Acid (2N)	SLS, CHE3688
Superscript™ First-Strand Synthesis System for RT-PCR kit	ThermoFisher, 11904018
Taq DNA Polymerase	ThermoFisher, 18038-026
TaqMan® Universal PCR Master Mix (2x)	ThermoFisher, 10525395
Taqman 96 well plate and strips	Netascientific, 410021 AND 410024
Triton X-100	Sigma-Aldrich, X-100
Trypsin Inhibitor	ThermoFisher, 17075-029
Trypsin-EDTA solution (1x)	Sigma-Aldrich, T3924-500ML
Tween® 20	Sigma-Aldrich, P-1379
VectaMount Permanent Mounting Medium	Vector labs H-5000
VectaShield™ Hard+Set Mounting Media with DAPI	Vector Laboratories, H-1500
96 well assay plate	Corning, 9107

Mammalian cells and cell culture material (list)

Item	**Supplier**
100 mM Sodium Pyruvate solution	ThermoFisher, 11360-039
200 mM L-Glutamine solution	ThermoFisher, 25030-024
All-trans Retinoic Acid	Sigma-Aldrich, R2625
BEGM Basal Medium	Lonza, CC-3171
2ml 13 mg/ml bovine pituitary extract 0.5ml mg/ml hydrocortisone 0.5 ml 0.5 µg/ml human recombinant epidermal growth factor 0.5 ml 0.5 mg/ml epinephrine 0.5 ml 10 mg/ml transferrin 0.5 ml 5 mg/ml insulin 0.5 ml 0.1 µg/ml retinoic acid 0.5 ml 6.5 µg/ml triiodothyronine 0.5 ml 50µg/ml gentamicin/amphotericin B	Lonza, CC-3170
Chamber well slides (1.7cm2)	BD Falcon, 354114
DMEM high glucose culture medium	ThermoFisher, 11960-085
Dulbecco's PBS with Ca + Mg phosphate buffered saline	Sigma-Aldrich, D8662
ECIS 8W10E PET array	IBIDI, 72010
HBEC (primary cells; Donors 195307, 124040, 355687, 369144)	Lonza, CC-2540
Non-essential Amino Acids (x100)	ThermoFisher, 11140-035
Penicillin/Streptomycin/Fungizone	Sigma-Aldrich, A-5955
PureCol Type 1 Bovine Collagen Solution	Advanced BioMatrix, 5005-B
Transwell® 6.5mm with 0.4µm Pore Polyester Membrane Insert for 24-well plates	Corning, 3470
Vented 75cm tissue culture flasks	Corning, 430641

8.2 Appendix 2: Individual TEER profiles for HBEC donors



TEER profiles of HBEC Donors 3 (195307), 4 (124040), 5 (355687), 6 (369144) from day 7 to 21 ALI.

8.3 Appendix 3: Assay detection ranges of analytes measured using Luminex

8.3.1 Chemokine and Cytokine Assay Ranges

Analyte	Standard curve range (pg/mL)
IL-8/CXCL8	17.7-7,310
MIP-1α/CCL3	314-25,440
MIP-1β/CCL4	145-11,720
MDC/CCL22	58.0-14,100
GM-CSF	27.2-6,610
VEGF	8.12-1,970
IL-4	16.9-4,100
IL-6	20.1-4,880
IL-10	14.8-3,600
TNF- α	19.8-4,800
IL-1β	10.0-2,430
IL-2	28.5-6,920
IL-17A	18.6-4,530
MCP-4/CCL13	6.17-1,500
MCP-1/CCL2	43.5-3,520
IL-12 p70	249-60,540
Eotaxin/CCL11	123-29,800
Eotaxin-3/CCL26	27.7-6,740
IFN-γ	18.9-1,530
IL-5	15.8-3,830
TARC/CCL17	94.2-22,900

8.3.2 scuPAR, PAI-1 and uPA Luminex Assay Ranges

Analyte	Standard curve range (pg/mL)
scuPAR	103000 – 1609 pg/ml
PAI-1	48900 - 760 pg/ml
uPA	32200 – 503 pg/ml

9 References

Global Initiative for Asthma Guidelines 2016.

ACEVEDO, N., REINIUS, L. E., GRECO, D., GREF, A., ORSMARK-PIETRAS, C., PERSSON, H., PERSHAGEN, G., HEDLIN, G., MELÉN, E., SCHEYNIUS, A., KERE, J. & SÖDERHÄLL, C. 2015. Risk of childhood asthma is associated with CpG-site polymorphisms, regional DNA methylation and mRNA levels at the GSDMB/ORMDL3 locus. *Hum Mol Genet,* 24**,** 875-90.

AITKEN, M. L., VILLALON, M., VERDUGO, P. & NAMEROFF, M. 1991. Enrichment of subpopulations of respiratory epithelial cells using flow cytometry. *Am J Respir Cell Mol Biol,* 4**,** 174-8.

AL-MUHSEN, S., JOHNSON, J. R. & HAMID, Q. 2011. Remodeling in asthma. *J Allergy Clin Immunol,* 128**,** 451-62; quiz 463-4.

ALLGAYER, H. 2010. Translational research on u-PAR. *Eur J Cancer,* 46**,** 1241-51.

ALMASI, C. E., HØYER-HANSEN, G., CHRISTENSEN, I. J. & PAPPOT, H. 2009. Prognostic significance of urokinase plasminogen activator receptor and its cleaved forms in blood from patients with non-small cell lung cancer. *APMIS,* 117**,** 755-61.

ANTHONY JF GRIFFITHS, J. H. M., DAVID T SUZUKI, RICHARD C LEWONTIN, AND WILLIAM M GELBART 2000. *An Introduction to Genetic Analysis. 7th edition.*, W.H. Freeman.

AOSHIBA, K. & NAGAI, A. 2004. Differences in airway remodeling between asthma and chronic obstructive pulmonary disease. *Clin Rev Allergy Immunol,* 27**,** 35-43.

BAI, J., SMOCK, S. L., JACKSON, G. R., MACISAAC, K. D., HUANG, Y., MANKUS, C., OLDACH, J., ROBERTS, B., MA, Y. L., KLAPPENBACH, J. A., CRACKOWER, M. A., ALVES, S. E. & HAYDEN, P. J. 2015. Phenotypic responses of differentiated asthmatic human airway epithelial cultures to rhinovirus. *PLoS One,* 10**,** e0118286.

BARNIG, C. & LEVY, B. D. 2015. Innate immunity is a key factor for the resolution of inflammation in asthma. *Eur Respir Rev,* 24**,** 141-53.

BARTON SJ, K. G., VONK JM, BROWNING CA, NOLTE IM, STEWART CE, BAINBRIDGE S, MUTCH S, ROSE-ZERILLI MJ, POSTMA DS, MANIATIS N, HENRY AP, HALL IP, HOLGATE ST, TIGHE P, HOLLOWAY JW, SAYERS I. 2009. PLAUR polymorphisms are associated with asthma, PLAUR levels, and lung function decline. *J Allergy Clin Immunol*.

BARTON, S. J., KOPPELMAN, G. H., VONK, J. M., BROWNING, C. A., NOLTE, I. M., STEWART, C. E., BAINBRIDGE, S., MUTCH, S., ROSE-ZERILLI, M. J., POSTMA, D. S., MANIATIS, N., HENRY, A. P., HALL, I. P., HOLGATE, S. T., TIGHE, P., HOLLOWAY, J. W. & SAYERS, I. 2009. PLAUR polymorphisms

are associated with asthma, PLAUR levels, and lung function decline. *J Allergy Clin Immunol,* 123**,** 1391-400.e17.

BAXI, S. N. & PHIPATANAKUL, W. 2010. The role of allergen exposure and avoidance in asthma. *Adolesc Med State Art Rev,* 21**,** 57-71, viii-ix.

BEAUFORT, N., LEDUC, D., ROUSSELLE, J. C., MAGDOLEN, V., LUTHER, T., NAMANE, A., CHIGNARD, M. & PIDARD, D. 2004. Proteolytic regulation of the urokinase receptor/CD87 on monocytic cells by neutrophil elastase and cathepsin G. *J Immunol,* 172**,** 540-9.

BERAIR, R., SAUNDERS, R. & BRIGHTLING, C. E. 2013. Origins of increased airway smooth muscle mass in asthma. *BMC Med,* 11**,** 145.

BERGELSON, J. M. 2009. Intercellular junctional proteins as receptors and barriers to virus infection and spread. *Cell Host Microbe,* 5**,** 517-21.

BERGERON, C., TULIC, M. K. & HAMID, Q. 2010. Airway remodelling in asthma: from benchside to clinical practice. *Can Respir J,* 17**,** e85-93.

BLASI, F. & CARMELIET, P. 2002. uPAR: a versatile signalling orchestrator. *Nat Rev Mol Cell Biol,* 3**,** 932-43.

BLASI, F. & SIDENIUS, N. 2010. The urokinase receptor: focused cell surface proteolysis, cell adhesion and signaling. *FEBS Lett,* 584**,** 1923-30.

BOERS, J. E., AMBERGEN, A. W. & THUNNISSEN, F. B. 1998. Number and proliferation of basal and parabasal cells in normal human airway epithelium. *Am J Respir Crit Care Med,* 157**,** 2000-6.

BOHADANA, A., TECULESCU, D. & MARTINET, Y. 2004. Mechanisms of chronic airway obstruction in smokers. *Respir Med,* 98**,** 139-51.

BORISH, L. 2016. The immunology of asthma: Asthma phenotypes and their implications for personalized treatment. *Ann Allergy Asthma Immunol,* 117**,** 108-14.

BOSTANTZOGLOU, C., DELIMPOURA, V., SAMITAS, K., ZERVAS, E., KANNIESS, F. & GAGA, M. 2015. Clinical asthma phenotypes in the real world: opportunities and challenges. *Breathe (Sheff),* 11**,** 186-93.

BREITLING, R., ARMENGAUD, P., AMTMANN, A. & HERZYK, P. 2004. Rank products: a simple, yet powerful, new method to detect differentially regulated genes in replicated microarray experiments. *FEBS Letters,* 573**,** 83-92.

BRIMS, F. J., CHAUHAN, A. J., HIGGINS, B. & SHUTE, J. K. 2009. Coagulation factors in the airways in moderate and severe asthma and the effect of inhaled steroids. *Thorax,* 64**,** 1037-43.

BTS/SIGN 2016. British guideline on the management of asthma. British Thoracic Society Scottish Intercollegiate Guidelines, Network.

BUSH 2012. Chapter 11: Genome-Wide Association Studies. *PLOS: Computational Biology*.

BUSSE, W. W., HOLGATE, S., KERWIN, E., CHON, Y., FENG, J., LIN, J. & LIN, S. L. 2013. Randomized, double-blind, placebo-controlled study of

brodalumab, a human anti-IL-17 receptor monoclonal antibody, in moderate to severe asthma. *Am J Respir Crit Care Med,* 188**,** 1294-302.

BÉGIN, P. & NADEAU, K. C. 2014. Epigenetic regulation of asthma and allergic disease. *Allergy Asthma Clin Immunol,* 10**,** 27.

BØNNELYKKE, K. & OBER, C. 2016. Leveraging gene-environment interactions and endotypes for asthma gene discovery. *J Allergy Clin Immunol,* 137**,** 667-79.

BØNNELYKKE, K., SLEIMAN, P., NIELSEN, K., KREINER-MØLLER, E., MERCADER, J. M., BELGRAVE, D., DEN DEKKER, H. T., HUSBY, A., SEVELSTED, A., FAURA-TELLEZ, G., MORTENSEN, L. J., PATERNOSTER, L., FLAATEN, R., MØLGAARD, A., SMART, D. E., THOMSEN, P. F., RASMUSSEN, M. A., BONÀS-GUARCH, S., HOLST, C., NOHR, E. A., YADAV, R., MARCH, M. E., BLICHER, T., LACKIE, P. M., JADDOE, V. W., SIMPSON, A., HOLLOWAY, J. W., DUIJTS, L., CUSTOVIC, A., DAVIES, D. E., TORRENTS, D., GUPTA, R., HOLLEGAARD, M. V., HOUGAARD, D. M., HAKONARSON, H. & BISGAARD, H. 2014. A genome-wide association study identifies CDHR3 as a susceptibility locus for early childhood asthma with severe exacerbations. *Nat Genet,* 46**,** 51-5.

CAMPBELL, A. M., CHANEZ, P., VIGNOLA, A. M., BOUSQUET, J., COURET, I., MICHEL, F. B. & GODARD, P. 1993. Functional characteristics of bronchial epithelium obtained by brushing from asthmatic and normal subjects. *Am Rev Respir Dis,* 147**,** 529-34.

CARR, T. F., BERDNIKOVS, S., SIMON, H. U., BOCHNER, B. S. & ROSENWASSER, L. J. 2016. Eosinophilic bioactivities in severe asthma. *World Allergy Organ J,* 9**,** 21.

CASTELLANI, S., GUERRA, L., FAVIA, M., DI GIOIA, S., CASAVOLA, V. & CONESE, M. 2012. NHERF1 and CFTR restore tight junction organisation and function in cystic fibrosis airway epithelial cells: role of ezrin and the RhoA/ROCK pathway. *Lab Invest,* 92**,** 1527-40.

CESARMAN-MAUS, G. & HAJJAR, K. A. 2005. Molecular mechanisms of fibrinolysis. *Br J Haematol,* 129**,** 307-21.

CHAE, E. J., KIM, T. B., CHO, Y. S., PARK, C. S., SEO, J. B., KIM, N. & MOON, H. B. 2011. Airway Measurement for Airway Remodeling Defined by Post-Bronchodilator FEV1/FVC in Asthma: Investigation Using Inspiration-Expiration Computed Tomography. *Allergy Asthma Immunol Res,* 3**,** 111-7.

CHAMBERS, R. C. & SCOTTON, C. J. 2012. Coagulation cascade proteinases in lung injury and fibrosis. *Proc Am Thorac Soc,* 9**,** 96-101.

CHIN, L. S., RAYNOR, M. C., WEI, X., CHEN, H. Q. & LI, L. 2001. Hrs interacts with sorting nexin 1 and regulates degradation of epidermal growth factor receptor. *J Biol Chem,* 276**,** 7069-78.

CHIOU, S. J., WANG, C. C., TSENG, Y. S., LEE, Y. J., CHEN, S. C., CHOU, C. H., CHUANG, L. Y., HONG, Y. R., LU, C. Y., CHIU, C. C. & CHIGNARD, M. 2016. A novel role for β2-microglobulin: a precursor of antibacterial chemokine in respiratory epithelial cells. *Sci Rep,* 6**,** 31035.

CHU, E. K., CHENG, J., FOLEY, J. S., MECHAM, B. H., OWEN, C. A., HALEY, K. J., MARIANI, T. J., KOHANE, I. S., TSCHUMPERLIN, D. J. & DRAZEN, J. M. 2006. Induction of the plasminogen activator system by mechanical stimulation of human bronchial epithelial cells. *Am J Respir Cell Mol Biol,* 35**,** 628-38.

CHUNG, K. F. 2015. Targeting the interleukin pathway in the treatment of asthma. *Lancet,* 386**,** 1086-96.

CHUNG, K. F. & BARNES, P. J. 1999. Cytokines in asthma. *Thorax,* 54**,** 825-57.

CLIFFORD, R. L., JONES, M. J., MACISAAC, J. L., MCEWEN, L. M., GOODMAN, S. J., MOSTAFAVI, S., KOBOR, M. S. & CARLSTEN, C. 2017. Inhalation of diesel exhaust and allergen alters human bronchial epithelium DNA methylation. *J Allergy Clin Immunol,* 139**,** 112-121.

CONESA, A., MADRIGAL, P., TARAZONA, S., GOMEZ-CABRERO, D., CERVERA, A., MCPHERSON, A., SZCZEŚNIAK, M. W., GAFFNEY, D. J., ELO, L. L., ZHANG, X. & MORTAZAVI, A. 2016. A survey of best practices for RNA-seq data analysis. *Genome Biol,* 17**,** 13.

CONTOLI, M., SANTUS, P. & PAPI, A. 2015. Small airway disease in asthma: pathophysiological and diagnostic considerations. *Curr Opin Pulm Med,* 21**,** 68-73.

CORRIGAN, C. J. 2002. Asthma refractory to glucocorticoids: the role of newer immunosuppressants. *Am J Respir Med,* 1**,** 47-54.

CROSBY, L. M. & WATERS, C. M. 2010. Epithelial repair mechanisms in the lung. *Am J Physiol Lung Cell Mol Physiol,* 298**,** L715-31.

CRYSTAL, R. G., RANDELL, S. H., ENGELHARDT, J. F., VOYNOW, J. & SUNDAY, M. E. 2008. Airway epithelial cells: current concepts and challenges. *Proc Am Thorac Soc,* 5**,** 772-7.

CURRAN, D. R. & COHN, L. 2010. Advances in mucous cell metaplasia: a plug for mucus as a therapeutic focus in chronic airway disease. *Am J Respir Cell Mol Biol,* 42**,** 268-75.

DAVIES, D. E. 2014. Epithelial barrier function and immunity in asthma. *Ann Am Thorac Soc,* 11 Suppl 5**,** S244-51.

DE BOER, W. I., SHARMA, H. S., BAELEMANS, S. M., HOOGSTEDEN, H. C., LAMBRECHT, B. N. & BRAUNSTAHL, G. J. 2008. Altered expression of epithelial junctional proteins in atopic asthma: possible role in inflammation. *Can J Physiol Pharmacol,* 86**,** 105-12.

DE WATER, R., WILLEMS, L. N., VAN MUIJEN, G. N., FRANKEN, C., FRANSEN, J. A., DIJKMAN, J. H. & KRAMPS, J. A. 1986. Ultrastructural localization of bronchial antileukoprotease in central and peripheral human airways by a gold-labeling technique using monoclonal antibodies. *Am Rev Respir Dis,* 133**,** 882-90.

DEGRYSE, B., RESNATI, M., CZEKAY, R. P., LOSKUTOFF, D. J. & BLASI, F. 2005. Domain 2 of the urokinase receptor contains an integrin-interacting epitope with intrinsic signaling activity: generation of a new integrin inhibitor. *J Biol Chem,* 280**,** 24792-803.

DERYUGINA, E. I. & QUIGLEY, J. P. 2012. Cell surface remodeling by plasmin: a new function for an old enzyme. *J Biomed Biotechnol,* 2012**,** 564259.

DINARELLO, C. A. 2010. Anti-inflammatory Agents: Present and Future. *Cell,* 140**,** 935-50.

DOUWES, J., GIBSON, P., PEKKANEN, J. & PEARCE, N. 2002. Non-eosinophilic asthma: importance and possible mechanisms. *Thorax,* 57**,** 643-8.

DURRANI, S. R., VISWANATHAN, R. K. & BUSSE, W. W. 2011. What effect does asthma treatment have on airway remodeling? Current perspectives. *J Allergy Clin Immunol,* 128**,** 439-48; quiz 449-50.

ELIAS, J. A., ZHU, Z., CHUPP, G. & HOMER, R. J. 1999. Airway remodeling in asthma. *J Clin Invest,* 104**,** 1001-6.

ELLIS, V., PYKE, C., ERIKSEN, J., SOLBERG, H. & DANØ, K. 1992. The urokinase receptor: involvement in cell surface proteolysis and cancer invasion. *Ann N Y Acad Sci,* 667**,** 13-31.

ERLE, D. J. & SHEPPARD, D. 2014. The cell biology of asthma. *J Cell Biol,* 205**,** 621-31.

EVANS, M. J. & PLOPPER, C. G. 1988. The role of basal cells in adhesion of columnar epithelium to airway basement membrane. *Am Rev Respir Dis,* 138**,** 481-3.

EXCOFFON, K. J., GUGLIELMI, K. M., WETZEL, J. D., GANSEMER, N. D., CAMPBELL, J. A., DERMODY, T. S. & ZABNER, J. 2008. Reovirus preferentially infects the basolateral surface and is released from the apical surface of polarized human respiratory epithelial cells. *J Infect Dis,* 197**,** 1189-97.

FAHY, J. V. & DICKEY, B. F. 2010. Airway mucus function and dysfunction. *N Engl J Med,* 363**,** 2233-47.

FANG, Z. & CUI, X. 2011. Design and validation issues in RNA-seq experiments. *Brief Bioinform,* 12**,** 280-7.

FAURA TELLEZ, G., WILLEMSE, B. W., BROUWER, U., NIJBOER-BRINKSMA, S., VANDEPOELE, K., NOORDHOEK, J. A., HEIJINK, I., DE VRIES, M., SMITHERS, N. P., POSTMA, D. S., TIMENS, W., WIFFEN, L., VAN ROY, F., HOLLOWAY, J. W., LACKIE, P. M., NAWIJN, M. C. & KOPPELMAN, G. H. 2016. Protocadherin-1 Localization and Cell-Adhesion Function in Airway Epithelial Cells in Asthma. *PLoS One,* 11**,** e0163967.

FEI, Y., WEBB, R., COBB, B. L., DIRESKENELI, H., SARUHAN-DIRESKENELI, G. & SAWALHA, A. H. 2009. Identification of novel genetic susceptibility loci for Behçet's disease using a genome-wide association study. *Arthritis Res Ther,* 11**,** R66.

FERLAND, C., GUILBERT, M., DAVOINE, F., FLAMAND, N., CHAKIR, J. & LAVIOLETTE, M. 2001. Eotaxin promotes eosinophil transmigration via the activation of the plasminogen-plasmin system. *J Leukoc Biol,* 69**,** 772-8.

FERRARIS, G. M., SCHULTE, C., BUTTIGLIONE, V., DE LORENZI, V., PIONTINI, A., GALLUZZI, M., PODESTÀ, A., MADSEN, C. D. & SIDENIUS, N. 2014. The

interaction between uPAR and vitronectin triggers ligand-independent adhesion signalling by integrins. *EMBO J,* 33**,** 2458-72.

FISCHER, A. H., JACOBSON, K. A., ROSE, J. & ZELLER, R. 2008. Hematoxylin and Eosin Staining of Tissue and Cell Sections. *Cold Spring Harbor Protocols,* 2008**,** pdb.prot4986.

FISCHER, H. & WIDDICOMBE, J. H. 2006. Mechanisms of acid and base secretion by the airway epithelium. *J Membr Biol,* 211**,** 139-50.

FORBES, B., SHAH, A., MARTIN, G. P. & LANSLEY, A. B. 2003. The human bronchial epithelial cell line 16HBE14o- as a model system of the airways for studying drug transport. *Int J Pharm,* 257**,** 161-7.

FROEHLICH, J., VERSAPUECH, M., MEGRELIS, L., LARGETEAU, Q., MEUNIER, S., TANCHOT, C., BISMUTH, G., DELON, J. & MANGENEY, M. 2016. FAM65B controls the proliferation of transformed and primary T cells. *Oncotarget,* 7**,** 63215-63225.

FUERST, E., FOSTER, H. R., WARD, J. P., CORRIGAN, C. J., COUSINS, D. J. & WOSZCZEK, G. 2014. Sphingosine-1-phosphate induces pro-remodelling response in airway smooth muscle cells. *Allergy,* 69**,** 1531-9.

GAO, P. S., KAWADA, H., KASAMATSU, T., MAO, X. Q., ROBERTS, M. H., MIYAMOTO, Y., YOSHIMURA, M., SAITOH, Y., YASUE, H., NAKAO, K., ADRA, C. N., KUN, J. F., MORO-OKA, S., INOKO, H., HO, L. P., SHIRAKAWA, T. & HOPKIN, J. M. 2000. Variants of NOS1, NOS2, and NOS3 genes in asthmatics. *Biochem Biophys Res Commun,* 267**,** 761-3.

GASTON, B., DRAZEN, J. M., LOSCALZO, J. & STAMLER, J. S. 1994. The biology of nitrogen oxides in the airways. *Am J Respir Crit Care Med,* 149**,** 538-51.

GAUTHIER, M., RAY, A. & WENZEL, S. E. 2015. Evolving Concepts of Asthma. *Am J Respir Crit Care Med,* 192**,** 660-8.

GEORAS, S. N. & REZAEE, F. 2014. Epithelial barrier function: at the front line of asthma immunology and allergic airway inflammation. *J Allergy Clin Immunol,* 134**,** 509-20.

GIAEVER, I. & KEESE, C. R. 1991. Micromotion of mammalian cells measured electrically. *Proc Natl Acad Sci U S A,* 88**,** 7896-900.

GIAVER, I. & KEESE, C. R. 1993. Micromotion of mammalian cells measured electrically. *Proceedings of the National Academy of Sciences of the United States of America,* 90**,** 1634-1634.

GIULIETTI, M., OCCHIPINTI, G., PRINCIPATO, G. & PIVA, F. 2016. Weighted gene co-expression network analysis reveals key genes involved in pancreatic ductal adenocarcinoma development. *Cell Oncol (Dordr),* 39**,** 379-88.

GOLEBSKI, K., RÖSCHMANN, K. I., TOPPILA-SALMI, S., HAMMAD, H., LAMBRECHT, B. N., RENKONEN, R., FOKKENS, W. J. & VAN DRUNEN, C. M. 2013. The multi-faceted role of allergen exposure to the local airway mucosa. *Allergy,* 68**,** 152-60.

GORDON, E. D., PALANDRA, J., WESOLOWSKA-ANDERSEN, A., RINGEL, L., RIOS, C. L., LACHOWICZ-SCROGGINS, M. E., SHARP, L. Z., EVERMAN, J. L., MACLEOD, H. J., LEE, J. W., MASON, R. J., MATTHAY, M. A., SHELDON, R.

T., PETERS, M. C., NOCKA, K. H., FAHY, J. V. & SEIBOLD, M. A. 2016. IL1RL1 asthma risk variants regulate airway type 2 inflammation. *JCI Insight,* 1**,** e87871.

GOTO, K., OUE, N., HAYASHI, T., SHINMEI, S., SAKAMOTO, N., SENTANI, K., TEISHIMA, J., MATSUBARA, A. & YASUI, W. 2014. Oligophrenin-1 is associated with cell adhesion and migration in prostate cancer. *Pathobiology,* 81**,** 190-8.

GRAINGE, C. L., LAU, L. C., WARD, J. A., DULAY, V., LAHIFF, G., WILSON, S., HOLGATE, S., DAVIES, D. E. & HOWARTH, P. H. 2011. Effect of bronchoconstriction on airway remodeling in asthma. *N Engl J Med,* 364**,** 2006-15.

GRAS, D., CHANEZ, P., VACHIER, I., PETIT, A. & BOURDIN, A. 2013. Bronchial epithelium as a target for innovative treatments in asthma. *Pharmacol Ther,* 140**,** 290-305.

GRASEMANN, H. 2001. [Genetics of the neuronal NO synthase (NOS1) in the etiology of bronchial asthma]. *Pneumologie,* 55**,** 390-5.

GRAYSON, M. H. 2006. Lung dendritic cells and the inflammatory response. *Ann Allergy Asthma Immunol,* 96**,** 643-51; quiz 652-3, 678.

GREEN, R. H., BRIGHTLING, C. E. & BRADDING, P. 2007. The reclassification of asthma based on subphenotypes. *Curr Opin Allergy Clin Immunol,* 7**,** 43-50.

GREEN, R. H., BRIGHTLING, C. E., MCKENNA, S., HARGADON, B., PARKER, D., BRADDING, P., WARDLAW, A. J. & PAVORD, I. D. 2002. Asthma exacerbations and sputum eosinophil counts: a randomised controlled trial. *Lancet,* 360**,** 1715-21.

GRUENERT, D. C., FINKBEINER, W. E. & WIDDICOMBE, J. H. 1995. Culture and transformation of human airway epithelial cells. *Am J Physiol,* 268**,** L347-60.

GÅRDSVOLL, H., GILQUIN, B., LE DU, M. H., MÉNÈZ, A., JØRGENSEN, T. J. & PLOUG, M. 2006. Characterization of the functional epitope on the urokinase receptor. Complete alanine scanning mutagenesis supplemented by chemical cross-linking. *J Biol Chem,* 281**,** 19260-72.

HACKETT, N. R., SHAYKHIEV, R., WALTERS, M. S., WANG, R., ZWICK, R. K., FERRIS, B., WITOVER, B., SALIT, J. & CRYSTAL, R. G. 2011. The human airway epithelial basal cell transcriptome. *PLoS One,* 6**,** e18378.

HACKETT, T. L., DE BRUIN, H. G., SHAHEEN, F., VAN DEN BERGE, M., VAN OOSTERHOUT, A. J., POSTMA, D. S. & HEIJINK, I. H. 2013. Caveolin-1 controls airway epithelial barrier function. Implications for asthma. *Am J Respir Cell Mol Biol,* 49**,** 662-71.

HACKETT, T. L., WARNER, S. M., STEFANOWICZ, D., SHAHEEN, F., PECHKOVSKY, D. V., MURRAY, L. A., ARGENTIERI, R., KICIC, A., STICK, S. M., BAI, T. R. & KNIGHT, D. A. 2009. Induction of epithelial-mesenchymal transition in primary airway epithelial cells from patients with asthma by transforming growth factor-beta1. *Am J Respir Crit Care Med,* 180**,** 122-33.

HALAPI, E. & BJORNSDOTTIR, U. S. 2009. Overview on the current status of asthma genetics. *Clin Respir J,* 3**,** 2-7.

HAMMAD, H., CHIEPPA, M., PERROS, F., WILLART, M. A., GERMAIN, R. N. & LAMBRECHT, B. N. 2009. House dust mite allergen induces asthma via Toll-like receptor 4 triggering of airway structural cells. *Nat Med,* 15**,** 410-6.

HARDYMAN, M. A., WILKINSON, E., MARTIN, E., JAYASEKERA, N. P., BLUME, C., SWINDLE, E. J., GOZZARD, N., HOLGATE, S. T., HOWARTH, P. H., DAVIES, D. E. & COLLINS, J. E. 2013. TNF-α-mediated bronchial barrier disruption and regulation by src-family kinase activation. *J Allergy Clin Immunol,* 132**,** 665-675.e8.

HAY, D. W. 1999. Putative mediator role of endothelin-1 in asthma and other lung diseases. *Clin Exp Pharmacol Physiol,* 26**,** 168-71.

HEIJINK, I. H., BRANDENBURG, S. M., NOORDHOEK, J. A., POSTMA, D. S., SLEBOS, D. J. & VAN OOSTERHOUT, A. J. 2010a. Characterisation of cell adhesion in airway epithelial cell types using electric cell-substrate impedance sensing. *Eur Respir J,* 35**,** 894-903.

HEIJINK, I. H., KIES, P. M., KAUFFMAN, H. F., POSTMA, D. S., VAN OOSTERHOUT, A. J. & VELLENGA, E. 2007. Down-regulation of E-cadherin in human bronchial epithelial cells leads to epidermal growth factor receptor-dependent Th2 cell-promoting activity. *J Immunol,* 178**,** 7678-85.

HEIJINK, I. H., VAN OOSTERHOUT, A. & KAPUS, A. 2010b. Epidermal growth factor receptor signalling contributes to house dust mite-induced epithelial barrier dysfunction. *Eur Respir J,* 36**,** 1016-26.

HIROTA, N. & MARTIN, J. G. 2013. Mechanisms of airway remodeling. *Chest,* 144**,** 1026-32.

HOLGATE, S. T. 2008. The airway epithelium is central to the pathogenesis of asthma. *Allergol Int,* 57**,** 1-10.

HOLGATE, S. T. 2011. Pathophysiology of asthma: what has our current understanding taught us about new therapeutic approaches? *J Allergy Clin Immunol,* 128**,** 495-505.

HOLGATE, S. T., LACKIE, P., WILSON, S., ROCHE, W. & DAVIES, D. 2000. Bronchial epithelium as a key regulator of airway allergen sensitization and remodeling in asthma. *Am J Respir Crit Care Med,* 162**,** S113-7.

HOLGATE, S. T. & POLOSA, R. 2008. Treatment strategies for allergy and asthma. *Nat Rev Immunol,* 8**,** 218-30.

HOLGUIN, F., BLEECKER, E. R., BUSSE, W. W., CALHOUN, W. J., CASTRO, M., ERZURUM, S. C., FITZPATRICK, A. M., GASTON, B., ISRAEL, E., JARJOUR, N. N., MOORE, W. C., PETERS, S. P., YONAS, M., TEAGUE, W. G. & WENZEL, S. E. 2011. Obesity and asthma: an association modified by age of asthma onset. *J Allergy Clin Immunol,* 127**,** 1486-93.e2.

HU, J., JO, M., EASTMAN, B. M., GILDER, A. S., BUI, J. D. & GONIAS, S. L. 2014. uPAR Induces Expression of Transforming Growth Factor β and Interleukin-4 in Cancer Cells to Promote Tumor-Permissive Conditioning of Macrophages. *The American Journal of Pathology,* 184**,** 3384-3393.

HUBER, D., BALDA, M. S. & MATTER, K. 2000. Occludin modulates transepithelial migration of neutrophils. *J Biol Chem,* 275**,** 5773-8.

IERODIAKONOU, D., PORTELLI, M. A., POSTMA, D. S., KOPPELMAN, G. H., GERRITSEN, J., HACKEN, N. H. T. T., TIMENS, W., BOEZEN, H. M., VONK, J. M. & SAYERS, I. 2016a. Urokinase plasminogen activator receptor polymorphisms and airway remodelling in asthma.

IERODIAKONOU, D., PORTELLI, M. A., POSTMA, D. S., KOPPELMAN, G. H., GERRITSEN, J., TEN HACKEN, N. H., TIMENS, W., BOEZEN, H. M., VONK, J. M. & SAYERS, I. 2016b. Urokinase plasminogen activator receptor polymorphisms and airway remodelling in asthma. *Eur Respir J,* 47**,** 1568-71.

IERODIAKONOU, D., POSTMA, D. S., KOPPELMAN, G. H., BOEZEN, H. M., GERRITSEN, J., TEN HACKEN, N., TIMENS, W. & VONK, J. M. 2011. E-cadherin gene polymorphisms in asthma patients using inhaled corticosteroids. *Eur Respir J,* 38**,** 1044-52.

INOUE, K., TAKANO, H., SHIMADA, A. & SATOH, M. 2009. Metallothionein as an anti-inflammatory mediator. *Mediators Inflamm,* 2009**,** 101659.

INUZUKA, K., OGATA, Y., NAGASE, H. & SHIROUZU, K. 2000. Significance of coexpression of urokinase-type plasminogen activator, and matrix metalloproteinase 3 (stromelysin) and 9 (gelatinase B) in colorectal carcinoma. *J Surg Res,* 93**,** 211-8.

JEON, B. N., YOON, J. H., KIM, M. K., CHOI, W. I., KOH, D. I., HUR, B., KIM, K., KIM, K. S. & HUR, M. W. 2016. Zbtb7c is a molecular 'off' and 'on' switch of Mmp gene transcription. *Biochim Biophys Acta,* 1859**,** 1429-1439.

JIRTLE, R. L. & SKINNER, M. K. 2007. Environmental epigenomics and disease susceptibility. *Nat Rev Genet,* 8**,** 253-62.

JO, M., LESTER, R. D., MONTEL, V., EASTMAN, B., TAKIMOTO, S. & GONIAS, S. L. 2009. Reversibility of epithelial-mesenchymal transition (EMT) induced in breast cancer cells by activation of urokinase receptor-dependent cell signaling. *J Biol Chem,* 284**,** 22825-33.

KABATA, H., MORO, K., KOYASU, S., FUKUNAGA, K., ASANO, K. & BETSUYAKU, T. 2016. Mechanisms to Suppress ILC2-induced Airway Inflammation. *Ann Am Thorac Soc,* 13 Suppl 1**,** S95.

KARYADI, D. M., GEYBELS, M. S., KARLINS, E., DECKER, B., MCINTOSH, L., HUTCHINSON, A., KOLB, S., MCDONNELL, S. K., HICKS, B., MIDDHA, S., FITZGERALD, L. M., DERYCKE, M. S., YEAGER, M., SCHAID, D. J., CHANOCK, S. J., THIBODEAU, S. N., BERNDT, S. I., STANFORD, J. L. & OSTRANDER, E. A. 2017. Whole exome sequencing in 75 high-risk families with validation and replication in independent case-control studies identifies TANGO2, OR5H14, and CHAD as new prostate cancer susceptibility genes. *Oncotarget,* 8**,** 1495-1507.

KAUFFMANN, F. & DEMENAIS, F. 2012. Gene-environment interactions in asthma and allergic diseases: challenges and perspectives. *J Allergy Clin Immunol,* 130**,** 1229-40; quiz 1241-2.

KLOEPFER, K. M. & GERN, J. E. 2010. Virus/allergen interactions and exacerbations of asthma. *Immunol Allergy Clin North Am,* 30**,** 553-63, vii.

KNIGHT, D. A. & HOLGATE, S. T. 2003. The airway epithelium: structural and functional properties in health and disease. *Respirology,* 8**,** 432-46.

KOJIMA, T., GO, M., TAKANO, K., KUROSE, M., OHKUNI, T., KOIZUMI, J., KAMEKURA, R., OGASAWARA, N., MASAKI, T., FUCHIMOTO, J., OBATA, K., HIRAKAWA, S., NOMURA, K., KEIRA, T., MIYATA, R., FUJII, N., TSUTSUMI, H., HIMI, T. & SAWADA, N. 2013. Regulation of tight junctions in upper airway epithelium. *Biomed Res Int,* 2013**,** 947072.

KOLTSOVA, E. K. & LEY, K. 2010. The mysterious ways of the chemokine CXCL5. *Immunity,* 33**,** 7-9.

KOVACIC, M. B., MYERS, J. M., WANG, N., MARTIN, L. J., LINDSEY, M., ERICKSEN, M. B., HE, H., PATTERSON, T. L., BAYE, T. M., TORGERSON, D., ROTH, L. A., GUPTA, J., SIVAPRASAD, U., GIBSON, A. M., TSORAS, A. M., HU, D., ENG, C., CHAPELA, R., RODRÍGUEZ-SANTANA, J. R., RODRÍGUEZ-CINTRÓN, W., AVILA, P. C., BECKMAN, K., SEIBOLD, M. A., GIGNOUX, C., MUSAAD, S. M., CHEN, W., BURCHARD, E. G. & HERSHEY, G. K. 2011. Identification of KIF3A as a novel candidate gene for childhood asthma using RNA expression and population allelic frequencies differences. *PLoS One,* 6**,** e23714.

KUO, C. H., YANG, S. N., KUO, H. F., LEE, M. S., HUANG, M. Y., HUANG, S. K., LIN, Y. C., HSIEH, C. C. & HUNG, C. H. 2016. Cysteinyl leukotriene receptor antagonist epigenetically modulates cytokine expression and maturation of human myeloid dendritic cells. *Pulm Pharmacol Ther,* 39**,** 28-37.

KURAMOTO, E., NISHIUMA, T., KOBAYASHI, K., YAMAMOTO, M., KONO, Y., FUNADA, Y., KOTANI, Y., SISSON, T. H., SIMON, R. H. & NISHIMURA, Y. 2009. Inhalation of urokinase-type plasminogen activator reduces airway remodeling in a murine asthma model. *Am J Physiol Lung Cell Mol Physiol,* 296**,** L337-46.

LAING, E. & SMITH, C. P. 2010. RankProdIt: A web-interactive Rank Products analysis tool. *BMC Res Notes,* 3**,** 221.

LAMBRECHT, B. N. & HAMMAD, H. 2012. The airway epithelium in asthma. *Nat Med,* 18**,** 684-92.

LANGLOIS, A., FERLAND, C., TREMBLAY, G. M. & LAVIOLETTE, M. 2006. Montelukast regulates eosinophil protease activity through a leukotriene-independent mechanism. *J Allergy Clin Immunol,* 118**,** 113-9.

LARUSCH, G. A., MAHDI, F., SHARIAT-MADAR, Z., ADAMS, G., SITRIN, R. G., ZHANG, W. M., MCCRAE, K. R. & SCHMAIER, A. H. 2010. Factor XII stimulates ERK1/2 and Akt through uPAR, integrins, and the EGFR to initiate angiogenesis. *Blood,* 115**,** 5111-20.

LAWRENCE, T., WILLOUGHBY, D. A. & GILROY, D. W. 2002. Anti-inflammatory lipid mediators and insights into the resolution of inflammation. *Nat Rev Immunol,* 2**,** 787-95.

LE VISAGE, C., DUNHAM, B., FLINT, P. & LEONG, K. W. 2004. Coculture of mesenchymal stem cells and respiratory epithelial cells to engineer a human composite respiratory mucosa. *Tissue Eng,* 10**,** 1426-35.

LI, X., HAWKINS, G. A., AMPLEFORD, E. J., MOORE, W. C., LI, H., HASTIE, A. T., HOWARD, T. D., BOUSHEY, H. A., BUSSE, W. W., CALHOUN, W. J.,

CASTRO, M., ERZURUM, S. C., ISRAEL, E., LEMANSKE, R. F., SZEFLER, S. J., WASSERMAN, S. I., WENZEL, S. E., PETERS, S. P., MEYERS, D. A. & BLEECKER, E. R. 2013. Genome-wide association study identifies TH1 pathway genes associated with lung function in asthmatic patients. *J Allergy Clin Immunol,* 132**,** 313-20.e15.

LIANG, L., WILLIS-OWEN, S. A., LAPRISE, C., WONG, K. C., DAVIES, G. A., HUDSON, T. J., BINIA, A., HOPKIN, J. M., YANG, I. V., GRUNDBERG, E., BUSCHE, S., HUDSON, M., RÖNNBLOM, L., PASTINEN, T. M., SCHWARTZ, D. A., LATHROP, G. M., MOFFATT, M. F. & COOKSON, W. O. 2015. An epigenome-wide association study of total serum immunoglobulin E concentration. *Nature,* 520**,** 670-4.

LIBERZON, A., BIRGER, C., THORVALDSDÓTTIR, H., GHANDI, M., MESIROV, J. P. & TAMAYO, P. 2015. The Molecular Signatures Database (MSigDB) hallmark gene set collection. *Cell Syst,* 1**,** 417-425.

LIM, R. H., KOBZIK, L. & DAHL, M. 2010. Risk for asthma in offspring of asthmatic mothers versus fathers: a meta-analysis. *PLoS One,* 5**,** e10134.

LIN, C. H. & CHENG, S. L. 2016. A review of omalizumab for the management of severe asthma. *Drug Des Devel Ther,* 10**,** 2369-78.

LIU, X., LAN, Y., ZHANG, D., WANG, K., WANG, Y. & HUA, Z. C. 2014a. SPRY1 promotes the degradation of uPAR and inhibits uPAR-mediated cell adhesion and proliferation. *Am J Cancer Res,* 4**,** 683-97.

LIU, Y., ZHOU, J. & WHITE, K. P. 2014b. RNA-seq differential expression studies: more sequence or more replication? *Bioinformatics,* 30**,** 301-4.

LOCKSLEY, R. M. 2010. Asthma and allergic inflammation. *Cell,* 140**,** 777-83.

LÖTVALL, J., AKDIS, C. A., BACHARIER, L. B., BJERMER, L., CASALE, T. B., CUSTOVIC, A., LEMANSKE, R. F., WARDLAW, A. J., WENZEL, S. E. & GREENBERGER, P. A. 2011. Asthma endotypes: a new approach to classification of disease entities within the asthma syndrome. *J Allergy Clin Immunol,* 127**,** 355-60.

MADSEN, C. D., FERRARIS, G. M., ANDOLFO, A., CUNNINGHAM, O. & SIDENIUS, N. 2007. uPAR-induced cell adhesion and migration: vitronectin provides the key. *J Cell Biol,* 177**,** 927-39.

MANEECHOTESUWAN, K., KASETSINSOMBAT, K., WONGKAJORNSILP, A. & BARNES, P. J. 2016. Simvastatin up-regulates adenosine deaminase and suppresses osteopontin expression in COPD patients through an IL-13-dependent mechanism. *Respir Res,* 17**,** 104.

MANETTI, M., ROSA, I., MILIA, A. F., GUIDUCCI, S., CARMELIET, P., IBBA-MANNESCHI, L. & MATUCCI-CERINIC, M. 2014. Inactivation of urokinase-type plasminogen activator receptor (uPAR) gene induces dermal and pulmonary fibrosis and peripheral microvasculopathy in mice: a new model of experimental scleroderma? *Ann Rheum Dis,* 73**,** 1700-9.

MAQUERLOT, F., GALIACY, S., MALO, M., GUIGNABERT, C., LAWRENCE, D. A., D'ORTHO, M. P. & BARLOVATZ-MEIMON, G. 2006. Dual role for plasminogen activator inhibitor type 1 as soluble and as matricellular regulator of epithelial alveolar cell wound healing. *Am J Pathol,* 169**,** 1624-32.

MARCELLO, C. & CARLO, L. 2016. Asthma phenotypes: the intriguing selective intervention with Montelukast. *Asthma Res Pract,* 2**,** 11.

MASELLI, D. J., VELEZ, M. I. & ROGERS, L. 2016. Reslizumab in the management of poorly controlled asthma: the data so far. *J Asthma Allergy,* 9**,** 155-62.

MAUROY, B., FILOCHE, M., WEIBEL, E. R. & SAPOVAL, B. 2004. An optimal bronchial tree may be dangerous. *Nature,* 427**,** 633-6.

MCKINLEY, L., ALCORN, J. F., PETERSON, A., DUPONT, R. B., KAPADIA, S., LOGAR, A., HENRY, A., IRVIN, C. G., PIGANELLI, J. D., RAY, A. & KOLLS, J. K. 2008. TH17 cells mediate steroid-resistant airway inflammation and airway hyperresponsiveness in mice. *J Immunol,* 181**,** 4089-97.

MINETA, K., YAMAMOTO, Y., YAMAZAKI, Y., TANAKA, H., TADA, Y., SAITO, K., TAMURA, A., IGARASHI, M., ENDO, T., TAKEUCHI, K. & TSUKITA, S. 2011. Predicted expansion of the claudin multigene family. *FEBS Lett,* 585**,** 606-12.

MIRANDA, C., BUSACKER, A., BALZAR, S., TRUDEAU, J. & WENZEL, S. E. 2004. Distinguishing severe asthma phenotypes: role of age at onset and eosinophilic inflammation. *J Allergy Clin Immunol,* 113**,** 101-8.

MITCHELL, P. D., EL-GAMMAL, A. I. & O'BYRNE, P. M. 2016. Emerging monoclonal antibodies as targeted innovative therapeutic approaches to asthma. *Clin Pharmacol Ther,* 99**,** 38-48.

MODENA, B. D., TEDROW, J. R., MILOSEVIC, J., BLEECKER, E. R., MEYERS, D. A., WU, W., BAR-JOSEPH, Z., ERZURUM, S. C., GASTON, B. M., BUSSE, W. W., JARJOUR, N. N., KAMINSKI, N. & WENZEL, S. E. 2014. Gene expression in relation to exhaled nitric oxide identifies novel asthma phenotypes with unique biomolecular pathways. *Am J Respir Crit Care Med,* 190**,** 1363-72.

MOFFATT, M. F., GUT, I. G., DEMENAIS, F., STRACHAN, D. P., BOUZIGON, E., HEATH, S., VON MUTIUS, E., FARRALL, M., LATHROP, M., COOKSON, W. O. & CONSORTIUM, G. 2010. A large-scale, consortium-based genomewide association study of asthma. *N Engl J Med,* 363**,** 1211-21.

MOFFATT, M. F., KABESCH, M., LIANG, L., DIXON, A. L., STRACHAN, D., HEATH, S., DEPNER, M., VON BERG, A., BUFE, A., RIETSCHEL, E., HEINZMANN, A., SIMMA, B., FRISCHER, T., WILLIS-OWEN, S. A., WONG, K. C., ILLIG, T., VOGELBERG, C., WEILAND, S. K., VON MUTIUS, E., ABECASIS, G. R., FARRALL, M., GUT, I. G., LATHROP, G. M. & COOKSON, W. O. 2007. Genetic variants regulating ORMDL3 expression contribute to the risk of childhood asthma. *Nature,* 448**,** 470-3.

MOHEIMANI, F., HSU, A. C., REID, A. T., WILLIAMS, T., KICIC, A., STICK, S. M., HANSBRO, P. M., WARK, P. A. & KNIGHT, D. A. 2016. The genetic and epigenetic landscapes of the epithelium in asthma. *Respir Res,* 17**,** 119.

MONDINO, A., RESNATI, M. & BLASI, F. 1999. Structure and function of the urokinase receptor. *Thromb Haemost,* 82 Suppl 1**,** 19-22.

MONTUORI, N., VISCONTE, V., ROSSI, G. & RAGNO, P. 2005. Soluble and cleaved forms of the urokinase-receptor: degradation products or active molecules? *Thromb Haemost,* 93**,** 192-8.

MOORE, W. C., MEYERS, D. A., WENZEL, S. E., TEAGUE, W. G., LI, H., LI, X., D'AGOSTINO, R., CASTRO, M., CURRAN-EVERETT, D., FITZPATRICK, A. M., GASTON, B., JARJOUR, N. N., SORKNESS, R., CALHOUN, W. J., CHUNG, K. F., COMHAIR, S. A., DWEIK, R. A., ISRAEL, E., PETERS, S. P., BUSSE, W. W., ERZURUM, S. C., BLEECKER, E. R. & NATIONAL HEART, L. N., AND BLOOD INSTITUTE'S SEVERE ASTHMA RESEARCH PROGRAM 2010. Identification of asthma phenotypes using cluster analysis in the Severe Asthma Research Program. *Am J Respir Crit Care Med,* 181**,** 315-23.

MYÖHÄNEN, H. & VAHERI, A. 2004. Regulation and interactions in the activation of cell-associated plasminogen. *Cell Mol Life Sci,* 61**,** 2840-58.

NAKAWAH, M. O., HAWKINS, C. & BARBANDI, F. 2013. Asthma, chronic obstructive pulmonary disease (COPD), and the overlap syndrome. *J Am Board Fam Med,* 26**,** 470-7.

NALLAR, S. C., LIN, L., SRIVASTAVA, V., GADE, P., HOFMANN, E. R., AHMED, H., REDDY, S. P. & KALVAKOLANU, D. V. 2011. GRIM-1, a novel growth suppressor, inhibits rRNA maturation by suppressing small nucleolar RNAs. *PLoS One,* 6**,** e24082.

NANZER, A. M., CHAMBERS, E. S., RYANNA, K., RICHARDS, D. F., BLACK, C., TIMMS, P. M., MARTINEAU, A. R., GRIFFITHS, C. J., CORRIGAN, C. J. & HAWRYLOWICZ, C. M. 2013. Enhanced production of IL-17A in patients with severe asthma is inhibited by 1α,25-dihydroxyvitamin D3 in a glucocorticoid-independent fashion. *J Allergy Clin Immunol,* 132**,** 297-304.e3.

NICODEMUS-JOHNSON, J., MYERS, R. A., SAKABE, N. J., SOBREIRA, D. R., HOGARTH, D. K., NAURECKAS, E. T., SPERLING, A. I., SOLWAY, J., WHITE, S. R., NOBREGA, M. A., NICOLAE, D. L., GILAD, Y. & OBER, C. 2016a. DNA methylation in lung cells is associated with asthma endotypes and genetic risk. *JCI Insight,* 1**,** e90151.

NICODEMUS-JOHNSON, J., NAUGHTON, K. A., SUDI, J., HOGARTH, K., NAUREKAS, E. T., NICOLAE, D. L., SPERLING, A. I., SOLWAY, J., WHITE, S. R. & OBER, C. 2016b. Genome-Wide Methylation Study Identifies an IL-13-induced Epigenetic Signature in Asthmatic Airways. *Am J Respir Crit Care Med,* 193**,** 376-85.

NOCKER, R. E., SCHOONBROOD, D. F., VAN DE GRAAF, E. A., HACK, C. E., LUTTER, R., JANSEN, H. M. & OUT, T. A. 1996. Interleukin-8 in airway inflammation in patients with asthma and chronic obstructive pulmonary disease. *Int Arch Allergy Immunol,* 109**,** 183-91.

NOGUCHI, E., SAKAMOTO, H., HIROTA, T., OCHIAI, K., IMOTO, Y., SAKASHITA, M., KUROSAKA, F., AKASAWA, A., YOSHIHARA, S., KANNO, N., YAMADA, Y., SHIMOJO, N., KOHNO, Y., SUZUKI, Y., KANG, M. J., KWON, J. W., HONG, S. J., INOUE, K., GOTO, Y., YAMASHITA, F., ASADA, T., HIROSE, H., SAITO, I., FUJIEDA, S., HIZAWA, N., SAKAMOTO, T., MASUKO, H., NAKAMURA, Y., NOMURA, I., TAMARI, M., ARINAMI, T., YOSHIDA, T., SAITO, H. & MATSUMOTO, K. 2011. Genome-wide association study identifies HLA-DP as a susceptibility gene for pediatric asthma in Asian populations. *PLoS Genet,* 7**,** e1002170.

NOH, H., HONG, S. & HUANG, S. 2013a. Role of urokinase receptor in tumor progression and development. *Theranostics,* 3**,** 487-95.

NOH, H., HONG, S. & HUANG, S. 2013b. Role of Urokinase Receptor in Tumor Progression and Development. *Theranostics,* 3**,** 487-495.

NUTU, M., WEIJDEGÅRD, B., THOMAS, P., BERGH, C., THURIN-KJELLBERG, A., PANG, Y., BILLIG, H. & LARSSON, D. G. 2007. Membrane progesterone receptor gamma: tissue distribution and expression in ciliated cells in the fallopian tube. *Mol Reprod Dev,* 74**,** 843-50.

NYKJAER, A., PETERSEN, C. M., MØLLER, B., JENSEN, P. H., MOESTRUP, S. K., HOLTET, T. L., ETZERODT, M., THØGERSEN, H. C., MUNCH, M. & ANDREASEN, P. A. 1992. Purified alpha 2-macroglobulin receptor/LDL receptor-related protein binds urokinase.plasminogen activator inhibitor type-1 complex. Evidence that the alpha 2-macroglobulin receptor mediates cellular degradation of urokinase receptor-bound complexes. *J Biol Chem,* 267**,** 14543-6.

OBER, C. 2016. Asthma Genetics in the Post-GWAS Era. *Ann Am Thorac Soc,* 13 Suppl 1**,** S85-90.

OBER, C. & VERCELLI, D. 2011. Gene-environment interactions in human disease: nuisance or opportunity? *Trends Genet,* 27**,** 107-15.

OHTA, A. & SITKOVSKY, M. 2014. Extracellular adenosine-mediated modulation of regulatory T cells. *Front Immunol,* 5**,** 304.

ORDOÑEZ, C., FERRANDO, R., HYDE, D. M., WONG, H. H. & FAHY, J. V. 2000. Epithelial desquamation in asthma: artifact or pathology? *Am J Respir Crit Care Med,* 162**,** 2324-9.

OSHIKAWA, K., KUROIWA, K., TAGO, K., IWAHANA, H., YANAGISAWA, K., OHNO, S., TOMINAGA, S. I. & SUGIYAMA, Y. 2001. Elevated soluble ST2 protein levels in sera of patients with asthma with an acute exacerbation. *Am J Respir Crit Care Med,* 164**,** 277-81.

OSSOVSKAYA, V. S. & BUNNETT, N. W. 2004. Protease-activated receptors: contribution to physiology and disease. *Physiol Rev,* 84**,** 579-621.

PAN, Q., NING, Y., CHEN, L. Z., ZHANG, S., LIU, Z. Z., YANG, X. X., WEI, W., WEI, H., LI, Q. G., YUE, H. N. & WANG, J. X. 2012. Association of MHC class-III gene polymorphisms with ER-positive breast cancer in Chinese Han population. *Genet Mol Res,* 11**,** 4299-306.

PARKER, J., SARLANG, S., THAVAGNANAM, S., WILLIAMSON, G., O'DONOGHUE, D., VILLENAVE, R., POWER, U., SHIELDS, M., HEANEY, L. & SKIBINSKI, G. 2010. A 3-D well-differentiated model of pediatric bronchial epithelium demonstrates unstimulated morphological differences between asthmatic and nonasthmatic cells. *Pediatr Res,* 67**,** 17-22.

PEASE, J. E. & SABROE, I. 2002. The role of interleukin-8 and its receptors in inflammatory lung disease: implications for therapy. *Am J Respir Med,* 1**,** 19-25.

PELAIA, G., VATRELLA, A., BUSCETI, M. T., GALLELLI, L., CALABRESE, C., TERRACCIANO, R. & MASELLI, R. 2015. Cellular mechanisms underlying eosinophilic and neutrophilic airway inflammation in asthma. *Mediators Inflamm,* 2015**,** 879783.

PETROS, Z., MAKONNEN, E. & AKLILLU, E. 2017. Genome-Wide Association Studies for Idiosyncratic Drug-Induced Hepatotoxicity: Looking Back-Looking Forward to Next-Generation Innovation. *OMICS,* 21**,** 123-131.

PEZZULO, A. A., STARNER, T. D., SCHEETZ, T. E., TRAVER, G. L., TILLEY, A. E., HARVEY, B. G., CRYSTAL, R. G., MCCRAY, P. B. & ZABNER, J. 2011. The air-liquid interface and use of primary cell cultures are important to recapitulate the transcriptional profile of in vivo airway epithelia. *Am J Physiol Lung Cell Mol Physiol,* 300**,** L25-31.

PIRAZZOLI, V., FERRARIS, G. M. & SIDENIUS, N. 2013. Direct evidence of the importance of vitronectin and its interaction with the urokinase receptor in tumor growth. *Blood,* 121**,** 2316-23.

PLOUG, M. 2003. Structure-function relationships in the interaction between the urokinase-type plasminogen activator and its receptor. *Curr Pharm Des,* 9**,** 1499-528.

PLOUG, M., RØNNE, E., BEHRENDT, N., JENSEN, A. L., BLASI, F. & DANØ, K. 1991. Cellular receptor for urokinase plasminogen activator. Carboxyl-terminal processing and membrane anchoring by glycosyl-phosphatidylinositol. *J Biol Chem,* 266**,** 1926-33.

POLDERMAN, T. J., BENYAMIN, B., DE LEEUW, C. A., SULLIVAN, P. F., VAN BOCHOVEN, A., VISSCHER, P. M. & POSTHUMA, D. 2015. Meta-analysis of the heritability of human traits based on fifty years of twin studies. *Nat Genet,* 47**,** 702-9.

POLOSA, R. & THOMSON, N. C. 2013. Smoking and asthma: dangerous liaisons. *Eur Respir J,* 41**,** 716-26.

PORTELLI, M. & SAYERS, I. 2016. Genome-Wide Association Studies in Asthma.

PORTELLI, M. A. 2013. *The role and regulation of the urokinase receptor in asthma and COPD.* University of Nottingham.

PORTELLI, M. A., MOSELEY, C., STEWART, C. E., POSTMA, D. S., HOWARTH, P., WARNER, J. A., HOLLOWAY, J. W., KOPPELMAN, G. H., BRIGHTLING, C. & SAYERS, I. 2016. Airway and peripheral urokinase plasminogen activator receptor is elevated in asthma, and identifies a severe, nonatopic subset of patients. *Allergy*.

PORTELLI, M. A., SIEDLINSKI, M., STEWART, C. E., POSTMA, D. S., NIEUWENHUIS, M. A., VONK, J. M., NURNBERG, P., ALTMULLER, J., MOFFATT, M. F., WARDLAW, A. J., PARKER, S. G., CONNOLLY, M. J., KOPPELMAN, G. H. & SAYERS, I. 2014. Genome-wide protein QTL mapping identifies human plasma kallikrein as a post-translational regulator of serum uPAR levels. *FASEB J,* 28**,** 923-34.

PORTELLI, M. A., STEWART, C. E., HALL, I. P., BRIGHTLING, C. E. & SAYERS, I. 2015. Cigarette Smoke and the Induction of Urokinase Plasminogen Activator Receptor In Vivo: Selective Contribution of Isoforms to Bronchial Epithelial Phenotype. *Am J Respir Cell Mol Biol,* 53**,** 174-83.

PRUIM 2010. LocusZoom: regional visualization of genome-wide association scan results. *Bioinformatics*.

PURCELL, S., NEALE, B., TODD-BROWN, K., THOMAS, L., FERREIRA, M. A., BENDER, D., MALLER, J., SKLAR, P., DE BAKKER, P. I., DALY, M. J. & SHAM, P. C. 2007. PLINK: a tool set for whole-genome association and population-based linkage analyses. *Am J Hum Genet,* 81**,** 559-75.

PYKE, C., ERIKSEN, J., SOLBERG, H., NIELSEN, B. S., KRISTENSEN, P., LUND, L. R. & DANØ, K. 1993. An alternatively spliced variant of mRNA for the human receptor for urokinase plasminogen activator. *FEBS Lett,* 326**,** 69-74.

QIU, Y., ZHU, J., BANDI, V., GUNTUPALLI, K. K. & JEFFERY, P. K. 2007. Bronchial mucosal inflammation and upregulation of CXC chemoattractants and receptors in severe exacerbations of asthma. *Thorax,* 62**,** 475-82.

RABBANI, S. A., ATEEQ, B., ARAKELIAN, A., VALENTINO, M. L., SHAW, D. E., DAUFFENBACH, L. M., KERFOOT, C. A. & MAZAR, A. P. 2010. An Anti-Urokinase Plasminogen Activator Receptor Antibody (ATN-658) Blocks Prostate Cancer Invasion, Migration, Growth, and Experimental Skeletal Metastasis In Vitro and In Vivo. *Neoplasia (New York, N.Y.),* 12**,** 778-788.

RACKEMANN, F. M. 1947. A working classification of asthma. *Am J Med,* 3**,** 601-6.

RACKEMANN, F. M. 1950. Other factors besides allergy in asthma. *J Am Med Assoc,* 142**,** 534-8.

RAEBURN, D. & WEBBER, S. E. 1994. Proinflammatory potential of the airway epithelium in bronchial asthma. *Eur Respir J,* 7**,** 2226-33.

RAGHU, H., NALLA, A. K., GONDI, C. S., GUJRATI, M., DINH, D. H. & RAO, J. S. 2012. uPA and uPAR shRNA inhibit angiogenesis via enhanced secretion of SVEGFR1 independent of GM-CSF but dependent on TIMP-1 in endothelial and glioblastoma cells. *Mol Oncol,* 6**,** 33-47.

RAGNO, P. 2006. The urokinase receptor: a ligand or a receptor? Story of a sociable molecule. *Cell Mol Life Sci,* 63**,** 1028-37.

RAHNAMA, F., TOFTGÅRD, R. & ZAPHIROPOULOS, P. G. 2004. Distinct roles of PTCH2 splice variants in Hedgehog signalling. *Biochem J,* 378**,** 325-34.

RAMASAMY, A., KUOKKANEN, M., VEDANTAM, S., GAJDOS, Z. K., COUTO ALVES, A., LYON, H. N., FERREIRA, M. A., STRACHAN, D. P., ZHAO, J. H., ABRAMSON, M. J., BROWN, M. A., COIN, L., DHARMAGE, S. C., DUFFY, D. L., HAAHTELA, T., HEATH, A. C., JANSON, C., KÄHÖNEN, M., KHAW, K. T., LAITINEN, J., LE SOUEF, P., LEHTIMÄKI, T., MADDEN, P. A., MARKS, G. B., MARTIN, N. G., MATHESON, M. C., PALMER, C. D., PALOTIE, A., POUTA, A., ROBERTSON, C. F., VIIKARI, J., WIDEN, E., WJST, M., JARVIS, D. L., MONTGOMERY, G. W., THOMPSON, P. J., WAREHAM, N., ERIKSSON, J., JOUSILAHTI, P., LAITINEN, T., PEKKANEN, J., RAITAKARI, O. T., O'CONNOR, G. T., SALOMAA, V., JARVELIN, M. R., HIRSCHHORN, J. N. & COLLABORATORS, A. A. G. C. 2012. Genome-wide association studies of asthma in population-based cohorts confirm known and suggested loci and identify an additional association near HLA. *PLoS One,* 7**,** e44008.

RAVA 2015. Gene-environment interactions in the study of asthma in the postgenomewide association studies era. *Curr Opin Allergy Clin Immunol*.

RAY, A., ORISS, T. B. & WENZEL, S. E. 2015. Emerging molecular phenotypes of asthma. *Am J Physiol Lung Cell Mol Physiol,* 308**,** L130-40.

REILLY, M. T., FAULKNER, G. J., DUBNAU, J., PONOMAREV, I. & GAGE, F. H. 2013. The role of transposable elements in health and diseases of the central nervous system. *J Neurosci,* 33**,** 17577-86.

REYNOLDS, S. D., GIANGRECO, A., POWER, J. H. & STRIPP, B. R. 2000. Neuroepithelial bodies of pulmonary airways serve as a reservoir of progenitor cells capable of epithelial regeneration. *Am J Pathol,* 156**,** 269-78.

ROBINSON, D. S., HAMID, Q., YING, S., TSICOPOULOS, A., BARKANS, J., BENTLEY, A. M., CORRIGAN, C., DURHAM, S. R. & KAY, A. B. 1992. Predominant TH2-like bronchoalveolar T-lymphocyte population in atopic asthma. *N Engl J Med,* 326**,** 298-304.

ROGERS, A. V., DEWAR, A., CORRIN, B. & JEFFERY, P. K. 1993. Identification of serous-like cells in the surface epithelium of human bronchioles. *Eur Respir J,* 6**,** 498-504.

ROGERS, M. F., THOMAS, J., REDDY, A. S. & BEN-HUR, A. 2012. SpliceGrapher: detecting patterns of alternative splicing from RNA-Seq data in the context of gene models and EST data. *Genome Biology,* 13**,** 1-17.

ROTH, H. M., WADSWORTH, S. J., KAHN, M. & KNIGHT, D. A. 2012. The airway epithelium in asthma: developmental issues that scar the airways for life? *Pulm Pharmacol Ther,* 25**,** 420-6.

SAJJAN, U., WANG, Q., ZHAO, Y., GRUENERT, D. C. & HERSHENSON, M. B. 2008. Rhinovirus disrupts the barrier function of polarized airway epithelial cells. *Am J Respir Crit Care Med,* 178**,** 1271-81.

SCHNEEBERGER, E. E. & LYNCH, R. D. 2004. The tight junction: a multifunctional complex. *Am J Physiol Cell Physiol,* 286**,** C1213-28.

SCHNEIDERMAN, J., BORDIN, G. M., ADAR, R., SMOLINSKY, A., SEIFFERT, D., ENGELBERG, I., DILLEY, R. B., THINNES, T. & LOSKUTOFF, D. J. 1998. Patterns of expression of fibrinolytic genes and matrix metalloproteinase-9 in dissecting aortic aneurysms. *Am J Pathol,* 152**,** 703-10.

SHANNON, J. M., MCCORMICK-SHANNON, K., BURHANS, M. S., SHANGGUAN, X., SRIVASTAVA, K. & HYATT, B. A. 2003. Chondroitin sulfate proteoglycans are required for lung growth and morphogenesis in vitro. *Am J Physiol Lung Cell Mol Physiol,* 285**,** L1323-36.

SHETTY, S., BHANDARY, Y. P., SHETTY, S. K., VELUSAMY, T., SHETTY, P., BDEIR, K., GYETKO, M. R., CINES, D. B., IDELL, S., NEUENSCHWANDER, P. F., RUPPERT, C., GUENTHER, A., ABRAHAM, E. & SHETTY, R. S. 2010. Induction of tissue factor by urokinase in lung epithelial cells and in the lungs. *Am J Respir Crit Care Med,* 181**,** 1355-66.

SHIFREN, A., WITT, C., CHRISTIE, C. & CASTRO, M. 2012. Mechanisms of remodeling in asthmatic airways. *J Allergy (Cairo),* 2012**,** 316049.

SKADHAUGE, L. R., CHRISTENSEN, K., KYVIK, K. O. & SIGSGAARD, T. 1999. Genetic and environmental influence on asthma: a population-based study of 11,688 Danish twin pairs. *Eur Respir J,* 13**,** 8-14.

SKOVGAARD, D., PERSSON, M. & KJAER, A. 2016. PET imaging of urokinase-type plasminogen activator receptor (uPAR) in prostate cancer: current status and future perspectives. *Clin Transl Imaging,* 4**,** 457-465.

SLATER, M., TORR, E., HARRISON, T., FORRESTER, D., KNOX, A., SHAW, D. & SAYERS, I. 2016. The differential effects of azithromycin on the airway epithelium in vitro and in vivo. *Physiol Rep,* 4.

SMITH, E. R., CAYROU, C., HUANG, R., LANE, W. S., CÔTÉ, J. & LUCCHESI, J. C. 2005. A human protein complex homologous to the Drosophila MSL complex is responsible for the majority of histone H4 acetylation at lysine 16. *Mol Cell Biol,* 25**,** 9175-88.

SMITH, H. W. & MARSHALL, C. J. 2010. Regulation of cell signalling by uPAR. *Nat Rev Mol Cell Biol,* 11**,** 23-36.

SPINA, D. 1998. Epithelium smooth muscle regulation and interactions. *Am J Respir Crit Care Med,* 158**,** S141-5.

STEWART 2009. PLAUR polymorphisms and lung function in UK smokers. *BMC Medical Genetics*.

STEWART, C. E., HALL, I. P., PARKER, S. G., MOFFAT, M. F., WARDLAW, A. J., CONNOLLY, M. J., RUSE, C. & SAYERS, I. 2009. PLAUR polymorphisms and lung function in UK smokers. *BMC Med Genet,* 10**,** 112.

STEWART, C. E., NIJMEH, H. S., BRIGHTLING, C. E. & SAYERS, I. 2012a. uPAR regulates bronchial epithelial repair in vitro and is elevated in asthmatic epithelium. *Thorax,* 67**,** 477-87.

STEWART, C. E., NIJMEH, H. S., BRIGHTLING, C. E. & SAYERS, I. 2012b. uPAR regulates bronchial epithelial repair in vitro and is elevated in asthmatic epithelium. *Thorax,* 67**,** 477-487.

STEWART, C. E. & SAYERS, I. 2009. Characterisation of urokinase plasminogen activator receptor variants in human airway and peripheral cells. *BMC Mol Biol,* 10**,** 75.

STEWART, C. E., TORR, E. E., MOHD JAMILI, N. H., BOSQUILLON, C. & SAYERS, I. 2012c. Evaluation of differentiated human bronchial epithelial cell culture systems for asthma research. *J Allergy (Cairo),* 2012**,** 943982.

STEWART, C. E., TORR, E. E., MOHD JAMILI, N. H., BOSQUILLON, C. & SAYERS, I. 2012d. Evaluation of Differentiated Human Bronchial Epithelial Cell Culture Systems for Asthma Research. *Journal of Allergy,* 2012**,** 11.

STRIETER, R. M. 2002. Interleukin-8: a very important chemokine of the human airway epithelium. *Am J Physiol Lung Cell Mol Physiol,* 283**,** L688-9.

SUBRAMANIAN, A., TAMAYO, P., MOOTHA, V. K., MUKHERJEE, S., EBERT, B. L., GILLETTE, M. A., PAULOVICH, A., POMEROY, S. L., GOLUB, T. R., LANDER, E. S. & MESIROV, J. P. 2005. Gene set enrichment analysis: a knowledge-based approach for interpreting genome-wide expression profiles. *Proc Natl Acad Sci U S A,* 102**,** 15545-50.

SZEFLER, S. J., WENZEL, S., BROWN, R., ERZURUM, S. C., FAHY, J. V., HAMILTON, R. G., HUNT, J. F., KITA, H., LIU, A. H., PANETTIERI, R. A.,

SCHLEIMER, R. P. & MINNICOZZI, M. 2012. Asthma outcomes: biomarkers. *J Allergy Clin Immunol,* 129**,** S9-23.

SZULCEK, R., BOGAARD, H. J. & VAN NIEUW AMERONGEN, G. P. 2014. Electric Cell-substrate Impedance Sensing for the Quantification of Endothelial Proliferation, Barrier Function, and Motility. *Journal of Visualized Experiments : JoVE***,** 51300.

TAKEYAMA, K., DABBAGH, K., LEE, H. M., AGUSTÍ, C., LAUSIER, J. A., UEKI, I. F., GRATTAN, K. M. & NADEL, J. A. 1999. Epidermal growth factor system regulates mucin production in airways. *Proc Natl Acad Sci U S A,* 96**,** 3081-6.

TAN, X. & CHEN, M. 2014. Association between Catechol-O-methyltransferase rs4680 (G>A) polymorphism and lung cancer risk. *Diagn Pathol,* 9**,** 192.

TANG, C. H. & WEI, Y. 2008. The urokinase receptor and integrins in cancer progression. *Cell Mol Life Sci,* 65**,** 1916-32.

TAYLOR, D. R., BATEMAN, E. D., BOULET, L. P., BOUSHEY, H. A., BUSSE, W. W., CASALE, T. B., CHANEZ, P., ENRIGHT, P. L., GIBSON, P. G., DE JONGSTE, J. C., KERSTJENS, H. A., LAZARUS, S. C., LEVY, M. L., O'BYRNE, P. M., PARTRIDGE, M. R., PAVORD, I. D., SEARS, M. R., STERK, P. J., STOLOFF, S. W., SZEFLER, S. J., SULLIVAN, S. D., THOMAS, M. D., WENZEL, S. E. & REDDEL, H. K. 2008. A new perspective on concepts of asthma severity and control. *Eur Respir J,* 32**,** 545-54.

TERADA, H., URANO, T. & KONNO, H. 2005. Association of interleukin-8 and plasminogen activator system in the progression of colorectal cancer. *Eur Surg Res,* 37**,** 166-72.

THOMAS, M. 2015. Why aren't we doing better in asthma: time for personalised medicine? *NPJ Prim Care Respir Med,* 25**,** 15004.

THOMSEN, S. F. 2015. Genetics of asthma: an introduction for the clinician. *Eur Clin Respir J,* 2.

THOMSEN, S. F., DUFFY, D. L., KYVIK, K. O. & BACKER, V. 2010. Genetic influence on the age at onset of asthma: a twin study. *J Allergy Clin Immunol,* 126**,** 626-30.

TINDEMANS, I., SERAFINI, N., DI SANTO, J. P. & HENDRIKS, R. W. 2014. GATA-3 function in innate and adaptive immunity. *Immunity,* 41**,** 191-206.

TRIVEDI, A., PAVORD, I. D. & CASTRO, M. 2016. Bronchial thermoplasty and biological therapy as targeted treatments for severe uncontrolled asthma. *Lancet Respir Med,* 4**,** 585-92.

TSUKITA, S., YAMAZAKI, Y., KATSUNO, T. & TAMURA, A. 2008. Tight junction-based epithelial microenvironment and cell proliferation. *Oncogene,* 27**,** 6930-8.

UYTTERSPROT, N., COSTAGLIOLA, S. & MIOT, F. 1998. A new tool for efficient transfection of dog and human thyrocytes in primary culture. *Mol Cell Endocrinol,* 142**,** 35-9.

VAREILLE, M., KIENINGER, E., EDWARDS, M. R. & REGAMEY, N. 2011. The airway epithelium: soldier in the fight against respiratory viruses. *Clin Microbiol Rev,* 24**,** 210-29.

VASSALLI, J. D., BACCINO, D. & BELIN, D. 1985. A cellular binding site for the Mr 55,000 form of the human plasminogen activator, urokinase. *J Cell Biol,* 100**,** 86-92.

VERMEER, P. D., DENKER, J., ESTIN, M., MONINGER, T. O., KESHAVJEE, S., KARP, P., KLINE, J. N. & ZABNER, J. 2009. MMP9 modulates tight junction integrity and cell viability in human airway epithelia. *Am J Physiol Lung Cell Mol Physiol,* 296**,** L751-62.

VIRCHOW, J. C. 2009. [Asthma--a small airway disease: concepts and evidence]. *Pneumologie,* 63 Suppl 2**,** S96-101.

VON MUTIUS, E. & VERCELLI, D. 2010. Farm living: effects on childhood asthma and allergy. *Nat Rev Immunol,* 10**,** 861-8.

WADSWORTH, S., DORSCHIED, D. & YANG, J. 2012. *IL-13, Asthma and Glycosylation in Airway Epithelial Repair*, INTECH.

WAIN, L. V., ODENTHAL-HESSE, L., ABUJABER, R., SAYERS, I., BEARDSMORE, C., GAILLARD, E. A., CHAPPELL, S., DOGARU, C. M., MCKEEVER, T., GUETTA-BARANES, T., KALSHEKER, N., KUEHNI, C. E., HALL, I. P., TOBIN, M. D. & HOLLOX, E. J. 2014. Copy number variation of the beta-defensin genes in europeans: no supporting evidence for association with lung function, chronic obstructive pulmonary disease or asthma. *PLoS One,* 9**,** e84192.

WALSH, G. M. 2017. Biologics targeting IL-5, IL-4 or IL-13 for the treatment of asthma - an update. *Expert Rev Clin Immunol,* 13**,** 143-149.

WAN 2012. Genome-wide association study to identify genetic determinants of severe asthma. *Thorax*.

WAN, Y. I., SHRINE, N. R., SOLER ARTIGAS, M., WAIN, L. V., BLAKEY, J. D., MOFFATT, M. F., BUSH, A., CHUNG, K. F., COOKSON, W. O., STRACHAN, D. P., HEANEY, L., AL-MOMANI, B. A., MANSUR, A. H., MANNEY, S., THOMSON, N. C., CHAUDHURI, R., BRIGHTLING, C. E., BAFADHEL, M., SINGAPURI, A., NIVEN, R., SIMPSON, A., HOLLOWAY, J. W., HOWARTH, P. H., HUI, J., MUSK, A. W., JAMES, A. L., BROWN, M. A., BALTIC, S., FERREIRA, M. A., THOMPSON, P. J., TOBIN, M. D., SAYERS, I., HALL, I. P. & CONSORTIUM, A. A. G. 2012. Genome-wide association study to identify genetic determinants of severe asthma. *Thorax,* 67**,** 762-8.

WANG, A., YOKOSAKI, Y., FERRANDO, R., BALMES, J. & SHEPPARD, D. 1996. Differential regulation of airway epithelial integrins by growth factors. *Am J Respir Cell Mol Biol,* 15**,** 664-72.

WANG, I. M., STEPANIANTS, S., BOIE, Y., MORTIMER, J. R., KENNEDY, B., ELLIOTT, M., HAYASHI, S., LOY, L., COULTER, S., CERVINO, S., HARRIS, J., THORNTON, M., RAUBERTAS, R., ROBERTS, C., HOGG, J. C., CRACKOWER, M., O'NEILL, G. & PARÉ, P. D. 2008. Gene expression profiling in patients with chronic obstructive pulmonary disease and lung cancer. *Am J Respir Crit Care Med,* 177**,** 402-11.

WANG, Q., WANG, Y., ZHANG, Y. & XIAO, W. 2013. The role of uPAR in epithelial-mesenchymal transition in small airway epithelium of patients with chronic obstructive pulmonary disease. *Respir Res,* 14**,** 67.

WANG, Y. H. & WILLS-KARP, M. 2011. The potential role of interleukin-17 in severe asthma. *Curr Allergy Asthma Rep,* 11**,** 388-94.

WEGENER, J., KEESE, C. R. & GIAEVER, I. 2000. Electric cell-substrate impedance sensing (ECIS) as a noninvasive means to monitor the kinetics of cell spreading to artificial surfaces. *Exp Cell Res,* 259**,** 158-66.

WEI, Y., TANG, C.-H., KIM, Y., ROBILLARD, L., ZHANG, F., KUGLER, M. C. & CHAPMAN, H. A. 2007. Urokinase Receptors Are Required for α5β1 Integrin-mediated Signaling in Tumor Cells. *Journal of Biological Chemistry,* 282**,** 3929-3939.

WEIBEL, E. 1963. Morphometry of the Human Lung. New York; Academic.

WEIBEL, E. 1984. *T**he Pathway for Oxygen: Structure and Function in the Mammalian Respiratory System***, Harvard University Press.

WENZEL, S. E. 2012. Asthma phenotypes: the evolution from clinical to molecular approaches. *Nat Med,* 18**,** 716-25.

WENZEL, S. E., SCHWARTZ, L. B., LANGMACK, E. L., HALLIDAY, J. L., TRUDEAU, J. B., GIBBS, R. L. & CHU, H. W. 1999. Evidence that severe asthma can be divided pathologically into two inflammatory subtypes with distinct physiologic and clinical characteristics. *Am J Respir Crit Care Med,* 160**,** 1001-8.

WESOLOWSKA-ANDERSEN, A. & SEIBOLD, M. A. 2015. Airway molecular endotypes of asthma: dissecting the heterogeneity. *Curr Opin Allergy Clin Immunol,* 15**,** 163-8.

WHITSETT, J. A. & ALENGHAT, T. 2015. Respiratory epithelial cells orchestrate pulmonary innate immunity. *Nat Immunol,* 16**,** 27-35.

WOODMAN, L. B., WAN, W. Y., MILONE, R., GRACE, K., SOUSA, A., WILLIAMSON, R. & BRIGHTLING, C. E. 2013. Synthetic response of stimulated respiratory epithelium: modulation by prednisolone and iKK2 inhibition. *Chest,* 143**,** 1656-66.

WOODRUFF, P. G., BOUSHEY, H. A., DOLGANOV, G. M., BARKER, C. S., YANG, Y. H., DONNELLY, S., ELLWANGER, A., SIDHU, S. S., DAO-PICK, T. P., PANTOJA, C., ERLE, D. J., YAMAMOTO, K. R. & FAHY, J. V. 2007. Genome-wide profiling identifies epithelial cell genes associated with asthma and with treatment response to corticosteroids. *Proc Natl Acad Sci U S A,* 104**,** 15858-63.

WOODRUFF, P. G., MODREK, B., CHOY, D. F., JIA, G., ABBAS, A. R., ELLWANGER, A., KOTH, L. L., ARRON, J. R. & FAHY, J. V. 2009. T-helper type 2-driven inflammation defines major subphenotypes of asthma. *Am J Respir Crit Care Med,* 180**,** 388-95.

WU, J., LIN, R., HUANG, J., GUAN, W., OETTING, W. S., SRIRAMARAO, P. & BLUMENTHAL, M. N. 2014. Functional Fcgamma receptor polymorphisms are associated with human allergy. *PLoS One,* 9**,** e89196.

XIAO, C., PUDDICOMBE, S. M., FIELD, S., HAYWOOD, J., BROUGHTON-HEAD, V., PUXEDDU, I., HAITCHI, H. M., VERNON-WILSON, E., SAMMUT, D., BEDKE, N., CREMIN, C., SONES, J., DJUKANOVIĆ, R., HOWARTH, P. H., COLLINS, J. E., HOLGATE, S. T., MONK, P. & DAVIES, D. E. 2011. Defective epithelial barrier function in asthma. *Journal of Allergy and Clinical Immunology,* 128**,** 549-556.e12.

XIAO, W., HSU, Y. P., ISHIZAKA, A., KIRIKAE, T. & MOSS, R. B. 2005a. Sputum cathelicidin, urokinase plasminogen activation system components, and cytokines discriminate cystic fibrosis, COPD, and asthma inflammation. *Chest,* 128**,** 2316-26.

XIAO, W., HSU, Y. P., ISHIZAKA, A., KIRIKAE, T. & MOSS, R. B. 2005b. Sputum cathelicidin, urokinase plasminogen activation system components, and cytokines discriminate cystic fibrosis, COPD, and asthma inflammation. *Chest,* 128.

XIE, F., YUAN, Y., XIE, L., RAN, P., XIANG, X., HUANG, Q., QI, G., GUO, X., XIAO, C. & ZHENG, S. 2017. miRNA-320a inhibits tumor proliferation and invasion by targeting c-Myc in human hepatocellular carcinoma. *Onco Targets Ther,* 10**,** 885-894.

YAMAYA, M., FINKBEINER, W. E., CHUN, S. Y. & WIDDICOMBE, J. H. 1992. Differentiated structure and function of cultures from human tracheal epithelium. *Am J Physiol,* 262**,** L713-24.

YEUNG, K. Y. & RUZZO, W. L. 2001. Principal component analysis for clustering gene expression data. *Bioinformatics,* 17**,** 763-774.

YICK, C. Y., ZWINDERMAN, A. H., KUNST, P. W., GRÜNBERG, K., MAUAD, T., DIJKHUIS, A., BEL, E. H., BAAS, F., LUTTER, R. & STERK, P. J. 2013. Transcriptome sequencing (RNA-Seq) of human endobronchial biopsies: asthma versus controls. *Eur Respir J,* 42**,** 662-70.

ZHAN, C., YAN, L., WANG, L., SUN, Y., WANG, X., LIN, Z., ZHANG, Y., SHI, Y., JIANG, W. & WANG, Q. 2015. Identification of immunohistochemical markers for distinguishing lung adenocarcinoma from squamous cell carcinoma. *J Thorac Dis,* 7**,** 1398-405.

ZHANG, A. T., LANGLEY, A. R., CHRISTOV, C. P., KHEIR, E., SHAFEE, T., GARDINER, T. J. & KRUDE, T. 2011. Dynamic interaction of Y RNAs with chromatin and initiation proteins during human DNA replication. *J Cell Sci,* 124**,** 2058-69.

ZHANG, Y., HUA, S., ZHANG, A., KONG, X., JIANG, C., DENG, D. & WENLONG, B. 2013. Association between polymorphisms in COMT, PLCH1, and CYP17A1, and non-small-cell lung cancer risk in Chinese nonsmokers. *Clin Lung Cancer,* 14**,** 45-9.

ZHANG, Y., XIAO, W., JIANG, Y., WANG, H., XU, X., MA, D., CHEN, H. & WANG, X. 2012. Levels of components of the urokinase-type plasminogen activator system are related to chronic obstructive pulmonary disease parenchymal destruction and airway remodelling. *J Int Med Res,* 40**,** 976-85.

ZHANG, Y., XU, X., ZHANG, M., WANG, X., BAI, X., LI, H., KAN, L., ZHOU, Y., NIU, H. & HE, P. 2016. MicroRNA-663a is downregulated in non-small cell lung

cancer and inhibits proliferation and invasion by targeting JunD. *BMC Cancer,* 16**,** 315.

ZHAO, B., GANDHI, S., YUAN, C., LUO, Z., LI, R., GÅRDSVOLL, H., DE LORENZI, V., SIDENIUS, N., HUANG, M. & PLOUG, M. 2015. Mapping the topographic epitope landscape on the urokinase plasminogen activator receptor (uPAR) by surface plasmon resonance and X-ray crystallography. *Data in Brief,* 5**,** 107-113.